

AD736260

# Laminar Flow Forced Convection Heat Transfer and Flow Friction in Straight and Curved Ducts— A Summary of Analytical Solutions

by

R. K. Shah and A. L. London



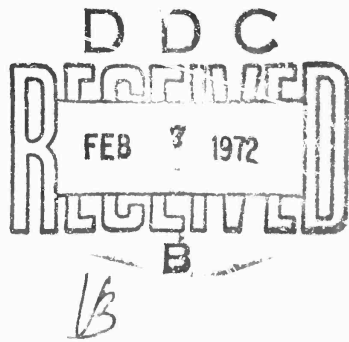
Technical Report No. 75

Prepared under Contract Nonr 225(91)

(NR-090-342)

for

Office of Naval Research



Department of Mechanical Engineering  
Stanford University  
Stanford, California

NATIONAL TECHNICAL  
INFORMATION SERVICE  
SP-2000-74-1215

November 1971

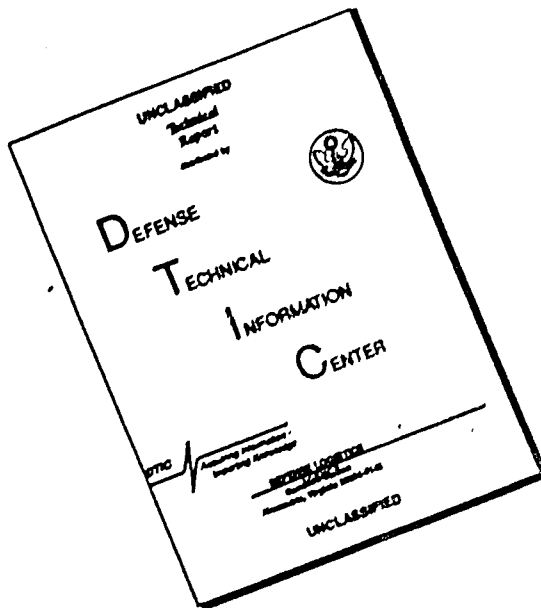
DISTRIBUTION STATEMENT A

Approved for public release.  
Distribution Unlimited

J

31

# **DISCLAIMER NOTICE**



**THIS DOCUMENT IS BEST  
QUALITY AVAILABLE. THE COPY  
FURNISHED TO DTIC CONTAINED  
A SIGNIFICANT NUMBER OF  
PAGES WHICH DO NOT  
REPRODUCE LEGIBLY.**

Page	Location	Wrong	Correct
8	Eq. (7a)	$h(t_w - t_m)$	$hP(t_w - t_m)$
9	Eq. (8a)	$h(t_{w,m} - t_m)$	$hP(t_{w,m} - t_m)$
11	3rd line after Eq. (10b)	peripheral	peripheral
21	8th line from the top	dissipation with the	dissipation within the
24	Eq. (24)	$\int_{-a}^a \dots + \int_{-b}^b \dots$	$[\int_{-a}^a \dots + \int_{-b}^b \dots]$
32	3rd line from the top	depending	dependent
59	11th line from the top	Sadikov [104] linearized	Sadikov [104] simplified
64	3rd line from the bottom	(H)	(H)
67	Last line	equals zero	equal to zero and one respectively
68	11th line from the	fluix	fluid
69	2nd line from the bottom	peripheral	peripheral
93	Last line of 2nd paragraph	from one sided	from the first order one sided
102	1st line	internal heat	internal thermal energy
136	1st line	thermal sources	thermal energy sources
149	Table 28, last	$\phi = 90, Nu_{H2} = -$	$\phi = 90, Nu_{H2} = 2.923$ [57]
170	2nd line from the last	work thermal energy	work and thermal energy
171	2nd line from the first	result.	results.
176	2nd line from the first	wall heater	wall heated
207	2nd line in 3rd paragraph	in Fig. 60(a),	in Fig. 61(a),
251	Eq. (237)	$\frac{x}{4L} \frac{P}{D_h} \frac{1}{Gz}$	$\frac{x}{4L} \frac{P}{D_h} \frac{1}{Gz} \left( = \frac{P}{4D_h} \frac{1}{Gz} \right) \text{ if}$ the flow length L is treated as a length variable

Unclassified

Security Classification

**DOCUMENT CONTROL DATA - R & D**

(Security classification of title, body of abstract and indexing annotation must be entered when the overall report is classified)

1. ORIGINATING ACTIVITY (Corporate author) Stanford University Mechanical Engineering Department Stanford, California 94305		2a. REPORT SECURITY CLASSIFICATION Unclassified
		2b. GROUP
3. REPORT TITLE Laminar Flow Forced Convection Heat Transfer and Flow Friction in Straight and Curved Ducts -- A Summary of Analytical Solutions		
4. DESCRIPTIVE NOTES (Type of report and inclusive dates)		
5. AUTHOR(S) (First name, middle initial, last name) Ramesh K. Shah, A. L. London		
6. REPORT DATE November 15, 1971	7a. TOTAL NO. OF PAGES 308	7b. NO. OF REFS 309
8a. CONTRACT OR GRANT NO. Nonr 225(91)	9a. ORIGINATOR'S REPORT NUMBER(S) TR No. 75	
b. PROJECT NO.		
c.		
d.		
10. DISTRIBUTION STATEMENT The distribution of this document is unlimited.		
11. SUPPLEMENTARY NOTES	12. SPONSORING MILITARY ACTIVITY Office of Naval Research NR-090-342 Washington, D.C. 20360	
13. ABSTRACT <p>The theoretical laminar flow solutions for heat transfer and flow friction are of considerable importance in the development of new types of compact heat exchangers. Generally the higher the degree of compactness, the lower is the Reynolds number and the greater is the relevance of the theory solutions.</p> <p>In this report these solutions are compiled, using a common format, for twenty one straight ducts and four curved ducts. The steady state, constant properties, Newtonian fluid flowing through a stationary, two-dimensional duct is considered. The effects of free convection, mass transfer and change of phase are omitted. Some new analytical solutions are obtained by writing a general computer program for the following ducts: rectangular, isosceles triangular, rounded corner equilateral triangular and sine ducts.</p> <p>Application of the analytical solutions to the gas turbine regenerator is discussed. Specific recommendations are made for further work.</p>		

DD FORM 1 NOV 65 1473

Unclassified

Security Classification

LAMINAR FLOW FORCED CONVECTION HEAT TRANSFER AND  
FLOW FRICTION IN STRAIGHT AND CURVED DUCTS --  
A SUMMARY OF ANALYTICAL SOLUTIONS

Technical Report No. 75

Prepared under Contract Nonr 225(91)  
(NR-090-342)

for  
Office of Naval Research

Reproduction in whole or in part is permitted for  
any purpose of the United States Government

Department of Mechanical Engineering  
Stanford University  
Stanford, California

November 1971

Report Prepared By:

R. K. Shah  
A. L. London

Approved By:

A. L. London  
Project Supervisor

Unclassified

Security Classification

14. KEY WORDS	LINK A		LINK B		LINK C	
	ROLE	WT	ROLE	WT	ROLE	WT
Laminar flow analysis for ducts						
Forced convection heat transfer						
Flow friction						
Compact heat exchangers						

Unclassified

Security Classification

## ABSTRACT

Theoretical laminar flow solutions for heat transfer and flow friction are of considerable importance in the development of new types of compact heat exchangers. Generally the higher the degree of compactness, the lower is the Reynolds number and the greater is the relevance of the theory solutions.

In this report these solutions are compiled, using a common format, for twenty one straight ducts and four curved ducts. The steady state, constant properties, Newtonian fluid flowing through a stationary, two-dimensional duct is considered. The effects of free convection, mass transfer and change of phase are omitted. Some new analytical solutions are obtained by writing a general computer program for the following ducts: rectangular, isosceles triangular, rounded corner equilateral triangular and sine ducts.

Application of the analytical solutions to the gas turbine regenerator is discussed. Specific recommendations are made for further work.

## ADDENDUM

The following important paper appeared in the literature after the present report was almost completed.

J. E. Porter, Heat transfer at low Reynolds number (highly viscous liquids in laminar flow) -- Industrial research fellow report, Trans. Instn chem. Engrs 49, 1-29 (1971).

With the cooperation of thirty industries, Porter compiled the laminar flow solutions for Newtonian as well as non-Newtonian fluids with constant and variable fluid properties. The purpose of the survey was to identify those areas which presented difficulties in thermal designs of chemical, plastic, food etc. industrial problems. He suggested the best design equations available to date and made specific recommendations for future investigation.

The present report is limited to constant properties Newtonian gas flows in laminar regime, in contrast to the very general problem considered by Porter. However, the present report is much more exhaustive in the more limited area and thus complements the work of Porter.

## TO THE READER

An effort was made to compile the laminar flow analytical solutions from all available literature sources. However, it is probable that several important sources may not have come to our attention. We will be grateful for any information in this respect. Any other suggestions and criticisms will also be appreciated.

R. K. Shah  
A. L. London

## ACKNOWLEDGMENTS

This research was sponsored by the Office of Naval Research under the contract Nonr 225(91), NR-090-342.

The authors are grateful to Dr. Wibulswas for furnishing written permission to reproduce the data of Tables 17, 19, 20, 21, 22, 26 and 29 from his Ph.D. thesis. Also, the authors express their thanks to the following researchers for providing the following tabular information: Prof. Manohar for Table 5; Prof. Ratkowsky for Tables 41b and 43b; Prof. Schmidt for Tables 6, 7, 8b, 11b, 12, 14, 15, 24 and 25; Prof. Ash for Tables 2 and 9; and Prof. Haji-Sheikh for the results of circular sector ducts of Table 28. Additionally, extensive correspondence was carried out with Prof. Sparrow, Prof. Cheng, Prof. Perkins, Dr. Iyczkowski, Dr. Hobler, Prof. Snyder, Dr. Hsu and Mr. Akiyama.

Mr. R. N. Noyes of the General Motors Technical Center made important contributions in the early stages of the development of the computer program used in this work. The GM program, patterned after Sparrow and Haji-Sheikh's [57] provided valuable guide lines for the present program.

The difficult task of typing this report was done by Miss Jan Elliott with her uncommon expertise. Mr. Dale Sekijima did the drafting of many illustrations. The authors thank Jan and Dale for their excellent work.

## TABLE OF CONTENTS

	Page
ABSTRACT . . . . .	iii
ACKNOWLEDGMENT . . . . .	v
LIST OF TABLES . . . . .	ix
LIST OF FIGURES . . . . .	xiv
NOMENCLATURE . . . . .	xx
I. INTRODUCTION . . . . .	1
II. MATHEMATICAL FORMULATION . . . . .	4
III. DEFINITIONS AND GENERAL CORRELATIONS . . . . .	23
IV. GENERAL METHODS . . . . .	48
V. ANALYTICAL SOLUTIONS . . . . .	61
Part 1. STRAIGHT DUCTS . . . . .	62
1. CIRCULAR DUCT . . . . .	62
2. PARALLEL PLATES . . . . .	96
3. RECTANGULAR DUCTS . . . . .	116
4. ISOSCELES TRIANGULAR DUCTS . . . . .	134
5. EQUILATERAL TRIANGULAR DUCT WITH ROUNDED CORNERS . . . . .	147
6. RIGHT TRIANGULAR DUCTS . . . . .	148
7. SINE DUCTS . . . . .	153
8. CIRCULAR SECTOR DUCTS . . . . .	155
9. CIRCULAR SEGMENT DUCTS . . . . .	157
10. CIRCULAR DUCTS WITH DIAMETRICALLY OPPOSITE FLAT SIDES . . . . .	158
11. REGULAR POLYGONAL DUCTS . . . . .	159
12. CUSPED DUCTS . . . . .	161
13. ELLIPTICAL DUCTS . . . . .	162
14. MOON SHAPED DUCTS . . . . .	168
15. CARDIOID DUCTS . . . . .	170
16. CONCENTRIC ANNULAR DUCTS . . . . .	172
17. ECCENTRIC ANNULAR DUCTS . . . . .	192
18. ANNULAR SECTOR DUCTS . . . . .	196
19. REGULAR POLYGONAL DUCTS WITH CENTRAL CIR- CULAR CORES . . . . .	199
20. CIRCULAR DUCTS WITH CENTRAL REGULAR POLYGONAL CORES . . . . .	201
21. LONGITUDINAL FLOW BETWEEN CYLINDERS . . . . .	204
22. MISCELLANEOUS GEOMETRIES . . . . .	209

	Page
PART 2. CURVED DUCTS . . . . .	212
23. CURVED CIRCULAR DUCTS . . . . .	213
24. CURVED RECTANGULAR DUCTS . . . . .	219
25. CURVED ELLIPTICAL DUCTS . . . . .	222
26. CURVED CONCENTRIC ANNULAR DUCTS . . . . .	222
VI. DISCUSSION AND COMPARISONS . . . . .	223
VII. SUMMARY AND CONCLUSIONS . . . . .	243
VIII. RECOMMENDATIONS . . . . .	248
REFERENCES . . . . .	253
APPENDIX A . . . . .	279

## LIST OF TABLES

Table		Page
1	Summary of heat transfer boundary conditions for fully developed laminar flow through ducts .	15
2	<u>Circular duct</u> $Nu_T$ as a function of $Pe$ for fully developed laminar flow, from Ash [123] . . .	64
3	<u>Circular, Parallel plates, Elliptical and Sine ducts</u> $Nu_o$ and $Nu_{Rl}$ as a function of $R_w$ for fully developed laminar flow . . . . .	64
4	<u>Circular duct</u> $Nu_o$ and $Nu_{Rl}$ as functions of $R_w$ and $Pe$ for fully developed laminar flow .	68
5	<u>Circular duct</u> $u_{max}/u_m$ , $\Delta p/(\rho u_m^2/2g_c)$ , $f_{app}^{app Re}$ and $K(x)$ as a function of $x^+ (= x/D_h Re)$ for developing laminar flow, from Manohar [137] . . .	70
6	<u>Circular duct</u> $f_{app}^{app Re}$ and $K(x)$ as a function of $x^+$ for $Re = 100, 500$ and $10,000$ , from Schmidt [138] . . . . .	72
7	<u>Circular duct</u> energy content of the fluid for developing temperature profile (developed velocity profile) when fluid axial heat conduction is considered, from Schmidt [138] . . . . .	80
8a	<u>Circular duct</u> $Nu_{x,T}$ , $Nu_{m,T}$ and $Nu_{x,H}$ as functions of $x^*$ and $Pr$ for simultaneously developing flow, from graphical results of Hornbeck [113] . . . . .	90
8b	<u>Circular duct</u> $Nu_{x,T}$ , $\Phi_x$ and $\Phi$ for fully developed and simultaneously developing flow, $Re = 500$ , $Pr = 0.707$ , from Schmidt [138] . . . .	94
9	<u>Parallel plates</u> $Nu_T$ as a function of $Pe$ for fully developed laminar flow, from Ash [123] . .	101
10	<u>Parallel plates</u> $u/u_m$ and flow $Q$ as a function of $x^+$ for developing laminar flow, from Bodoia [181] . . . . .	103

Table	Page
11a	<u>Parallel plates</u> $u_{max}/u_m$ , $\Delta p^*$ , $f_{app} Re$ and $K(x)$ as a function of $x^+$ ( $= x/D_h Re$ ) for developing laminar flow, from Bodoia [181] . . . . . $10^4$
11b	<u>Parallel plates</u> $f_{app} Re$ and $\bar{K}(x)$ as a function of $x^+$ for $Re = 10,000, 500$ and $100$ , from Schmidt [138] . . . . . $10^4$
12	<u>Parallel plates</u> energy content of the fluid for developing temperature profile (developed velocity profile) when fluid axial heat conduction is considered, from Schmidt [138] . . . . . 108
13	<u>Rectangular ducts</u> $fRe$ , $K(\infty)$ , $L_{hy}^+$ , $Nu_T$ , $Nu_{H1}$ and $Nu_{H2}$ for fully developed laminar flow, when all four walls are transferring the heat . 117
14	<u>Rectangular ducts</u> $Nu_T$ for fully developed laminar flow, when one or more walls are transferring the heat, from Schmidt [138] . . . . . 120
15	<u>Rectangular ducts</u> $Nu_{H1}$ for fully developed laminar flow when one or more walls are transferring the heat, from Schmidt [138] . . . . . 122
16	<u>Square duct</u> $Nu_{H3}$ for fully developed laminar flow, from Lyczkowski et al. [11] . . . . . 125
17	<u>Rectangular ducts</u> $Nu_{x,T}$ and $Nu_{m,T}$ as functions of $x^*$ and $\alpha^*$ for fully developed velocity profiles, from Wibulswas [116] . . . . . 128
18	<u>Rectangular ducts</u> $Nu_{x,T}$ as functions of $x^*$ and $\alpha^*$ for fully developed velocity profiles, from Lyczkowski et al. [11] . . . . . 128
19	<u>Rectangular ducts</u> $Nu_{x,H1}$ and $Nu_{m,H1}$ as functions of $x^*$ and $\alpha^*$ for fully developed velocity profiles, from Wibulswas [116] . . . . . 131
20	<u>Rectangular ducts</u> $Nu_{m,T}$ as functions of $x^*$ and $\alpha^*$ for simultaneously developing profiles, $Pr = 0.72$ , from Wibulswas [116] . . . . . 132

Table		Page
21	<u>Rectangular ducts</u> $Nu_{x,H1}$ and $Nu_{m,H1}$ as functions of $x^*$ and $\alpha^*$ for simultaneously developing profiles, $Pr = 0.72$ , from Wibulswas [116] . . . . .	132
22	<u>Rectangular ducts (<math>\alpha^*=0.5</math>)</u> $Nu_{m,H1}$ as functions of $x^*$ and $Pr$ for simultaneously developing profiles from Wibulswas [116] . . . . .	133
23	<u>Isosceles triangular ducts</u> $u_{max}/u_m$ , $K(\infty)$ , $L_{hy}^+$ , $fRe$ , $Nu_T$ , $Nu_{H1}$ and $Nu_{H2}$ for fully developed laminar flow, from Shah [60] . . . . .	139
24	<u>Isosceles triangular ducts</u> $Nu_T$ for fully developed laminar flow when one or more walls are transferring the heat, from Schmidt [138] . . . . .	140
25	<u>Isosceles triangular ducts</u> $Nu_{H1}$ for fully developed laminar flow, when one or more walls are transferring the heat, from Schmidt [138] . . . . .	142
26	<u>Equilateral triangular duct</u> $Nu_{x,T}$ , $Nu_{m,T}$ , $Nu_{x,H1}$ and $Nu_{m,H1}$ as functions of $x^*$ and $Pr$ , from Wibulswas [116] . . . . .	144
27	<u>Equilateral triangular duct with no, one, two and three rounded corners</u> geometrical, flow and heat transfer characteristics, from Shah [60] . . . . .	146
28	<u>Right triangular and Circular sector ducts</u> $fRe$ , $K(\infty)$ , $Nu_{H1}$ and $Nu_{H2}$ for fully developed laminar flow . . . . .	149
29	<u>Right-angled isosceles triangular duct</u> $Nu_{x,T}$ , $Nu_{m,T}$ , $Nu_{x,H1}$ and $Nu_{m,H1}$ for $Pr = \infty$ , 0.72 and 0, from Wibulswas [116] . . . . .	151
30	<u>Sine ducts</u> $u_{max}/u_m$ , $K(\infty)$ , $L_{hy}^+$ , $fRe$ , $Nu_T$ , $Nu_{H1}$ and $Nu_{H2}$ for fully developed laminar flow, from Shah [60] . . . . .	152

Table		Page
31	<u>Circular segment ducts, Circular ducts with diametrically opposite flat sides and Moon shaped ducts</u> $fRe$ , $K(\infty)$ , $Nu_{H1}$ and $Nu_{H2}$ for fully developed laminar flow . . . . .	157
32	<u>Regular polygonal ducts</u> $fRe$ , $Nu_{H1}$ and $Nu_{H2}$ and <u>Cusped ducts</u> $fRe$ for fully developed laminar flow . . . . .	161
33	<u>Elliptical ducts</u> $fRe$ , $K(\infty)$ , $L_{hy}^+$ , $Nu_{H1}$ and $Nu_T$ for fully developed laminar flow . . . . .	165
34	<u>Concentric annular ducts</u> $fRe$ , $K(\infty)$ , $L_{hy}^+$ , $Nu_T$ and $Nu_H$ for fully developed laminar flow. . . . .	175
35	Fundamental solutions for concentric annular ducts . . . . .	176
36	<u>Concentric annular ducts</u> fundamental solutions of first, second, third and fourth kind for the fully developed laminar flow . . . . .	177
37	<u>Concentric annular ducts</u> Nusselt numbers for specified constant temperatures and axial heat fluxes at inner and outer walls for fully developed laminar flow . . . . .	180
38	<u>Eccentric annular ducts</u> $fRe$ for fully developed laminar flow, from graphical results of Jonsson [268] . . . . .	193
39	<u>Eccentric annular ducts</u> $Nu_H$ for fully developed laminar flow, from Cheng and Hwang [55] . . . . .	195
40	<u>Annular sector ducts</u> $fRe$ for fully developed laminar flow . . . . .	196
41a	<u>Regular polygonal ducts with central circular cores</u> $fRe$ for fully developed laminar flow, from Cheng and Jamil [54] . . . . .	200
41b	<u>Regular polygonal ducts with central circular cores</u> $fRe$ for fully developed laminar flow, from Ratkowsky [271] . . . . .	200

Table	Page
42 <u>Regular polygonal ducts with central circular cores</u> $Nu_{H1}$ for fully developed laminar flow, from Cheng and Jamil [54] . . . . .	197
43a <u>Circular duct with central regular polygonal cores</u> $f_{Re}$ for fully developed laminar flow, from Jamil [235] . . . . .	202
43b <u>Circular duct with central regular polygonal cores</u> $f_{Re}$ for fully developed laminar flow, from Ratkowsky [271] . . . . .	202
44 <u>Circular duct with central regular polygonal cores</u> $Nu_{H1}$ for fully developed laminar flow, from Jamil [235] . . . . .	202
45 <u>Longitudinal flow between cylinders (triangular array)</u> $f_{Re}$ , $Nu_{H1}$ , $Nu_{H2}$ for fully developed laminar flow . . . . .	206
46 <u>Curved circular ducts</u> $f_c/f_s$ and $Nu_{H1,c}/Nu_{H,s}$ for fully developed laminar flow . . . . .	214
47 <u>Curved rectangular ducts</u> $f_{Re}$ and $Nu_{H1}$ for fully developed laminar flow, $Pr = 0.73$ , from Akiyama [281] . . . . .	218
48 <u>Curved square duct</u> $f_{Re}$ and $Nu_{H1}$ for fully developed laminar flow; the influence of $Pr$ on $f_{Re}$ and $Nu_{H1}$ , from Akiyama [281] . . . . .	221
49      Idealizations of wall thermal conductivity for some thermal boundary conditions . . . . .	225
50      Solutions for heat transfer and friction for fully developed flow . . . . .	228
51      Summary index of available laminar flow solutions for straight and curved ducts . . . . .	244

LIST OF FIGURES

Figure		Page
1	A two-dimensional duct . . . . .	5
2	Energy transfer terms in the duct wall cross section for finite peripheral conduction . . .	10
3	(H <sub>4</sub> ) temperature variations along the tube length . . . . .	12
4	Thermal circuit representation of the resistances . . . . .	13
5	A cross section of a rectangular duct . . . . .	24
6	Energy transfer terms and temperature distribution with the fluid axial heat conduction . .	40
7	Cosine heat flux variation along circular tube periphery . . . . .	66
8	<u>Circular duct</u> $Nu_{H4}$ for fully developed laminar flow, from Hasegawa and Fujita [10] . .	67
9	<u>Circular duct</u> $f_{app} Re$ for developing laminar flow . . . . .	74
10	<u>Circular duct</u> $K(x)$ for developing laminar flow . . . . .	74
11	<u>Circular duct</u> energy content of the fluid for developing temperature profile when fluid axial heat conduction is considered, from Schmidt [138] . . . . .	81
12	<u>Circular duct</u> $Nu_{m,T}$ as functions of $x^*$ and $Pe$ for simultaneously developing flow, from Hornbeck [113] . . . . .	90
13	<u>Circular duct</u> $Nu_{x,T}$ as functions of $x^*$ and $Pe$ for simultaneously developing flow . . . . .	92
14	<u>Circular duct</u> $Nu_{x,H}$ as functions of $x^*$ and $Pe$ for simultaneously developing flow, from Hornbeck [113] . . . . .	92

Figure		Page
15	Four fundamental problems for parallel plates .	97
16	Temperature profiles for four fundamental problems . . . . .	98
17	Specification of wall temperatures and heat fluxes for parallel plates . . . . .	99
18	<u>Parallel plates</u> energy content of the fluid for developing temperature profile when fluid axial heat conduction is considered, from Schmidt [138] . . . . .	108
19	<u>Rectangular ducts</u> $f_{Re}$ , $K(\infty)$ and $L_{hy}^+$ for fully developed laminar flow . . . . .	118
20	<u>Rectangular ducts</u> $Nu_T$ , $Nu_{H1}$ and $Nu_{H2}$ for fully developed laminar flow . . . . .	118
21	<u>Rectangular ducts</u> $Nu_T$ for fully developed laminar flow, when one or more walls are transferring the heat, from Schmidt [138] . . . . .	120
22	<u>Rectangular ducts</u> $Nu_{H1}$ for fully developed laminar flow, when one or more walls are transferring the heat, from Schmidt [138] . . . . .	122
23	<u>Rectangular ducts</u> $Nu_{x,T}$ for fully developed velocity profile; the influence of $\alpha^*$ on $Nu_{x,T}$ . Similar influence can be expected for $Nu_{m,T}$ , $Nu_{x,H1}$ and $Nu_{m,H1}$ of Tables 17, 19 and 20 . . . . .	129
24	<u>Rectangular ducts</u> ( $\alpha^*=0.5$ ) $Nu_{m,H1}$ as functions of $x^*$ and $Pr$ for simultaneously developing profiles, from Wibulswas [116] . . . . .	133
25	An equilateral triangular duct . . . . .	134
26	An isosceles triangular duct . . . . .	136
27	<u>Isosceles triangular ducts</u> $f_{Re}$ , $K(\infty)$ and $L_{hy}^+$ for fully developed laminar flow . . . . .	138

Figure		Page
28	<u>Isosceles triangular ducts</u> $Nu_T$ , $Nu_{H1}$ and $Nu_{H2}$ for fully developed laminar flow . . . . .	138
29	<u>Isosceles triangular ducts</u> $Nu_T$ for fully de- veloped laminar flow, when one or more walls are transferring the heat, from Schmidt [138] . . . . .	140
30	<u>Isosceles triangular ducts</u> $Nu_{H1}$ for fully developed laminar flow, when one or more walls are transferring the heat, from Schmidt [138] . . . . .	142
31	<u>Equilateral triangular duct</u> $Nu_{x,T}$ ; the in- fluence of $Pr$ on $Nu_{x,T}$ from Wibulswas [116]. Similar influence can be expected for $Nu_{m,T}$ , $Nu_{x,H1}$ and $Nu_{m,H1}$ of Table 26 . . . . .	144
32	An equilateral triangular duct with rounded corners . . . . .	147
33	A right-angled isosceles triangular duct . . . . .	148
34	<u>Right triangular ducts</u> $fRe$ , $K(\infty)$ and $Nu_{H1}$ for fully developed laminar flow, from Sparrow and Haji-Sheikh [230] . . . . .	149
35	<u>Right-angled isosceles triangular duct</u> $Nu_{x,T}$ as functions of $x^*$ and $Pr$ , from Wibulswas [116] . . . . .	151
36	A sine duct . . . . .	153
37	<u>Sine ducts</u> $fRe$ , $K(\infty)$ and $L_{hy}^+$ for fully de- veloped laminar flow . . . . .	154
38	<u>Sine ducts</u> $Nu_T$ , $Nu_{H1}$ and $Nu_{H2}$ for fully developed laminar flow . . . . .	154
39	<u>Circular segment ducts</u> $fRe$ , $K(\infty)$ , $Nu_{H1}$ and $Nu_{H2}$ for fully developed laminar flow . . . . .	156

Figure	Page
40 <u>Circular sector ducts</u> $f_{Re}$ , $K(\infty)$ , $Nu_{H1}$ and $Nu_{H2}$ for fully developed laminar flow, from [57] . . . . .	156
41 <u>Circular ducts with diametrically opposite flat</u> sides $f_{Re}$ and $Nu_{H1}$ for fully developed laminar flow, from Cheng and Jamil [54,235] . . .	158
42 <u>Regular polygonal ducts</u> $f_{Re}$ , $Nu_{H1}$ and $Nu_{H2}$ for fully developed laminar flow . . . . .	160
43      An elliptical duct . . . . .	162
44 <u>Elliptical ducts</u> $f_{Re}$ and $L_{hy}^+$ for fully de- veloped laminar flow . . . . .	164
45 <u>Elliptical ducts</u> $Nu_T$ and $Nu_{H1}$ for fully de- veloped laminar flow . . . . .	164
46      A moon shaped duct . . . . .	168
47 <u>Moon shaped ducts</u> $f_{Re}$ for fully developed laminar flow . . . . .	169
48      A cardioid duct . . . . .	170
49      A concentric annular duct . . . . .	172
50 <u>Concentric annular ducts</u> $f_{Re}$ , $K(\infty)$ and $L_{hy}^+$ for fully developed laminar flow . . . . .	174
51 <u>Concentric annular ducts</u> $Nu_T$ and $Nu_H$ for fully developed laminar flow . . . . .	174
52 <u>Concentric annular ducts</u> $Nu_i$ and $Nu_o$ for constant temperatures on both walls for fully de- veloped laminar flow . . . . .	180
53 <u>Concentric annular ducts</u> $Nu_i$ and $Nu_o$ for constant axial heat fluxes on both walls for fully developed laminar flow . . . . .	184
54 <u>Eccentric annular ducts</u> $f_{Re}$ for fully devel- oped laminar flow . . . . .	193

Figure	Page
55 <u>Eccentric annular ducts</u> $Nu_H$ for fully developed laminar flow . . . . .	195
56 <u>Annular sector ducts</u> $fRe$ for fully developed laminar flow . . . . .	197
57 <u>Regular polygonal ducts with central circular cores</u> $fRe$ for fully developed laminar flow, from Ratkowsky [271] . . . . .	198
58 <u>Regular polygonal ducts with central circular cores</u> $Nu_{H1}$ for fully developed laminar flow, from Cheng and Jamil [54] . . . . .	198
59 <u>Circular duct with central regular polygonal cores</u> $fRe$ for fully developed laminar flow, from Ratkowsky [271] . . . . .	203
60 <u>Circular duct with central regular polygonal cores</u> $Nu_{H1}$ for fully developed laminar flow, from Jamil [235] . . . . .	203
61      Triangular and square array arrangements for longitudinal flow between cylinders . . . . .	204
62 <u>Longitudinal flow between cylinders</u> $fRe$ , $Nu_{H1}$ and $Nu_{H2}$ for fully developed laminar flow . . . . .	206
63      Geometries and results considered by Gunn and Darling [274] . . . . .	209
64      An internally finned tube . . . . .	211
65 <u>Curved circular duct</u> $f_c/f_s$ and $Nu_{H1,c}/Nu_{H,s}$ for fully developed laminar flow . . . . .	214
66 <u>Curved rectangular ducts</u> $f_c/f_s$ for fully developed laminar flow, from Cheng and Akiyama [280] . . . . .	218
67 <u>Curved rectangular ducts</u> $Nu_{H1,c}/Nu_{H1,s}$ for fully developed laminar flow, from Cheng and Akiyama [280] . . . . .	220
68 <u>Curved square duct</u> $Nu_{H1,c}/Nu_{H1,s}$ as functions of $K$ and $Pr$ for fully developed laminar flow, from Cheng and Akiyama [280] . . . . .	220

Figure		Page
69	Fluid temperature profiles for $\textcircled{H}$ and $\textcircled{T}$ boundary conditions . . . . .	229
70	Flow area "goodness" factors for some duct geometries of Table 50 . . . . .	230
71	Volume "goodness" factors for some duct geom- tries of Table 50 . . . . .	230
72	Corner effects for limiting geometries . . . .	233
73	Comparison of flow friction behavior -- isosceles triangular and sine ducts . . . .	240
74	Comparison of heat transfer behavior -- isosceles triangular and sine ducts . . . .	240

## NOMENCLATURE

### English letter symbols

A	heat transfer or flow friction area
$A_c$	flow cross section area
a	radius of a circular duct, half width of rectangular duct, semi-major axis of the elliptical duct, half base width of triangular or sine duct, $a > b$ for rectangular and elliptical ducts with symmetric heating
$a'$	duct wall thickness
$B_1, B_2$	constants; see Eq. (76)
b	half spacing of parallel plates, half height of rectangular duct, semi-minor axis of elliptical duct, half height of triangular or sine duct, $b \leq a$ for rectangular and elliptical ducts with symmetric heating
b	amplitude of cosine heat flux variation around the periphery of a circular duct; see Fig. 7
C	flow stream capacity rate, $W_{cp}$
$c_1$	a pressure gradient parameter, $(dp/dx)/(\mu/g_c)$
$c_2$	a temperature gradient parameter, $(\partial t/\partial x)/a$
$c_3$	thermal energy source parameter, $S/k$
$c_4$	a parameter, $c_1 c_2$
$c_5$	a parameter, $c_3/c_4 a^2$
$c_6$	a parameter, $g_c (dp/dx)/\rho c_p (\partial t/\partial x)$
$c_p$	specific heat of the fluid at constant pressure
$D_h$	hydraulic diameter of the duct or flow passages, $D_h = 4r_h$
$E(m)$	complete elliptical integral of second kind
f	"Fanning" or "small" friction factor, for fully developed flow if no subscript, $\tau/(\rho u_m^2/2g_c)$ , dimensionless

$f_{ave}$	average Fanning friction factor in hydrodynamic entry length, defined by Eq. (26), dimensionless
$f_{app}$	apparent Fanning friction factor, defined by Eq. (34), dimensionless
$f_D$	"Darcy" or "large" friction factor, $4f$ , dimensionless
G	fluid mass velocity, $\rho u_m$
$g_c$	proportionality factor in Newton's second law of motion
(H)	boundary condition referring to constant and uniform axial as well as peripheral wall heat flux, also uniform peripheral wall temperature; boundary condition valid only for the circular tube, parallel plates, and annular ducts
(H1)	boundary condition referring to constant axial wall heat flux with uniform peripheral wall temperature, expressed by Eq. (7)
(H2)	boundary condition referring to constant axial wall heat flux with uniform peripheral wall heat flux, expressed by Eq. (8)
(H3)	boundary condition referring to constant axial wall heat flux with finite peripheral wall heat conduction, expressed by Eq. (9)
(H4)	boundary condition referring to exponential axial wall heat flux with uniform peripheral wall temperature, expressed by Eq. (10)
h	convective heat transfer coefficient, for fully developed flow if no subscript is used
J	mechanical to thermal energy conversion factor
j	Colburn heat transfer modulus, $StPr^{2/3}$ , dimensionless
K	Dean number, $Re \sqrt{a/R}$ , dimensionless
$K(x)$	pressure drop increment due to hydrodynamic entrance region, defined by Eq. (35), dimensionless
$K(\infty)$	$K(x)$ evaluated at $x \rightarrow \infty$ , defined by Eq. (31), dimensionless

$K_f$	flow friction modulus, $fRe$ , dimensionless
$K_h$	heat transfer modulus, $jRe$ , dimensionless
$K_p$	peripheral wall heat conduction parameter, $k_w a'/kD_h$ , dimensionless
$k$	thermal conductivity, for fluid if no subscript
$L$	length of the duct
$L_{hy}$	hydrodynamic entrance length, defined as the duct length required to achieve the duct centerline (maximum) velocity as 99% of the corresponding fully developed magnitude when entering flow is uniform
$L_{th}$	thermal entrance length, defined as the duct length required to achieve the value of local Nusselt number $Nu_x$ as 1.05 $Nu_{fd}$
$L_{hy}^+$	dimensionless hydrodynamic entrance length, $L_{hy}/D_h Re$
$L_{th}^*$	dimensionless thermal entrance length, $L_{th}/D_h Pe$
$m$	a parameter for elliptical duct geometry, $\sqrt{1 - 1/\alpha^*^2}$
$Nu$	Nusselt number, for fully developed flow if neither $x$ nor $m$ appear as subscript, $hD_h/k$ , dimensionless
$Nu_x, ( )$	local Nusselt number for the thermal entrance region. The second subscript in ( ) designates the associated thermal boundary condition. The local Nusselt number is an average value with respect to perimeter at any given cross section $x$
$Nu_o$	overall Nusselt number associated with $(R1)$ boundary condition, defined by Eq. (49a), dimensionless
$N_{tu}$	number of heat transfer units, $h_m A/Wc_p$ , $St L/r_h$ , dimensionless
$n$	number of sides of a regular polygon or a cusped duct
$n$	outer normal direction to the duct wall

$n^*$	dimensionless distance $n/D_h$ measured along the outer normal direction
P	wetted perimeter of the duct
Pe	Péclet number, $Pe = RePr = D_h u_m / \alpha$ , dimensionless
Pr	Prandtl number, $\mu c_p / k$ , dimensionless
p	fluid static pressure
$\Delta p^*$	dimensionless pressure drop, $\Delta p / (\rho u_m^2 / 2g_c)$
Q	a parameter for the curved duct heat transfer, $(K^2 Pr)^{1/4}$ , dimensionless
Q	volumetric flow rate
$q'$	heat transfer rate per unit length of the duct
$q''$	heat flux, heat transfer rate per unit heat transfer surface area of the duct
$q_r''$	incident radiative heat flux
R	radius of curvature of the centerline of the curved duct
Re	Reynolds number, $GD_h / \mu$ , dimensionless
$R_w$	dimensionless wall thermal resistance, defined by Eq. (54)
(R1)	boundary condition referring to finite thermal resistance at the wall, expressed by Eq. (11)
(R2)	boundary condition referring to radiative flux at the wall, expressed by Eq. (12)
r	radial distance in cylindrical coordinates
$r_h$	hydraulic radius of the duct, $A_c / P$
$r_i$	inner radius of concentric annular duct or radius of circular centered core of a regular polygonal duct
$r_j$	radius of heat transferring wall of the concentric annular duct

$r_o$	outer radius of a concentric annular duct or radius of a circular duct having regular polygon as centered core
$r^*$	$r_i/r_o$
$r_j^*$	$r_j/r_c$
S	thermal energy source function, thermal energy generated per unit volume of the fluid
St	Stanton number, $h/Gc_p$ , dimensionless
s	distance along the periphery $\Gamma$ of the duct
s	half of the tube bundle pitch; see Fig. 61
T	temperature of the fluid, on the absolute scale, $^{\circ}\text{R}$ or $^{\circ}\text{K}$
(T)	boundary condition referring to constant and uniform wall temperature, both axially and peripherally, expressed by Eq. (6)
(Δt)	thermal boundary condition expressed by Eq. (21)
t	temperature of the fluid to a specified arbitrary datum, $^{\circ}\text{F}$ or $^{\circ}\text{C}$
$t_a$	ambient fluid temperature; see Fig. 4
$t_m$	bulk average fluid temperature, defined by Eq. (45)
$t_w$	wall or fluid temperature at the duct wall $\Gamma$
U	wall conductance with suffix w, i or o; $U_o$ is defined by Eq. (48)
u	fluid axial velocity, fluid velocity component in x direction
$u_m$	average axial velocity, defined by Eq. (22)
v	fluid velocity component in y direction or radial direction
w	fluid mass flow rate through the duct
w	fluid velocity component in z direction
$x^+$	$10^3 x^+$
$x^*$	$10^3 x^*$

x	axial coordinate in cartesian and cylindrical systems
$x^+$	dimensionless axial coordinate for hydrodynamic entrance region, $x/D_h Re$
$x^*$	dimensionless axial coordinate for thermal entrance region, $x/D_h Pe$
$x'$	$2x^*$
y	a spatial coordinate in cartesian coordinate system
z	a spatial coordinate in cartesian coordinate system

Greek letter symbols

$\alpha$	thermal diffusivity, $k/\rho c_p$
$\alpha_w$	absorptivity of wall material, dimensionless
$\alpha^*$	aspect ratio of rectangular, isosceles triangular, elliptical and sine duct, $\alpha^* = 2b/2a$ , for a symmetrical geometry with symmetrical heating, otherwise $\alpha^* = 2a/2b$ , so that it ranges from 0 to 1
$\beta$	a function of $x$ alone, defined by Eq. (104)
$\Gamma$	periphery of the duct
$\gamma$	radiative wall heat flux boundary condition parameter, $\epsilon_w \sigma T_e^3 D_h / k$ , dimensionless
$\Delta, \delta$	prefixes denoting a difference
$\delta$	a parameter, $\mu c_1^2 D_h^3 / k (\partial t / \partial n)_\Gamma$
$\epsilon$	heat exchanger effectiveness, the ratio of actual heat transfer rate to the thermodynamically limited, maximum possible heat transfer rate as would be realized only in a counterflow heat exchanger of infinite area, dimensionless
$\epsilon_w$	emissivity of the wall
$\epsilon(x)$	mean velocity weighing factor; see Eq. (106)
$\zeta$	ratio of thermal to hydrodynamic boundary layer thickness

$\eta$	a parameter to account fluid viscous dissipation, $\mu u_m^2 / q'' D_h$ , dimensionless
$\theta_{w-m}$	dimensionless wall to fluid bulk mean temperature difference, defined by Eq. (94)
$\theta$	angular coordinate in cylindrical coordinate system
$\theta$	dimensionless fluid temperature when used with subscript
$\theta_m$	dimensionless fluid temperature for $\textcircled{T}$ , defined by Eq. (76)
$\Lambda(x)$	a parameter defined by Eq. (106)
$\lambda$	exponential axial wall heat flux parameter, defined by Eq. (10a)
$\mu$	dynamic fluid viscosity coefficient; see footnote on p. 24
$\nu$	kinematic fluid viscosity coefficient, $\mu/\rho$
$\xi_1$	perpendicular distance from center of duct to side of the regular polygon; see Fig. 57
$\xi_2$	distance measured from the center to the corner of a regular polygon; see Fig. 59
$\rho$	fluid density
$\sigma$	Stefan-Boltzmann constant
$\tau$	wall shear stress due to skin friction
$\Phi$	dimensionless wall heat flux for concentric annular ducts when used with superscript and subscript, defined by Eq. (134)
$\Phi$	dimensionless total wall heat flux for $\textcircled{T}$ boundary condition, $q'' D_h / k(t_w - t_e)$
$\Phi_x$	dimensionless local wall heat flux for $\textcircled{T}$ boundary condition, $q_x'' D_h / k(t_w - t_e)$
$\phi$	half apex angle of isosceles triangular, sinusoidal, circular sector, circular segment flat sided circular ducts and moon shaped ducts

$\phi$	effectiveness coefficient; see Eq. (73)
$\nabla$	denotes gradient, derivative with respect to normal direction
<u>Subscript</u>	
c	curved duct
e	initial value at $x = 0$ (at entrance) or where the heat transfer starts, e.g. $x_e$
fd	fully developed laminar flow
H	referring to $(H)$ boundary condition
H1	referring to $(H_1)$ boundary condition
H2	referring to $(H_2)$ boundary condition
H3	referring to $(H_3)$ boundary condition
H4	referring to $(H_4)$ boundary condition
i	inner surface of the concentric annular duct
lm	logarithmic mean
m	mean
max	maximum
min	minimum
o	outer surface of the concentric annular duct
R1	referring to $(R_1)$ boundary condition
R2	referring to $(R_2)$ boundary condition
s	straight duct
T	referring to $(T)$ boundary condition
x	denoting arbitrary section along the duct length, a local value as opposed to a mean value
w	wall
$\infty$	referring to fully developed laminar flow

Superscript

\*,+ designates a normalized or dimensionless quantity

## I. INTRODUCTION

Interest in heat exchanger surfaces with a high ratio of heat transfer area to core volume is increasing at an accelerated pace. The primary reasons for the use of these more compact surfaces is that a smaller, lighter weight and lower cost exchanger is the result. These gains are brought about by both the direct geometric advantage of higher "area density" and because forced convection heat transfer in small dimension passages generally results in higher heat transfer coefficients (heat transfer power per unit area and temperature difference) for a specified flow friction power per unit area.

The flow passages for these compact or high area density surfaces have a small hydraulic radius. Consequently, with gas flows particularly, the heat exchanger design range for Reynolds number usually falls well within the laminar flow regime. It follows then that the theory derived laminar flow solutions for friction and heat transfer in ducts of various flow cross-section geometries become important and these solutions are the subject matter of this report. A direct application of these results may be in the development of new surfaces with improved characteristics. A critical examination of the theory solutions may prove to be fruitful because there is a wide range for the heat transfer coefficient, at a given friction power for different cross-section geometries.

It has long been realized that laminar flow heat transfer is dependent on the duct geometry, flow inlet velocity profile, and the wall temperature and/or heat flux boundary conditions. These conditions are difficult to control in the laboratory, nevertheless there is a substantial ongoing experimental research effort devoted to this task. A theory base is needed in order to interpret the experimental results

and to extrapolate these results for the task of designing practical heat exchanger systems. However, it is recognized that this theory is founded on idealizations of geometry and boundary conditions that are not necessarily well duplicated either in application or even in the laboratory. The development of this theory base has been a fertile field of applied mathematics since the early days of the science of heat transfer. Today, by the application of modern computer technology, analysis to some degree has exceeded experimental verification.

Drew [1]<sup>1</sup> in 1931 prepared a compilation of existing theory results for heat transfer. Dryden et al. [2] in 1932 compiled the fully developed laminar flow solutions for ducts of various geometries. Later several literature surveys were made for particular geometries. In 1961, Rohsenow and Choi [3] presented a limited compilation of solutions for simple cylindrical ducts. Kays and London [4] published a compilation in 1964 pertinent to compact heat exchangers. The theoretical development as well as the details of analysis are described in depth by Kays [5] in 1966.

The specific objectives of this report are the following:

- (1) To provide an up-to-date compilation of available analytical solutions with results in numerical and graphical non-dimensionalized form.
- (2) To present an unified treatment for the nomenclature and dimensionless flow friction and heat transfer characteristics.
- (3) To fill some of the gaps where solutions are needed because of the current state of the art of the gas turbine regenerator applications.

---

<sup>1</sup>The numbers in brackets denote references at the end of the report.

(4) To indicate those areas where applied mathematicians may make their contributions.

Primarily english language literature up to December 1970 is reviewed. The available analytical solutions for the laminar flow friction and heat transfer through twenty one straight ducts and four curved ducts are described. Whenever possible, the results are summarized in tabular and graphical form.

Emphasis is given to the analytical solutions for heat transfer and flow friction for fully developed and developing flow through axisymmetric and two-dimensional straight and curvilinear ducts. Only the forced convection steady laminar flow of constant property Newtonian fluid through a stationary duct is considered. Magnetohydrodynamic flows, electrically conducting flows, the high temperature (heat radiating) flows etc. are not considered. Also omitted are the effects of natural convection, change of phase, mass transfer, chemical reaction, etc.

The applicable momentum and energy equations with appropriate boundary conditions are outlined in Chapter II to describe the flow characteristics and heat transfer through the duct. The definitions and general correlation schemes for the laminar duct flow and heat transfer problem are described in Chapter III. The general methods used in the heat transfer literature to solve the problems formulated in Chapter II are presented in Chapter IV. Chapter V describes the solutions obtained for various duct geometries. Comparisons and discussion of analytical solutions and thermal boundary conditions are presented in Chapter VI. Conclusions and summary of these solutions are presented in Chapter VII. Recommendations for future studies and presentation of new work are made in Chapter VIII. Appendix A lists the technical journals from which laminar flow heat transfer literature has been located.

## II. MATHEMATICAL FORMULATION

The applicable momentum and energy equations with appropriate boundary conditions are outlined to describe the flow characteristics and heat transfer through the duct. The solutions to these equations for a particular geometry will be described in Chapter V.

### II.1 Fully Developed Flow

Far downstream from the flow entrance region of the duct, the fluid velocity no longer depends upon the axial distance  $x$ , and the flow becomes hydrodynamically fully developed; i.e.

$$u = u(y, z) \quad \text{or} \quad u(r, \theta) \quad \text{only} \quad (1)$$

For several of thermal boundary conditions, as described below the dimensionless temperature profile also becomes invariant with the axial distance, thereby designated as thermally developed flow. In this case,

$$\frac{\partial}{\partial x} \left[ \frac{t_{w,m} - t}{t_{w,m} - t_m} \right] = 0 \quad (2)$$

Note, however,  $t$  is a function of  $x$  as well as  $y$  and  $z$ , unlike  $u$ .

The terminology "fully developed flow" or "fully developed laminar flow" will be used throughout the report when the flow is both hydrodynamically and thermally developed.

#### II.1.1 Flow Friction

Consider a steady state, fully developed laminar flow in a two-dimensional stationary cylindrical duct bounded by a closed curve  $\Gamma$  (Fig. 1). Also assume that the fluid is incompressible and the fluid properties  $\rho, c_p, k$  are constant, independent of fluid temperature, and the body forces,

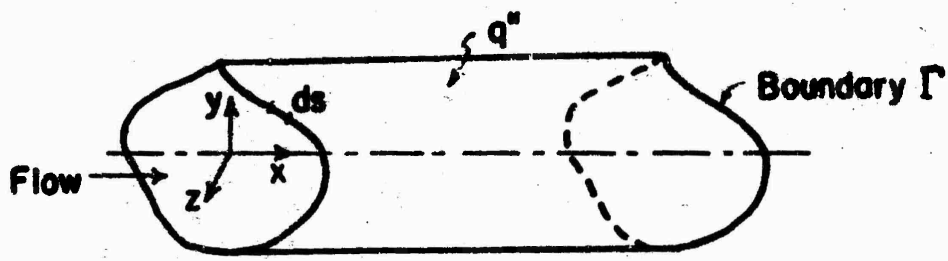


Fig. 1 A two-dimensional duct

viz., gravity, centrifugal, Coriolis, electromagnetic etc. do not exist. The applicable differential momentum equation is [5]

$$\nabla^2 u = \frac{g_c}{\mu} \frac{dp}{dx} = c_1 \quad (3)$$

where  $x$  is the axis of the duct and  $c_1$  is defined as the pressure drop parameter. The  $\nabla^2$  is the two-dimensional Laplacian operator. Note that the right hand side of Eq. (3) is independent of  $(y, z)$  or  $(r, \theta)$ , so it is designated as a constant  $c_1$ . Eq. (3) in cartesian coordinates is

$$\frac{\partial^2 u}{\partial y^2} + \frac{\partial^2 u}{\partial z^2} = c_1 \quad (3a)$$

and in cylindrical coordinates is

$$\frac{1}{r} \frac{\partial}{\partial r} \left( r \frac{\partial u}{\partial r} \right) + \frac{1}{r^2} \frac{\partial^2 u}{\partial \theta^2} = c_1 \quad (3b)$$

The boundary condition for the velocity problem is no slip boundary condition, namely,

$$u = 0 \quad \text{on } \Gamma . \quad (4)$$

By the definition of fully developed laminar flow of the incompressible fluid, the solution of the continuity equation (conservation of mass) is implicitly given by Eq. (1). Moreover, the continuity equation is already built into Eq. (3). Consequently, the continuity equation is not required separately<sup>2</sup> for the solution of fully developed laminar flow friction and the heat transfer problem described below.

### II.1.2 Heat Transfer

In addition to the idealizations made for flow friction problem, it is assumed that there is no mass diffusion, chemical reaction, electromagnetic effects etc., but there may be uniform intensity thermal energy sources (erroneously referred to as heat sources) present within the fluid. The governing differential energy equation for a perfect gas or an incompressible fluid is as follows [5], after the introduction of the rate equations for the heat conduction and shear stress.

$$k\nabla^2 t = \frac{k u}{\alpha} \frac{\partial t}{\partial x} - S - \frac{\mu}{g_c J} \left[ \left( \frac{\partial u}{\partial y} \right)^2 + \left( \frac{\partial u}{\partial z} \right)^2 \right] \quad (5)$$

Here again the flow is assumed steady, laminar, fully developed with constant  $\mu$  and  $k$ . When the axial thermal conduction is not neglected in the fluid, the  $\nabla^2$  is a three-dimensional Laplacian operator. On the right hand side of the Eq. (5), the second term represents the thermal energy sources within the fluid, while the third term represents part of the work done by the fluid on adjacent layers due to action of shear forces. This third term is usually referred to as viscous dissipation or unfortunately as friction heat in the literature. Under the assumptions mentioned as above, Eq. (5) is exact for incompressible liquids,  $\rho = \text{constant}$ .

---

<sup>2</sup>The continuity equation, in addition to the momentum equation, is required separately for the exact solution of developing velocity profile in the duct entrance region.

However, for perfect gases, there is an additional assumption involved that the  $u(dp/dx)/J$  term is negligible, so it does not appear in Eq. (5). This latter term is conventionally referred to as the gas compression work. It appears in the energy equation when the energy conservation equation is manipulated with the momentum equation, canceling the kinetic energy term [5].

Note that if Eq. (5) is operated by  $\nabla^2$ , the right hand side of Eq. (5) would contain  $\nabla^2 u$  which equals to  $c_1$  from Eq. (3). The resulting equation will be a fourth order differential equation for the dependent variable  $t$ .

The boundary conditions associated with Eq. (5) will be discussed separately in the following section.

### II.1.3 Heat Transfer Boundary Conditions

A variety of boundary conditions can be specified for the heat transfer problem. These boundary conditions can be categorized in two classes. In the first class, the peripheral wall temperature or wall heat flux is uniform. In the second class, the peripheral wall temperature or wall heat flux is arbitrary. The boundary conditions of the first class are described by an equation form in the following subsections. The boundary conditions of the second class are analyzed by the superposition methods [6,7,8].

For all the boundary conditions of class one and two, the fully developed laminar Nusselt number is found to be independent of  $x$ ,  $Pr$  and  $Re$ , but dependent on the duct geometry and other relevant parameters.

#### II.1.3.1 Specified Wall Temperature Distribution

The wall temperature is arbitrarily specified along the periphery of the duct and is constant in the axial direction. The case of arbitrary peripheral temperature is not investigated in the literature. The case of constant and uniform wall temperature for the whole duct is a boundary

condition of considerable technical importance. It occurs for the heat transfer in condensers and evaporators etc. where the temperature of the fluid on one side is approximately uniform and constant, and the thermal resistance on the constant fluid temperature side is relatively small. In this case,

$$t|_{\Gamma} = t_w = \text{a constant, independent of } (x,y,z) \quad (6)$$

The uniform and constant wall temperature condition can, however, be pictured in two ways: (a) thermal resistance of wall and other side of the fluid is zero and the temperature of ambient fluid is constant (Fig. 4). In this case, the axial wall thermal conductivity can be arbitrary but the radial thermal conductivity is infinite, (b) infinite wall thermal conductivity in axial and peripheral directions as well as radial. This boundary condition will be referred to as  $\mathbb{T}$  boundary condition. The Nusselt number or related parameters evaluated for this case will have a suffix T.

#### II.1.3.2 Specified Wall Heat Flux Distribution

The wall heat flux distribution is specified in axial as well as peripheral direction. The following four special cases of this boundary condition have been considered in the literature. Arbitrary variations in peripheral wall temperature or wall heat flux can be handled by the superposition techniques [6,7,8]. For the case of circular tube and parallel plates, the  $\mathbb{H}_1$ ,  $\mathbb{H}_2$  and  $\mathbb{H}_3$  boundary conditions described below are identical and hence will be designated as  $\mathbb{H}$  boundary condition.

- (a) Constant axial wall heat flux with uniform peripheral wall temperature,  $\mathbb{H}_1$

$$q' = Wc_p \frac{dt_m}{dx} = h(t_w - t_m) = \text{constant} \quad (7a)$$

$$t|_{\Gamma} = t_w = \text{a constant, independent of } (y, z) \quad (7b)$$

For this boundary condition, the wall thermal conductivity  $k_w$  is implicitly assumed to be zero in the axial direction and infinite in the peripheral direction. This means wall thermal resistance is infinite in the axial direction and zero in the peripheral direction. This boundary condition will be referred to as  $(H1)$  with the Nusselt number having  $H1$  as a suffix. It may be difficult to achieve  $(H1)$  boundary condition in practice for noncircular ducts [9]. However, mathematically it is the most amenable, and consequently, most frequently investigated boundary condition in the literature for noncircular ducts.

- (b) Constant axial wall heat flux with uniform peripheral wall heat flux,  $(H2)$

$$q' = Wc_p \frac{dt}{dx} = h(t_{w,m} - t_m) = \text{constant} \quad (8a)$$

$$k \frac{\partial t}{\partial n}|_{\Gamma} = \text{a constant, independent of } (y, z) \quad (8b)$$

This boundary condition corresponds to having zero  $k_w$  in axial as well as peripheral direction (infinite wall thermal resistance in axial and peripheral direction). It will be referred to as  $(H2)$  boundary condition. It is a limiting case of the more realistic boundary condition  $(H3)$  described below.

- (c) Constant axial wall heat flux with finite peripheral wall heat conduction,  $(H3)$ . From the steady state energy balance on the wall element  $ds$  of unit depth in Fig. 2, the temperature distribution in the wall is related to

the wall heat flux as follows:

$$q'' = k \frac{\partial t}{\partial n} \Big|_{\Gamma} + k_w \frac{\partial^2}{\partial s^2} \int_n^{n+a'} t_w dn = 0 \quad (9a)$$

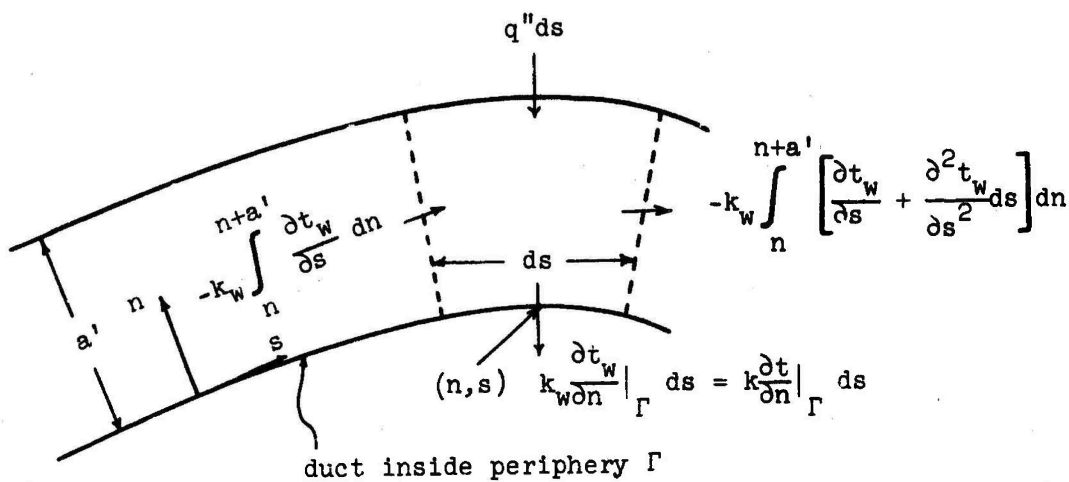


Fig. 2 Energy transfer terms in the duct wall cross section for finite peripheral conduction

It is assumed that the axial  $k_w$  is zero. The temperature across any cross section for a thin wall may be taken as uniform. If the thin wall thickness  $a'$  is uniform, then

$$\int_n^{n+a'} t_w dn \approx a' t \Big|_{\Gamma}$$

After dividing  $n$  and  $s$  by the characteristic dimension  $D_h$ , Eq. (9a) reduces to

$$\frac{q''D_h}{k} - \frac{\partial t}{\partial n^*} \Big|_{\Gamma} + K_p \frac{\partial^2 t}{\partial s^*^2} \Big|_{\Gamma} = 0 \quad (9b)$$

where  $K_p = \frac{k_w a'}{k D_h}$  = peripheral heat conduction parameter.

This boundary condition will be referred to as  $(H3)$ .

The  $K_p = \infty$  and  $0$  corresponds to the  $(H1)$  and  $(H2)$  boundary conditions respectively.

Electric resistance heating, nuclear heating and counterflow heat exchangers with fluid thermal capacity rates being equal are some examples that approximate  $(H3)$  boundary condition.

(d) Exponential axial wall heat flux,  $(H4)$

$$q'_x = q'_e e^{\lambda x^*} \quad (10a)$$

$$t \Big|_{\Gamma} = t_w = \text{a constant, independent of } (y, z) \quad (10b)$$

In this case, it is also implicitly assumed that the wall thermal conductivity is zero in axial direction and infinite in peripheral direction. This boundary condition will be referred to as  $(H4)$ . The  $(H1)$  and  $(T)$  boundary conditions are special cases of the general exponential wall heat flux boundary condition as described below. For the case of circular tube, with varying values of  $\lambda$ , the wall and fluid bulk mean temperatures obtained are shown in Fig. 3 [10]. For the circular duct, the  $(H1)$  and  $(T)$  boundary conditions are special cases of  $(H4)$  boundary condition with  $\lambda=0$  and  $-14.632$  respectively. The  $(H4)$  boundary condition with an appropriate value of  $\lambda$  can be used to approximate either the parallel or counterflow heat exchangers where the temperature distribution varies exponentially along the duct.

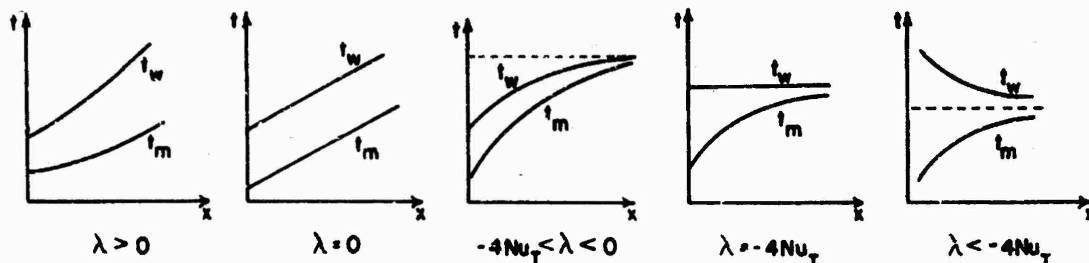


Fig. 3 (H4) temperature variations along the tube length

### III.1.3.3 Heat Flux at the Wall Dependent Upon the Wall Temperature

The local wall heat flux is dependent linearly or non-linearly on the local wall temperature. Two special cases of this boundary condition are technically important and have been considered in the literature, namely the finite wall thermal resistance and the radiant flux surface conditions.

- (a) Finite thermal resistance at the wall, (R1). The duct wall, transferring heat to the fluid, has a finite thermal resistance in the normal direction. The wall thermal resistance,  $1/U_w$ , is composed of two thermal resistances (wall and outside wall to fluid) as shown in Fig. 4 and is expressed as

$$\frac{1}{U_w} = \frac{a'}{k_w} + \frac{1}{h_a} \quad (11a)$$

This boundary condition, will be referred to as (R1), for the finite wall thermal resistance, is expressed as

$$k \left. \frac{\partial t}{\partial n} \right|_{\Gamma} = U_w (t_a - t_w) \quad (11b)$$

$$t \Big|_{\Gamma} = t_w = \text{a constant, independent of } (y, z)$$

It is implicitly assumed that the peripheral  $k_w$  is infinite, the axial  $k_w$  is zero, and the radial or normal  $k_w$  is finite. The normal  $k_w$  is used in the expression for  $U_w$ , Eq. (11a). The ambient fluid temperature  $t_a$  is assumed to be uniform and constant. The wall thermal resistance  $1/U_w$  always has been treated as a constant in the theoretical analysis.

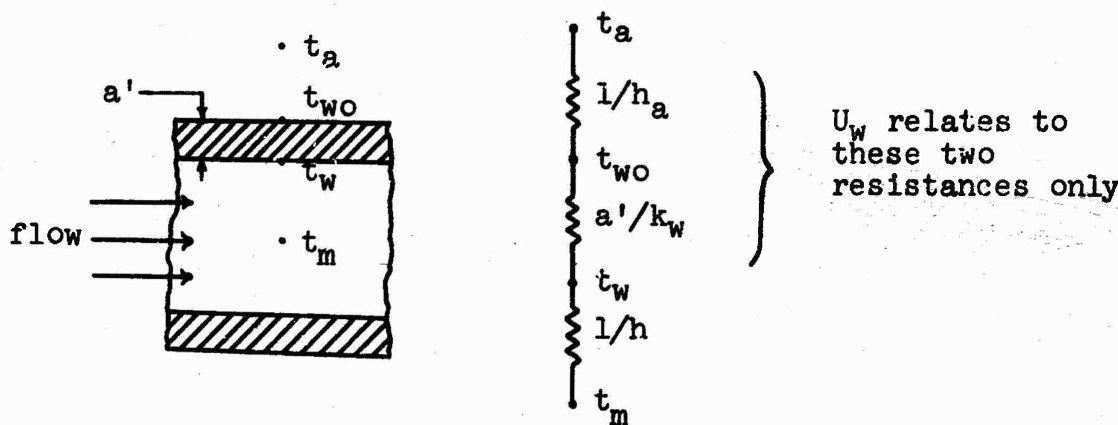


Fig. 4 Thermal circuit representation of the resistances

Two limiting cases are of interest: (1) If the wall thermal resistance  $1/U_w$  is zero, the  $\textcircled{R1}$  boundary condition reduces to  $\textcircled{T}$  boundary condition. (2) If  $1/U_w \gg 1/h$ , then  $q''$  is virtually independent of  $1/h$  and  $q''$  tends to be a constant, if  $(t_a - t_w) \approx \text{constant}$ . Hence, if the wall thermal resistance  $1/U_w$  is infinite, it reduces to  $\textcircled{H1}$  boundary condition.

- (b) Nonlinear radiant-flux boundary condition,  $\textcircled{R2}$ . When the duct wall is radiating the thermal energy to the environment at zero degree absolute temperature, this boundary condition, referred to as  $\textcircled{R2}$ , is encountered.

$$-k \frac{\partial T}{\partial n} \Big|_{\Gamma} = \epsilon_w \sigma T_w^4 \quad (12a)$$

$T \Big|_{\Gamma} = T_w$  = a constant, independent of  $(y, z)$

It is implicitly assumed that the wall thermal conductivity is infinite in peripheral direction, while it is zero in the axial direction. Heat transfer to and from the surfaces in a vacuum may be an area of application of the  $\textcircled{R2}$  boundary condition.

Non-dimensionalizing the temperature and the normal direction with  $T_e$  and  $D_h$  respectively, the boundary condition (12a) reduces to

$$\frac{\partial T^*}{\partial n^*} \Big|_{\Gamma} = -\gamma T_w^{*4} \quad (12b)$$

where the radiation parameter  $\gamma = \epsilon_w \sigma T_e^3 D_h / k$ . Similar to limiting cases of  $\textcircled{R1}$  boundary condition, for  $\gamma$  equals infinite and zero, the  $\textcircled{R2}$  boundary condition reduces to  $\textcircled{T}$  and  $\textcircled{H1}$  boundary conditions respectively.

A more generalized boundary condition, which takes into account the peripheral wall heat conduction as well as the dependency of local wall heat flux upon the local wall temperature [e.g.  $\textcircled{R1}$  and  $\textcircled{R2}$  ], is discussed by Liczkowski et al. [11].

All the boundary conditions outlined in this section are summarized in Table 1.

## II.2 Hydrodynamically Developing Flow

As the fluid flows through a duct, its velocity profile undergoes a change from its initial entrance form to that of a fully developed profile at an axial location far downstream from the entrance. The hydrodynamically developing flow

Table 1. Summary of heat transfer boundary conditions  
for fully developed laminar flow through ducts

Designation	Description	Equations
(T)	Constant and uniform wall temperature peripherally as well as axially	$t _{\Gamma} = t_w$ , a constant independent of $(x,y,z)$
(H1)	Constant axial wall heat flux with uniform peripheral wall temperature	$q' = Wc_p \frac{dt}{dx} = \text{constant}$ $t _{\Gamma} = t_w$ , a constant independent of $(y,z)$
(H2)	Constant axial wall heat flux with uniform peripheral wall heat flux	$q' = Wc_p \frac{dt}{dx} = \text{constant}$ $k \frac{\partial t}{\partial n} _{\Gamma} = \text{constant}$
(H3)	Constant axial wall heat flux with finite peripheral wall heat conduction	$q' = Wc_p \frac{dt}{dx} = \text{constant}$ $\frac{q'' D_h}{k} - \frac{\partial t}{\partial n^*} _{\Gamma} + K_p \frac{\partial^2 t}{\partial s^* 2} _{\Gamma} = 0$
(H4)	Exponential axial wall heat flux	$q'_x = q'_e e^{\lambda x^*}$ $t _{\Gamma} = t_w$ , a constant independent of $(y,z)$
(R1)	Finite thermal resistance at the wall	$k \frac{\partial t}{\partial n} _{\Gamma} = U_w (t_a - t_w)$ $t _{\Gamma} = t_w$ , a constant independent of $(y,z)$
(R2)	Nonlinear radiant-flux boundary condition	$-k \frac{\partial T}{\partial n} _{\Gamma} = \epsilon_w \sigma T_w^4$ $T _{\Gamma} = T_w$ , a constant independent of $(y,z)$

region is referred to as that region from entrance to where the fully developed invariant conditions are achieved. The definition of hydrodynamic entrance length will be presented in Chapter III.

The axial pressure gradient is higher in the entrance region than that in the fully developed region due to two effects: (a) the increase in momentum or fluid as the velocity profile becomes less uniform, and (b) the higher wall shear caused by higher transverse velocity gradients.

The determination of velocity profile, wall shear stress distribution, pressure drop, and the location to achieve invariant flow conditions etc. is considered as the solution to hydrodynamically developing flow problem (also referred to as hydrodynamic entry length problem).

All the idealizations made in the fully developed case are still applicable here. Additionally, the rate of change of shear stress  $\mu(\partial^2 u / \partial x^2)$  (also referred to as the diffusion of vorticity) in axial direction is treated as zero. Even though the physical concept<sup>3</sup> of boundary layer introduced by Prandtl is not applicable to the developing duct flow, the boundary layer idealizations,

$$u \gg v, w \quad (13a)$$

$$\frac{\partial u}{\partial y}, \frac{\partial u}{\partial z} \gg \frac{\partial u}{\partial x}, \frac{\partial v}{\partial x}, \frac{\partial v}{\partial y}, \frac{\partial v}{\partial z}, \frac{\partial w}{\partial x}, \frac{\partial w}{\partial y}, \frac{\partial w}{\partial z} \quad (13b)$$

---

<sup>3</sup>A momentum or velocity boundary layer is a thin region very close to the body surface or wall where the influence of fluid viscosity is predominant. The remainder of the flow field can to a good approximation be treated as inviscid and can be analyzed by the potential flow theory.

are also a good approximation for laminar flow in ducts. As a result, it is found that the fluid pressure is a function of  $x$  only. The governing boundary layer momentum equation, for axially symmetric flow, in cylindrical coordinates is [5]

$$u \frac{\partial u}{\partial x} + v \frac{\partial u}{\partial r} = - \frac{g_c}{\rho} \frac{dp}{dx} + v \left( \frac{\partial^2 u}{\partial r^2} + \frac{1}{r} \frac{\partial u}{\partial r} \right) \quad (14a)$$

and in cartesian coordinates,

$$u \frac{\partial u}{\partial x} + v \frac{\partial u}{\partial y} + w \frac{\partial u}{\partial z} = - \frac{g_c}{\rho} \frac{dp}{dx} + v \left( \frac{\partial^2 u}{\partial y^2} + \frac{\partial^2 u}{\partial z^2} \right) \quad (14b)$$

The no slip boundary condition for this case is

$$u, v, w = 0 \quad \text{on } \Gamma \quad (15)$$

An initial condition is also required, and usually uniform velocity profile is assumed at the entrance.

$$u = u_e = u_m \quad \text{at } x = 0 \quad (16)$$

In addition, the continuity equation needs to be solved simultaneously. In cylindrical coordinates [5], it is

$$\frac{\partial u}{\partial x} + \frac{\partial v}{\partial r} + \frac{v}{r} = 0 \quad (17a)$$

and in cartesian coordinates [5],

$$\frac{\partial u}{\partial x} + \frac{\partial v}{\partial y} + \frac{\partial w}{\partial z} = 0. \quad (17b)$$

The solution to the hydrodynamic entry length problem is obtained by solving the Eqs. (17) and (14) simultaneously with the boundary and initial conditions of Eqs. (15) and (16).

### II.3 Thermally Developing Flow

As the fluid (at different temperature than that of the duct walls) flows through the duct, its temperature profile changes from uniform at the point where heating started to an invariant form downstream. The thermal entry length is referred to as duct length required to attain fully developed invariant temperature profile. The definition of thermal entry length will be given in Chapter III.

Thermal entry length problem is classified in three categories: (i) the velocity profile is fully developed and remains fixed while the temperature profile develops, (ii) the simultaneous development of velocity and temperature profile, and (iii) at some point in the hydrodynamic entry region, the temperature profile starts developing. The first problem is an excellent approximation for high Prandtl number fluids for which the velocity profile develops much more rapidly than the temperature profile. For fluids with  $Pr \approx 1$ , the second problem approximates the actual situation in most cases. The third problem is important for some special cases when either  $Pr < 1$  or high viscous fluid ( $Pr \gg 1$ ) flow in short ducts (small values of  $L/D_h$ ).

The rate of heat transfer and consequently the heat transfer coefficient  $h$  (and Nusselt number) are higher in the thermal entrance region than that in the fully developed region due to higher fluid temperature gradients at the wall.

The determination of temperature profile, wall heat flux distributions, local and mean Nusselt numbers (or  $h$ ), and the location to achieve invariant dimensionless temperature profile etc. is considered as the solution to the thermal entry length problem.

All the idealizations made in the fully developed case are still applicable except that the axial heat conduction, thermal energy sources and viscous dissipation within the fluid are neglected. Also, the boundary layer idealizations, Eq. (13) and

$$\frac{\partial t}{\partial y}, \frac{\partial t}{\partial z} \gg \frac{\partial t}{\partial x} \quad (18)$$

are invoked. Refer to footnote 3 on p. 16 and associated discussion. The governing boundary layer energy equation for the developing laminar temperature profile of a perfect gas or an incompressible liquid is [5]

$$u \frac{\partial t}{\partial x} + v \frac{\partial t}{\partial r} = \alpha \left( \frac{\partial^2 t}{\partial r^2} + \frac{1}{r} \frac{\partial t}{\partial r} + \frac{\partial^2 t}{\partial x^2} \right) \quad (19a)$$

in cylindrical coordinates, and

$$u \frac{\partial t}{\partial x} + v \frac{\partial t}{\partial y} + w \frac{\partial t}{\partial z} = \alpha \left( \frac{\partial^2 t}{\partial y^2} + \frac{\partial^2 t}{\partial z^2} + \frac{\partial^2 t}{\partial x^2} \right) \quad (19b)$$

in cartesian coordinates. Eq. (19a) includes the idealization that the heating is axially symmetrical.

In addition to the heat transfer boundary conditions, an initial condition is also required and is normally employed as the uniform temperature at the point where heating (or cooling) started.

$$t = t_e \quad \text{at} \quad x = x_e \quad (20)$$

For the exact solution to the thermal entry length problem, the continuity and momentum equations need to be solved first.

### II.3.1 Heat Transfer Boundary Conditions

Heat transfer boundary conditions for a thermally developing flow can be categorized in two classes: (i) Those boundary conditions of Section II.1.3 (Table 1), where  $t_w$ ,  $q''$ ,  $R_w$  etc. are axially constant. (Also the axially constant  $(t_w - t_m)$  boundary condition, to be discussed, would fall in this class.) (ii) Arbitrarily specified axial distribution of  $t_w$ ,  $q''$ ,  $R_w$  etc.

#### II.3.1.1 Axially Constant $t_w$ , $q''$ , $R_w$ , $(t_w - t_m)$ etc.

All the heat transfer boundary conditions outlined in Section II.1.3 and summarized in Table 1 are also applied to thermally developing flow. Additionally, the  $\Delta t$  boundary condition, defined in Eq. (21), will be considered, since the counterflow heat exchanger with  $C_{min}/C_{max} = 1$  (e.g. the gas turbine regenerator) has a boundary condition between  $(H_3)$  and  $\Delta t$ .

$$\Delta t = t_w - t_m = \text{a constant independent of } x \quad (21)$$

$$t|_{\Gamma} = t_w = \text{a constant, independent of } (y, z)$$

In case of the fully developed flow, the constant wall heat flux boundary condition  $(H_1)$  is the same as the constant wall to fluid bulk mean temperature difference boundary condition  $\Delta t$ . This is because the heat transfer coefficient  $h$  is found to be independent of  $x$  in fully developed laminar flow. However, for the case of thermally developing flow, the  $(H_1)$  and  $\Delta t$  boundary conditions are different, as the heat transfer coefficient is dependent on  $x$  along the thermal entrance. In the gas turbine regenerator literature, the  $(H_1)$  boundary condition, Eq. (7), is exclusively employed or implied, except for the case of circular tube considered by Kays [12].

### II.3.1.2 Axially Arbitrarily Specified $t_w$ , $q''$ , $R_w$ etc.

The axial distribution of wall surface temperature, wall heat flux, wall thermal resistance or wall radiant heat flux is specified arbitrarily. The solution of energy equation with this class of boundary condition can be obtained by the superposition techniques if the energy equation is linear and homogeneous. This is the situation when the thermal energy sources and viscous dissipation with the fluid are neglected. Then a sum of solutions is again a solution. Thus by superposing thermal entrance solutions for axially constant  $t_w$ ,  $q''$  etc., any arbitrary axial variations in  $t_w$ ,  $q''$  etc. can be handled.

The general thermal entry length problem with arbitrary axial variations in wall temperature has been considered by [5,13,14]. The same problem with arbitrary axial variations in wall heat flux has been tackled by [5,15,16].

### II.3.1.3 Axial Wall Heat Conduction

Wall heat conduction axially generally lowers the heat transfer coefficient for the duct flow. The importance of taking axial wall heat conduction into account has been realized [4], and some work has been done in this area.

Rotem [17] considered the effect of axial wall heat conduction in the beginning of thermal entrance region. He presented a method for rapid, approximate calculation of both the temperature and film coefficient for two cases of almost isothermal wall and constant heat flux wall.

Davis and Gill [18] analyzed the laminar Poiseuille-Couette flow between parallel plates with finite axial heat

conduction in solid. The Poiseuille flow<sup>5</sup> and Couette flow<sup>6</sup> are special cases of the Poiseuille-Couette flow. They considered the constant axial heat flux at the outside wall boundary. They concluded that the axial conduction in the solid boundary can significantly affect the temperature field in the fluid phase and lower the Nusselt number associated with the heat transfer.

---

<sup>5</sup>Fully developed, steady state, laminar flow of an incompressible fluid through a stationary circular or parallel plate duct is referred to as Poiseuille or Hagen-Poiseuille flow. The viscosity of the fluid is specified as constant, and the body forces are absent. The invariant velocity profile obtained for the Poiseuille flow is parabolic at any cross-section of the duct.

<sup>6</sup>Fully developed, steady state, laminar flow of an incompressible fluid between two parallel plates (one of which is at rest, the other moving at a constant velocity parallel to itself) is referred to as Couette flow. The viscosity of the fluid is assumed as constant, and there are no body forces. The invariant velocity profile obtained for the Couette flow is linear at any cross-section of the duct.

### III. DEFINITIONS AND GENERAL CORRELATIONS

In the previous chapter, appropriate differential equations as well as the boundary conditions were outlined for the laminar flow friction and heat transfer problem for single and multiply connected cylindrical ducts. The friction factor, Nusselt number and other associated dimensionless terms, which are used by an engineer in practice, are defined in this section. Also presented are the relationships between these terms and the solution to the problems formulated in the previous section.

#### III.1 Flow Friction

From an engineering point of view, it is important to know how much power will be needed to flow the fluid through the heat exchanger. The fluid pumping power is proportional to the pressure drop in the fluid across the heat exchanger. The pressure drop in fully developed flow occurs due to the wall shear. While in the developing flow, it occurs due to the wall shear and the change in momentum (flow acceleration) across the two duct sections of interest. Throughout the analysis and result of this report, considerations of abrupt contraction and expansion losses at the duct entrance and exit are omitted as well as form drag and flow acceleration pressure effects due to density changes. In design applications, these factors also have to be considered [4]. Fortunately, these factors are additive for the evaluation of total pressure drop.

The velocity distribution for a given duct geometry is determined from the applicable Eq. (3) or (14). The mean velocity  $u_m$  and the local wall shear stress  $\tau_x$  are then evaluated. They are defined as

$$u_m = \frac{1}{A_c} \int_{A_c} u dA_c \quad (22)$$

For the Newtonian fluid flowing through a circular duct, the local wall shear stress is given by [5]

$$\tau_x = \frac{\mu}{g_c} \left( \frac{\partial u}{\partial r} \right)_{r=a} \quad (23)^7$$

The local wall shear stress for other duct geometries can be expressed similarly for the cartesian coordinate system. Except where more detailed information is needed, the local wall shear stress is consistently defined as average wall shear stress with respect to the perimeter of the duct; e.g. for the axisymmetric flow in a rectangular duct, Fig. 5, at any cross section  $x$ ,

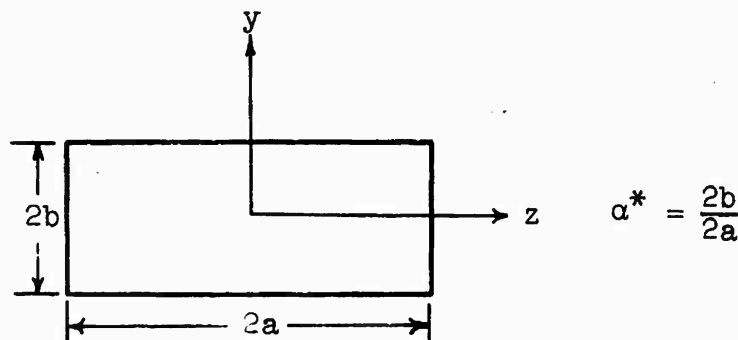


Fig. 5 A cross section of a rectangular duct

$$\tau_x = \frac{\mu}{2g_c(a+b)} \int_{-a}^a \left( \frac{\partial u}{\partial y} \right)_{y=b} dz + \int_{-b}^b \left( \frac{\partial u}{\partial z} \right)_{z=a} dy \quad (24)$$

The local and average Fanning friction factors are subsequently determined. They are defined as

---

<sup>7</sup> The dynamic viscosity coefficient  $\mu$  defined here is the  $g_c$  times the usual fluid dynamics dynamic viscosity coefficient. Hence note that Newton's second law of motion is not invoked in Eq. (23), even though  $g_c$  appears in that equation.

$$f_x = \frac{\tau_x}{\rho u_m^2 / 2 g_c} \quad (25)$$

$$f_{ave} = \frac{\frac{1}{x} \int_0^x \tau_x dx}{\rho u_m^2 / 2 g_c} \quad (26)$$

For constant density flow in the duct of Fig. 1, pressure drop from the section  $x = 0$  to  $x$  can be found by applying Newton's second law of motion and conservation of matter as

$$\frac{\Delta p}{\rho u_m^2 / 2 g_c} = f_{ave} \frac{x}{r_h} + \frac{2}{A_c} \int_{A_c} \left(\frac{u}{u_m}\right)^2 dA_c - 2 \quad (27)$$

where  $f_{ave}$  is given by Eq. (26),  $u$  is the velocity profile at the cross section  $x$ . However, this representation of pressure drop is not useful for engineering calculations because first the  $f_{ave}$  and the velocity profile  $u$  are needed as a function of  $x$  and then the integral must be evaluated. Alternative means of evaluating  $\Delta p$  will be presented in the following subsections.

In addition to the pressure drop and velocity distribution in the entrance region of flow, the knowledge of hydrodynamic entrance length is essential. The hydrodynamic entrance length,  $L_{hy}$ , is defined as the duct length required to achieve the duct centerline (maximum) velocity as 99% of the corresponding fully developed magnitude when the entering flow is uniform.

### III.1.1 Fully Developed Flow

In case of fully developed flow through a duct, the velocity profile is invariant across any flow cross section.

Consequently, the wall shear stress does not change axially, and the average friction factor is the same as the local friction factor for that part of the duct beyond the hydrodynamic entry length. In this case, the constant density flow pressure drop across two flow cross sections separated by a distance  $L$  takes the following form instead of Eq. (27).

$$\frac{\Delta p}{\rho u_m^2 / 2g_c} = f \frac{L}{r_h} \quad (28)^8$$

In fully developed region, Eq. (28) may be rearranged, using the definitions of  $Re$  and  $c_1$ , to

$$fRe = - \frac{c_1 D_h^2}{2u_m} \quad (29)$$

Also, based on the solution of differential equation (3), it can be shown that

$$fRe = K_f \quad (30)$$

where  $K_f$  is a constant dependent on the geometry of the duct cross section, and  $Re$  is the Reynolds number based on hydraulic diameter.

In a long duct, in which fluid enters at a uniform velocity profile, the effect of the entrance region, as men-

---

<sup>8</sup>In the literature, the "large" or Darcy friction factor is also used. It is defined such that

$$f_D = 4f$$

and the right hand side of Eq. (28) becomes  $f_D L/D_h$ .

tioned earlier, is to increase the pressure drop compared to that for the fully developed flow. This increment in pressure drop, designated as  $K(\infty)$ , is defined by

$$\frac{\Delta p}{\rho u_m^2/2g_c} = f_{fd} \frac{L}{r_h} + K(\infty) \quad (31)$$

In heat exchanger analysis, only the knowledge of entrance length and  $f_{fd}$  is sufficient to establish the total pressure drop; a detailed investigation of velocity and pressure distribution in the flow field is not needed. Lundgren et al. [19] devised an approximate analytical method for calculating  $K(\infty)$  for the ducts of arbitrary cross section. They obtained

$$K(\infty) = \frac{2}{A_c} \int_{A_c} \left[ \left( \frac{u_{fd}}{u_m} \right)^3 - \left( \frac{u_{fd}}{u_m} \right)^2 \right] dA_c \quad (32)$$

Thus the fully developed velocity profile ( $u_{fd}/u_m$ ) from the solution of Eq. (3) is needed to evaluate  $K(\infty)$ . The  $f_D$ ,  $Re$  and  $K(\infty)$  were determined for circular tube, elliptical ducts, rectangular ducts, isosceles triangular ducts and the concentric annular ducts in [19]. McComas [20] extended this analysis to approximately determine the hydrodynamic entry length. He assumed Schiller velocity profile [21] but only dealt with the inviscid core, i.e., the flow along the center line of the tube was assumed to be inviscid up to the axial location where the boundary layer had completely filled the duct. He also imposed the condition that the center line was the line of maximum velocity for the fully developed flow. The hydrodynamic entrance length, from his analysis, is given by

$$L_{hy}^+ = \frac{L_{hy}}{D_h Re} = \frac{\left(\frac{u_{max}}{u_m}\right)^2 - 1 - K(\infty)}{f K_f} \quad (33)$$

McComas presented in tabular form the  $L_{hy}$ ,  $(u_{max}/u_m)$ ,  $K(\infty)$  and  $K_f = fRe$  for fully developed laminar flow through circular, elliptical, annular, rectangular and isosceles triangular ducts.

### III.1.2 Hydrodynamically Developing Flow

In the fully developed region, the velocity distribution is obtained from the solution of Eq. (3) with boundary condition of Eq. (4). The friction factor and incremental pressure drop are then determined from Eqs. (25) or (29) and (32) respectively.

In case of hydrodynamically developing flow, the velocity distribution is obtained from the solution of Eqs. (14) and (17) with the boundary and initial conditions of Eqs. (15) and (16). The friction factor and incremental pressure drop are then calculated from the following equations.

As in Eq. (27), the pressure drop from  $x = 0$  to  $x$  is obtained as

$$\frac{\Delta p}{\rho u_m^2/2g_c} = f_{ave} \frac{x}{r_h} + \frac{2}{A_c} \int_{A_c} \left(\frac{u}{u_m}\right)^2 dA_c - 2$$

However, as noted before this representation of pressure drop is operationally not convenient. Therefore, it is presented in the following two ways for engineering calculations:

$$\frac{\Delta p}{\rho u_m^2/2g_c} = f_{app} \frac{x}{r_h} \quad (34)$$

$$\frac{\Delta p}{\rho u_m^2/2g_c} = f_{fd} \frac{x}{r_h} + K(x) \quad (35)$$

These equations define the apparent Fanning friction factor  $f_{app}$  and the pressure drop increment  $K(x)$  due to entrance region. The  $K(x)$  consists of two additive components:

(i) the momentum change between the entrance section  $x = 0$  and the downstream section  $x$ , and (ii) accumulated increment in wall shear between a developing and a fully developed flow. The value of  $K$  increase monotonically from 0 at  $x = 0$  to a constant value in the fully developed region.

The  $f_{app}$ ,  $K(x)$  and  $L_{hy}^+$ , based on the solution of Eq. (14) are found to have the functional form as follows.

$$f_{app} = f_{app}\left(\frac{x}{D_h Re}\right) \quad (36)$$

$$K(x) = K\left(\frac{x}{D_h Re}\right) \quad (37)$$

$$L_{hy}^+ = \frac{L_{hy}}{D_h Re} = \text{constant (depending on duct geometry)} \quad (38)$$

If the boundary layer assumptions are not invoked, but rather complete Navier-Stokes equations are solved, the functional forms are found as

$$f_{app} = f_{app}\left(\frac{x}{D_h Re}, Re\right) \quad (39)$$

$$K(x) = K\left(\frac{x}{D_h Re}, Re\right) \quad (40)$$

$$L_{hy}^+ = L_{hy}^+(Re) \quad (41)$$

### III.2 Heat Transfer

For the duct fluid flow problem involving heat transfer, wall heat flux  $q''$  and fluid and wall temperatures are required. If the fluid inlet conditions are given, the outlet

conditions can be determined, if the wall heat flux distribution is known along with the flow path geometry. Alternatively, if the inlet and outlet conditions are known, the length of the duct (or a heat exchanger) of a given cross sectional geometry can be determined from the wall heat flux distribution. The formulae for  $q''$  and other related heat transfer parameters follow.

The peripheral average heat flux at the wall for a fluid flowing through a duct is given by Fourier's law of heat conduction as

$$q'' = -k(\nabla t)_{w,m} \quad (42)$$

This equation is the rate equation for the conduction heat transfer. Considering the general case of nonuniform peripheral heating, the mean temperature gradient at the wall in Eq. (42) is obtained by averaging with respect to the periphery  $\Gamma$  of the duct.

The convection rate equation, defining the heat transfer conductance is

$$q'' = h(t_{w,m} - t_m) \quad (43)$$

where  $t_{w,m}$  and  $t_m$  are the mean temperature of wall and bulk mean temperature of the fluid respectively, defined as

$$t_{w,m} = \frac{1}{P} \int_{\Gamma} t_w ds \quad (44)$$

$$t_m = \frac{1}{A_c u_m} \int_{A_c} u t dA_c \quad (45)$$

In a thermal circuit representation such as Fig. 4,  $1/h$  signifies a thermal resistance between  $t_{w,m}$  and  $t_m$  potentials. In some of the solutions outlined in Chapter V, the  $h$  will

be either infinity or negative. This means the temperature difference ( $t_{w,m} - t_m$ ) is either zero or negative even though the heat flux is finite and directed into the fluid.

From Eqs. (42) and (43), the wall heat flux is given by

$$q'' = -k(Vt)_{w,m} = h(t_{w,m} - t_m) \quad (46)$$

Once the temperature field is known,  $(Vt)_{w,m}$  can be evaluated and  $h$  can be determined from Eq. (46).

In case of  $\textcircled{R1}$  boundary condition, the overall heat transfer coefficient  $U_o$  is of primary practical importance. The  $U_o$  is defined from

$$q'' = U_o(t_a - t_m) \quad (47)$$

where from Fig. 4,

$$\frac{1}{U_o} = \frac{1}{h_{R1}} + \frac{1}{U_w} \quad (48)$$

The laminar flow heat transfer results are generally correlated in terms of dimensionless heat transfer modulus, the Nusselt number, defined as

$$Nu = \frac{hD_h}{k} \quad (49)$$

where  $D_h$  is the hydraulic diameter of flow passages based on the flow wetted perimeter. In case of  $\textcircled{R1}$  boundary condition, the overall Nusselt number, defined as

$$Nu_o = \frac{U_o D_h}{k} , \quad (49a)$$

is operationally convenient. In absence of thermal energy sources, viscous dissipation and axial heat conduction within

the fluid, the fully developed laminar flow Nusselt number is found to be a constant, independent of  $x$ ,  $\text{Pr}$  and  $\text{Re}$  but depending upon the duct cross section and the boundary conditions of Table 1. Clearly it is more convenient to present the Nusselt number rather than other dimensionless heat transfer modulus such as  $St$  which does depend on  $\text{Re}$  and  $\text{Pr}$ . Note that from the definition of individual moduli

$$\text{Nu} = \text{St Re Pr}$$

The Nusselt number can also be presented in terms of the fluid bulk mean temperature gradient along the flow length. In absence of the thermal energy sources, viscous dissipation, and fluid axial heat conduction, an energy balance on the duct length  $\delta x$  will yield

$$q''P \delta x = (\rho A_c u_m) c_p \frac{dt_m}{dx} \delta x \quad (50)$$

Combining Eqs. (43), (49) and (50) with the definition of hydraulic diameter,

$$\text{Nu} = \frac{D_h^2 u_m}{4\alpha(t_{w,m} - t_m)} \frac{dt_m}{dx} \quad (51)$$

This result will be useful later in the discussion of Section V.4.1.2.2.

For fully developed turbulent flow in cylindrical passages, the heat transfer data are well correlated by plotting a Colburn factor (a counterpart of the friction factor) versus Reynolds number for the moderate Prandtl number range ( $0.5 \leq \text{Pr} \leq 10$ ). This correlation is not strongly dependent on passage cross section geometry, provided that the characteristic dimension used in  $\text{Re}$  is the hydraulic diameter. The Colburn factor  $j$  is defined as

$$j = St \Pr^{2/3} = \frac{Nu}{Re} \Pr^{-1/3} \quad (52)$$

To be consistent with turbulent flow correlations and because  $St$  is more closely related to the  $N_{tu}$ , a convenient design parameter, the laminar flow heat transfer design data for heat exchangers are also presented in terms of  $j$  versus  $Re$  plot. With Prandtl number as a constant and for fully developed laminar flow, Eq. (52) becomes

$$jRe = K_h (= Nu\Pr^{-1/3}), \text{ a constant} \quad (53)$$

The similarity of Eqs. (30) and (53) is of interest.

For the  $(R_l)$  boundary condition, the dimensionless wall thermal resistance is defined as the ratio of wall thermal resistance to the pure conductive fluid thermal resistance for a conduction path length  $D_h$ , i.e.

$$R_w = \frac{1/U_w}{D_h/k} = \frac{k}{U_w D_h} \quad (54)$$

The reciprocal of  $R_w$  has been called variously the wall Nusselt number and the wall Biot number in the literature. But as  $1/R_w$  does not have the usual physical significance assigned either to Nusselt number or Biot number, this unfortunate terminology should be replaced. The wall thermal resistance parameter  $R_w$ , which does have a simple physical significance of its own, is used for this purpose.

### III.2.1 Fully Developed Flow

As discussed earlier, in fully developed flow, an invariant nondimensional axial temperature profile results for the previously described wall temperature boundary conditions. The temperature profile, solution of Eq. (5), can be described in a closed form for simple geometries or de-

terminated by other methods discussed in the next chapter. Knowing the temperature distribution, the  $h$  and hence  $Nu$  are determined from Eqs. (46) and (49).

(a) T Boundary Condition. The Nusselt number for fully developed, laminar flow heat transfer is found to be a function of  $Pe$ .

$$Nu_T = Nu_T( Pe ) \quad (55)$$

Here  $Pe$ , the Féclét number, is associated with the effect of axial heat conduction within the fluid. Hennecke [22] shows that for  $Pe > 50$ , the axial fluid heat conduction can be neglected, and  $Nu_T$  is a constant as a consequence. The effect of thermal energy sources and viscous dissipation on  $Nu_T$  has not been investigated.

(b) H1 and H2 Boundary Condition. The fully developed laminar flow Nusselt number for these boundary conditions is expressed in the following functional forms.

$$Nu_{H1} = Nu_{H1} \left( \frac{SD_h}{q}, \eta \right) \quad (56)$$

$$Nu_{H2} = Nu_{H2} \left( \frac{SD_h}{q}, \delta \right) \quad (57)$$

where  $SD_h/q$  and  $\eta$  (or  $\delta$ ) represent respectively the effect of uniform intensity thermal energy sources and the viscous dissipation in the fluid. For these thermal boundary conditions, the axial heat conduction within the fluid is constant, and consequently does not affect the Nusselt number. Tyagi [23, 24, 25, 26] concludes that if  $|\eta|$  or  $|\delta| \geq 0.1$ , the effect of viscous dissipation is significant. Cheng [27] concludes that the effect of viscous dissipation is greatest for the circular duct, decreases for the regular polygonal

duct with decreasing number of sides, and is least for the equilateral triangular duct.

(c) H3 Boundary Condition. For finite peripheral wall heat conduction, the Nusselt number is a function of the peripheral conduction parameter  $K_p$ .

$$Nu_{H3} = Nu_{H3}(K_p) \quad (58)$$

(d) H4 Boundary Condition. For exponential wall heat flux boundary condition, Eq. (10), the Nusselt number is a function of the exponent  $\lambda$ .

$$Nu_{H4} = Nu_{H4}(\lambda) \quad (59)$$

when the effect of fluid axial heat conduction, thermal energy sources and viscous dissipation is neglected.

(e) R1 Boundary Condition. For finite thermal resistance at the wall, the fully developed laminar flow Nusselt number is found as

$$Nu_{R1} = Nu_{R1}(R_w, Pe) \quad (60)$$

where the effect of axial heat conduction in the fluid is represented by the dependency on Péclet number,  $Pe$ . The effect of thermal energy sources and viscous dissipation is not investigated so far.

(f) R2 Boundary Condition. For the non-linear radiant flux boundary condition, the fully developed laminar flow Nusselt number is found as a function of  $\gamma$ .

$$Nu_{R2} = Nu_{R2}(\gamma) \quad (61)$$

where  $\gamma = \epsilon_w \sigma T_e^3 D_h / k$ .

### III.2.2 Thermally Developing Flow

In developing temperature profile case, the solution of Eq. (19), the fluid temperature distribution is obtained by one of the methods outlined in the next chapter for a given boundary condition. Knowing the temperature distribution, the dimensionless heat transfer characteristics for a given duct under specified boundary condition is analytically correlated by either of the following two methods: (i) generally accepted and well-known Nusselt number correlation, and (ii) recently proposed [28] dimensionless temperature correlation. It will be shown that the recently proposed correlation is an extension of the Nusselt number correlation. These correlations, specifically for  $(T)$  and  $(\dot{m})$  boundary conditions, will be described below.

In addition, the knowledge of thermal entrance length is essential. The thermal entrance length,  $L_{th}$ , is defined as the duct length required to achieve the value of local Nusselt number  $Nu_x$  as  $1.05 Nu_{fd}$ . The local Nusselt number is defined as

$$Nu_x = \frac{h_x D_h}{k} \quad (62)$$

where the local heat transfer coefficient is defined the same way as in Eq. (43)

$$h_x = \frac{q''_x}{t_{w,m} - t_m} = \frac{-k(\nabla t)_{w,m}}{t_{w,m} - t_m} \quad (63)$$

In case of uniform peripheral surface temperature,  $t_{w,m} = t_w$ , and  $(\nabla t)_{w,m} = (\nabla t)_w$ .

The local Nusselt number depends upon the axial distance from the point where heating (or cooling) started. The dimensionless axial distance is defined as

$$x^* = \frac{x}{D_h Pe} = \frac{x}{D_h Re Pr} \quad (64)$$

With this choice of  $x^*$ , the energy equation for the Graetz problem<sup>9</sup> becomes parameter free. Throughout the thermal entrance heat transfer literature, the  $x^*$  or  $1/x^*$  is designated as the Graetz number. McAdams [29] defines the Graetz number quite differently as  $Gz = Wc_p/kL = PeP/4L$ . To avoid the confusion of the definition of Graetz number, the  $x^*$  will be used as the dimensionless axial distance. The  $x^+$  defined by Kays [5] is simply related to  $x^*$  as  $x^+ = 2x^*$ .

First the case of fully developed velocity profile and developing temperature profile will be considered. Next the combined entry length problem will be discussed.

### III.2.2.1 Hydrodynamically Developed Flow

#### (a) T Boundary Condition

In this case, fluid bulk mean temperature distribution, the local and total wall heat flux are unknown. Knowing one of these three unknowns, the required heat transfer surface area and remaining unknowns can be determined. For this purpose, two different ways of correlation have been proposed: (i) Nusselt number correlation, (ii) dimensionless temperature correlation.

(i) Nusselt Number Correlation. Based on the solution of Eq. (19), the local and mean Nusselt numbers are presented as a function of the dimensionless distance  $x^*$ . The local Nusselt number is defined by Eq. (62). The mean Nusselt number is defined as

$$Nu_m = \frac{h_m D}{k} \quad (65)$$

$$h_m = \frac{1}{x} \int_0^x h_x dx \quad (66)$$

---

<sup>9</sup>The Graetz problem is described in Chapter V, Section 1.3.1.

In absence of axial heat conduction, viscous dissipation and the thermal energy sources within the fluid, based on the simple energy balance, Eqs. (50) and (66), it can be shown, for uniform inlet fluid temperature  $t_e$ , that

$$\epsilon = \frac{t_m(x) - t_e}{t_w - t_e} = 1 - \exp\left(-\frac{h_m P x}{W c_p}\right) = 1 - e^{-N_t u} \quad (67)$$

By multiplying numerator and denominator on the left hand side of Eq. (67) by  $W c_p$ , it can be interpreted as the ratio of the actual heat transferred in distance  $x$  to thermodynamically maximum possible heat transfer. This ratio is referred to as the effectiveness,  $\epsilon$ , of the heat exchanger [4]. If the fluid bulk mean temperature  $t_m$  at outlet ( $x=L$ ) of the duct is known,  $h_m L$  can be determined from Eq. (67). From the known solution  $Nu_m = Nu_m(x^*)$ , by iteration the length  $L$  and hence the heat transfer area can be calculated. As  $h_m$  does not vary much except very close to inlet, only two iterations would suffice in practice. If the heat transfer area  $A$  is known,  $t_m$  can be calculated directly from Eq. (67). The total wall heat flux from  $x=0$  to  $x$  is

$$q = W c_p \epsilon (t_w - t_e) = W c_p (t_m - t_e) \quad (68)$$

Alternatively,

$$q = P \int_0^x q''_x dx \quad (69)$$

by manipulation of Eqs. (65), (68) and (69), it can be shown that

$$q = h_m A (\Delta t)_{\text{lm}} \quad (70)$$

where

$$(\Delta t)_{lm} = \frac{[t_w - t_e] - [t_w - t_m(x)]}{\ln \frac{t_w - t_e}{t_w - t_m}} \quad (71)$$

However, when the axial heat conduction within the fluid is considered, a simple relationship of Eq. (67) or (68) does not result. The local Nusselt number is defined by Eq. (62) as before. The total wall heat transfer rate cannot be calculated based on the mean Nusselt number defined previously, Eq. (65). Instead, the dimensionless total wall heat flux  $\Phi$  defined as follows is determined and presented as a function of the dimensionless distance  $x^*$ .

$$\Phi = \frac{qD_h}{kA(t_w - t_e)} \quad (72)$$

and is evaluated from

$$\Phi = \frac{D_h}{k(t_w - t_e)} \frac{1}{x} \int_0^x q''_x dx \quad (72a)$$

where  $q''_x$  is given by Eq. (63). Note that inappropriately this dimensionless wall heat transfer rate  $\Phi$  has been termed a mean Nusselt number in [22] and [30]. The "mean heat transfer coefficient" in  $\Phi$  does not represent a thermal conductance in a thermal circuit for a heat exchanger nor does it approach to the fully developed value at large  $x^*$  (when  $x^* \rightarrow \infty$ ).

If the effect of axial heat conduction in the fluid is considered in the energy balance, Eq. (50), it can be shown that the Eq. (67) transforms to

$$\mathcal{E} = 1 - \phi(x^*, Pe)e^{-N_{tu}} \quad (73)$$

where  $\phi(x^*, Pe)$  is designated as the effectiveness coefficient by Stein [30a]. But in Eq. (73), the  $N_{tu}$  is defined based on the  $h_m$  rather than the  $h_x$  as is done by Stein [30a].

The energy transfer terms and the qualitative fluid bulk mean temperature distribution are shown in Fig. 6, when the axial heat conduction within the fluid is present. The dotted line in Fig. 6 represents the fluid bulk mean temperature distribution when the fluid axial heat conduction

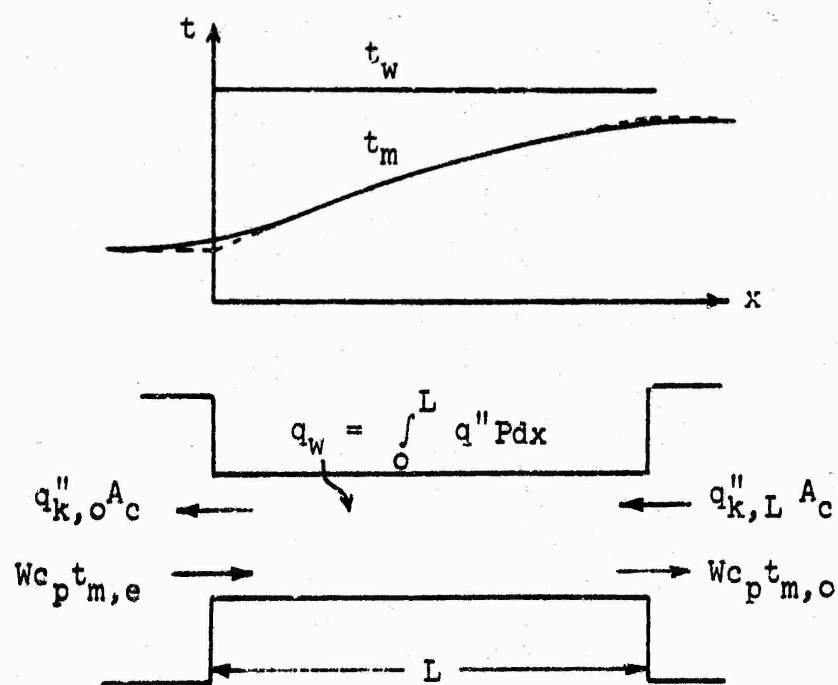


Fig. 6 Energy transfer terms and temperature distribution with the fluid axial heat conduction

is not present. The fraction energy content of the fluid is defined as that fraction of heat transfer that is not conducted away from the fluid. Algebraically,

$$\text{fraction energy content of the fluid} = \frac{W_c p (t_{m,o} - t_{m,e})}{q_w} \quad (74)$$

To determine the wall heat flux, in addition to the knowledge of  $\epsilon$ , the fraction energy content of the fluid is needed, so that the energy conducted away from the fluid can be calculated.

Thus to apply the conventional heat exchanger design theory [4], when the effect of fluid axial heat conduction is considered, the solution to the  $\Theta$  heat transfer problem should include  $Nu_{x,T}$ ,  $Nu_{m,T}$  or  $\Phi$  and  $\phi$  or the energy content of the fluid as functions of  $x^*$  and  $Pe$  for each duct geometry. The thermal entry length for a given duct geometry, in this case, has the functional form

$$L_{th}^* = L_{th}^*(Pe) . \quad (75)$$

According to Hennecke [22], the effect of fluid axial heat conduction may be neglected for  $Pe > 50$  and  $x^* \geq 0.01$ .

(ii) Dimensionless Temperature Correlation. This method is recently proposed by Baehr and Hicken [28]. The local dimensionless fluid bulk mean temperature is presented as function of  $x^*$ .

$$\vartheta_m(x^*) = \frac{t_m(x^*) - t_e}{t_w - t_e} = 1 - \exp[-B_1 \sqrt{x^*} - B_2 x^*] \quad (76)$$

where they have tabulated, the constants  $B_1$  and  $B_2$  for the circular tube and rectangular duct of  $x^* = 0, 0.1, 0.2, 0.5$  and  $1$ . It can be shown that the dimensionless local wall heat flux is

$$\frac{q'' D_h}{k(t_w - t_e)} = \Phi(x) = \frac{1}{\pi} \frac{d\vartheta_m}{dx^*} \quad (77)$$

$$= \frac{1}{4} \left( \frac{B_1}{2\sqrt{x^*}} + B_2 \right) \exp(-B_1 \sqrt{x^*} - B_2 x^*)$$

Introducing approximations, Baehr and Hicken have inverted Eq. (76) so that

$$x^* = x^*(\vartheta_m) \quad (78)$$

In design application using this correlation, if the fluid exit bulk mean temperature,  $t_m$ , is given, the  $x^*$  and hence the heat transfer surface area can be explicitly calculated from Eq. (78). Alternatively, if the heat transfer area is specified, then the fluid exit temperature can be evaluated from Eq. (76). So it appears that this method is operationally useful compared to Nusselt number correlation. However, the comparison of Eqs. (67) and (76) reveals that

$$\epsilon = \vartheta_m \quad (79)$$

$$N_{tu} = 4x^* \text{Nu}_{m,T} = B_1 \sqrt{x^*} + B_2 x^* \quad (80)$$

$$\text{or} \quad \text{Nu}_{m,T} = \frac{B_2}{4} + \frac{B_1}{4\sqrt{x^*}} \quad (81)$$

So that the conventional  $\text{Nu}_{m,T}(x^*)$  is approximated by the above best fit curve and the constants  $B_1$  and  $B_2$  are determined. Consequently, it appears that the proposed new correlation is just an extension of the conventional Nusselt number correlation. The  $\text{Nu}_{x,T}$  and  $\vartheta_m$  are related as follows.

$$\text{Nu}_{x,T} = \frac{1}{4} \frac{d\vartheta_m}{dx^*} \frac{1}{1-\vartheta_m} = \frac{B_2}{4} + \frac{B_1}{8\sqrt{x^*}} \quad (82)$$

The correlation method of Eq. (76) is essentially the  $\epsilon-N_{tu}$  approach [4] for the heat exchanger with  $C_{min}/C_{max} = 0$ . Baehr and Hicken compared their scheme with the  $(\Delta t)_{lm}$

approach and showed that their proposed procedure is operationally more convenient than the  $(\Delta t)_{\text{bm}}$  approach for the calculations of heating surfaces from heat transfer area. This view is also supported in [4].

(b) H1 Boundary Condition

In this case, the axial wall and fluid bulk mean temperature distribution is unknown. Two quite similar ways of correlation have been proposed for this purpose.

(i) Nusselt Number Correlation. Based on the solution of energy equation (19), the local Nusselt number is presented as a function of  $x^*$ ,

$$\frac{h_x D}{k} = \text{Nu}_{x,H1} = \text{Nu}_{x,H1}(x^*) \quad (83)$$

The local heat flux  $q''_x$  and total heat transfer rate  $q$  (from  $x = 0$  to  $x$ ) are given by

$$q''_x = h_x [t_w(x) - t_m(x)] = \text{constant} \quad (84)$$

$$q = \int_0^x q''_x dA = q''_x A \quad (85)$$

$$q = Wc_p [t_m(x) - t_e] \quad (86)$$

From these four equations (83) through (86), the total heat transfer rate, heat transfer area or terminal temperature can be calculated, when any one is unknown. There is no need to evaluate the mean heat transfer coefficient. It is also interesting to note that the dimensionless temperature ratio, similar to the effectiveness  $\epsilon$  and  $\vartheta_m$  in case of  $\textcircled{T}$ , is dependent on  $h_x$  only as it can be easily shown that

$$\frac{t_m(x) - t_e}{t_w(x) - t_e} = \frac{N_{tu,x}}{1 + N_{tu,x}} \quad (87)$$

where

$$N_{tu,x} = \frac{h_x P x}{W c_p}$$

However, in a heat exchanger having approximately  $H_1$  boundary condition (e.g. counterflow heat exchanger, although it has close to  $H_3$  boundary condition), an overall conductance  $U_o$  is needed. In this case, the mean heat transfer coefficient on each side of the heat exchanger is needed and it can be determined from

$$h_{m,H1} = \frac{1}{x} \int_0^x h_{x,H1} dx \quad (88)$$

Alternatively, for operational convenience the  $Nu_{m,H1}$  can be evaluated as a function of  $x^*$  for the given duct cross section. In this case, the total heat transfer rate is related to  $h_{m,H1}$  from  $Nu_{m,H1}$  as

$$q = h_{m,H1} A (\Delta t)_{ave} \quad (89)$$

where

$$(\Delta t)_{ave} = \left[ \frac{1}{x} \int_0^x \frac{1}{t_w(x) - t_m(x)} dx \right]^{-1} \quad (90)$$

Before proceeding to the second correlation scheme, the effect of fluid axial heat conduction may be mentioned. The functional relationship is found as

$$Nu_{x,H1} = Nu_{x,y1}(x^*, Pe) \quad (91)$$

$$L_{th,H1}^* = L_{th,H1}^*(Pe) \quad (92)$$

Similar relationship holds for  $Nu_{m,H1}$ . The effect of fluid axial heat conduction is smaller for  $\textcircled{H1}$  boundary condition in comparison to  $\textcircled{T}$  boundary condition. According to Hennecke [22], the effect of axial heat conduction may be neglected for the fluids with  $Pe > 10$  for  $x^* \geq 0.01$ .

(ii) Dimensionless Temperature Correlation. This method has been recently proposed by Baehr and Hicken [28]. The dimensionless temperature is presented as a function of  $x^*$  and its fully developed value, i.e.,

$$\theta_{w-m}(x^*) = \theta_{w-m}(\infty) [1 - \exp(-B_1 \sqrt{x^*} - B_2 x^*)] \quad (93)$$

where

$$\theta_{w-m}(x) = \frac{t_w(x) - t_m(x)}{q_x'' D_h / k} \quad (94)$$

Along with this, Eqs. (85) and (86) are used to determine the heat transfer rate, heat transfer area or terminal temperatures. Baehr and Hicken [28] tabulated the values of  $\theta_{w-m}(\infty)$ , and the constants  $B_1$  and  $B_2$  for the circular tube and parallel plates.

The  $\theta_{w-m}$  and  $Nu_{x,H1}$  correlations methods are essentially the same since from Eqs. (84) and (94) it follows that

$$\theta_{w-m}(x) = \frac{1}{Nu_{x,H1}} \quad (95)$$

### (c) $\textcircled{H2}$ Boundary Condition

The local Nusselt number and the thermal entrance length are correlated in the following functional form.

$$Nu_{x,H2} = Nu_{x,H2}(x^*, Pe) \quad (96)$$

$$L_{th,H2}^* = L_{th,H2}^*(Pe) \quad (97)$$

Similar relationship holds for  $Nu_{m,H2}$ . The Pe number is associated with the effect of fluid axial heat conduction, which has not been investigated yet for  $\textcircled{H2}$  boundary condition.

(d)  $R_1$  Boundary Condition

In this case,

$$Nu_{x,R1} = Nu_{x,R1}(x^*, R_w, Pe) \quad (98)$$

$$L_{th,R1}^* = L_{th,R1}^*(R_w, Pe) \quad (99)$$

and similar relationship holds for  $Nu_{m,R1}$ , where Péclét number is associated with the influence of fluid axial heat conduction.

(e)  $R_2$  Boundary Condition

The local Nusselt number and thermal entry length are presented as

$$Nu_{x,R2} = Nu_{x,R2}(x^*, \gamma) \quad (100)$$

$$L_{th,R2}^* = L_{th,R2}^*(\gamma) \quad (101)$$

where  $\gamma$  is the radiation parameter,  $\epsilon_w \sigma T_e^3 D_h / k$ .

### III.2.2.2 Simultaneously Developing Flow

For simultaneously developing velocity and temperature profile, the Prandtl number becomes an additional parameter influencing the Nusselt number. While the velocity

development is independent of Prandtl number, the temperature development is dependent on Prandtl number. Hence, when the axial heat conduction, thermal energy sources and viscous dissipation within the fluid are neglected, the thermal entrance Nusselt number for  $\textcircled{T}$ ,  $\textcircled{H1}$  and  $\textcircled{H2}$  boundary conditions is given by

$$Nu_x = Nu_x(x^*, Pr) \quad (102)$$

If the axial thermal conduction within the fluid is considered as in the case of liquid metals,

$$Nu_x = Nu_x(x^*, Pr, PrRe) \quad (103a)$$

or

$$Nu_x = Nu_x(x^*, Pr, Re) \quad (103b)$$

For  $\textcircled{R1}$  and  $\textcircled{R2}$  boundary conditions, additional parameters  $R_w$  and  $\gamma$  appear respectively in the above equations.

The fully developed velocity profile with developing temperature profile case considered in Section III.2.2.1 is a special case of simultaneous development of velocity and temperature profiles with  $Pr = \infty$ .

#### IV. GENERAL METHODS

The governing differential equations and the associated boundary conditions for the laminar velocity and temperature profiles for the duct flow are outlined in Chapter II. The various definitions and general correlation schemes viewed from an engineering point are described in Chapter III. In this chapter, the general methods used in the heat transfer literature are presented to solve the problems formulated in Chapter II and arrive at the dimensionless parameters of Chapter III.

##### IV.1 Fully Developed Flow

Hydrodynamically and thermally fully developed laminar flow friction and heat transfer solutions are obtained by the following eight methods.

(1) Exact or Approximate Solutions by Analogy Method. Marco and Han [31] and Cheng [32] pointed out that the following four Dirichlet problems are related to each other:

- a. Torsion of prismatical bars
- b. Fully developed laminar flow
- c. Uniformly loaded, simply supported polygonal plates
- d. Fully developed laminar heat transfer

Considering (a) and (b), the stress function in torsion theory [33] has the identical differential equation and boundary condition as that of the laminar velocity field for the duct flow. Hence, based on the known solutions of torsion of prismatical bars, the velocity distribution and  $fRe$  can be determined, as is done for the case of rectangular and moon shaped ducts in this report.

Consider (c) and (d), the governing differential equation is fourth order for the small deflection of thin polygonal plates, under uniform lateral load and simply supported along

all edges [34]. This differential equation and the associated boundary conditions for the thin plate problem are identical to the  $H_1$  laminar temperature field in the duct flow, provided that the axial heat conduction, thermal energy sources and viscous dissipation within the fluid are neglected. For the plates with curvilinear boundaries, the adjustment of Poisson's ratio is required so that the boundary condition of nonslip flow may be satisfied [31,32]. As noted in Section II.1.2, the solution to a fourth order differential equation for the  $H_1$  temperature problem will simultaneously provide the solution for the velocity problem. Consequently, based on the known solutions of the thin plate problem, the  $H_1$  temperature and velocity distributions,  $Nu_{H_1}$  and  $fRe$  can be determined. The  $Nu_{H_1}$  for rectangular, equilateral triangular, right angled isosceles triangular, semicircular [31], and circular sector [6] ducts were evaluated by this method.

As mentioned above, knowing the solution of thin plate problem,  $fRe$  and  $Nu_{H_1}$  as well as velocity, stress, and temperature distribution etc. can be calculated. Cheng [32, 35] has shown how to apply the Moiré and point matching methods (used to obtain approximate solutions for the thin plate problem) for the laminar  $H_1$  heat transfer problem.

(2) Exact Solutions by the Method of Complex Variables. This method is limited to the cases where the velocity and temperature fields are deducible directly from the equations of the boundary curves such as equilateral triangular and elliptical ducts. Only the  $H_1$  boundary condition is considered by Tao [36]. Sastry [37] applied Tao's method [36] to confocal ellipses for the  $H_1$  boundary condition.

(3) Exact or Approximate Solutions by Conformal Mapping. Any duct cross section which can be mapped exactly or approximately, by conformal transformation, onto a unit circle

can be analyzed by this method. Tao has considered the cardioid duct [38,39], hexagonal duct [38] and Pascal's limacon [39] for  $H_1$  boundary condition, and cardioid duct [40] for  $H_2$  boundary condition. Tao, in his analysis, included the effect of thermal energy sources, but neglected the effect of viscous dissipation, gas compression work and the axial heat conduction within the fluid. Sastry applied Tao's method [39] for curvilinear polygonal ducts [41] for the  $H_1$  boundary condition. Sastry [42] also considered the general power series mapping function; and presented the formulae for  $u$ ,  $u_m$ ,  $t$ ,  $t_m$ ,  $q''$  and  $Nu$  for the  $H_1$  boundary condition. Examples were worked out for cardioid and ovaloid cross sectional ducts. Tyagi extended Tao's work by including the effect of viscous dissipation for the  $H_1$  boundary condition [23] for equilateral triangular and elliptical ducts and  $H_2$  boundary condition [24] for the cardioid duct. Tyagi also extended Tao's work by including viscous dissipation and gas compression work for the  $H_1$  [25] and  $H_2$  [26] boundary conditions for the cardioid duct.

Cesarella et al. [43] proposed an approximate conformal mapping technique for the thermal entrance  $Nu_{x,T}$  through the duct of arbitrary cross section with  $T$  boundary condition. As an asymptote,  $Nu_T$  can be calculated from the results for  $Nu_{x,T}$ . Only the slug flow solutions and the Graetz problem were solved [43].

(4) Approximate Solutions by Finite Difference Method. The differential momentum and energy equations are put into the finite difference form, and the solution is carried out by hand or by a digital computer using standard techniques such as relaxation, Gaussian elimination etc. Clark and Kays [44] employed the relaxation technique and obtained  $Nu_T$  and  $Nu_{H1}$  for rectangular ducts and the equilateral triangular duct. Schmidt and Newell [45] employed the

Gaussian elimination technique with an iterative refinement and obtained  $Nu_T$  and  $Nu_{H1}$  for rectangular and isosceles triangular ducts. Lyczkowski et al. [11] utilized the extended Dufort-Frankel method and determined  $Nu_T$  for rectangular ducts and  $Nu_{H3}$  for the square duct. Sherony and Solbrig [46] also used the Dufort-Frankel method and evaluated  $fRe$  and  $Nu_T$  for the sine duct. Dwyer and Berry [47] employed the Gaussian elimination method and determined  $Nu_{H2}$  for longitudinal laminar flow over a rod bundle arranged in an equilateral triangular array.

Methods (5) and (6) described below are powerful, computationally fast, and accurate to any desired degree for the  $(H1)$  and  $(H2)$  boundary conditions, hence are now preferred over numerical finite difference method.

### (5) Approximate Closed Form Solutions by the Point

Matching Method. After an appropriate change of dependent variables, the momentum and energy equations can be represented as two-dimensional Laplace equation. The general solution to this equation is obtained by a linear combination of harmonic functions in form of an infinite series. This series is truncated at finite number of terms  $n$ . The  $n$  points are selected on the periphery  $\Gamma$  either equidistance or equiangular. The boundary condition is satisfied at these  $n$  pre-chosen points exactly to determine the  $n$  unknown coefficients of the truncated series. The velocity of temperature distribution is then obtained in a closed form series with these coefficients. The  $(H1)$  and  $(H2)$  are the only boundary conditions treated to date by the point-matching method. The limitations of the point-matching method are discussed by Sparrow in Cheng's paper [32]. The well known algebraic-trigonometric polynomials, obtained by the general solution of Laplace equation by the separation of variables method, were employed in the following cases: the  $fRe$  and  $Nu_{H1}$  for the longitudinal flow over cylinders arranged in

arrays by Sparrow et al. [48,49], the fRe for isosceles triangular ducts by Sparrow [50], the fRe ,  $Nu_{H1}$  and  $Nu_{H2}$  for the regular polygonal ducts by Cheng [51,52], the fRe for the cusped, regular polygonal, equilateral triangular, elliptical and rectangular ducts by Shih [53], the fRe and  $Nu_{H1}$  for the regular polygonal ducts with a central circular core by Cheng and Jamil [54], the  $Nu_{H1}$  for eccentric annuli by Cheng and Hwang [55] and fRe and  $Nu_{H1}$  for cylindrical ducts with central regular polygonal cores by Cheng and Jamil [56]. The linear combination of polynomial harmonic functions, the real and imaginary parts of the analytical function  $(x + iy)^n$  where n is an integer, were used to calculate fRe ,  $Nu_{H1}$  and  $Nu_{H2}$  for the circular segment duct by Sparrow and Haji-Sheikh [57] and the fRe and  $Nu_{H1}$  for circular ducts with diametrically opposite flat sided duct by Cheng and Jamil [56].

(6) Approximate Closed Form Solutions by Least-Square-Fitting of Harmonic Functions. This method differs from the point-matching method that more than n points (usually 2n to 3n points) along the boundary are employed to determine n unknown coefficients in the truncated series harmonic function solution for the Laplace equation. The coefficients of the series are evaluated numerically by the least square fit. Thus, the exact fit to these pre-chosen points is sacrificed in favor of a better fit to the boundary as a whole. The fRe were obtained by this method for regular polygonal ducts with circular centered core by Ratkowsky and Epstein [58] and for the circular ducts with regular polygonal centered cores by Hagan and Ratkowsky [59]. Shah [60] obtained fRe ,  $K(\infty)$  ,  $Nu_{H1}$  and  $Nu_{H2}$  for rectangular, isosceles triangular, sine and equilateral triangular ducts with rounded corners. The algebraic-trigonometric polynomials were employed for the solution of Laplace equation in [58, 59, 60].

(7) Approximate, Variational Methods. A variational method for fully developed laminar flow in non-circular ducts was proposed by Sparrow and Siegel [61] for the  $H_1$  and  $H_2$  boundary conditions. Examples were worked out for the square duct, rectangular duct with  $\alpha^* = 0.1$  and a circular sector duct. Gupta [62] formulated a variational approach for the laminar heat transfer with  $H_1$  boundary condition with the fluid axial heat conduction included. Stewart [63] determined the accuracy of variational flow calculations by applying a reciprocal variational principle, with the example of a square duct. A variational approach for  $T$  boundary condition was presented by Pnueli [64], where the upper and lower bounds for Nusselt numbers were obtained for the circular and square duct.

Finlayson and Scriven [65] discussed and critically reviewed the different variational methods used for the transport and transformation processes. They concluded that the different methods used in the literature did not possess the advantages associated with the genuine variational principles, and no general variational principle can be devised for the transport and transformation processes. They showed that the variational methods of approximation, used in the literature, were equivalent to the more straight forward Galerkin method or another closely related version of weighted residuals.

(8) Approximate Method for Very Small Aspect Ratio Ducts. MacLaine-Cross [66] presented an approximate method for calculating fully developed laminar flow  $f_{Re}$ ,  $Nu_{H1}$ , and  $K(\infty)$  for the ducts with low height-to-width ratio and without abrupt variations in height across their width. The method is similar to the one used for torsion of a narrow rectangular bar by Timoshenko and Goodier [33]. In the limit, the  $f_{Re}$ ,  $Nu_{H1}$  and  $K(\infty)$  approach the cor-

responding values for parallel plates. An example was worked for hexagonal duct with a low height-to-width ratio.

James [67] outlined a simple method to determine the fully developed  $Nu_T$  for the narrow ducts (of low aspect ratio). As an example, he calculated  $Nu_T$  for an elliptical duct of  $\gamma^* = 0$ .

#### IV.2 Hydrodynamic Developing Flow

For the hydrodynamic entry length problem, five methods have been used to solve Eq. (14) which incorporates the boundary layer type idealizations of Eq. (13). Numerical methods are used exclusively for the complete Navier-Stokes equations. The methods for the boundary layer type hydrodynamic entry length problem are described first.

(1) Integral. The flow cross section is treated as having two regions, a boundary layer developing near the wall and an inviscid fluid core. This approach was first applied by Schiller [21] for flow in a circular tube and a parallel plate channel. He used a parabolic velocity distribution in the boundary layer and Bernoulli's equation (potential flow dynamical equation) in the inviscid core to determine the pressure distribution in the axial direction. Shapiro et al. [68] modified this method by employing cubic and quartic velocity profiles in the boundary layer. Campbell and Slattery [69] further refined the method by taking viscous dissipation into account in the boundary layer. Gubin and Levin [70] assumed a logarithmic velocity profile in the boundary layer, and presented the velocity distribution for the circular tube in tabular and graphical form.

(2) Axially Patched Solutions. The entrance region is divided into two sections. Near the entrance a boundary layer approach is used and an approximate solution is obtained in terms of a perturbation of Blasius boundary layer solution.

Far downstream, where the flow is nearly fully developed, the solution is obtained in terms of small perturbations of the fully developed solution. These solutions are "patched" (joined smoothly) at some appropriate axial location to obtain a complete entrance region solution. This method was first used by Schlichting [71,72] for the parallel plate channel and by Atkinson-Goldstein [73] for the circular tube. Collins and Schowalter [74] refined Schlichting's method by retaining more terms in the series of upstream and downstream solutions.

(3) Linearization of Momentum Equation. The above two methods yield the discontinuous solution for the velocity and pressure distribution in the hydrodynamic entrance region. Langhaar [75] proposed a method which yields continuous solution in the entrance region of a circular tube. He linearized the nonlinear inertia term, left hand side of Eq. (14a) as follows.

$$u \frac{\partial u}{\partial x} + v \frac{\partial u}{\partial r} = v \beta^2(x) u \quad (104)$$

where  $\beta$  is a function of  $x$  only. Langhaar's linearization is rigorous in the unsheared central core. His solution appears satisfactory at the tube centerline, very near the entrance or far from the entrance. Langhaar's approach of linearization was used by Han for rectangular ducts [76] and for parallel plates [77], by Han and Cooper [78] for the equilateral triangular duct, and by Sugino [79] and Heaton et al. [80] for annular ducts.

Targ [81] linearized the inertia term of momentum equation (14a) for circular tube as follows.

$$u \frac{\partial u}{\partial x} + v \frac{\partial u}{\partial r} = u_m \frac{\partial u}{\partial x} \quad (105)$$

He also replaced  $(dp/dx)/\rho$  with  $(2v/a)(\partial u/\partial r)$  to obtain a solution. Chang and Atabeck [82] used Targ's linearization approach for annular ducts<sup>10</sup>. In case of circular tube, Targ's solution, which neglects the contribution of momentum change to pressure gradient, results in the velocity profile developing too slowly near the entrance.

It may be noted that Langhaar and Targ's linearization is exact (a) at entrance if the uniform velocity is assumed, (b) at all points on the wall of the duct, since  $\partial u/\partial x$  and  $v$  both vanish there, and (c) in the fully developed region where  $\partial u/\partial x$  and  $v$  become zero.

Sparrow et al. [83] employed the following linearization to the momentum equation

$$\epsilon(x) u_m \frac{\partial u}{\partial x} = \Lambda(x) + v \left[ \frac{1}{r} \frac{\partial}{\partial r} \left( r \frac{\partial u}{\partial r} \right) \right] \quad (106)$$

where  $\epsilon(x)$  is the mean velocity weighting factor and  $\Lambda(x)$  stands for the  $dp/dx$  term plus the residual inertia terms. This linearization is similar to Targ's but embodies a more general linearization of the inertia term than that used by Targ. Sparrow et al. [83] matched the pressure gradients from the momentum and mechanical energy equation to evaluate  $\epsilon(x)$ . This linearization is restricted to the case where the velocity profile depends on only one cross sectional coordinate, e.g. circular tubes and parallel plates [83], and annular ducts [84]. Wiginton and Wendt [85] and Fleming and Sparrow [86] independently generalized this linearization to the case where velocity profiles depend upon two cross sectional coordinates, e.g., rectangular and isosceles triangular ducts. The convergence of solution by the method of [85] is more rapid than that by [86].

---

<sup>10</sup>Unless specified, the annular duct means a concentric annular duct.

(4) Numerical Finite Difference Method. The continuity and momentum equations are reduced to the finite difference form and the numerical solution is carried out on a computer. This method is used by Bodoia and Osterle [87] for parallel plates, by Hornbeck [88], Christiansen and Lemmon [89] and Manohar [90] for a circular tube, by Manohar [91] for annular ducts, and by Montgomery and Wibulswas [92] for rectangular ducts.

(5) Numerical Finite Difference Method with Transformation of the Initial Value Problem to a Boundary Value Problem. If the fully developed velocity profile, the  $fRe$  factor, and the hydrodynamic entrance length  $L_{hy}^+$  are known for a given duct geometry, the initial value problem for the hydrodynamic entrance region can be transformed into a boundary value problem. The detailed velocity distribution, friction factor and pressure distribution can then be obtained for a given Reynolds number by numerically solving the boundary value problem. Miller [93] employed this technique and worked out the hydrodynamic entrance length solution for the square and equilateral triangular duct at  $Re = 10^3$  from the hydrodynamic entrance length  $L_{hy}^+$  given by McComas [20].

In all of the above five methods, the boundary layer type idealizations, Eq. (13), are invoked. However, several papers deal directly with the numerical solution of complete Navier-Stokes equations without invoking the boundary layer idealizations. Vrentas et al. [94], Friedmann et al. [95], and Schmidt and Zeldin [96] solved the hydrodynamic entry length problem for circular tube, Wang and Longwell [97], and Gillis and Brandt [98] solved it for parallel plates using the complete Navier-Stokes equations.

#### IV.3 Thermally Developing Flow

#### IV.3.1 Hydrodynamically Fully Developed Flow

The thermal entrance solutions are obtained by the following methods.

(1) Eigen Solution. Most of the solutions of thermally developing and hydrodynamically developed flow are obtained by the eigenvalue method; particularly the circular tube, parallel plates, rectangular ducts, elliptical ducts and annular ducts. The axial heat conduction and thermal energy sources within the fluid are also considered for circular tubes.

The infinite series solution, obtained by the above method, for the thermal entrance problem converges very slowly near  $x^* = 0$ . Lévèque [99] provided a solution for the thermal entrance region near  $x^* = 0$  (very close to the point of step change in the boundary condition). Newman [100] refined Lévèque solution by retaining the first three terms of the Lévèque series. Burghardt and Dubis [101] also formulated a simple method for the thermal entrance region near  $x^* = 0$ .

(2) Variational Methods. Sparrow and Siegel [102] developed a variational method for the thermal entrance region for H1 boundary condition. They neglected the effect of axial heat conduction, thermal energy sources and viscous dissipation in the fluid. Examples were worked out for a circular tube, parallel plates and a square duct. Tao [103] proposed a variational approach for the thermal entrance region for the prescribed wall temperature and wall temperature gradient boundary conditions. He included the effect of viscous dissipation and internal thermal energy generation. He obtained the thermal entrance temperature distribution for the circular and elliptical ducts.

(3) Conformal Mapping Method. Casarella et al. [43] proposed an approximate, conformal mapping method for the thermal entrance  $Nu_{x,T}$  for the ducts of arbitrary cross section. Slug flow solutions were carried out for circular, cardioid, corrugated, square and hexagonal ducts. Laminar flow solution was carried out for the circular tube only.

(4) Simplified Energy Equation. In this approximate method, the variable coefficients energy equation is reduced to the constant coefficient linear equation and then is solved. No momentum or continuity equation is needed. Sadikov [104] linearized the energy equation (19b) as follows after neglecting  $\alpha(\partial^2 t / \partial x^2)$ .

$$\epsilon u_m \frac{\partial t}{\partial x} = \alpha \left( \frac{\partial^2 t}{\partial y^2} + \frac{\partial^2 t}{\partial z^2} \right) \quad (107)$$

where the correction factor  $\epsilon = 0.346 Pr^{-1/3}$  is based on heat transfer for laminar flow over a flat plate. Based on the simplification procedure, this equation is valid in the entrance region where the boundary layer on a wall is not significantly affected by the opposing wall. With this, he solved the thermal entry length problem for parallel plates with entering fluid at uniform [105] and non-uniform [106] temperature. In both cases, the wall temperature was assumed linearly varying with the axial distance. Sadikov [104] also studied the thermal entry length problem, based on the simplified energy equation, in rectangular ducts with given wall heat flux boundary condition.

(5) Numerical Finite Difference Method. The energy equation is expressed in the finite difference form and a solution is carried out on a computer. Grigull and Tratz [107] employed this technique for the circular tube and Montgomery and Wibulswas [108] employed for the rectangular ducts to obtain the  $(T)$  and  $(H)$  temperature distribution and Nusselt numbers.

(6) Monte Carlo Method.<sup>11</sup> Chandler et al. [109] showed how the Monte Carlo method can be applied to the laminar forced convection heat transfer problem. They considered the thermal entry problem for parallel plates with  $\Theta$  boundary condition.

### 3.2 Simultaneously Developing Flow

The thermal entrance solutions are obtained by the following methods.

(1) Semi-Numerical Method. The velocity profile is obtained from the linearization of momentum equation. Consequently, employing this velocity profile, the temperature distribution is obtained by numerical methods. Employing Langhaar type velocity profile [75], the numerical solutions were carried out for the circular tube by Kays [12], McMordie and Emery [110] and Butterworth and Hazell [111], for the parallel plates by Han [77] and for the annular ducts by Heaton et al. [80]. Employing Sparrow's velocity profile [83], the numerical solution was carried out for the circular tube by Kakaç and Özgü [112].

(2) Complete Numerical Method. Both the velocity and temperature distribution is obtained by solving the corresponding momentum and energy equations numerically. The thermal entry solutions were carried out for the circular tube [113,114,90], parallel plates [115], rectangular ducts [92], equilateral triangular and isosceles right triangular ducts [116].

---

<sup>11</sup> Monte Carlo method has been defined as the technique of solving a problem by putting in random numbers and getting out random answers.

## V. ANALYTICAL SOLUTIONS

The governing differential equations and the boundary conditions were outlined in Chapter II for the laminar flow and heat transfer through a cylindrical duct. This chapter describes all the solutions available to the authors from the heat transfer literature for two dimensional ducts. In reviewing the literature for each geometry, the chronological history is not presented. Instead, the material is presented in order for each boundary condition and its subdivisions. The presentation is divided into two parts: (1) straight ducts and (2) curved ducts.

No attempt has been made to present the detailed solutions for any geometry. Instead, only the final results, useful to a heat transfer designer are presented. In particular, the maximum available information from the following list of parameters is presented for each geometry:  $u$ ,  $u_m$ ,  $fRe$ ,  $K(\infty)$ ,  $L_{hy}^+$  and Nusselt numbers corresponding to the boundary conditions of Table I. For each geometry, the above information is presented both in tabular and graphical form. The original tabular and graphical information is augmented when possible in light of (i) more information obtained by corresponding with authors, (ii) the knowledge of limiting cases of boundary conditions or the geometries, and (iii) calculating more detailed and accurate results on the Stanford computer whenever readily feasible.

For convenient reference, the table number, figure number and source for the  $fRe$ ,  $Nu_T$ ,  $Nu_{H1}$ ,  $Nu_{H2}$  and hydrodynamic and thermal entrance length solutions for each geometries are summarized in Chapter VII.

## Part 1. Straight Ducts

### 1. CIRCULAR DUCT

Mathematically, the circular tube is the simplest cylindrical geometry after parallel plates. Practically, it is the geometry most commonly used for fluid flow and heat transfer. Circular tube laminar fully developed and developing flow has been analyzed in great detail for various boundary conditions, including the effect of thermal energy sources, viscous dissipation, fluid axial heat conduction and vorticity diffusion etc. The results are outlined below.

#### 1.1 Fully Developed Flow

The velocity profile and friction factor for the fully developed laminar flow through a circular tube of radius,  $a$ , with co-ordinate axes located at the center of the tube are [5]

$$u = \frac{c_1}{4}(r^2 - a^2) \quad (108)$$

$$u_m = -\frac{c_1 a^2}{8} \quad (109)$$

$$fRe = 16 \quad (110)$$

The heat transfer results are described separately for each boundary condition.

##### 1.1.1 Uniform Surface Temperature, $\mathbb{T}$

The problem was first handled by Graetz in 1885 [117, 118], now famous as Graetz problem, and later quite independently by Nusselt in 1910 [119]; where they evaluated the first three terms of infinite series solution for hydrodynamically developed and thermally developing flow with  $\mathbb{T}$  boundary condition. Their asymptotic Nusselt number for the

fully developed flow was presented as  $Nu_T = 3.66$ . A more precise magnitude is

$$Nu_T = 3.6567935 \quad (111)$$

for the case when the fluid axial heat conduction, viscous dissipation and thermal energy sources within the fluid are neglected. The temperature distribution  $t_T$  may be inferred from [13].

Pahor and Strand [120] included the effect of axial heat conduction in the fluid and graphically presented the fully developed Nusselt number as a function of Péclét number. Also they formulated the following asymptotic expressions.

$$Nu_T = 3.6570 \left(1 + \frac{1.232}{Pe^2} + \dots\right) \quad Pe \gg 1 \quad (112a)$$

$$Nu_T = 4.1805 \left(1 - 0.0439 Pe + \dots\right) \quad Pe \ll 1 \quad (112b)$$

Labuntsov [121] also considered the same problem, and presented the asymptotic  $Nu_T$  as a function of Péclét number in a tabular form. Hennecke [22], along with the thermal entrance length solution, presented graphically the fully developed  $Nu_T$  as a function of Péclét number. Ash and Heinbockel [122] refined the work of Pahor and Strand [120]. They obtained the temperature distribution in terms of the confluent hypergeometric function. They graphically presented the  $Nu_T$  as a function of  $Pe$ . Their numerical results [123] are listed in Table 2.

### 1.1.2 Specified Wall Heat Flux Distribution and $\textcircled{H}$

Glaser [124] provided a solution for the fully developed laminar flow with the  $\textcircled{H}$  boundary condition. As mentioned earlier, the circular tube geometry is unique<sup>12</sup> because  $\textcircled{H1}$ ,

<sup>12</sup>The parallel plate geometry is also unique for the identical reason.

Table 2: Circular duct  $Nu_T$  as a function of  $Pe$  for fully developed laminar flow, from Ash [123]

$Pe$	$Nu_T$	$Pe$	$Nu_T$	$Pe$	$Nu_T$
$\infty$	3.6568	6	3.744	0.5	4.098
60	3.660	5	3.769	0.4	4.118
50	3.660	4	3.805	0.3	4.134
40	3.661	3	3.852	0.2	4.150
30	3.663	2	3.925	0.1	4.167
20	3.670		4.030	0.04	4.170
10	3.697	0.9	4.043	0.03	4.175
9	3.705	0.8	4.059	0.02	4.175
8	3.714	0.7	4.071	0.01	4.175
7	3.728	0.6	4.086	0.001	4.182
				0	4.1805

Table 3. Circular, Parallel plates, Elliptical and Sine ducts  $Nu_O$  and  $Nu_{R1}$  as a function of  $R_w$  for fully developed laminar flow<sup>13</sup>

Circular Duct [131]			Parallel Plates [131]		
$R_w$	$Nu_O$	$Nu_{R1}$	$R_w$	$Nu_O$	$Nu_{R1}$
0	3.657	3.657	0	7.541	7.541
0.005	3.603	3.669	0.0125	6.940	7.599
0.025	3.398	3.713	0.025	6.422	7.650
0.05	3.167	3.763	0.05	5.576	7.731
0.10	2.777	3.844	0.075	4.918	7.793
0.15	2.464	3.908	0.125	3.970	7.881
0.25	2.000	4.000	0.25	2.667	8.000
0.50	1.347	4.124	0.50	1.604	8.095
1.00	0.8085	4.223	$\infty$	0	8.235
$\infty$	0	4.364			

Elliptical Duct with $a^*=0.8$ [238]			Sine Duct with $a^*=a/b=.5$ [46]		
$R_w$	$Nu_O$	$Nu_{R1}$	$R_w$	$Nu_O$	$Nu_{R1}$
0.0	3.669	3.669	0	2.12	2.12
0.2	2.206	3.948	0.01236	2.043	2.096
1.0	0.8068	4.175	0.1236	1.587	1.974
10.0	0.09775	4.344	1.236	0.5285	1.524
$\infty$	0	5.233	12.36	0.07678	1.508
			123.6	0.008044	1.415

<sup>13</sup>For circular, parallel plates and elliptical ducts,  $Nu_{R1}$ , for the limiting case  $R_w = 0$  and  $\infty$ , correspond to (T) and (H) boundary conditions. Unlike other ducts, the sine duct  $Nu_{R1}$  decreases with an increasing value of  $R_w$  [46].

(H2) and (H3) boundary conditions yield the same heat transfer results for both developed and developing velocity and temperature profiles. For this boundary condition, the axial heat conduction within the fluid is constant. Consequently, it does not affect the Nusselt number. Thus  $Nu_H$  is independent of the Pe number. Tao [36] outlined the fully developed solution for (H) boundary condition using a complex variables technique; he included thermal energy sources in the fluid. Madejski [125] considered the effect of gas work  $u(dp/dx)/J$  on the temperature distribution when  $q'' = 0$ , and observed an effect of temperature drop, similar to the Rangue effect. Tyagi [23] extended Tao's work to include the influence of viscous dissipation on heat trans. r. His results for the temperature profile and Nusselt number are given by

$$t_H = \frac{c_4}{64}(r^2 - a^2)[(r^2 - 3a^2 - 16a^2 c_5) + c_6 \{ r^2 - 3a^2 - 2(r^2 - a^2) \}] \quad (113)$$

$$t_{m,H} = \frac{11c_4 a^2}{384} \left[ 1 + \frac{64}{11} c_5 + \frac{5}{11} c_6 \right] \quad (114)$$

$$Nu_H = \frac{48}{11} \left[ \frac{1 + 8 c_5 + c_6}{1 + \frac{64}{11} c_5 + \frac{5}{11} c_6} \right] \quad (115)$$

where the constants  $c_1$ ,  $c_2$ ,  $c_3$ ,  $c_4$  are characterized in the nomenclature, and

$$c_5 = \frac{c_3}{c_4 a^2} = - \frac{1}{8 \left[ 1 + \frac{q''}{S r_h} \right]} \quad (116)$$

$$c_6 = \frac{\mu c_1}{k c_2} = \frac{-32\mu u_m^2}{D_h^2 \left[ S + \frac{q''}{r_h} \right] J g_c} \quad (117)$$

In absence of thermal energy sources and viscous dissipation,

$$Nu_H = \frac{48}{11} = 4.3636364 \quad (118)$$

Reynolds [126] considered the effect of arbitrary peripheral heat flux on fully developed Nusselt numbers with constant axial heat flux per unit length. Of the particular interest is the cosine heat flux variation as shown in Fig. 7.

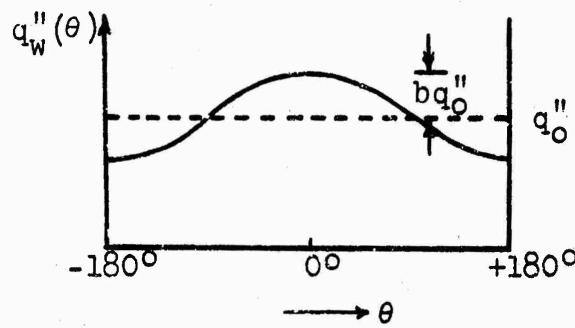


Fig. 7 Cosine heat flux variation along circular tube periphery

The peripheral fully developed Nusselt number is obtained as

$$Nu_H(\theta) = \frac{1 + b\cos\theta}{\frac{11}{48} + \frac{b}{2}\cos\theta} \quad (119)$$

Reynolds [7] extended his work by including the effect of heat conduction in peripheral direction with arbitrary peripheral heat flux, but constant axial wall heat flux.

### 1.1.3 Exponential Wall Heat Flux, $H^4$

Hall et al. [127] first showed that the axially invariant fluid temperature profile, Eq. (2), results for the exponential wall heat flux distribution in axial direction, Eq. (10). Hasegawa and Fujita [10] also independently found

that the fully developed situation arises when the axial wall heat flux is exponential. They solved the energy equation numerically, and determined the  $Nu_{H4}$  as a function of the exponent  $\lambda$  as shown in Fig. 8. They demonstrated that the  $(H)$  and  $(T)$  boundary conditions are the special cases of  $(H4)$  boundary condition, with  $\lambda = 0$ , and  $-14.627$  respectively. The wall and fluid bulk mean temperatures for various values of  $\lambda$  are shown in Fig. 3.

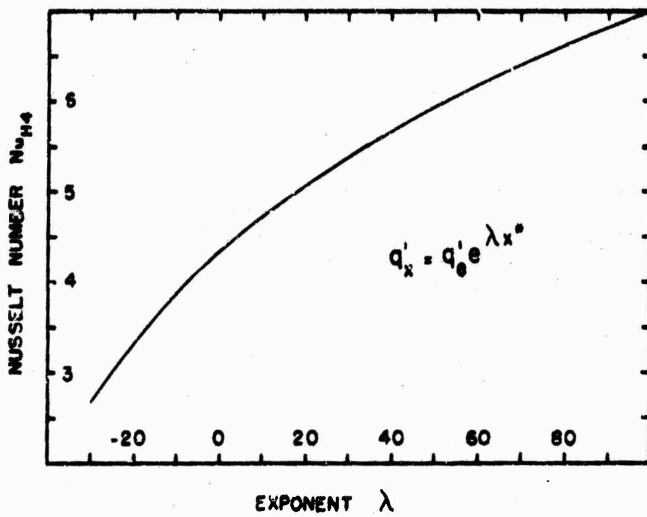


Fig. 8 Fully developed  $Nu_{H4}$ , from [10]

Graber [128] also studied the axial exponential wall heat flux distribution in circular tube, parallel plates and annular ducts. He introduced a parameter  $F_o = dt_w/dt_o$ . The  $F_o$  is the ratio of the temperature gradients  $dt_w/dx$  along the wall transferring the heat and  $dt_o/dx$  in the fluid at the point where the temperature gradient normal to wall reduces to zero. The  $F_o$  and  $\lambda$  are related by

$$\frac{1}{F_o} = 1 + Nu_{H4} \left[ \frac{4Nu_{H4}}{4Nu_{H4} + \frac{1+r^*}{r_j^*} \lambda} - 1 \right] \quad (120)$$

where  $r^*$  and  $r_j^*$  equals zero for the circular tube.

The 0 and 1 values of  $F_o$  correspond to the boundary conditions  $\textcircled{T}$  and  $\textcircled{H}$  respectively. The  $Nu_{H4}/Nu_{H1}$  ratio was presented graphically as a function of  $F_o$  (range from -2 to 8) with  $r^*$  (0-1) as a parameter.

Some experimental verification of the  $\textcircled{H4}$  boundary condition for the turbulent flow has been presented in [10, 129, 130].

#### 1.1.4 Finite Wall Thermal Resistance, $\textcircled{R1}$

Based on the Sideman et al. [131] results for the thermal entry length solution for the  $\textcircled{R1}$  boundary condition, the fully developed  $Nu_{R1}$  and  $Nu_o$  are calculated and presented in Table 3 for the circular duct along with the similar results for parallel plates, elliptical ducts and sine ducts. Hsu [132] included the flux axial heat conduction with  $\textcircled{R1}$  boundary condition. Based on his results, the fully developed  $Nu_{R1}$  and  $Nu_o$  were calculated and are presented as a function of Péclét number in Table 4.

Table 4. Circular duct  $Nu_o$  and  $Nu_{R1}$  as functions of  $R_w$  and  $Pe$  for fully developed laminar flow, from Hsu [132].

$R_w$	$Pe = \infty$		$Pe = 100$		$Pe = 50$		$Pe = 30$	
	$Nu_o$	$Nu_{R1}$	$Nu_o$	$Nu_{R1}$	$Nu_o$	$Nu_{R1}$	$Nu_o$	$Nu_{R1}$
0.25	2.000	4.000	1.999	3.995	1.995	3.981	1.987	3.947
0.05	3.167	3.763	3.164	3.759	3.157	3.748	3.138	3.722
0.005	3.602	3.669	3.599	3.665	3.590	3.655	3.567	3.632

$R_w$	$Pe = 20$		$Pe = 10$		$Pe = 5$		$Pe = 1$	
	$Nu_o$	$Nu_{R1}$	$Nu_o$	$Nu_{R1}$	$Nu_o$	$Nu_{R1}$	$Nu_o$	$Nu_{R1}$
0.25	1.970	3.863	1.821	3.586	1.662	2.843	0.6580	0.7875
0.05	3.104	3.674	2.740	3.447	2.506	2.865	0.9202	0.9645
0.005	3.525	3.588	3.325	3.381	2.808	2.848	1.0113	1.0164

Toor [133] investigated the effect of gas compression work  $u(dp/dx)/J$  on heat transfer for the (R1) boundary condition, and showed that the gas work can have significant influence on temperature profiles.

### 1.1.5 Radiant Flux Boundary Condition, (R2)

The fully developed  $Nu_{R2}$  may be inferred from the thermal entry length solution of Chen [134] as a function of  $\gamma$ . Kadaner et al. [135] also analyzed the radiant wall heat flux boundary condition. They approximated within 0.5 percent of their  $Nu_{R2}$  values by the following equation

$$Nu_{R2} = \frac{4.364 + 3.66\gamma T_a^3}{1 + \gamma T_a^3} \quad (121)$$

where  $T_a$  is the outside fluid temperature normalized to the fluid inlet temperature  $T_e$ .

### 1.2 Hydrodynamically Developing Flow

Hydrodynamic entry length problem was first analyzed by Boussinesq [136,73] by considering perturbation about the fully developed Poiseuille profile. His infinite series solution was fairly adequate downstream, but poor near the entrance. Atkinson-Goldstein [73] represented the stream function by a power series to find a solution to Eq. (14) for axial position close to the inlet. They then joined this solution with the one obtained by Boussinesq method to obtain a velocity distribution in the entire entrance region. Schiller [21] solved the problem by an integral method assuming developing boundary layer (of parabolic arc) in the entrance region with impressed pressure gradient and a straight potential core in the remaining central cross section. This method is good at the entrance, but poor at downstream. Shapiro et al. [68] refined Schiller's solution by using cubic and quartic velocity profiles in the boundary

Table 5. Circular duct  $u_{max}/u_m$ ,  $\Delta p/(\rho u_m^2/2g_c)$ ,  $f_{app} Re$  and  $K(x)$  as a function of  $x^+ (= x/D_h Re)$  for developing laminar flow, from Manohar [137]

$x/(D_h Re)$	$u_{max}/u_m$	$\Delta p/(\rho u_m^2/2g_c)$	$f_{app} Re$	$K(x)$
0.000075	1.06011	0.10695865	350.529	0.1022
0.000150	1.08271	0.15537634	258.961	0.1458
0.000275	1.10940	0.21388836	194.444	0.1963
0.000400	1.13032	0.26073870	162.962	0.2391
0.000525	1.14800	0.30101158	143.339	0.2674
0.000675	1.16647	0.34376495	127.320	0.3006
0.000925	1.19291	0.40615480	109.772	0.3470
0.001175	1.21577	0.46119542	98.127	0.3860
0.001425	1.23615	0.51118190	89.621	0.4200
0.001725	1.25826	0.56633064	82.077	0.4559
0.002225	1.49100	0.66978957	73.010	0.5074
0.002725	1.32008	0.72569772	66.578	0.5513
0.003225	1.34648	0.79610395	61.713	0.5897
0.003725	1.37085	0.86230301	57.873	0.6239
0.004225	1.39357	0.92513389	54.7^2	0.6547
0.004725	1.41497	0.98521656	52.128	0.6828
0.005225	1.43523	1.04297360	49.903	0.7086
0.005825	1.45828	1.10971400	47.627	0.7369
0.006825	1.49414	1.21577760	44.534	0.7790
0.007825	1.52733	1.31664510	42.065	0.8158
0.008825	1.55826	1.41332200	40.037	0.8485
0.009825	1.58720	1.50656550	38.335	0.6776
0.010825	1.61430	1.59690420	36.880	0.9041
0.011825	1.63970	1.68478840	35.619	0.9280
0.012925	1.66349	1.77051920	34.513	0.9447
0.013825	1.68578	1.85440190	33.533	0.9696
0.014825	1.70632	1.93662C80	32.658	0.9878
0.015825	1.72611	2.01739360	31.870	1.0046
0.016825	1.74432	2.09683910	31.157	1.0200
0.017825	1.76132	2.17512670	30.507	1.0393
0.018825	1.77720	2.25232450	29.911	1.0475
0.019825	1.79202	2.32859250	29.364	1.0558
0.020825	1.80534	2.40395460	28.859	1.0712
0.022025	1.82200	2.49336460	28.302	1.0838
0.024025	1.84619	2.64003780	27.472	1.1024
0.026025	1.86668	2.78426040	26.746	1.1157
0.028025	1.88447	2.92638480	26.105	1.1328
0.030025	1.90997	3.06670290	25.535	1.1451
0.032025	1.91351	3.20546730	25.023	1.1529
0.034025	1.92533	3.34287760	24.562	1.1653
0.036025	1.93567	3.47911690	24.144	1.1735
0.038025	1.94673	3.61433020	23.763	1.1807
0.040025	1.95265	3.74865080	23.414	1.1871
0.042025	1.95900	3.88218600	23.095	1.1929
0.044025	1.96570	4.01503720	22.800	1.1974
0.046025	1.97104	4.14728660	22.527	1.2017
0.048025	1.97573	4.27900720	22.275	1.2054
0.050025	1.97986	4.41026680	22.040	1.2087
0.052025	1.98348	4.54111300	21.822	1.2115
0.053625	1.98606	4.64553280	21.657	1.2135

layer. Campbell and Slattery [69] improved Schiller's solution by taking viscous dissipation into account in the boundary layer, and the pressure drop was evaluated from the mechanical energy balance to all of the fluid in the tube. Gubin and Levin [70] employed a logarithmic velocity profile in the boundary layer and solved the hydrodynamic entry length problem by the integral method. They presented the velocity distribution in tabular and graphical form.

All of the above solutions exhibit a discontinuity in the velocity and pressure distribution in the entrance region. Langhaar [75] proposed a linearization of momentum equation [see Eq. (104)] and subsequently solved the momentum equation by an integral method. The linearization is rigorous in the unsheared central core. His solution appears satisfactory at the tube centerline, and very near the entrance or far from the entrance.

Targ [81] introduced another approach of linearization, Eq. (105), which is a special case of the linearization [Eq. (106)] performed by Sparrow et al. [83]. In Targ's solution, which neglects the contribution of momentum change to the pressure gradient, velocity profiles develop more slowly near the entrance than is predicted by the numerical solution. The velocity profiles by Sparrow et al. [83] are nearly identical with the numerical solutions described below.

Hornbeck [88] introduced a finite difference scheme for the hydrodynamic entry length problem of circular tube. He linearized the momentum equation at any cross section  $x = x_1$  by means of velocity at  $x = x_1 - \Delta x$ . Christiansen and Lemmon [89] and Manohar [90] solved the non-linear momentum equation numerically iteratively, thus avoiding any error due to linearization. The  $u_{\max}/u_m$ ,  $\Delta p/(\rho u_m^2/2g_c)$ ,  $f_{app}^{Re}$  and  $K(x)$  for the hydrodynamic entrance region of a circular tube are presented in Table 5.<sup>15</sup> The  $f_{app}^{Re}$  and  $K(x)$

<sup>15</sup>The tabular  $x^+$ ,  $u_{\max}/u_m$  and  $\Delta p/(\rho u_m^2/2g_c)$  were provided by Manohar [137].

Table 6. Circular duct  $f_{app}^{-1/2}$  and  $K(x)$  as a function of  $x^+$  for  $Re = 100$ , 500 and 10,000, from Schmidt [138]

$\eta/(D_h Re)$	Re = 10,000		Re = 500		Re = 100	
	$f_{app}^{-1/2}$	$K(x)$	$f_{app}^{-1/2}$	$K(x)$	$f_{app}^{-1/2}$	$K(x)$
0.0000614	424.795	0.1004	653.622	0.1566	382.372	0.09003
0.0000946	348.148	0.1257	519.700	0.1906	403.421	0.1466
0.0001296	297.720	0.1461	434.820	0.2172	386.035	0.1919
0.0001666	262.775	0.1645	375.886	0.2399	359.384	0.2289
0.0002059	236.495	0.1816	331.809	0.2601	331.930	0.2602
0.0002475	215.939	0.1979	297.370	0.2785	306.466	0.2875
0.0002917	199.010	0.2135	269.386	0.2956	283.701	0.3123
0.0003387	184.733	0.2286	246.071	0.3117	263.638	0.3355
0.0003889	174.531	0.2435	226.208	0.3270	245.815	0.3575
0.0004425	161.916	0.2583	209.029	0.3417	229.987	0.3788
0.0005000	152.500	0.2730	194.000	0.3560	215.850	0.3997
0.0005615	144.094	0.2877	180.693	0.3699	203.088	0.4202
0.0006280	136.622	0.3025	168.747	0.3837	191.358	0.4405
0.0007000	129.429	0.3176	157.929	0.3974	180.571	0.4606
0.0007780	122.973	0.3329	148.102	0.4111	170.563	0.4810
0.0008625	117.014	0.3485	139.188	0.4250	161.304	0.5013
0.0009545	111.495	0.3646	131.034	0.4392	152.668	0.5218
0.0010555	106.265	0.3811	123.461	0.4537	144.517	0.5426
0.0011665	101.362	0.3983	116.450	0.4687	136.789	0.5636
0.0012895	96.690	0.4162	109.912	0.4844	129.416	0.5850
0.0014260	92.245	0.4349	103.816	0.5009	122.381	0.6068
0.0015785	87.999	0.4540	98.103	0.5184	115.636	0.6291
0.0017500	83.014	0.4754	92.714	0.5370	109.129	0.6519
0.0019445	79.962	0.4975	87.012	0.5570	102.848	0.6755
0.0021665	76.143	0.5212	82.757	0.5796	96.752	0.6998
0.0024230	72.418	0.5468	78.134	0.6022	90.804	0.7250
0.0027220	68.783	0.5747	73.687	0.6281	85.012	0.7514
0.0030760	65.195	0.6053	69.381	0.6568	79.345	0.7794
0.0035000	61.664	0.6393	65.214	0.6890	73.807	0.8093
0.0040185	58.161	0.6777	61.135	0.7255	68.383	0.8420
0.0046665	54.664	0.7217	57.126	0.7677	63.066	0.8789
0.0055000	51.141	0.7731	53.145	0.8172	57.909	0.9260
0.0061100	47.562	0.8345	49.162	0.8768	52.634	0.9739
0.0081650	43.846	0.9095	45.088	0.9500	47.782	1.0380
0.0105000	39.881	1.0030	40.786	1.0410	42.667	1.1200
0.0143900	35.371	1.1150	35.997	1.1510	37.178	1.2190
0.0221650	29.418	1.2340	30.302	1.2680	30.945	1.3250
0.0455000	23.220	1.3140	23.396	1.3460	23.676	1.3970

are plotted as a function of  $x^+$  in Figs. 9 and 10 respectively ( $Re \rightarrow \infty$  case).

All of the above hydrodynamic entry length solutions involve the idealizations of Eq. (13) (boundary layer type assumptions), i.e., axial diffusion of vorticity and the radial pressure gradients are neglected. Vrentas et al. [94] first solved the complete Navier-Stokes equations without invoking the boundary layer assumptions. They assumed a stream tube to extend from the entrance of the real tube to minus infinity where the axial velocity was considered to be uniform. They numerically solved the two coupled elliptical equations, and determined the velocity and pressure distribution, the pressure drop increment  $K(x)$  and the entry length for  $Re = 0, 1, 50, 150, 250$  and  $\infty$ . The momentum equation for  $Re = \infty$  corresponds to the boundary layer type equation, Eq. (14). Friedmann et al. [95] also solved the complete Navier-Stokes equations numerically for the Reynolds number range 0 to 500. They reported the velocity distribution in tabular form as well as graphically as functions of  $Re$  and  $x/D_h$ , and the hydrodynamic entry length as a function of  $Re$ . Schmidt and Zeldin [96] also solved the complete Navier-Stokes equations numerically for the case of circular tube and parallel plates. They used a different technique than that in Ref. [94] in forming the difference equations and the method of finding pressure. They reported the non-dimensional pressure distribution and the cross sectional area average  $\bar{K}(x)$  for  $Re = 100, 500$  and  $10000$ . Their results are presented in Table 6 and Figs. 9 and 10 [138].

### 1.3 Thermally Developing Flow

#### 1.3.1 Hydrodynamically Developed Flow

##### 1.3.1.1 Specified Wall Temperature Distribution

As previously mentioned, the study of heat transfer in laminar flow through a closed conduit was first made by

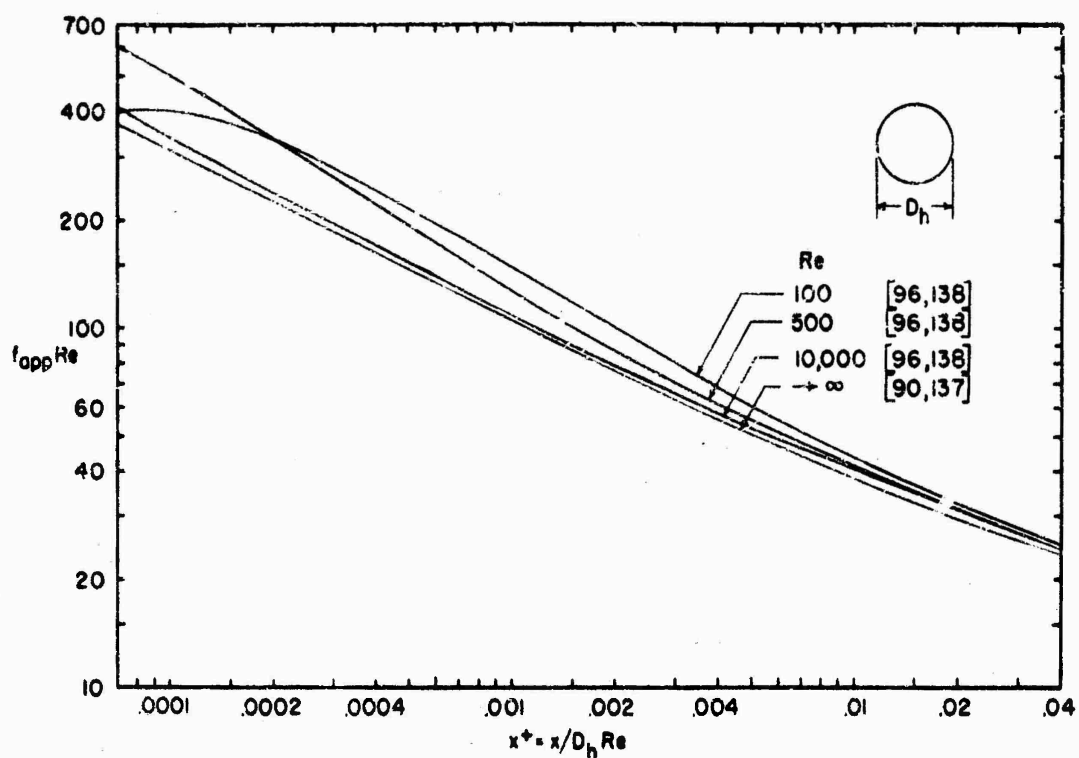


Fig. 9 Circular duct  $f_{app}Re$  for developing laminar flow.

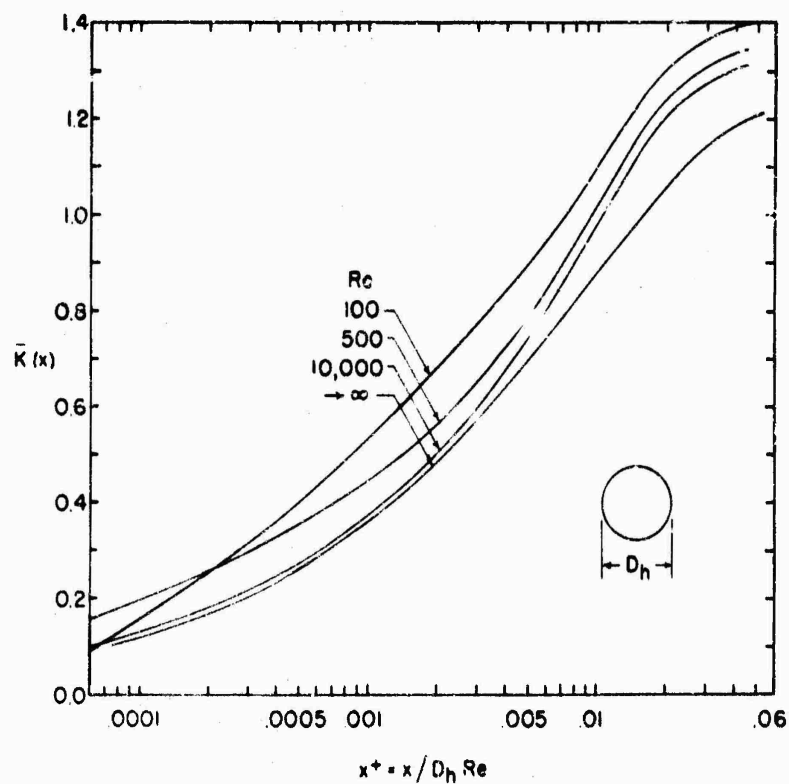


Fig. 10 Circular duct  $K(x)$  for developing laminar flow.

Graetz [117,118] in 1885 and later independently by Nusselt [119] in 1910. They considered the incompressible fluid with constant physical properties flowing through a circular tube and having fully developed laminar velocity profile and developing temperature profile. The circular tube was maintained at a constant and uniform temperature (i.e.  $\textcircled{T}$ ) different from the uniform temperature of fluid at the entrance. The axial heat conduction, viscous dissipation, gas compression work  $u(dp/dx)/J$  and the thermal energy sources within the fluid were neglected. The resulting energy equation is

$$\frac{\partial^2 t}{\partial r^2} + \frac{1}{r} \frac{\partial t}{\partial r} = \frac{u}{\alpha} \frac{\partial t}{\partial x} \quad (122a)$$

with initial and boundary conditions as

$$t = t_e = \text{constant} \quad \text{for } x \leq 0 \quad (122b)$$

$$t = t_w = \text{constant} \quad \text{at } r = a \quad (122c)$$

and the velocity profile  $u$  is given by Eq. (108). The above problem is now well known as the Graetz problem, sometimes also referred to as Graetz-Nusselt problem. If the duct in question is not a circular tube, the problem is usually referred to as the Graetz type problem.

Graetz and Nusselt obtained the first two and three terms respectively of an infinite series (known as Graetz series) solution for the fluid temperature and the local Nusselt numbers as a function of dimensionless axial distance  $x^*$ , now sometimes known as the Graetz number.<sup>16</sup> The Graetz

---

<sup>16</sup>To avoid the confusion of various definitions used for the Graetz number, the dimensionless distance is termed as  $x^*$ . See further discussion on p. 37.

series converges uniformly for all non zero  $x^*$ , but the convergence is very slow near the thermal entrance point and the three terms are not sufficient. Lévêque [99] alleviated this difficulty with his flat plate solution as an asymptotic approximation near the thermal entrance point. The Lévêque solution has been extended by Newman [100] by providing three terms of the Lévêque series; only the first term was provided by Lévêque in his original solution. Thus, the temperature distribution and the local Nusselt number can accurately be determined from  $x^* = 0$  to about 0.01 by the extended Lévêque solution.

Abramowitz [139] and Lipkis [140] employed a fairly rapidly converging series solution of the Graetz equation, and obtained first five eigenvalues and eigenconstants. Asymptotic expressions were presented for the higher eigenvalues and eigenconstants. Sellers et al. [13] independently extended the original work of Graetz by determining the first ten eigenvalues and eigenconstants for the Graetz problem, and presented the asymptotic formulae for the higher eigenvalues and eigenconstants. Sellers et al. considered the  $\mathbb{T}$  boundary condition, arbitrary wall temperature (specialized to linear variations in wall temperature) and prescribed wall heat flux boundary conditions. The  $\mathbb{H}$  heat transfer problem was worked out by an inversion method. Brown [141] outlined a comprehensive literature study of the Graetz problem. He evaluated and tabulated more accurately (10 decimal point accuracy) the first eleven eigenvalues and eigenconstants for the Graetz problem. He also presented the first six eigenfunctions. Larkin [142] extended the tabulation of Brown by presenting the sixth through fifteenth eigenfunctions. As mentioned above, the higher eigenvalues and eigenconstants are estimated by means of asymptotic formulae presented by Sellers et al. [13].

Kuga [143] solved the Graetz problem by reducing the Sturm-Liouville type governing differential equation to a Fredholm integral equation, and obtained numerically the first ten eigenvalues and six eigenfunctions and constants.

Grigull and Tratz [107] solved the Graetz problem numerically by the finite difference method. The dimensionless temperature distribution, local and mean Nusselt numbers were presented graphically as a function of  $x^*$ . For  $x^* \geq 0.001$ , they have approximated by the following equations  $Nu_{x,T}$  and  $Nu_{m,T}$  within 0.5 percent of their numerical solution (with  $x^* = 10^3 x^*$  for numerical convenience).

$$Nu_{x,T} = 3.655 + 6.874 x^{*-0.488} e^{-0.0572 x^*} \quad (123)$$

$$Nu_{m,T} = 3.655 + \frac{42.1}{x^{*0.64} (69.0 + x^{*1.64})^{0.301}} \quad (124)$$

Hicken [144] investigated the Graetz problem with non-uniform inlet temperature. He considered five different sinusoidal inlet fluid temperature profiles. He tabulated the eigenvalues and eigenconstants and presented the dimensionless fluid bulk mean temperature  $\vartheta_{m,T}$  as a function of  $x^*$ .

Instead of using the parabolic velocity distribution Lyche and Bird [145] and Whiteman and Drake [146] solved the Graetz problem for the general power law velocity distribution as

$$\frac{u}{u_m} = 2[1 - (\frac{r}{a})^n] \quad (125)$$

where  $n$  is an arbitrary number. Such velocity distribution is typical for non-Newtonian fluids.

For a fluid having vanishing viscosity with finite thermal conductivity and Prandtl number, if the flow is radically different from the parabolic profile at inlet, that profile will be maintained over a considerable distance from the entrance. To investigate the effect of the non-uniform inlet profiles, Barrow and Humphreys [147] analyzed the Graetz problem with slug, inverted conical and inverted parabolic velocity profile instead of the laminar parabolic profile for the whole flow length. They graphically presented  $Nu_{x,T}$  as a function of  $x^*$  for the different velocity profiles. Their results show that, for a given flow rate, increase in velocities near the wall results in a shortening of the thermal entry length and an increase in heat transfer coefficient, as expected.

The effect of internal thermal energy generation in the solution of Graetz problem was included by Topper [148] and Toor [149].

Singh [150] extended the work of Sellers et al. [13] by including the effect of axial heat conduction, viscous dissipation and prescribed internal thermal energy generation. He assumed that the fluid entered at uniform temperature at  $x = 0$ . He solved the associated Sturm-Liouville problem for the fluid temperature by expanding the fluid temperature in series of Bessel functions. He tabulated first four eigenvalues and the corresponding eigenfunctions for  $Pe = 100$  and  $1000$ . Also, the fluid bulk mean temperature and  $Nu_T$  as a function of  $x'$  ( $= 2x^*$ ) were tabulated for  $Pe = 100$  and  $1000$ , when the internal thermal energy generation and viscous dissipation were neglected.

Petukhov and Tsvetkov [151] included the effect of axial heat conduction in the Graetz problem. Uniform inlet temperature at  $x = 0$  is inconsistent with the inclusion of axial heat conduction. The  $x = 0$  is the section along the tube length where heat transfer starts and is not the entrance to the tube. Hence, they assumed the fluid to be at uniform

temperature  $t_e$  at  $x = -\infty$ , the wall region from  $x = -\infty$  to  $x = 0$  to be isothermal at temperature  $t_e$ , a step change in wall temperature at  $x = 0$ , and the region from  $x = 0$  to  $\infty$  isothermal (at temperature  $t_w > t_e$ ) and transferring heat to fluid. They obtained approximate temperature distribution numerically, and presented  $Nu_{x,T}$  for  $Pe = 1, 10$  and 45.

Shapovalov [152] included the effect of the fluid axial heat conduction in the Graetz problem, and obtained the fluid temperature distribution in terms of degenerate hypergeometric functions.

Bes [153] also solved the same problem as in [151] for circular tube and parallel plates for both  $\Theta$  and  $H$  boundary conditions. He found that for  $Pe < 15$ , longitudinal conduction is significant for the circular tube. Unfortunately, the paper utilizes unfamiliar symbols and terminology which makes an adequate evaluation difficult.

Hennecke [22] included the fluid axial heat conduction in the Graetz problem and analyzed it numerically by the finite difference method. He considered the same boundary condition of Petukhov and Tsvetkov [151], i.e., the flow channel extending from  $x = -\infty$  to  $x = \infty$  with the uniform inlet temperature at  $x = -\infty$  and a step change in wall temperature at  $x = 0$ . After solving the problem in two semi-infinite regions, the fluid temperature was matched at  $x = 0$ . The local Nusselt numbers and dimensionless wall heat fluxes  $\Phi$  and  $(\Phi x/a)$  were presented graphically as a function of  $x' (= 2x^*)$  for  $Pe = 1, 2, 5, 10, 20$  and 50. The thermal entry length was also presented graphically as a function of Péclét number.

Schmidt and Zeldin [30] independently investigated the Graetz problem numerically by the finite difference method with the effect of axial heat conduction within the fluid included. They considered the semi-infinite region

Table 7. Circular duct energy content of the fluid for developing temperature profile (developed velocity profile) when fluid axial heat conduction is considered, from Schmidt [138]

Pe = 1		Pe = 10		Pe = 25		Pe = 300	
x' = 2x*	energy content	x'	energy content	x'	energy content	x'	energy content
.00197	.000383	.000657	.01587	.000657	.0822	.000657	.8959
.00405	.000528	.00135	.02032	.00285	.165	.00135	.9032
.00624	.000786	.00452	.04697	.03641	.2273	.00208	.9211
.00855	.001045	.00855	.0738	.01099	.2964	.00285	.9330
.01099	.001364	.01381	.1002	.01709	.3595	.00366	.9415
.04397	.00336	.02098	.1304	.02564	.4201	.00452	.9479
.06294	.00573	.03134	.1650	.03846	.4808	.00544	.9530
.1154	.00925	.04762	.2062	.05983	.5444	.00641	.9572
.4077	.01827	.07692	.2576	.1026	.6141	.00744	.9607
.9488	.03024	.1453	.3257	.2308	.6878	.00855	.9636
1.4615	.0329	.3162	.3865	1.0000	.7196	.00973	.9662
3.0000	.0342	.4872	.4018			.01099	.9685
		1.0000	.4091			.01381	.9724
						.01709	.9755
						.02098	.9782
Pe = 50		Pe = 100		Pe = 200		Pe = 100,000	
x'	energy content						
.000657	.2277	.000657	.5059	.000693	.8053	.02564	.9806
.00135	.2577	.00135	.5366	.00142	.8183	.03134	.9826
.00452	.4167	.00235	.636	.00300	.8704	.03846	.9845
.00855	.5164	.00452	.6973	.00477	.8978	.04762	.9862
.01381	.5900	.00641	.7405	.00676	.9152	.05983	.9878
.02098	.6498	.00855	.7718	.00901	.9275		
.03134	.7019	.01099	.7974	.01158	.9368		
.04762	.7496	.01381	.8185	.01802	.9506		
.07692	.7954	.01709	.8366	.03303	.9646	.07692	.9893
.1026	.8180	.02098	.8524	.05019	.9718	.1026	.9907
.1453	.8402	.02564	.8665	.08108	.9780	.1453	.9920
.2308	.8605	.03845	.8912	.1532	.9834	.1795	.9926
.3162	.8688	.05983	.9128	.3333	.9866	.2308	.9932
.4872	.8746	.1026	.9324	1.0541	.9875	.3162	.9936
1.0000	.8772	.2398	.9497			.4872	.9940
						1.0000	.9941
Pe = 100,000		Pe = 100,000		Pe = 100,000		Pe = 100,000	
x'	energy content						
						.000657	.99988
						.00452	.99994
						.01235	.99997
						.04274	.99998
						.3162	.99999

$(0 \leq x < \infty)$  and uniform fluid temperature at inlet. The  $Nu_{x,T}$  and  $\Phi$  obtained by Schmidt and Zeldin [30] are generally higher than those obtained by Hennecke [22]. Part of the energy transferred from the wall to the fluid shows up as enthalpy rise of the fluid, and the rest is conducted by the fluid to the end headers. As the effect of axial heat conduction is more pronounced with decreasing Péclét number, the energy content of the fluid<sup>17</sup> (measured as enthalpy rise) reduces with decreasing Péclét number as shown in Fig. 11. Corresponding tabular information is presented in Table 7 [138]. This graph, Fig. 11, may be useful for the design of a high effectiveness heat exchanger, as the designer can now establish a criterion as to when to neglect the fluid axial heat conduction. If the thermal boundary condition of

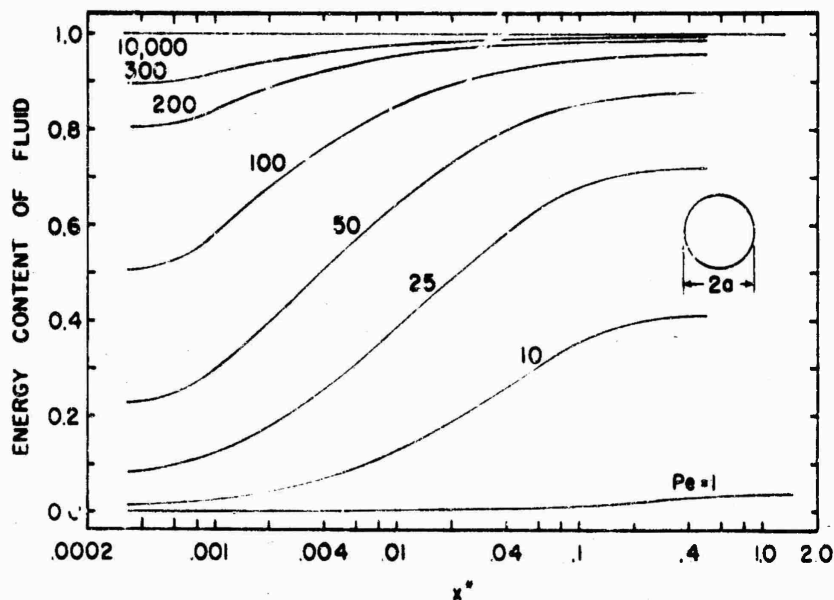


Fig. 11 Circular duct energy content of the fluid for developing temperature profile when fluid axial heat conduction is considered, from Schmidt [138].

<sup>17</sup> See Fig. 6 and associated discussion.

Hennecke [22] would have been employed, the effect of fluid axial conduction would not be as pronounced as found by Schmidt and Zeldin [30].

Jones [154] also included the axial heat conduction in the fluid for the Graetz problem for the circular tube extending from  $x = -\infty$  to  $x = \infty$  with a step change in wall temperature at  $x = 0$ . Closed form solution was obtained by employing the two-sided Laplace transform. The eigenvalues were presented in the form of an asymptotic expansion in Péclét number, unlike Singh's approach [150] where the eigenvalues and eigenfunctions are needed for each Péclét number. Similar to comparison of the Hennecke [22] and Schmidt and Zeldin's [30] results, Jones'  $Nu_{x,T}$  are lower than those by Singh [150]. Jones tabulated dimensionless bulk mean fluid temperature and  $Nu_{x,T}$  for  $Pe = 100, 200, 1000$  and  $2000$ . For  $x^* > 0.075$  and  $Pe > 200$ , the  $Nu_{x,T}$  was approximated as

$$Nu_{x,T} = 3.657[1 + 0.6072 e^{4(p_1-p_0)x^*}] \quad (126)$$

where the values of  $p_0$ ,  $p_1$  are tabulated below.

	$Pe = 200$	$Pe = 1000$	$Pe = 2000$
$p_0$	-3.65595	-3.65676	-3.65678
$p_1$	-22.2687	-22.3034	-22.3044

Specified arbitrary variation in wall temperature problem can be handled by superposition techniques from the known solution (eigenvalues and eigenconstants) of the Graetz problem. Sellers et al. [15] obtained the formulae for local Nusselt number, wall heat flux, and fluid bulk mean temperature when the wall temperature was varying linearly in axial direction. Kuga [143,155] obtained the solution for axially

varying sinusoidal wall temperature distribution. Grigull and Tratz [107] numerically obtained the solution for linearly varying wall temperature. They presented graphically the local Nusselt number as a function of  $x^*$  with a dimensionless temperature  $\theta_0$

$$\theta_0 = \frac{32}{3} \frac{(t_w - t_e)_e}{(dt_w/dx^*)}$$

as a parameter, where the temperature jump at the wall at  $x = x_e$  is non-dimensionalized by the wall temperature gradient. For small jumps ( $0 < \theta_0 < 1$ ), the local Nusselt number asymptotically approached to the value of 4.364 corresponding to  $(H)$  boundary condition. For large jumps, the local Nusselt number passed through a minimum and approached, for example, for  $\theta_0 = 50$ , a value of 3.66 corresponding to  $(T)$  boundary conditions. Shapovalov [156] considered the arbitrary wall temperature distribution with arbitrary initial condition, and obtained a solution in terms of hypergeometric functions. Any arbitrary axial wall temperature variation boundary condition can be handled by the Duhamel's superposition theorem, and is outlined in [5,13,14].

#### 1.3.1.2 Specified Heat Flux Distribution

Sellers et al. [13] analyzed the thermal entry length problem for the circular tube with uniform wall heat flux  $(H)$  boundary condition by an inversion method, knowing the solution to the Graetz problem. Siegel et al. [15] investigated the  $(H)$  thermally developing flow by the method of separation of variables and Sturm-Liouville theory, and obtained the eigensolution. They calculated first seven eigenvalues and eigenfunctions to six digit accuracy. In their analysis, they assumed fully developed velocity profile, uniform fluid temperature at entrance, and neglected the axial heat conduction, viscous dissipation, and the thermal-

energy sources within the fluid. Hsu [157] extended Siegel et al. work and reported first twenty eigenvalues and eigenconstants; also presented approximate formulae for higher eigenvalues and eigenconstants. Grigull and Tratz [107] attacked the same problem numerically by the finite difference method. They approximated the  $Nu_{x,H}$  with 0.5 percent to their numerical solution for  $x^* \geq 0.001$  as follows. With  $x^* = 10^3 x^*$ ,

$$Nu_{x,H} = 4.364 + 8.68 x^{*-0.506} e^{-0.041x^*} \quad (127)$$

Hicken [144] studied the same  $\textcircled{H}$  thermal entry problem as Siegel et al. [15] but with the non-uniform fluid temperature at inlet. He considered five different sinusoidal inlet fluid temperature profiles. He tabulated the eigenvalues and eigenconstants, and presented graphically the fluid bulk mean temperature  $\theta_{w-m}$  as a function of  $x^*$ .

Sparrow and Siegel [158] extended the analysis of Siegel et al. [15] by including the internal thermal energy generation. The thermal energy generation was allowed to vary in an arbitrary manner both longitudinally along the tube and radially across the cross section. Inman [159] experimentally studied the temperature distribution in laminar flow through an insulated circular tube with the internal thermal energy generation. His results were in excellent agreement with the theory prediction by Sparrow and Siegel [158].

Hsu [160] extended his work [157] by including the effect of axial heat conduction within the fluid for  $\textcircled{H}$  boundary condition. He considered the fluid entering at  $x = 0$  with uniform temperature profile, thus solved the problem for semi-infinite region ( $0 \leq x < \infty$ ). He tabulated first twelve eigenvalues and eigenconstants for the Péclét numbers of 5, 10, 20, 30, 50 and 100.

Hennecke [22] investigated the same problem as Hsu [160] i.e.,  $\textcircled{H}$  thermal entry length problem with inclusion of axial fluid heat conduction; but he considered the more consistent inlet fluid temperature condition, being uniform at  $x = -\infty$ . He solved the problem for the two semi-infinite region numerically by the finite difference method, and matched the solutions point by point at  $x = 0$ . He showed that while the value of Nusselt number at  $x = 0$  is infinite in the case of  $\textcircled{T}$  boundary condition, it has a finite value at  $x = 0$  which decreases with decreasing Péclet numbers for the  $\textcircled{H}$  boundary condition. The  $Nu_{x,H}$  were presented as a function of  $x' (= 2x^*)$  for  $Pe = 1, 2, 5, 10, 20$  and  $50$ . Unlike Hsu's [160] results, Hennecke's  $Nu_{x,H}$  has an inflection point at  $x^* \approx 0.0075$ .

Bes [153] also solved the same problem as Hennecke [22], and found that the longitudinal conduction is significant for  $Pe < 30$ .

Hsu [161] further considered the same problem as Hennecke [22], but solved it theoretically in a closed form. Hsu determined the first twenty eigenvalues and eigenfunctions for the heated and adiabatic regions. The  $Nu_{x,H}$  obtained by Hsu are in excellent agreement with the Hennecke's results.

Siegel et al. [15] also generalized the  $\textcircled{H}$  thermally developing flow problem to the case of arbitrary axial variations in heat flux by the superposition technique. For an arbitrary analytical axial wall heat flux distribution, Noyes [16] derived a closed form integrated solution for the local Nusselt number. Shapovalov [162] considered the arbitrary wall heat flux distribution with arbitrary initial condition and obtained the temperature distribution in terms of hypergeometric functions. Hsu [157] and Kuga [163] considered the sinusoidal axial wall heat flux. In the above cases, the peripheral wall heat flux distribution was assumed to be uniform. Bhattacharyya and Roy [164] considered

the variable peripheral wall heat flux distribution. They reported the eigenvalues and eigenconstants for the temperature distribution in the thermal entry region; and extended the thermal entry region problem to arbitrary wall heat flux in peripheral as well as the axial direction by applying Dutamel's superposition theorem.

#### 1.3.1.3. Finite Wall Thermal Resistance, $R_l$

Schenk and DuMoré [165] considered the finite thermal resistance at the wall of a circular tube. They tabulated the first three eigenvalues, eigenconstants, local Nusselt numbers and bulk mean fluid temperatures for the wall resistance parameter  $R_w = 1, 0.25, 0.025$  and  $0$ . The  $R_w = 0$  corresponds to the Graetz problem. The infinite series solution for the temperature distribution and  $Nu_{x,Rl}$  converges very slowly near the entrance region. Rosen and Scott [166] extended the Léveque solution for the finite wall resistance case. They presented the fluid bulk mean temperature and local Nusselt number in tabular and graphical form for various values of  $R_w$ . Sideman et al. [131] supplemented and extended the work of Schenk and DuMoré [165]. They presented first five eigenvalues and related constants for the thermal resistance parameter  $R_w = 1, 0.5, 0.25, 0.15, 0.10, 0.05, 0.025$  and  $0$ . Using the finite difference method, McKillop et al. [167] also analyzed the  $(R_l)$  thermal entrance problem for Newtonian and non-Newtonian fluids. The  $Nu_{x,Rl}$  were presented graphically for  $R_w = 0, 0.005, 0.025, 0.25, 1$  and  $\infty$ .

The fluid axial heat conduction has been neglected in the above analysis [131,165,167]. Hsu [132] also investigated the finite wall resistance thermal entry region problem with finite fluid axial heat conduction. He considered the wall thermal resistance parameter  $R_w = 0.25, .05$  and  $.005$ . For  $Pe = \infty$ , the first ten eigenvalues and related constants were presented; while for  $Pe = 100, 50,$

30, 20, 10 and 5, first twelve eigenvalues and related constants were presented. For  $Pe = 1$ , Hsu listed the first 20 eigenvalues and related constants.

#### 1.3.1.4 Radiant Flux Boundary Condition R2

Chen [134] analyzed the thermally developing and hydrodynamically fully developed laminar flow through a circular tube with the non-linear radiant-flux boundary condition of Eq. (12). He obtained an approximate solution in terms of the Liouville-Neumann series. He also carried out an exact iterative numerical solution to the same problem for a wide range of radiation parameter  $\gamma = (\epsilon_w \sigma T_e^5 D_h / k)$ . The results of  $Nu_{x,R2}$  were presented in tabular and graphical forms for  $\gamma = 0.1, 0.2, 0.5, 1, 2, 5, 10, 20$  and 50. In the range of  $0.001 \leq x^* \leq 0.1$  and  $\gamma \leq 20$ , his following approximation for  $Nu_{x,R2}$  agreed better than  $\pm 2$  percent with his numerical solution.

$$Nu_{x,R2} = \frac{2(0.928 - 0.023 \ln \gamma)}{\frac{11}{24} + \sum_{n=1}^{\infty} C_n R_n \exp(-2\beta_n^2 x^*)} \quad (128)$$

where  $C_n$ ,  $R_n$  and  $\beta_n$  are the eigenconstants, eigenfunctions at  $r = a$ , and eigenvalues for the H thermal entry region problem for the circular tube. They can be found from [157].

Benicio et al. [168] investigated the same problem analytically and experimentally. Analytically, the problem was solved by assuming the linearized radiation and an exponential kernel approximation. The wall heat flux  $q''_x/q''_e$  is plotted against  $x'$  ( $= 2x^*$ ) with the  $\gamma$  as a parameter. The results are in good agreement with Chen's result for  $x^* \geq 0.03$ . Their experimental results agree satisfactorily with the analysis, except in the region of entrance.

Sikka and Iqbal [169] considered the steady radiant heat flux being incident on one half of the tube circumference, while the fluid emanated heat through wall on all sides to absolute zero degree environment. This boundary condition may be approximated in some nuclear reactors and spacecraft. A solution by the finite difference method was obtained in the thermal entrance region for fully developed velocity profile. The local variations of wall temperature and the  $Nu_{x,R2}$  were delineated as a function of  $x' (= 2x^*)$  with  $\gamma$  and  $\psi$  as parameters, where  $\psi = \alpha_w^{1/3} a_r^{4/3} \sigma/k^{1/3}$ .

Kadaner et al. [135] also analyzed the radiant flux boundary condition thermal entry problem for the circular tube with fully developed laminar flow velocity profile. Graphically they presented  $Nu_{x,R2}$  as a function of  $x^*$  with  $\gamma$  as a parameter. The  $(H)$  and  $(T)$  local Nusselt number are shown as limiting cases when  $\gamma = 0$  and  $\infty$  respectively. Within the range of  $0.001 < x^* < 0.2$  and  $0.1 < \gamma < 50$  with ambient (outside fluid) temperature as zero, they presented the approximation

$$\frac{Nu_{x,R2}}{Nu_{x,H}} = 0.94 - \frac{0.0061 - 0.0053 \ln x^*}{1 + 0.0242 \ln x^*} \ln \gamma \quad (129)$$

which is accurate to within  $\pm 2$  percent of their solution.

### 1.3.2 Simultaneously Developing Flow

The thermal entry length problem for the circular tube with simultaneously developing velocity and temperature profile was first investigated numerically by Kays [12]. He considered the  $(T)$ ,  $(H)$  and  $(\Delta t)$  boundary conditions for the fluid with  $Pr = 0.7$ . The Langhaar velocity profile was employed. The radial velocity component and the fluid axial heat conduction [in Eq. (19a)] were neglected. The local and mean Nusselt numbers were tabulated and presented graphically. Goldberg [170] extended Kays' solution to

cover Prandtl number range of 0.5 to 5. Tien and Pawelek [171] analyzed the  $\textcircled{T}$  combined entry length problem for fluids with high Prandtl number. A solution was obtained by using Lévéque approximation and assuming very thin thermal boundary layer. The solution is thus valid for small  $x^*$ . They depicted the  $Nu_{x,T}$  and  $Nu_{m,T}$  as a function of  $4x^*$  (range  $10^{-5}$  to  $10^{-1}$ ) for  $Pr = 5, 10, 15, 20, 40$  and  $100$ .

Heaton et al. [80] used a different approach for the solution, though employing Langhaar velocity profile, and obtained a generalized entry region temperature profiles which could be used in the energy integral equation. The solutions were then obtained for the entire family of circular tube annuli for the constant axial heat flux boundary condition and  $Pr = 0.01, 0.7$  and  $10$ .

Petukhov et al. [172] also obtained the combined entry length solution for the laminar flow in a circular tube using Langhaar velocity profile. Other details are not known as the reference was not available to the authors.

Roy [173] considered three regions in the thermal entrance: simultaneous development of velocity and temperature profiles, fully developed velocity and developing temperature profiles, and both profiles developed. The problem was handled by an integral method for the  $\textcircled{H}$  boundary condition for  $Pr = 1, 10, 100$ , and  $1000$ .

Kakac and Özgü [112] employed Sparrow [83] velocity profile and obtained a numerical solution to the combined entry length problem for the  $\textcircled{T}$  and  $\textcircled{H}$  boundary condition and  $Pr = 0.7$ . The local Nusselt numbers determined were in good agreement with those of Ulrichson and Schmitz [174] for large  $x^*$ .

Ulrichson and Schmitz [174] refined Kays' work [12] by utilizing the axial velocity component of Langhaar solution and subsequently the radial component from the continuity equation. They found the effect of radial velocity on the

Table 8a. Circular duct  $Nu_{x,T}$ ,  $Nu_{m,T}$  and  $Nu_{x,H}$  as functions of  $x^*$  and  $Pr$  for simultaneously developing flow, from graphical results of Hornbeck [113]

$x^*$	$Nu_{x,T}$			$Nu_{m,T}$			$Nu_{x,T}$		
	Pr=0.7	Pr=2	Pr=5	Pr=0.7	Pr=2	Pr=5	Pr=0.7	Pr=2	Pr=5
0.0005	22.6	19.5	17.5	40.7	33.4	28.2	32.3	28.3	25.4
0.0006	21.0	18.1	16.1	37.8	31.0	26.6	29.8	26.4	23.7
0.0008	18.6	16.2	14.7	33.5	27.7	24.0	26.3	23.4	21.1
0.0010	16.8	14.8	13.5	30.6	25.2	22.1	23.7	21.2	19.2
0.0015	14.1	12.7	11.6	25.4	21.3	18.8	19.7	17.8	16.2
0.002	12.6	11.4	10.6	22.1	19.1	16.8	17.5	15.8	14.4
0.003	10.8	9.8	9.1	18.7	16.2	14.4	14.7	13.4	12.2
0.004	9.6	8.8	8.2	16.7	14.4	12.9	13.0	11.8	10.9
0.005	8.8	8.0	7.5	15.1	13.2	11.8	11.8	10.8	10.0
0.006	8.25	7.5	7.1	14.1	12.4	11.0	11.0	10.1	9.4
0.008	7.4	6.8	6.4	12.5	11.1	9.9	9.8	9.0	8.5
0.010	6.8	6.2	5.9	11.3	10.2	9.2	9.0	8.2	7.3
0.015	5.8	5.4	5.2	9.6	8.7	8.0	7.7	7.1	6.8
0.020	5.3	5.0	4.7	8.7	7.8	7.1	6.9	6.4	6.1
0.030	4.6	4.5	4.2	7.5	6.8	6.1	6.0	5.5	5.4
0.040	4.4	4.2	4.06	6.8	6.1	5.5	5.5	5.2	5.0
0.050	4.2	4.1	3.9	6.1	5.6	5.1	5.2	5.0	4.9
$\infty$	3.66	3.66	3.66	3.66	3.66	3.66	4.36	4.36	4.36

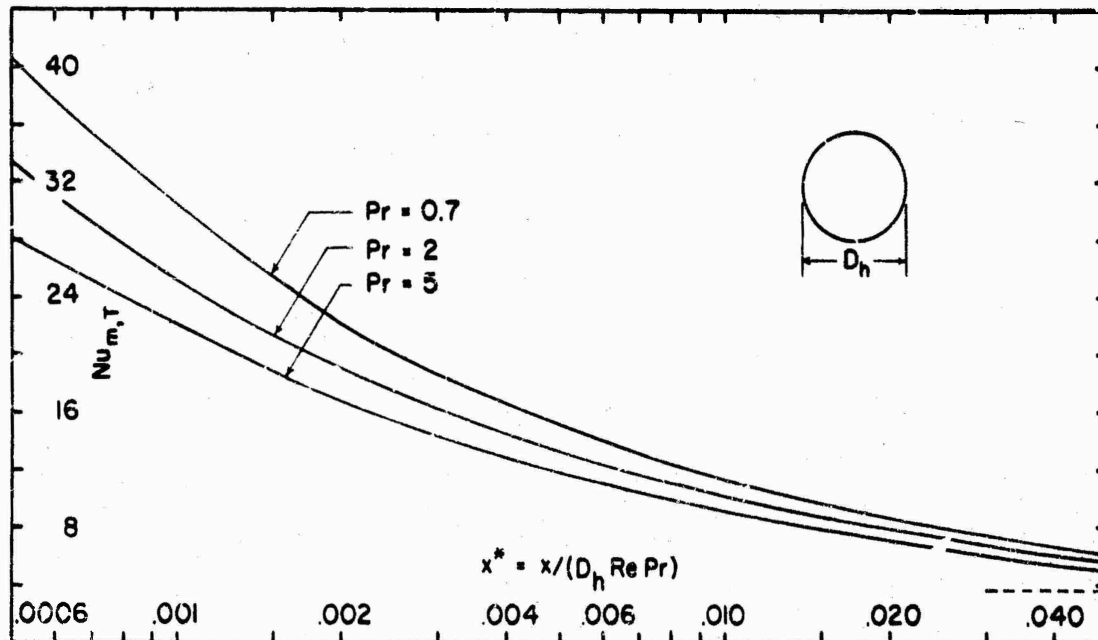


Fig. 12 Circular duct  $Nu_{m,T}$  as functions of  $x^*$  and  $Pe$  for simultaneously developing flow, from Hornbeck [113].

$Nu_x$  was significant only for  $x^* < 0.04$  for both  $\textcircled{T}$  and  $\textcircled{H}$  boundary condition and  $Pr = 0.7$ . In this region, the  $Nu_x$  obtained were lower than those determined by Kays [12]. Incidentally, the  $Nu_{x,T}$  and  $Nu_{x,H}$  are plotted against  $16x^*$  in present terminology, but the abscissa is misprinted consistently, it should have been  $x^*/1.6$  in [174].

Hornbeck [113] employed an all numerical finite difference method to solve to the combined entry length problem for the  $\textcircled{T}$  and  $\textcircled{H}$  boundary conditions and  $Pr = 0.7, 2$  and  $5$ . To obtain the velocity and subsequently temperature profiles in the entrance region, variable mesh sizes were used in the finite difference method, with the fine grid size near the entrance and near the wall with gradually increasing as the fully developed flow was approached. For  $Pr = 0.7$ , Hornbeck's  $Nu_{x,T}$  are consistently lower than those of Ulrichson and Schmitz, while  $Nu_{x,H}$  are in close agreement, except very close to the inlet. As no approximations were involved in determining the velocity profile, Hornbeck's solution is a refinement over the solution by Ulrichson and Schmitz [174]. Based on the graphical results of [113], as tabular results were not available, Figs. 12, 13, 14 and Table 8a were prepared for  $Nu_{x,T}$ ,  $Nu_{m,T}$  and  $Nu_{x,H}$  as functions of  $x^*$  and  $Pr$ .

Hornbeck also investigated the effect of variation in the inlet profile and viscous dissipation on the heat transfer. Using the modified Wang and Longwell [97] velocity profile at inlet, the obtained  $Nu_{m,T}$  and  $Nu_{x,H}$  versus  $x^*$  curves were found to be uniformly shifted upward and downward respectively from those obtained for uniform inlet velocity profile for  $x^* < 0.01$ . When the viscous dissipation was taken into account, the obtained  $Nu_{m,T}$  and  $Nu_{x,H}$  were also found to be uniformly shifted upward and downward respectively in comparison to those with no viscous dissipation.

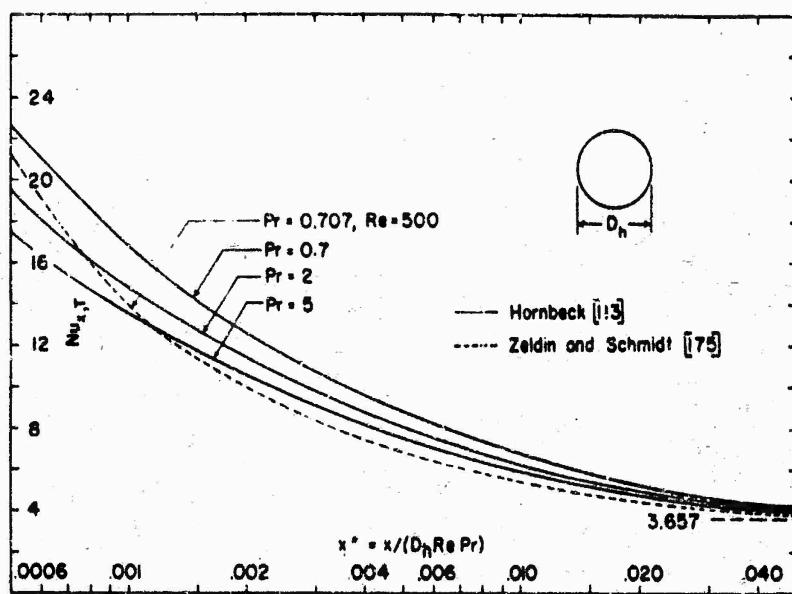


Fig. 13 Circular duct  $Nu_{x,T}$  as functions of  $x^*$  and  $Pe$  for simultaneously developing flow, from Hornbeck [113].

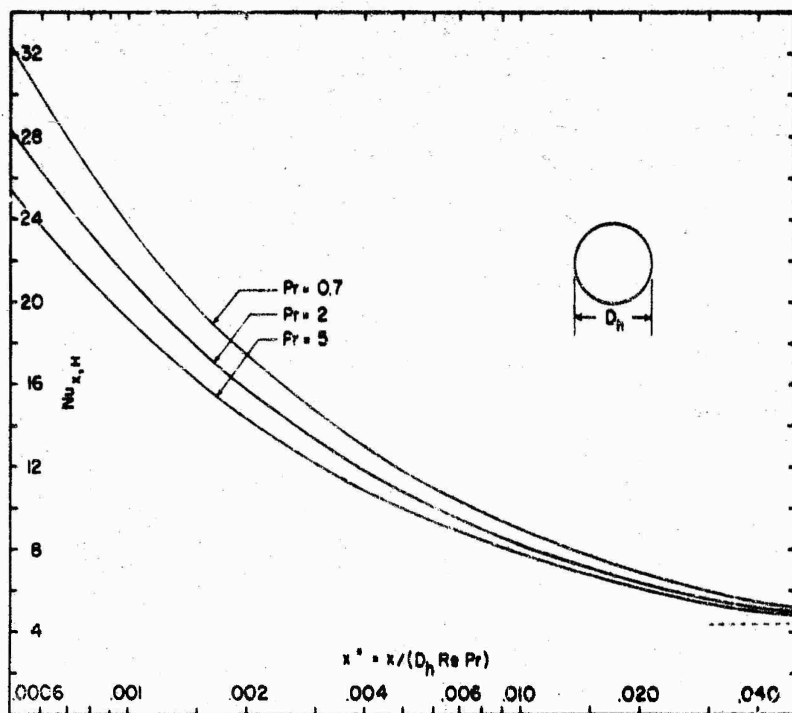


Fig. 14 Circular duct  $Nu_{x,H}$  as functions of  $x^*$  and  $Pe$  for simultaneously developing flow, from Hornbeck [113].

Bender [114] also numerically solved the combined entry length problem for the circular tube for the  $\Theta$  and  $H$  boundary conditions. Correspondingly, the fluid bulk mean temperature  $\theta_{m,T}$  and wall to fluid bulk mean temperature difference  $\theta_{w-m,H}$  were presented graphically as a function of  $x^*$  with Prandtl number as a parameter. The effect of temperature dependent fluid properties on the thermal entrance  $\theta_{w-m,H}$  was also considered.

Manohar [90] independently further refined the work of Ulrichson and Schmitz [174] by solving the non-linear momentum and energy equations numerically iteratively. For  $x^* < 0.04$ , Manohar obtained  $Nu_{x,T}$  lower and  $Nu_{x,H}$  higher than those by [174]. As Hornbeck [113] did not find this trend, this may be attributed to the possible error associated with the numeral values of the derivatives at the wall calculated from one sided difference formulae [137].

In the above analytical work, the effect of axial heat conduction in the fluid was neglected during the simultaneous development of the velocity and temperature profiles. This is a good approximation for the fluids with  $Pr > 0.1$ , but not for liquid metals with  $Pr < .03$ . McMordie and Emery [110] studied the simultaneous development of the velocity and  $H$  temperature profile in a circular tube with axial conduction effects in the fluid included. They used Langhaar's axial velocity profile and the subsequent radial velocity profile from the continuity equation. The local  $Nu_{x,H}$  were presented graphically for Prandtl numbers of 0.005, 0.01, 0.02, 0.03 and 0.7 as functions of  $x^*$  and Re numbers.

Recently, Zeldin and Schmidt [175] employed a velocity profile based on the complete Navier-Stokes equations and solved the  $\Theta$  thermal entry length problem Eq. (19a). They presented graphically the  $Nu_{x,T}$  and wall heat flux  $\Phi$  as a function of  $x'$  for  $Re = 500$  and  $Pr = 0.707$ . They also obtained a thermal entry length solution for the fully developed velocity profile.

Table 8b. Circular duct  $Nu_{x,T}$ ,  $\Phi_x$  and  $\Phi$  for fully developed and simultaneously developing flow,  $Re = 500$ ,  $Pr = 0.707$ , from Schmidt [138]

$x^* \times 10^2$	Fully Developed flow			Simultaneously developing flow		
	$Nu_{x,T}$	$\Phi_x$	$\Phi$	$Nu_{x,T}$	$\Phi_x$	$\Phi$
0.03258	20.65	20.10	23.25	20.38	27.42	53.17
0.06750	13.30	12.71	18.84	17.47	15.90	35.09
0.10395	10.89	10.24	16.02	13.62	12.15	27.20
0.14245	9.557	9.855	14.18	11.61	10.17	22.67
0.18315	8.566	7.916	12.86	10.32	8.893	19.66
0.22625	8.010	7.214	11.83	9.399	7.960	17.47
0.27195	7.496	6.657	11.00	8.693	7.251	15.79
0.32050	7.076	6.197	10.30	8.125	6.670	14.44
0.37720	6.724	5.805	9.705	7.653	6.162	13.32
0.42735	6.420	5.463	9.182	7.250	5.762	12.37
0.4863	6.155	5.160	8.716	6.901	5.393	11.55
0.5495	5.919	4.887	8.297	6.593	5.066	10.82
0.6175	5.702	4.638	7.914	6.318	4.770	10.18
0.6905	5.516	4.408	7.551	6.070	4.500	9.594
0.7690	5.341	4.195	7.233	5.845	4.252	9.064
0.8545	5.179	3.995	6.925	5.639	4.021	8.576
0.9475	5.030	3.806	6.636	5.449	3.806	8.123
1.0490	4.892	3.626	6.341	5.274	3.603	7.703
1.1600	4.762	3.453	6.098	5.111	3.411	7.308
1.2820	4.641	3.287	5.846	4.959	3.227	6.934
1.4170	4.528	3.127	5.603	4.818	3.052	6.579
1.5670	4.421	2.970	5.366	4.685	2.883	6.240
1.7345	4.321	2.816	5.130	4.561	2.719	5.915
1.9230	4.227	2.665	4.910	4.445	2.598	5.601
2.1370	4.140	2.515	4.687	4.337	2.401	5.297
2.3810	4.059	2.365	4.466	4.236	2.246	4.999
2.6625	3.984	2.215	4.246	4.143	2.902	4.708
2.9915	3.916	2.062	4.025	4.056	1.937	4.420
3.3800	3.855	1.906	3.801	3.979	1.781	4.135
3.346	3.802	1.743	3.573	3.910	1.620	3.848
4.416	3.758	1.573	3.338	3.849	1.454	3.599
5.130	3.722	1.392	3.092	3.796	1.280	3.264
6.045	3.695	1.197	2.831	3.754	1.094	2.958
7.265	3.677	0.9847	2.548	3.719	0.8955	2.635
8.975	3.665	0.7547	2.235	3.694	0.6835	2.288
11.540	3.659	0.5128	1.881	3.676	0.4634	1.908
15.810	3.657	0.2794	1.473	3.665	0.2521	1.483
24.360	3.656	0.09715	1.008	3.661	0.08760	1.009
50.00	3.655	0.01143	0.5026	3.661	0.01032	0.5019

They stated that the gas compression work term  $u(dp/dx)/J$  is not negligible for the gas; moreover, it is more appropriate to consider the gas as having a constant density along with constant  $\mu$  and  $k$ . With these idealizations, the energy Eq. (19a) is of the same form but the thermal diffusivity  $\alpha$  contains  $c_v$  instead of  $c_p$ . On this basis, with  $Pr = 0.505$  (air) based on  $c_v$  instead of 0.707 based on  $c_p$ , they determined the thermal entrance results. These are presented in Table 8b [138]. The  $Nu_{x,T}$  for simultaneously developing flow from this table are compared in Fig. 13 with Hornbeck's solution [113] obtained using the boundary layer type approximations.

To assess the order of magnitude of the gas compression work term  $u(dp/dx)/J$ , it will be compared with the convective term  $\rho c_p u_m (\partial t / \partial x)$  for  $(H)$  boundary condition (for which  $\partial t / \partial x$  is constant) as a convenience. If it is assumed that  $(dp/dx)$  is approximately constant, and both terms are integrated over the flow cross section area, the results will be  $u_m A_c (dp/dx)/J$  and  $(\rho u_m A_c) c_p (\partial t / \partial x)$ . Dividing these terms by the perimeter  $P$ , it can be shown that these terms are  $E_{std}$  [see Eq. (235)] and  $q''$  respectively. For a gas turbine regenerator application, the typical values of  $E_{std} = 0.005$   $hp/ft^2 \approx 12.5$  Btu/hr ft $^2$  and of  $q'' = 1500$  Btu/hr ft $^2$ . It can be concluded that the gas compression work would be negligible under these circumstances.

The  $Nu_{x,T}$  for  $Pr = 0.707$  shown in Fig. 13, derived for the two different sets of idealizations differ as much as 25%. Based on the above example (even though, it is for  $(H)$  rather than  $(T)$  and some additional idealizations are involved), the validity of idealizations and/or the numerical method of [175] is in question.

Recently, Butterworth and Hazell [111] considered the  $(H)$  heating started at different locations in the hydrodynamic entry length for  $Pr = 60 \sim 550$ . They used Langhaar's axial velocity profile. Their experimental results showed a close agreement with their theory predictions.

## 2. PARALLEL PLATES

The parallel plate duct is the simplest geometry amenable to mathematical treatment, even more so than the circular duct. Consequently laminar flow and heat transfer for the parallel plates have been analyzed in great detail. The analytical results for laminar flow and heat transfer follow.

### 2.1 Fully Developed Flow

The fully developed laminar velocity profile and friction factor for the plate spacing of  $2b$  with coordinate axes at the center are [3,176]

$$u = \frac{c_1}{2} (y^2 - b^2) \quad (130)$$

$$v_m = -\frac{1}{3} c_1 b^2 \quad (131)$$

$$fRe = 24 \quad (132)$$

The heat transfer results are described below separately for each of the boundary conditions.

#### 2.1.1 Uniform Wall Temperature and Wall Heat Flux, (T) and (H)

The (T) boundary condition problem was first studied by Nusselt [177] in 1923, and later independently by Léveque [99], Norris and Streid [178], and Hahnemann and Ghert [179]. Glaser [124] investigated the fully developed laminar heat transfer for (H) boundary conditions. The (H<sub>1</sub>), (H<sub>2</sub>) and (H<sub>3</sub>) boundary conditions are the same for parallel plates as is the case for the circular tube and is designated as the (H) boundary condition.

Depending upon the temperature or heat flux specified at either wall, there are four fundamental problems for the

heat transfer. These are shown in Fig. 15 and described below.

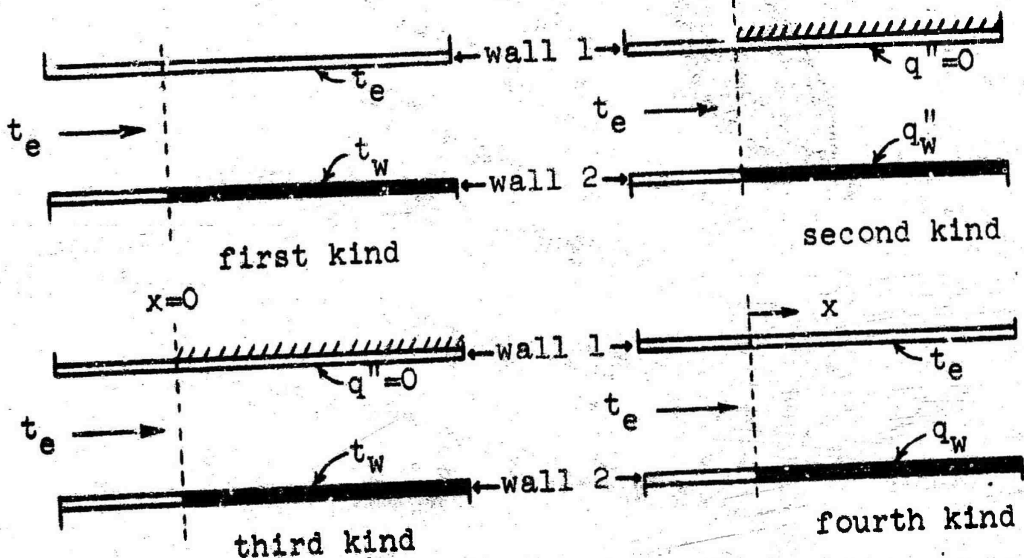


Fig. 15 Four fundamental problems for parallel plates

- (i) Fundamental problem of the first kind. On one wall a constant<sup>18</sup> temperature, different from the entering fluid temperature, is specified, while the other wall is at a constant temperature of the entering fluid.
- (ii) Fundamental problem of the second kind. On one wall a constant heat flux per unit length is specified, while the other wall is insulated (zero heat flux).
- (iii) Fundamental problem of the third kind. On one wall a constant temperature, different from the entering fluid temperature, is specified, while the other wall is insulated.

<sup>18</sup> Constant means constant both in time and space.

17. Fundamental problem of the fourth kind. On one wall a constant heat flux per unit length is specified, while the temperature of the other wall is constant at the temperature of the entering fluid.

McCuer, et al. [176] obtained the four fundamental solutions for the parallel plates. The fully developed temperature profiles corresponding to these four solutions are presented in Fig. 16 along with a thermal entrance profile.

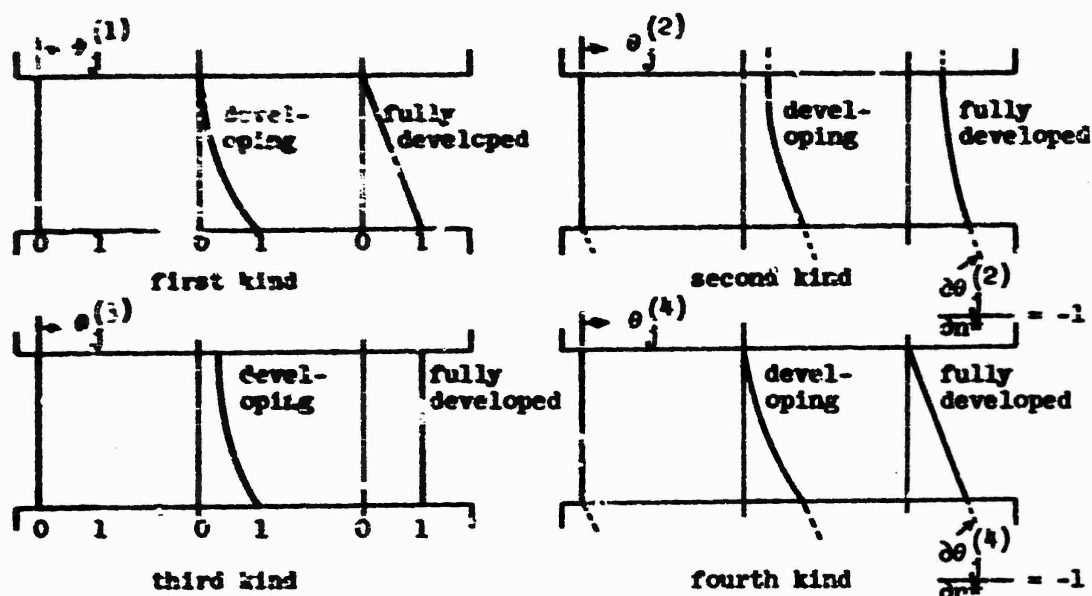


Fig. 16 Temperature profiles for four fundamental problems.

The dimensionless fluid temperatures and heat fluxes are defined as

$$\theta_j^{(1)}, \theta_j^{(3)} = \frac{t-t_e}{t_j-t_e} \quad (133a)$$

$$\theta_j^{(2)}, \theta_j^{(4)} = \frac{t-t_e}{q_j D_h / k} \quad (133b)$$

$$\phi_j^{(i)} = -D_h \frac{\partial \theta_j^{(i)}}{\partial n} \quad (134)$$

The suffix  $j$  stands for the heated surface  $j$ . The superscripts 1, 2 etc. stand for the fundamental solutions of first, second kind etc. The superscript i for the heat flux stands for 1, 2, 3 or 4 designating the fundamental solution.

The fully developed Nusselt numbers corresponding to these four solutions are

$$\text{First kind: } \text{Nu}_1 = \text{Nu}_2 = 4 \quad (135)$$

$$\text{Second kind: } \text{Nu}_1 = 0, \text{Nu}_2 = 5.385 \quad (136)$$

$$\text{Third kind: } \text{Nu}_1 = 9, \text{Nu}_2 = 4.861 \quad (137)$$

$$\text{Fourth kind: } \text{Nu}_1 = \text{Nu}_2 = 4 \quad (138)$$

where suffix 1 and 2 refer to walls 1 and 2 in Fig. 15. The Nusselt numbers are based on the temperature difference between bulk mean fluid temperature and the wall temperature.

As mentioned previously, if viscous dissipation and the internal thermal energy sources are neglected in energy Eq. (5), the resulting equation is linear and homogeneous; and then, any complex problem can be handled by the superposition of these four fundamental solutions. In particular, the fully developed Nusselt numbers for three cases of interest, as shown in Fig. 17, are as follows.

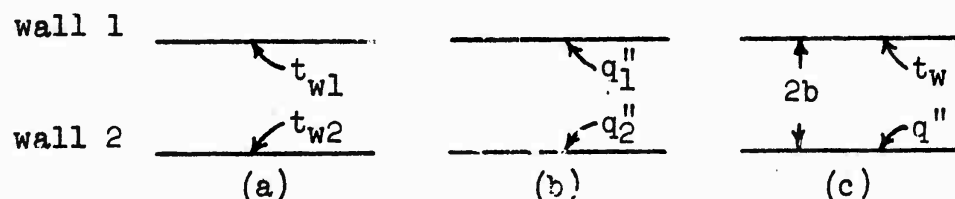


Fig. 17 Specification of wall temperatures and heat fluxes for parallel plates.

- (i) Constant but different temperatures specified at each wall, Fig. 17(a).

$$\text{If } t_{w1} \neq t_{w2}, \quad \text{Nu}_1 = 4, \quad \text{Nu}_2 = 1 \quad (139a)$$

$$\text{If } t_{w1} = t_{w2} = t_w, \quad \text{Nu}_T = 7.5407159 \quad (139b)$$

When the wall temperatures are unequal and  $L/r_h = \infty$ , Fig. 17a, the heat transfer is into the fluid at one wall and out of the other and this asymmetry is maintained in the limit as  $t_{w1}$  goes to  $t_{w2}$ . In contrast when  $t_{w1}, t_{w2} = t_w$ , a common magnitude, for  $L/r_h < \infty$  the heat transfer is symmetrical (either in or out) and this is maintained in the limit as  $L/r_h$  goes to  $\infty$ . Thus the apparent paradox of  $\text{Nu}_T \sim 1.9 \text{ Nu}_1$  in Eq. (139) is a result of comparing in the limit (and different limits) an asymmetrical heat transfer problem with a symmetrical one. In both situations the heat transfer flux goes to zero because the temperature difference for heat transfer goes to zero.

- (ii) Constant but different heat fluxes specified at each wall, Fig. 17(b).

$$\text{If } q_1'' \neq q_2'', \quad \text{Nu}_1 = \frac{140}{26-9(q_2''/q_1'')}, \quad \text{Nu}_2 = \frac{140}{26-9(q_1''/q_2'')} \quad (140a)$$

$$\text{If } q_1'' = q_2'', \quad \text{Nu}_H = 140/17 = 8.2352941 \quad (140b)$$

$$\text{If } q_1'' = 0 \quad (\text{the adiabatic wall}),$$

$$\text{Nu}_1 = 0, \quad \text{Nu}_2 = 5.3846154 \quad (140c)$$

- (iii) Constant temperature specified at one wall, uniform heat flux specified at the other wall ( $t_w \neq t_e$ ), Fig. 17(c).

$$\text{If } q'' \neq 0, \quad Nu_1 = 4, \quad Nu_2 = 4 \quad (141a)$$

$$\text{If } q'' = 0, \quad Nu_1 = 4.8618125, \quad Nu_2 = 0 \quad (141b)$$

Pahor and Strand [80] included the effect of axial heat conduction in the fluid for  $\Theta$  heat transfer problem. The  $\Theta$  temperature distribution was expressed in terms of the confluent hypergeometric functions. They graphically presented the fully developed  $Nu_T$  as a function of Pe number. They also formulated the following asymptotic formulae.

$$Nu_T = 7.540 \left( 1 + \frac{3.79}{Pe^2} + \dots \right) \quad Pe \gg 1 \quad (142a)$$

$$Nu_T = 8.118 \left( 1 - 0.031 Pe + \dots \right) \quad Pe \ll 1 \quad (142b)$$

Ash [123] also considered the effect of axial heat conduction in the fluid. The  $Nu_T$  as a function of Pe number are reported in Table 9.

Table 9. Parallel plates  $Nu_T$  as a function of Pe for fully developed laminar flow, from Ash [123].

Pe	$Nu_T$	Pe	$Nu_T$
$\infty$	7.5407	1.0572	7.9998
132.36	7.5408	0.8156	8.0242
92.24	7.5408	0.6508	8.0416
69.78	7.5408	0.5326	8.0546
28.86	7.5408	0.4444	8.0644
9.970	7.6310	0.02352	8.1144
3.548	7.8142	0.00616	8.1166
2.104	7.9084	0.000706	8.1176
1.4368	7.9640	0	8.118

Tao [36] included the internal heat generation for the laminar flow between parallel plates with  $(H)$  boundary condition and solved the problem by a complex variables technique. Tyagi [23] further extended the results of Tao by including viscous dissipation. The Nusselt number is given by Tyagi as

$$Nu_H = \frac{140}{17} \left[ \frac{1 + 3c_5 + c_6}{1 + \frac{42}{17}c_5 + \frac{8}{17}c_6} \right] \quad (143)$$

where  $c_5 = \frac{c_3}{c_4 b^2} = \frac{-1}{3 \left[ 1 + \frac{4q''}{SD_h} \right]}$  (144)

$$c_6 = \frac{\mu c_1}{kc_2} = \frac{-48\mu u_m^2}{D_h^2 \left[ S + \frac{4q''}{D_h} \right] Jg_c} \quad (145)$$

For special cases of no viscous dissipation  $c_6 = 0$ , and no internal thermal energy generation  $c_5 = 0$ .

### 2.1.2 Exponential Wall Heat Flux, $(H^4)$

Graber [128] studied the axial exponential wall heat flux distribution for parallel plates by introducing a parameter  $F_o$  defined in Section V.1.1.3. The  $Nu_{H4}/Nu_{H1}$  is graphically presented as a function of  $F_o$  (range from -2 to 8) in [128].

### 2.1.3 Finite Wall Thermal Resistance, $(R1)$

Based on the Sideman et al. [131] results for the thermal entry length solution for the  $(R1)$  boundary condition, the fully developed  $Nu_{R1}$  and  $Nu_o$  are calculated and presented in Table 3.

## 2.2 Hydrodynamically Developing Flow

Hydrodynamic entry length problem for parallel plates

Table 10. Parallel plates  $u/u_m$  and flow  $Q$  as a function  
of  $x^+$  for developing laminar flow, from Bodoia  
[181]

$y/b \diagdown x^+$	0.0625	0.125	0.250	0.375	0.500	0.625	0.750
0	1.0615	1.0751	1.1013	1.1244	1.1443	1.1615	1.1767
.1	1.0615	1.0751	1.1013	1.1244	1.1443	1.1615	1.1767
.2	1.0615	1.0751	1.1013	1.1244	1.1443	1.1615	1.1766
.3	1.0615	1.0751	1.1013	1.1244	1.1442	1.1613	1.1763
.4	1.0615	1.0751	1.1012	1.1243	1.1438	1.1604	1.1745
.5	1.0615	1.0751	1.1010	1.1234	1.1414	1.1555	1.1665
.6	1.0615	1.0750	1.0993	1.1176	1.1290	1.1351	1.1373
.7	1.0612	1.0725	1.0863	1.0874	1.0788	1.0655	1.0501
.8	1.0551	1.0485	1.0132	0.9665	0.9204	0.8798	0.8455
.9	0.9587	0.8655	0.7194	0.6204	0.5567	0.5136	0.4832
1.0	0.0000	0.0000	0.0000	0.0000	0.0000	0.0000	0.0000
Q	1.011	1.009	1.005	1.003	1.002	1.002	1.001

$y/b \diagdown x^+$	1.000	1.250	1.500	1.750	2.000	2.500	3.125
0	1.2031	1.2259	1.2463	1.2648	1.2818	1.3121	1.3441
.1	1.2030	1.2258	1.2460	1.2643	1.2811	1.3105	1.341
.2	1.2028	1.2252	1.2448	1.2623	1.2778	1.3043	1.3306
.3	1.2017	1.2228	1.2406	1.2556	1.2684	1.2887	1.3067
.4	1.1972	1.2144	1.2275	1.2373	1.2447	1.2542	1.2601
.5	1.1813	1.1893	1.1928	1.1935	1.1923	1.1871	1.1786
.6	1.1339	1.1253	1.1144	1.1030	1.0918	1.0715	1.0504
.7	1.0185	0.9896	0.9644	0.9429	0.9246	0.8950	0.8677
.8	0.7922	0.7535	0.7241	0.7011	0.6825	0.6541	0.6291
.9	0.4427	0.4162	0.3971	0.3825	0.3708	0.3534	0.3383
1.0	0.0000	0.0000	0.0000	0.0000	0.0000	0.0000	0.0000
Q	1.001	1.001	1.001	1.000	1.000	1.000	1.000

$y/b \diagdown x^+$	3.750	5.000	6.250	9.375	12.5	62.5	$\infty$
0	1.3707	1.4111	1.4388	1.4758	1.4903	1.499999	1.500
.1	1.3663	1.4039	1.4292	1.4629	1.4762	1.485000	1.485
.2	1.3511	1.3803	1.3993	1.4239	1.4336	1.440000	1.440
.3	1.3195	1.3357	1.3454	1.3573	1.3619	1.364000	1.365
.4	1.2626	1.2635	1.2628	1.2611	1.2604	1.260000	1.260
.5	1.1703	1.1565	1.1467	1.1336	1.1284	1.124999	1.125
.6	1.0337	1.0095	0.9938	0.9733	0.9553	0.959999	0.960
.7	0.8475	0.8197	0.8022	0.7796	0.7708	0.765000	0.765
.8	0.6112	0.5870	0.5720	0.5526	0.5451	0.540000	0.540
.9	0.3275	0.3132	0.3042	0.2926	0.2880	0.250000	0.285
1.0	0.0000	0.0000	0.0000	0.0000	0.0000	0.000000	0.000
Q	1.000	1.000	1.000	1.000	1.000	0.999999	1.000

Table 11a. Parallel plates  $u_{\text{max}}/u_{\infty}$ ,  $\Delta p^*$ ,  $f_{\text{app}} \text{Re}$  and  $K(x)$  as a function of  $x^+$  ( $= x/D_h \text{Re}$ ) for developing laminar flow, from Bodota [181]

$x/(D_h \text{Re})$	$u_{\text{max}}/u_{\infty}$	$\Delta p^*$	$f_{\text{app}} \text{Re}$	$K(x)$
0.000063	1.0615	0.12420	99.000	0.1102
0.000125	1.0751	0.15328	306.560	0.1413
0.000250	1.1013	0.21006	210.060	0.1861
0.000375	1.124	0.26150	174.332	0.2259
0.000500	1.1443	0.30648	153.140	0.2585
0.000625	1.1615	0.34612	130.446	0.2861
0.000750	1.1747	0.38164	117.113	0.3096
0.001000	1.2031	0.44436	111.090	0.3456
0.001250	1.2259	0.49984	99.968	0.3798
0.001500	1.2463	0.55044	91.740	0.4064
0.001750	1.2648	0.59746	85.351	0.4295
0.002000	1.2810	0.64170	80.212	0.4497
0.002500	1.3121	0.72384	72.384	0.4838
0.003125	1.3441	0.81784	65.427	0.5178
0.003750	1.3707	0.90498	60.332	0.5450
0.005000	1.4111	1.06516	53.258	0.5852
0.006250	1.4500	1.21262	48.505	0.6126
0.009375	1.4758	1.55014	41.337	0.6501
0.012500	1.4903	1.86538	37.308	0.6654
0.062500	1.49999	6.676036	26.704	0.6760

Table 11b. Parallel plates  $f_{\text{app}} \text{Re}$  and  $K(x)$  as a function of  $x^+$  for  $\text{Re} = 10000$ , 500 and 100, from Schmidt [138]

$x/(D_h \text{Re})$	Re = 10,000		Re = 500		Re = 100	
	$f_{\text{app}} \text{Re}$	$K(x)$	$f_{\text{app}} \text{Re}$	$K(x)$	$f_{\text{app}} \text{Re}$	$K(x)$
0.0000307	618.104	0.0739	1016.318	0.1228		
0.0000672	502.670	0.0921	904.934	0.1493	227.989	0.04011
0.0000648	425.837	0.1063	669.819	0.1695	316.489	0.07790
0.0000933	372.910	0.1109	576.121	0.1867	347.771	0.1106
0.0001029	333.636	0.1308	506.678	0.2020	353.460	0.1390
0.0001237	302.875	0.1420	452.534	0.2161	346.958	0.1638
0.0001458	277.851	0.1527	408.697	0.2291	334.701	0.1859
0.0001664	256.917	0.1632	372.178	0.2413	319.983	0.2059
0.01944	236.016	0.1735	341.077	0.2528	304.524	0.2244
0.0002213	223.637	0.1830	314.118	0.2639	289.207	0.2418
0.0002500	209.680	0.1937	290.415	0.2744	274.485	0.2585
0.0002809	197.381	0.2038	259.327	0.2846	260.442	0.2746
0.0003141	186.270	0.2139	250.381	0.2945	247.207	0.2905
0.0003350	175.139	0.2242	233.220	0.3041	234.722	0.3062
0.0003689	166.827	0.2346	217.559	0.3136	222.930	0.3219
0.0004312	158.206	0.2453	203.214	0.3229	211.763	0.3376
0.0004773	150.171	0.2561	189.983	0.3321	201.153	0.3525
0.0005278	142.639	0.2673	177.741	0.3415	191.034	0.3695
0.0005833	135.539	0.2789	166.377	0.3509	181.348	0.3858
0.0006447	128.812	0.2909	155.798	0.3405	172.038	0.4024
0.0007130	122.496	0.3035	145.926	0.3705	163.054	0.4194
0.0007892	116.279	0.3150	136.692	0.3810	154.350	0.4368
0.0008750	111.390	0.3304	128.513	0.3921	145.880	0.4546
0.0009722	106.706	0.3450	119.890	0.4040	137.603	0.4729
0.0010833	99.194	0.3605	112.205	0.4169	129.479	0.4917
0.0012115	93.625	0.3772	104.922	0.4309	121.468	0.5111
0.0013611	88.368	0.3951	97.983	0.4466	113.533	0.5310
0.0015379	83.392	0.4146	91.329	0.4634	105.640	0.5514
0.0017500	78.262	0.4358	86.899	0.4823	97.757	0.5723
0.0020093	73.137	0.4592	78.631	0.5034	89.860	0.5936
0.0023333	67.966	0.4850	72.452	0.5269	81.971	0.6154
0.0027500	62.681	0.5135	66.280	0.5531	73.966	0.6376
0.0033056	57.193	0.5467	60.014	0.5820	65.963	0.6606
0.0040833	51.365	0.5780	53.530	0.6130	57.899	0.6843
0.0052500	45.120	0.6115	46.687	0.6444	49.706	0.7078
0.0071944	38.246	0.6413	39.347	0.6724	41.310	0.7284
0.0110833	30.921	0.6615	31.596	0.6914	32.749	0.7426
0.03227500	23.349	0.6688	23.674	0.6983	24.221	0.7481

was first investigated by Schiller [21] by considering two regions in the flow cross section: (i) a boundary layer developing near the wall with impressed pressure gradient and (ii) a straight potential core in the remaining central cross section. This method provides good results at the entrance, but poor results downstream.

Schlichting [71,72] applied a perturbation method to solve the hydrodynamic entry length problem. His method consisted of smoothly joining two asymptotic series solutions, one based on perturbed Blasius' solution of external boundary layer development in the entrance region and second perturbed Hagen-Poiseuille solution of parabolic velocity distribution at the downstream. Collins and Schowalter [74] refined the solution by retaining more terms in Schlichting's upstream and downstream series velocity distribution. Their results approach to the numerical results of Bodoia and Osterle [87] described below.

For parallel plates, Han [77] used the same method of linearization of momentum equation as Langhaar [75] used for the circular tube. Sparrow et al. [83] used the stretched coordinate linearization, Eq. (106). Their results are in good agreement with Bodoia and Osterle's [87] numerical results.

Bodoia and Osterle [87] solved the problem numerically by linearizing the momentum equation at any cross section  $x = x_1$  by means of velocity at  $x = x_1 - \Delta x$ . The dimensionless velocity and pressure drop were calculated by the finite difference method using nine grid points between the centerline of the channel and one wall. Their results from [181] are presented in Tables 10 and 11a. The flow  $Q$  was first determined by evaluating the velocity profile by finite difference method and then numerically integrating the velocity profile. Theoretically  $Q$  should be 1. The variation of flow was found up to 1.1 percent from  $X^+ = 0$ .

to  $x^+ = 1.75$  ( $x^+ = 10^3 x^+$ ), thus establishing the accuracy of the solution. The convergence of solution was checked by considering fourteen instead of nine grid points for  $x^+$  up to 1. The error incurred was 0.2 percent, well within the inherent error of the finite difference formulation.

In all of the above solutions, the velocity distribution at the entrance was assumed to be uniform, and the idealizations made that the  $\mu(\partial^2 u / \partial x^2)$  and  $\partial p / \partial y$  terms in the momentum equations were negligible (same as boundary layer idealizations). Wang and Longwell [97] solved the complete Navier-Stokes equations for the parallel plates at  $Re = 300$ . Two cases were studied: (i) flat velocity distribution at the entrance, and (ii) flat velocity distribution far upstream of the entrance. Numerical results were presented for the velocity distribution and the pressure drop in the entrance region. The authors concluded that if the velocity distribution and the pressure gradients were required near the entrance region, the boundary layer type idealizations were not appropriate and full differential equations must be solved with realistic boundary conditions. Gillis and Brandt [98] also solved independently the complete Navier-Stokes equations for the parallel plates. Schmidt and Zeldin [96] also obtained a solution to complete Navier-Stokes equations. They reported non-dimensional pressure distribution and the cross sectional area average  $\bar{K}(x)$  for  $Re = 100, 500$  and  $10,000$ . Their  $f_{app} Re$  and  $\bar{K}(x)$  values are presented in Table 11b [138].

### 2.3 Thermally Developing Flow

#### 2.3.1 Hydrodynamically Developed Flow

##### 2.3.1.1 Fundamental Solutions of First and Second Kind

###### (a) Specified Wall Temperature Distribution

Thermal entry solutions for flow between parallel plates obtained up to 1961 are summarized by McCuen et

al. [176]. An approach similar to Graetz [117,118] was applied by Nusselt [177] for thermal entry length solution with  $\mathbb{T}$  boundary condition. As discussed in the circular duct section, this problem is known as the Graetz or Graetz-Nusselt problem.

Nusselt's infinite series solution was very slowly converging near the entrance region. Léveque [99,1] alleviated this difficulty by an approximate integral-type approach near the entrance region, and also obtained a solution for non-uniform wall temperature case.

An independent verification of Nusselt's result was done by Norris and Streid [178], Purday [182], Prins et al. [183], and Yih and Cermak [184]. Thus the determination of first three eigenvalues and eigenfunctions of series solution for  $Nu_{x,T}$  was completed. For higher eigenvalues and eigenfunctions, Sellers et al. [13] extended the Graetz-Nusselt problem for the circular tube and parallel plates by employing the WKBJ approximate method.<sup>19</sup> They derived the asymptotic expressions for the eigenvalues and eigenconstants. They presented the first ten eigenvalues and related constants from 0 to 4 decimal point accuracy. For the same problem, Brown [141] refined the work of Sellers et al. and reported the first ten eigenvalues and eigenconstants to ten decimal point accuracy.

Gupta [62] approached the Graetz-Nusselt problem by a variational method. Krishnamurty and Rao [185] employed Léveque approximation and derived an approximate formula for  $Nu_{x,T}$  with one or both sides heated. Empirically, the effect of natural convection and the temperature dependent viscosity were included in the approximate formula. Chandler

---

<sup>19</sup>The WKBJ method reduces a singular perturbation problem of an ordinary differential equation to a regular perturbation problem. The asymptotic solution is then obtained in terms of the perturbed parameter (e.g. large eigenvalue).

Table 12. Parallel plates energy content of the fluid for developing temperature profile (developed velocity profile) when fluid axial heat conduction is considered, from Schmidt [138]

Pe = 10		Pe = 25		Pe = 50		Pe = 100		x*	energy content				
x*	energy content	x*	energy content	x*	energy content	x*	energy content		Pe=200	Pe=300	Pe=400		
.000163	.00840	.000164	.00841	.000164	.00842	.000164	.00843	.00164	.6791	.8229	.8914		
.000337	.01111	.000337	.01111	.000337	.01111	.000337	.01111	.00337	.7024	.8362	.8998		
.000772	.01498	.000772	.01498	.000772	.01498	.000772	.01498	.00772	.5654	.9188			
.001543	.01886	.001543	.01886	.001543	.01886	.001543	.01886	.001543	.7816	.8853	.9114		
.003087	.03611	.003087	.03611	.003087	.03611	.003087	.03611	.003087	.8260	.9108	.9475		
.006277	.07636	.006277	.07636	.006277	.07636	.006277	.07636	.006277	.8551	.9269	.9571		
.012555	.1514	.012555	.1514	.012555	.1514	.012555	.1514	.012555	.8761	.9382	.9639		
.025110	.3028	.025110	.3028	.025110	.3028	.025110	.3028	.025110	.8924	.9468	.9693		
.050220	.6056	.050220	.6056	.050220	.6056	.050220	.6056	.050220	.9056	.9537	.9731		
.099440	.1293	.099440	.1293	.099440	.1293	.099440	.1293	.099440	.9167	.9593	.9765		
.198880	.2586	.198880	.2586	.198880	.2586	.198880	.2586	.198880	.9262	.9642	.9793		
.397760	.5172	.397760	.5172	.397760	.5172	.397760	.5172	.397760	.9346	.9684	.9817		
.795520	.1034	.795520	.1034	.795520	.1034	.795520	.1034	.795520	.9420	.9721	.9859		
.159100	.2068	.159100	.2068	.159100	.2068	.159100	.2068	.159100	.9489	.9754	.9877		
.318200	.4134	.318200	.4134	.318200	.4134	.318200	.4134	.318200	.9551	.9785	.9893		
.636400	.8268	.636400	.8268	.636400	.8268	.636400	.8268	.636400	.9693				
.127400	.1652	.127400	.1652	.127400	.1652	.127400	.1652	.127400	.9721				
Pe = 1		Pe = 1		Pe = 1		Pe = 1							
								.02208	.9048	.9193	.9813	.9908	
								.03236	.9186	.9193	.9840	.9923	
								.04487	.9310	.92564	.9864	.9934	
								.07381	.9406	.03022	.9875		
								.09726	.00237	.2600	.9488	.9885	.9940
								.14752	.008				
								.2308	.023				
								1.0000	.0331				

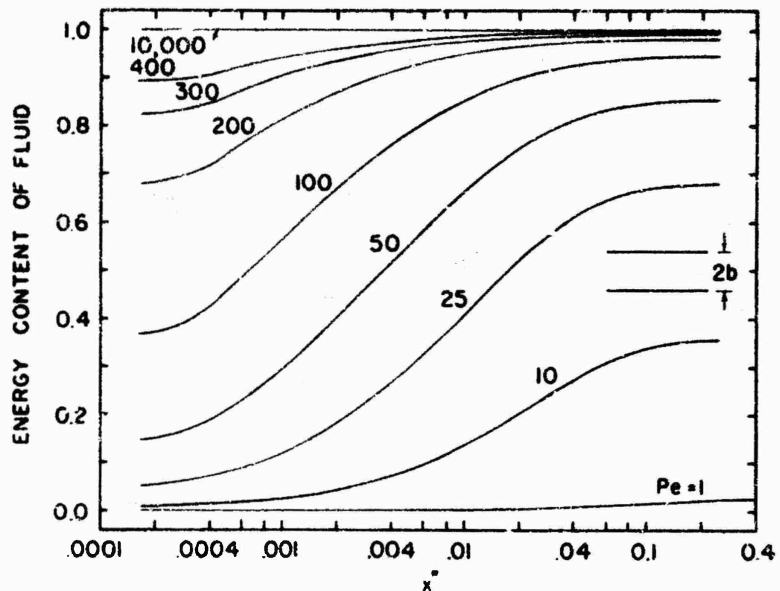


Fig. 18 Parallel plates energy content of the fluid for developing temperature profile when fluid axial heat conduction is considered, from Schmidt [138].

et al. [109] applied the Monte Carlo method to solve the Graetz-Nusselt problem for the parallel plates.

Bodnarescu [186] solved the Graetz-Nusselt problem and also considered the effect of axial heat conduction in fluid. Agrawal [187] included the effect of axial heat conduction and viscous dissipation in the fluid. He presented the eigenfunctions by infinite Fourier-sine series and derived an expression for the local temperature distribution and  $Nu_{x,T}$ , and outlined a detailed solution for  $Pe = 1$ . Bes [153] also included the effect of axial heat conduction. He found that for  $Pe < 30$ , the effect of axial heat conduction within the fluid is significant. Schmidt and Zeldin [30] also solved the Graetz-Nusselt problem with fluid axial heat conduction included. They employed the finite difference method for the semi-infinite region ( $0 \leq x < \infty$ ) with uniform temperature at inlet. They presented graphically the  $Nu_{x,T}$  and  $\Phi$  as a function of  $x'$  ( $= 2x^*$ ) with  $Pe$  as a parameter. Similar to the circular tube case, they also presented the energy content of the fluid as functions of  $x'$  and  $Pe$ . Their results [138] for the energy content of the fluid are presented in Table 12 and Fig. 18.

Sparrow et al. [188] included the effect of thermal energy sources within the fluid and obtained the thermal entry solution for both surfaces at equal and uniform temperatures as well as arbitrary temperature distribution. The thermal energy sources were assumed to have arbitrary longitudinal as well as cross sectionally symmetric transverse variations. The solution was obtained by the Graetz method. The first ten eigenvalues and eigenconstants for both walls at equal and uniform temperatures were presented in tabular form [188].

In all the following specified wall temperature cases considered, the effect of axial heat conduction, viscous dissipation and the thermal energy sources within the fluid

are neglected. Yih and Cermak [184] in 1951 used the superposition method and arrived at solutions for variable and unequal wall temperatures and insulated boundary conditions. The Yih and Cermak method was not generally used until it was outlined by Klein and Tribus [189] in 1953. Schenk and Beckers [190] considered a more general problem including wall thermal resistance and arbitrary inlet fluid distribution. Cess and Shaffer [191] summarized the first three even [13] and first three odd [184,190] eigenvalues and eigenconstants for the uniform and unequal wall temperatures, with asymptotic expressions for higher eigenvalues and eigenconstants. McCuen et al. [176] also solved the unequal wall temperature problem by superposition method and reported first four even and first three odd eigenvalues and eigenconstants, with asymptotic formulae for higher values. Hatton and Turton [192] independently solved the same problem, uniform and unequal wall temperatures. They reported the odd and even first eight (16 total), eigenvalues and eigenconstants with asymptotic formulae for higher values.

Sadikov used simplified energy Eq. (107) and solved the thermal entry length problem for parallel plates with entering fluid at uniform temperature [105] and nonuniform temperature [106]. In both cases, the wall temperature was assumed linearly varying with the axial distance. He presented graphically the local temperature distribution and the Nusselt numbers as a function of the axial distance.

#### (b) Specified Wall Heat Flux Distribution

The thermal entry length problem for uniform and equal wall heat fluxes,  $\textcircled{H}$  boundary condition, was first solved by Cess and Shaffer [193] using the method suggested by Siegel et al. [15]. They reported first three eigenvalues and constants for this problem with asymptotic expressions for higher values. Sparrow and Siegel [102] applied a variational method to the thermal entry length problem with equal and uniform wall heat fluxes.

Sparrow et al. [188] included the effect of thermal energy sources and obtained a thermal entry length solution for uniform and equal as well as arbitrary wall heat fluxes. They reported the first ten eigenvalues and constants in tabular form.

Hsu [161] theoretically investigated the effect of axial heat conduction within the fluid for the  $\textcircled{H}$  boundary condition. He considered the uniform fluid temperature profile at  $x = -\infty$ , the duct region from  $x = -\infty$  to  $x = 0$  isothermal at entering fluid temperature, and the uniform and equal wall heat fluxes from  $x = 0$  to  $x = \infty$ . He determined the first twenty eigenvalues and eigenconstants for the heated and adiabatic regions. The  $Nu_{x,H}$  were presented graphically as a function of  $32x^*/3$  with  $Pe$  as a parameter. The values of  $Pe$  used were 1, 2.5, 5, 10, 20, 30, 45 and  $\infty$ . In this plot, like the circular tube case, for finite values of  $Pe$ , the  $Nu_{x,H}$  is finite at  $x^* = 0$  and has an inflection point at  $x^* \approx 0.0015$ .

Cess and Shaffer [193] also applied the superposition theorem and presented the case of uniform and equal wall heat fluxes on both walls, but having arbitrary axial distribution. Cess and Shaffer [194] further extended their work by considering the uniform as well as arbitrary but unequal wall heat fluxes. For this problem, they reported first four odd eigenvalues and eigenconstants. Formulae were presented for higher values. The complete solution to this problem is obtained by combining these odd quantities with the even eigenvalues and constants determined for uniform and equal wall heat fluxes case [193]. They then generalized to arbitrary prescribed wall heat flux case. McCuen et al. [176] also presented the first three even and four odd eigenvalues and constants, and generalized the solution for the prescribed arbitrary axial wall heat flux distribution.

### 2.3.1.2 Fundamental Solutions of Third and Fourth Kind

The above solutions complete the fundamental solutions of first and second kind (Fig. 15) for the parallel plates. McCuen et al. [176] also obtained the thermal entry length solutions for the boundary conditions of the third and fourth kind. They summarized the results in tabular and graphical form for all four fundamental boundary conditions. With these results, the thermal entry length solution for any arbitrary combinations of wall heat fluxes and temperatures can be worked out provided that the axial heat conduction, viscous dissipation and thermal energy sources within the fluid are negligible.

### 2.3.1.3 Finite Wall Thermal Resistance

Does de Bye and Schenk [195] solved the thermal entry length problem for finite wall resistance ( $R_w = .025$  and  $.25$ ) with equal wall temperatures. Berry [196] also considered finite wall resistance for circular tube and parallel plates, but examples were worked out only for slug flow. Schenk [197] extended Berry's work considering fully developed laminar flow. Schenk and Beckers [198] dealt with the case of finite wall resistance and nonuniform inlet temperature profile. The calculations were made for a linear transverse temperature distribution at inlet with wall resistance parameter  $R_w = 0, 0.125$  and  $\infty$ . Butler and Plewes [199] treated the case of one wall at a uniform temperature ( $R_w = 0$ ) and the other wall insulated. Schenk [200] again solved this problem with the case of uninsulated wall having a finite thermal resistance,  $R_w = 0, 0.05$  and  $0.25$ . Dennis and Poots [201] used the Rayleigh approximate method to solve the problem treated by Does De Bye and Schenk as discussed above.

Sideman et al. [131] supplemented and extended the work of Schenk et al. [195,198] for the case of finite wall resistance. First five eigenvalues and eigenconstants were

tabulated for the wall thermal resistance parameter  $R_w = 0$ , 0.0125, 0.025, 0.05, 0.075, 0.125, 0.25 and 0.5. This thermal entrance solution is valid for fully developed laminar flow between parallel plates when neglecting the axial heat conduction, viscous dissipation and internal thermal energy generation. Sideman et al. [131] assumed a known value of the constant surface resistance for the thermal entry length solution. However, Davis and Gill [18] investigated the wall conduction effects on steady-state laminar Poiseuille-Couette flow<sup>20</sup> through parallel plates without a priori knowledge of the surface resistance. One wall was specified to be at the temperature of the entering fluid while the heat flux from outside to the other wall was specified constant. They concluded that the axial conduction in the wall of a heat transfer apparatus could significantly affect the temperature field in the fluid phase and lower the Nusselt number associated with the heat transfer.

### 2.3.2 Simultaneously Developing Flow

Simultaneous development of velocity and temperature profile for parallel plates was first considered by Sparrow [202] for the equal and uniform wall temperatures as well as one wall at uniform temperature and the other wall being insulated. Sparrow used Schiller's velocity profile and employed Kármán-Pohlhausen integral method. Slezkin [203] and Murakawa [204] considered theoretically simultaneous development of velocity and temperature distribution in the entrance region of tubes and ducts, but they did not present exact solutions of momentum and energy equations specifically. Stephan [205] employed approximate series solution for constant wall temperature case, and the average entrance region Nusselt numbers were approximated for  $\text{Pr}$  range of 0.1 to 1000 by the empirical relation

---

<sup>20</sup>See footnotes on p. 22

$$Nu_{m,T} = 7.55 + \frac{0.024(x^*)^{1.14}}{1 + 0.0358(x^*)^{0.64} (Pr)^{0.17}} \quad (146)$$

Hwan and Fan [115], utilizing the hydrodynamic entry length solution of Bodoia and Osterle [37], numerically solved the energy equation in the entrance region of parallel plates. The uniform and equal wall temperature case was investigated in Prandtl number range of 0.01 to 50. Their results agree with Eq. (146) within 3 percent. Mercer et al. [206] also solved numerically the equal wall temperature problem as well as one wall at a uniform temperature, the other being insulated. They reported results for a  $Pr = 0.7$  along with the results of an experimental investigation, and presented equations summarizing theoretical results. Miller and Lundberg [207] extended the work of Refs. [115,206] for a boundary condition of uniform, but unequal wall temperatures employing Bodoia velocity distribution [181].

Siegel and Sparrow [208] solved the case of equal and uniform wall heat fluxes by the same method used by Sparrow [202], i.e., employing Schiller's velocity profile. The local  $Nu_{x,H}$  were presented as functions of  $x^*$  and Prandtl numbers (from 0.01 to 50). Using a velocity profile based on Langhaar's approach, Han [77] also solved the equal and uniform wall heat flux case for the entrance region. The rate of approach of his local Nusselt number to its asymptotic value is quite different from Siegel and Sparrow's [208] approximate method. Miller [209] showed that Han's solution was in poor agreement with a similar solution employing the Schlichting velocity profile [71]. Hwan and Fan [115] also solved numerically the case of uniform and equal wall heat fluxes for the Prandtl number range of 0.1 to 50. Heaton et al. [80] used an approximate integral

method and Han's [77] hydrodynamic results to solve the thermal entry length problem for one wall having uniform heat flux with the other wall being insulated.

For an arbitrary variation in axial wall temperature and/or heat flux, the superposition principle can also be applied to four fundamental solutions for the simultaneously developing flow. However, at each step of axial wall temperature and/or heat flux, the velocity profile, developing in the entrance region, will be different. Hence, a large number of thermal entrance solutions, with the heating started at different locations in the hydrodynamic entry length, would be required for the superposition. As it is impractical to carry out such solutions, the basic problem of getting four fundamental solutions for the simultaneously developing flow has not been investigated. Instead, as mentioned above only one fundamental problem (of the second kind), having a direct practical application, has been solved by Heaton et al. [80].

### 3. RECTANGULAR DUCTS

For the rectangular duct fully developed  $f_{Re}$ ,  $Nu_{H1}$ ,  $Nu_{H2}$ , and  $Nu_T$  as well as the Nusselt numbers for different wall boundary conditions on each wall have been determined. The hydrodynamic entry length problem has also been solved. However, there remains a need for the refinement for the thermal entry length solutions for the simultaneously developing flow, which so far were obtained by neglecting the transverse velocity components  $v$  and  $w$ . The experience with the circular duct, discussed in Section V.i.3.2 indicated that this neglect is not valid near the thermal entrance.

#### 3.1 Fully Developed Flow

##### 3.1.1. Velocity Profile and Friction Factors

Fully developed velocity profile for the rectangular ducts has been determined from the analogy with the stress function in theory of elasticity [2,31,33].

Consider the cross section of rectangular duct as shown in Fig. 5 with flow direction in  $x$  axis. The velocity profile, the solution of Eq. (3a) with boundary condition of Eq. (4), from Ref. [33] is

$$u = - \frac{16c_1 a^2}{\pi^3} \sum_{n=1,3,\dots}^{\infty} \frac{1}{n^3} (-1)^{\frac{n-1}{2}} \left[ 1 - \frac{\cosh(n\pi y/2a)}{\cosh(n\pi b/2a)} \right] \cos \frac{n\pi z}{2a} \quad (147)$$

$$u_m = - \frac{c_1 a^2}{3} \left[ 1 - \frac{192}{\pi^5} \frac{a}{b} \sum_{n=1,3,\dots}^{\infty} \frac{1}{n^3} \tanh \frac{n\pi b}{2a} \right] \quad (148)$$

and

$$fRe = - \frac{8c_1 a^2}{u_m (1 + \frac{a}{b})^2} \quad (149)$$

The velocity profile of Eq. (147) is in excellent agreement with the experimental results of Holmes and Vermeulen [210].

The friction factors were calculated from Eq. (149) on the Stanford IBM 360/67 computer using double precision and taking first 30 terms in the series and were checked against 25 terms in series. Seven digit accuracy was thus established. The results are presented in Table 13 and Fig. 19.

Table 13. Rectangular ducts  $fRe$ ,  $K(\infty)$ ,  $L_{hy}^+$ ,  $Nu_T$ ,  $Nu_{H1}$  and  $Nu_{H2}$  for fully developed laminar flow, when all four walls are transferring the heat.

$\alpha^*$	$fRe$	$K(\infty)[20]$	$L_{hy}^+[20]$	$Nu_T[211]$	$Nu_{H1}$	$Nu_{H2}[60]$
1.000	14.22708	1.5515	0.0324	2.976	3.607949	3.091
0.900	14.26098				3.620452	
1/1.2	14.32808				3.645310	
0.800	14.37780				3.663823	
0.750	-	1.5203	0.0310		-	
1/1.4	14.56482			3.077	3.734193	
0.700	14.60538				3.749608	
2/3	14.71184			3.117[11]	3.790327	
0.600	14.97996				3.894556	
0.500	15.54806	1.3829	0.0255	3.391	4.123303	3.017
0.400	16.36810	1.2815	0.0217		4.471852	
1/3	17.08967			3.956	4.794796	
0.300	17.51209				4.989888	
0.250	18.23278	1.0759	0.0147	4.439	5.331064	2.930
0.200	19.07050				5.737689	
1/6	19.70220	0.9451	0.0110	5.137	6.049456	
1/7	20.19310				6.294041	
0.125	20.58464	0.8788	0.00938	5.597	6.490334	
1/9	20.90385				6.651060	
0.100	21.16888	0.8392	0.00855		6.784947	
0.050	22.47701	0.7613	0.00709		7.450827	
0.000	24.00000	0.6857	0.00588	7.540716	8.235294	8.235

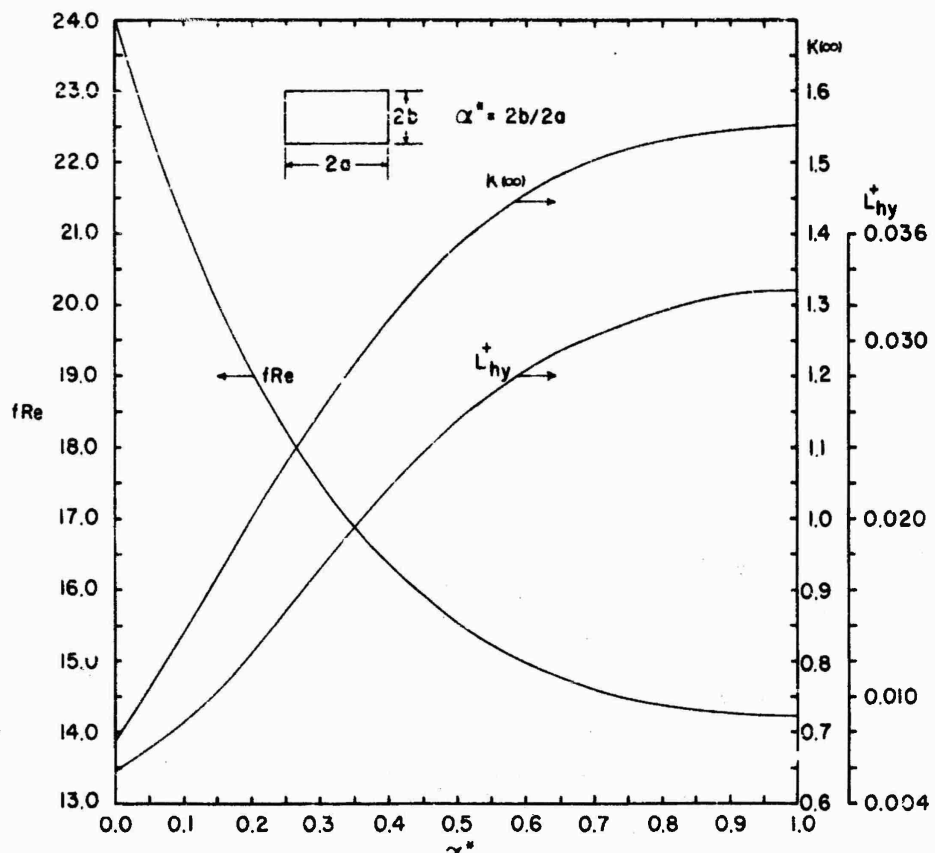


Fig. 19 Rectangular ducts  $fRe$  ,  $K(\infty)$  and  $L_{hy}^+$  for fully developed laminar flow.

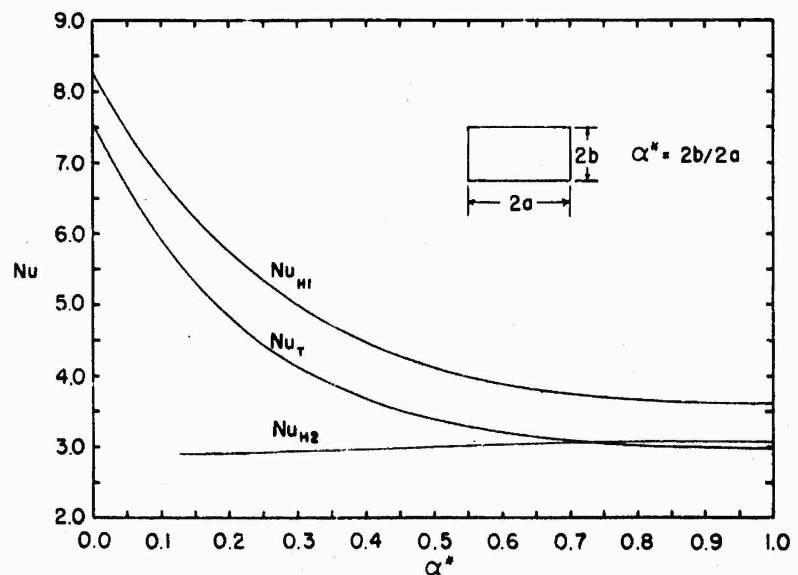


Fig. 20 Rectangular ducts  $Nu_T$  ,  $Nu_{H1}$  and  $Nu_{H2}$  for fully developed laminar flow.

Lundgren et al. [19] also determined  $f_D^{\text{Re}}$ ,  $K(\infty)$  and other flow parameters for the rectangular ducts. McComas [20] evaluated the hydrodynamic entrance length  $L_{hy}^+$  for the rectangular ducts. The  $K(\infty)$  and  $L_{hy}^+$  are also presented in Table 13 and Fig. 19. Shih [53] determined  $f_{\text{Re}}$  by the point matching method and presented the results graphically.

### 3.1.2 Specified Wall Temperature and $\langle T \rangle$

Clark and Kays [44] in 1953 were the first investigators to analyze the rectangular ducts in detail. They have numerically evaluated the fully developed  $Nu_T$  for  $\alpha^* = 0, 0.5$  and 1 when all four walls are uniformly and equally heated. Miles and Shih [211] refined the work of Clark and Kays by employing a  $40 \times 40\alpha^*$  grid instead of a  $10 \times 10\alpha^*$  grid size used for the finite difference method by Ref. [44]. They reported  $Nu_T$  for  $\alpha^* = 0.125, 1/6, 0.25, 1/3, 0.5, 1/1.4$  and 1. Along with the thermal entrance solution, Lyczkowski et al. [11] determined  $Nu_T$  for  $\alpha^* = 0.25, 0.5, 2/3$  and 1 by the finite difference method. The  $Nu_T$  for the rectangular duct are presented in Table 13 and Fig. 20.

Schmidt and Newell [45] considered one or more walls being heated at uniform surface temperature, the rest being at adiabatic condition. They solved the fully developed heat transfer problem by the finite difference method. The rectangular duct was divided into a system of  $20 \times 20$  subdivisions when the symmetry was present about both axes and  $20 \times 10$  subdivisions when the symmetry was present about one axis. A system of  $10 \times 10$  subdivisions was used when symmetry was not present about any axis, requiring that the complete duct be considered. According to Miles and Shih [211], the influence of grid size on calculated Nusselt numbers is eliminated, if the grid fineness of  $40 \times 40\alpha^*$  is employed. Consequently, the results for nonsymmetric heating may not be as accurate as those for the symmetric heating case of Table 14. After redefining the Nusselt number with

Table 14. Rectangular ducts  $Nu_T$  for fully developed laminar flow, when one or more walls are transferring the heat, from Schmidt [138]

$\frac{a}{b}$	$Nu_T$ Table 14	$Nu_T$ [138]				
		case 1 $\downarrow 2a \downarrow$ $\uparrow 2b$	case 2 $\downarrow 2b \downarrow$	case 3 $\uparrow 2a \uparrow$	case 4 $\uparrow 2b \uparrow$	case 5 $\downarrow 2a \downarrow$
0.0	7.541	7.541	7.541	7.541	0	4.861
0.1		6.858	6.095	6.399	0.4571	3.823
0.2		4.803	5.195	5.703	0.8330	3.330
0.3		4.114	4.579	5.224	1.148	2.996
0.4		3.670	4.154	4.884	1.416	2.768
0.5	5.691	3.881	3.842	4.619	1.647	2.613
0.6		3.198	-	-	-	2.509
0.7		3.083	3.408	4.192	2.023	2.442
0.8		3.014	-	-	-	2.401
0.9		2.980	-	-	-	2.381
1.0	2.976	2.970	3.018	3.703	2.437	2.375
1.4...		3.083	2.734	3.173	2.838	2.442
2.0	3.391	3.383	2.602	2.657	3.185	2.613
2.5		3.670	2.603	2.333	3.390	2.768
3.33...		4.114	2.703	1.946	3.626	2.996
5.0		4.803	2.982	1.467	3.909	3.330
10.0		5.858	3.590	0.3429	4.270	3.823
=	7.541	7.541	4.861	0	4.861	4.861

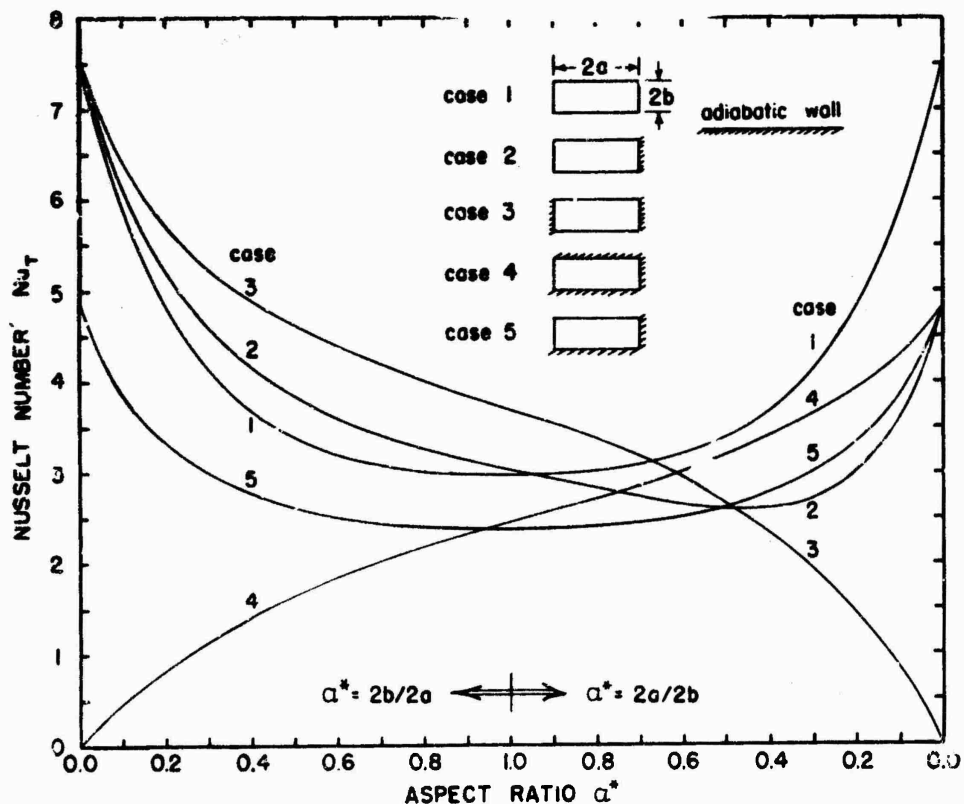


Fig. 21 Rectangular ducts  $Nu_T$  for fully developed laminar flow, when one or more walls are transferring the heat, from Schmidt [138].

the hydraulic diameter based on the wetted perimeter rather than the heated perimeter as was done in [45], the  $Nu_T$  [138] are reported in Table 14 and in Fig. 21.

Ikryannikov [212] obtained the  $\Theta$  temperature distribution in a rectangular duct by a finite integral Fourier sine transformation. In the energy Eq. (5), he neglected the convective term  $u(\partial t/\partial x)/a$ , thermal energy sources and the fluid axial heat conduction, but did not neglect the viscous dissipation. He presented graphically the maximum temperature at the mid-point of the channel as a function of the  $\alpha^*$  of the duct. The temperature distribution in the mid-plane of a square duct was also presented graphically.

### 3.1.3 Specified Wall Heat Flux and $\Theta_{H1}$

Glaser [124] obtained numerically, by the finite difference method, the fully developed  $Nu_{H1}$  only for the square duct. Clark and Kays [44] analyzed this problem for rectangular ducts in detail, by numerically evaluating the  $Nu_{H1}$  for  $\alpha^* = 0, 0.25, 1/3, 0.5, 1/1.4$  and 1. Miles and Shih [211] refined the calculations by employing a finer grid of  $40 \times 40\alpha^*$  instead of the  $10 \times 10\alpha^*$  grid. They determined the  $Nu_{H1}$  for  $\alpha^* = 0.125, 1/6, 0.25, 1/3, 0.5, 1/1.4$  and 1.

Marco and Han [31] derived the  $\Theta_{H1}$  temperature distribution for the rectangular ducts based on the existing solutions for the small deflection of thin plates under uniform lateral load with the plate being simply supported along all edges. The  $Nu_{H1}$  from [31] can be expressed as

Table 15. Rectangular ducts  $Nu_{H1}$  for fully developed laminar flow when one or more walls are transferring the heat, from Schmidt [138]

$\frac{2b}{\alpha}$	$Nu_{H1}$ Table 13	$Nu_{H1}$ [138]				
		case 1 $\frac{2a}{2b}$	case 2 $\frac{2b}{2a}$	case 3 $\frac{2b}{a}$	case 4 $\frac{a}{2b}$	case 5 $\frac{a}{2a}$
0.0	8.235	8.235	8.235	8.235	0	5.385
0.1	6.785	6.700	6.939	7.248	0.5377	4.410
0.2	5.738	5.704	6.072	6.561	0.9636	3.914
0.3	4.990	4.969	5.393	5.997	1.312	3.538
0.4	4.472	4.457	4.885	5.555	1.604	3.279
0.5	4.123	4.111	4.505	5.203	1.854	3.104
0.6	3.895	3.884	-	-	-	2.987
0.7	3.750	3.740	3.991	4.662	2.263	2.911
0.8	3.664	3.655	-	-	-	2.866
0.9	3.620	3.612	-	-	-	2.843
1.0	3.608	3.599	3.556	4.094	2.712	2.836
1.43..	3.750	3.740	3.195	3.508	3.149	2.911
2.0	4.123	4.111	3.146	2.947	3.539	3.104
2.5	4.472	4.457	3.169	2.598	3.777	3.279
3.33..	4.990	4.969	3.306	2.182	4.060	3.538
5.0	5.738	5.704	3.636	1.664	4.411	3.914
10.0	6.785	6.700	4.292	0.9746	4.851	4.410
$\infty$	8.235	8.235	5.385	0	5.385	5.385

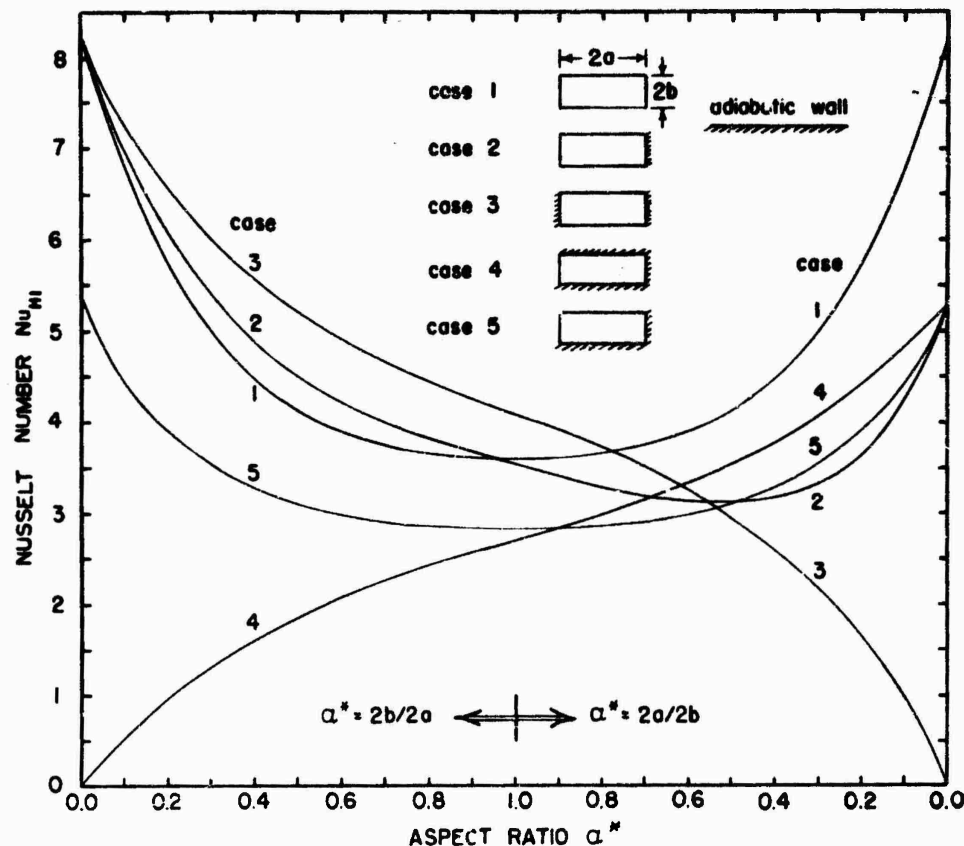


Fig. 22 Rectangular ducts  $Nu_{H1}$  for fully developed laminar flow, when one or more walls are transferring the heat, from Schmidt [138].

$$\text{Nu}_{H1} = \frac{64}{(1+\alpha^*)^2 \pi^2} \frac{\sum_{m=1,3,\dots}^{\infty} \sum_{n=1,3,\dots}^{\infty} \frac{1}{m^2 n^2 (m^2 + n^2 \alpha^{*2})}}{\sum_{m=1,3,\dots}^{\infty} \sum_{n=1,3,\dots}^{\infty} \frac{1}{m^2 n^2 (m^2 + n^2 \alpha^{*2})^3}} \quad (150)$$

The  $\text{Nu}_{H1}$  were evaluated on the Stanford IBM 360/67 computer from Eq. (150) using a double precision and taking 100 terms in each series. By this way, seven digit accuracy was obtained. The results are presented in Table 13 and Fig. 20.

Savino and Siegel [213] investigated the effect of unequal heat fluxes at adjacent walls of the duct on fully developed laminar heat transfer.

Schmidt and Newell [45] determined the Nusselt number numerically by finite difference method, when one or more walls having  $(H1)$  boundary condition, the other being at adiabatic condition. After redefining the Nusselt number with the hydraulic diameter based on the wetted perimeter rather than the heated perimeter as was done in [45], the Nusselt numbers [138] are listed in Table 15 and depicted in Fig. 22.

### 3.1.4 Specified Wall Heat Flux and $(H2)$

Cheng [214] analyzed the  $(H2)$  boundary condition with all four walls being heated. He arrived at a closed form expressions for the temperature distribution and  $\text{Nu}_{H2}$ , and calculated  $\text{Nu}_{H2}$  for  $\alpha^* = 0.1, 0.25, 0.5$  and  $1$ . There appears to be an error for  $\text{Nu}_{H2}$  for the square duct as pointed out by Sparrow and Siegel [61] and confirmed by Cheng [52]. Sparrow and Siegel [61] developed a variation approach for the  $(H2)$  boundary condition. Shah [60] employed the

method of least-square-fitting of algebraic-trigonometric polynomials to the boundary values and determined the  $Nu_{H2}$  (in addition to  $fRe$ ,  $K(\infty)$ ,  $L_{hy}^+$  and  $Nu_{H1}$ ) for the rectangular ducts. The results are presented in Table 13 and Fig. 20. The  $Nu_{H2}$  of Shah and Cheng are in good agreement.

Ikryannikov [115] studied the laminar heat transfer through rectangular ducts with uniform and constant axial wall heat flux, and arbitrary but the same peripheral heat flux distribution on each pair of the opposite walls. Particularly, he found and plotted the peripheral temperature distribution for the two problems: (i) On one pair of the opposite walls, the sinusoidal wall heat flux distribution was specified in the peripheral direction, the other pair of opposite walls being adiabatic. He considered  $\alpha^* = 2a/2t = 7, 5, 2, 1$ , and 0.2. (ii) On one pair of the opposite walls, the parabolic wall heat flux distribution was specified in the peripheral direction, the other pair of opposite walls being adiabatic. He considered  $\alpha^* = 2a/2b = 3.3, 2, 1, 0.2$  and 0.1.

### 3.1.5 Specified Wall Heat Flux and $(H3)$

Han [216] generalized the results of Marco and Han [31] by considering one pair of opposite walls as primary surface having  $(H1)$  boundary condition, and the other pair of opposite walls as extended surface or fins having  $(H3)$  boundary condition. On the extended surfaces, the heat is transferred from the primary surface to the fluid. Thus on those fins the temperature is not uniform in the peripheral direction like the primary surface, but the axial heat flux is uniform and constant. Han obtained the expressions for the temperature distribution and the fully developed Nusselt numbers. The Nusselt number is expressed functionally as

$$Nu = Nu_{H1} F_c \left( \frac{\alpha^* K_p}{1+\alpha^*}, \frac{1}{\alpha^*} \right) \quad (151)$$

where the  $Nu_{H1}$  is given by Eq. (150), and  $F_c$  is the correction factor dependent upon the fin parameter  $a^*K_p/(1+a^*)$  and the aspect ratio  $a^* = 2a/2b$ . The width of primary surface of rectangular channel is  $2a$  and the height of secondary surface (fins) of rectangular channel is  $2b$ . Han tabulated the correction factor for  $a^* = 1, 0.5, 0.25$  and  $0.2$  with the values of fin parameter as  $0, 1, 2, 4$  and  $10$ . The model analyzed by Han may be approximated, for example, in a counter-flow heat exchanger with equal thermal capacity rates for both fluids.

Siegel and Savino [8] considered the effect of peripheral wall heat conduction in broad walls with nonconducting insulated side walls. They extended their analysis to include different boundary conditions at the corners so that the effect of conduction in the insulated side walls could be studied [217].

Lyczkowski et al. [11] analyzed  $\textcircled{H3}$  boundary condition for the square duct and determined the  $Nu_{H3}$  numerically for  $K_p = 0, 0.5, 1.0$  and  $2.0$  as follows.

Table 16. Square duct  $Nu_{H3}$  for fully developed laminar flow

$K_p$	$Nu_{H3}$
0	3.23
0.5	3.41
1	3.47
2	3.52
$\infty$	3.608 [51]

It appears that the  $Nu_{H3}$  for  $K_p = 0$  by [11] has not converged to the expected limiting value of  $Nu_{H2} = 3.091^{21}$  [52].

<sup>21</sup>See Section II.1.3.2(c) for the limiting cases of  $Nu_{H3}$ .

However, the convergence may be better as  $K_p$  is increased.

### 3.2 Hydrodynamically Developing Flow

Hydrodynamic entry length problem for the rectangular duct has been solved approximately by the linearization of momentum equation. Han [76] used the Langhaar's linearization approach and presented the hydrodynamic entry length solution in tabular and graphical form for  $\alpha^* = 0, 0.125, 0.25, 0.5, 0.75$  and 1. The analysis of Han predicted somewhat more rapid flow development than observed experimentally [218,219]. Fleming and Sparrow [86] and Wiginton and Dalton [220] linearized the inertia terms in the boundary layer type momentum equation in a similar manner to Eq. (106), by introducing a stretched coordinate in the flow direction. References [86] and [220] methods are similar except that the convergence of the solution is more rapid for the later. Fleming and Sparrow [86] presented the hydrodynamic entry length solution for the rectangular ducts of aspect ratios 0.2 and 0.5, while Wiginton and Dalton [220]<sup>22</sup> reported the results for  $\alpha^* = 0.2, 0.25, 0.5$  and 1. For  $\alpha^* = 0.2$ , the pressure drop predicted by Wiginton and Dalton is about 2 to 3 percent higher than that by Fleming and Sparrow. For  $\alpha^* = 0.5$ , the pressure drop results of Refs. [86] and [220] are in excellent agreement. With the experimental data of Beavers et al. [221], the results of Refs. [86] and [220] are in good agreement.

### 3.3 Thermally Developing Flow

#### 3.3.1 Hydrodynamically Developed Flow

##### 3.3.1.1 Specified Wall Temperature and $\langle T \rangle$

Dennis et al. [222] considered the case of uniform and constant temperature on all four walls, and solved the

<sup>22</sup>The ordinate of Figs. 2, 4 and 6 of Ref. [220] is in error, it should start from 0 rather than 1.

thermal entry length problem for the fully developed laminar flow in rectangular ducts. They presented first three eigenvalues and eigenconstants for  $\alpha^* = 0.125, 0.25, 0.5, 2/3$  and 1. But these values, except the first term for rectangular ducts other than the square duct are in error [5,223].

Montgomery and Wibulswas [108] used the explicit finite difference method and solved the thermal entry length problem for the rectangular ducts with  $\alpha^* = 1/6, 0.2, 0.25, 1/3, 0.5$  and 1. They neglected the effect of axial heat conduction, viscous dissipation and the thermal energy sources within the fluid. Their  $Nu_{x,T}$  and  $Nu_{m,T}$  are presented in Table 17 [116]. The effect of  $\alpha^*$  on  $Nu_{x,T}$  for the developed velocity profile case is pictured in Fig. 23.

Lyczkowski et al. [11] considered a variety of thermal boundary conditions, such as, insulation on no walls, one wall, two walls and three walls with various finite wall thermal resistances and  $\mathbb{T}$  on the remaining walls. They used the modified DuFcrt and Frankai explicit finite difference method and numerically evaluated the thermal entry Nusselt numbers for  $\alpha^* = 0, 0.125, 0.25, 0.5$  and 1. The  $Nu_{x,T}$  versus  $x^*$  for  $\alpha^* = 0.25, 0.5$  and 1, when all four walls are heated, are presented in Table 18. The results of Tables 17 and 18 for  $\alpha^* = .25$  and 0.5 are in agreement within about 2 percent (except  $\alpha^* = 1$ ) as can be seen from Fig. 23 and reflects the differences obtained due to two different finite difference numerical methods. Authors believe that the results of Lyczkowski et al. [11] are more accurate.

Krishnamurty and Rao [224] employed the Lévèque approximation and arrived at an expression for local and mean Nusselt numbers for the rectangular ducts when one and all four walls transferred the heat. They included the effect of temperature dependent viscosity empirically.

DeWitt and Snyder [225] considered the fluid axial heat conduction and viscous dissipation, and solved the  $\mathbb{T}$  thermal

Table 17. Rectangular ducts  $Nu_{x,T}$  and  $Nu_{m,T}$  as functions of  $x^*$  and  $\alpha^*$  for fully developed velocity profiles, from Wibulswas [116]

$\frac{1}{\sqrt{x}}$	$Nu_{x,T}$						$Nu_{m,T}$					
	Aspect Ratio, $\alpha^*$						Aspect Ratio, $\alpha^*$					
	1.0	0.5	1/3	0.25	0.2	1/6	1.0	0.5	1/3	0.25	0.2	1/6
0	2.65	3.39	3.96	4.51	4.92	5.22	2.65	3.39	3.96	4.51	4.92	5.22
10	2.86	3.43	4.02	4.53	4.94	5.24	3.50	3.95	4.54	5.00	5.36	5.66
20	3.08	3.54	4.17	4.65	5.04	5.34	4.03	4.46	5.00	5.44	5.77	6.04
30	3.24	3.70	4.29	4.76	5.31	5.41	4.47	4.86	5.39	5.81	6.13	6.37
40	3.43	3.85	4.42	4.87	5.22	5.48	4.85	5.24	5.74	6.16	6.45	6.70
60	3.78	4.16	4.67	5.08	5.40	5.64	5.50	5.85	6.35	6.73	7.03	7.26
80	4.10	4.46	4.94	5.32	5.62	5.86	6.03	6.37	6.89	7.24	7.53	7.77
100	4.35	4.72	5.17	5.55	5.83	6.07	6.46	6.84	7.33	7.71	7.99	8.17
120	4.62	4.93	5.42	5.77	6.06	6.27	6.83	7.24	7.74	8.13	8.39	8.63
140	4.85	5.15	5.62	5.98	6.26	6.47	7.22	7.62	8.11	8.50	8.77	9.00
160	5.03	5.34	5.80	6.18	6.45	6.66	7.16	7.37	8.45	8.86	9.14	9.35
180	5.24	5.54	5.99	6.37	6.63	6.86	7.87	8.29	8.77	9.17	9.46	9.67
200	5.41	5.72	6.18	6.57	6.80	7.02	8.15	8.58	9.07	9.47	9.79	10.01

Table 18. Rectangular ducts  $Nu_{x,T}$  as functions of  $x^*$  and  $\alpha^*$  for fully developed velocity profiles, from Lyczkowski et al. [11]

$\alpha^* = 1$		$\alpha^* = 0.5$		$\alpha^* = 0.25$	
$x^*$	$Nu_{x,T}$	$x^*$	$Nu_{x,T}$	$x^*$	$Nu_{x,T}$
.00750	4.458	.004219	5.869	.002930	7.405
.01125	4.029	.006328	5.236	.004395	6.662
.01500	3.782	.008438	4.852	.005859	6.204
.01875	3.594	.01055	4.587	.007324	5.888
.02250	3.457	.01266	4.391	.008789	5.658
.02625	3.353	.01477	4.241	.01025	5.485
.03000	3.273	.01688	4.123	.01172	5.351
.03375	3.211	.01898	4.028	.01318	5.245
.03750	3.162	.02109	3.956	.01465	5.162
.05625	3.034	.04219	3.604	.02930	4.813
.07500	2.993	.06328	3.501	.05859	4.649
.09375	2.981	.08438	3.451	.10254	4.554
.1125	2.977	.12656	3.409	.14648	4.508
.1500	2.975	.14766	3.401	.21973	4.470
.1875	2.975	.16875	3.396	.25635	4.460
.2625	2.975	.17930	3.395	.28125	4.455

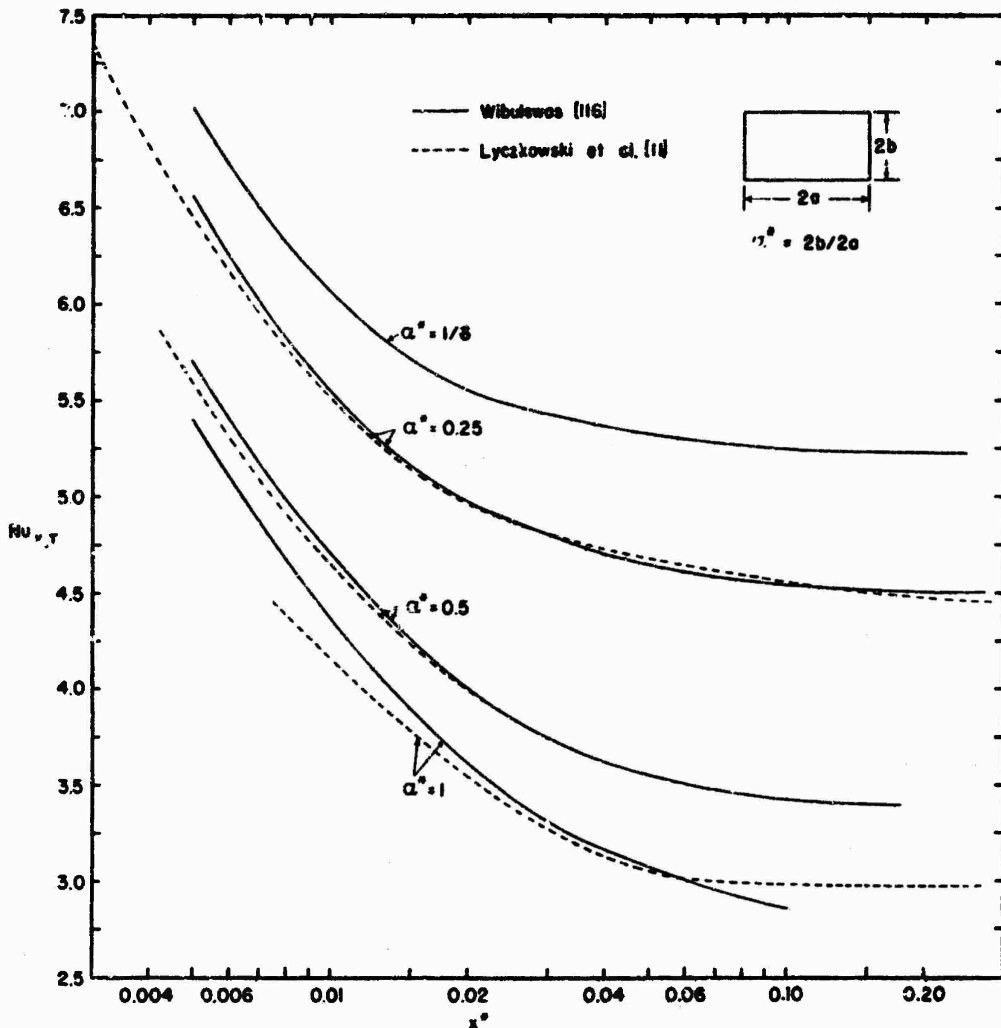


Fig. 23 Rectangular ducts  $\text{Nu}_{x,T}$  for fully developed velocity profile; the influence of  $\alpha^*$  on  $\text{Nu}_{x,T}$ . Similar influence can be expected for  $\text{Nu}_{m,T}$ ,  $\text{Nu}_{x,Hl}$  and  $\text{Nu}_{m,Hl}$  of Tables 17, 19 and 20.

entry length problem for rectangular ducts of  $\alpha^* = 0.1$ ,  $0.2$ ,  $0.5$  and  $1$ . The approximate series solution was obtained by the Galerkin method. The fluid bulk mean temperature and  $\text{Nu}_{x,T}$  were shown as a function of the dimensionless axial distance with Péclét number as a parameter. As the definitions used for the dimensionless variables and parameters are unconventional in [225], it is difficult to interpret the

thermal entry length solution in the present terminology.

### 3.3.1.2 Specified Heat Flux Distribution

Sparrow and Siegel [102] developed a variational method and calculated first two eigenvalues and eigenconstants for the square duct with  $\textcircled{H1}$  boundary condition.

Sadikov [104] studied the thermal entry length problem, based on his simplified energy equation, for rectangular ducts with prescribed wall heat flux boundary condition. Specifically, he presented graphically the local peripheral temperature and Nusselt number distribution with  $\textcircled{H2}$  boundary condition for  $\alpha^* = 1$  and 0.2. These results were plotted for  $\text{Pr} = 0.7$  and  $\text{Re} = 10^4$  with dimensionless axial distance as a parameter. Sadikov cited that, in the inlet section of a tube, the laminar flow was observed up to  $\text{Re} = 10^5$ .

Introducing the same assumptions as in the case of  $\textcircled{T}$ , Montgomery and Wibulswas [108] solved the thermal entry length problem for rectangular ducts of  $\alpha^* = 0.25, 1/3, 0.5$  and 1 with  $\textcircled{H1}$  boundary condition. Their  $Nu_{x,H1}$  and  $Nu_{m,H1}$  are reported in Table 19 [116].

Based on the same method employed for the specified wall temperature problem, Lyczkowski et al. [11] analyzed the thermal entry length problem for a variety of thermal boundary conditions, namely, insulation on no walls, one wall, two walls and three walls with various finite wall thermal resistances and  $\textcircled{H1}$  on the remaining walls.

Hicken [226] determined the temperature distribution in the thermal entrance region of rectangular ducts with arbitrary but uniform and constant axial heat flux specified on each wall. Graphically presented were the variation in wall to fluid bulk mean temperature difference,  $(4D_h/P)\theta_{w-m}$ , over the periphery for a square duct when one, two, three and four walls were equally heated. Also presented were the  $(4D_h/P)\theta_{w-m}$  over the periphery for  $\alpha^* = 0.1$  when all four

Table 19. Rectangular ducts  $Nu_{x,Hl}$  and  $Nu_{m,Hl}$  as functions of  $x^*$  and  $a^*$  for fully developed velocity profile, from Wibulswas [116]

$\frac{1}{x^*}$	$Nu_{x,Hl}$				$Nu_{m,Hl}$			
	Aspect Ratio, $a^*$				Aspect Ratio, $a^*$			
	1.0	0.5	1/3	0.25	1.0	0.5	1/3	0.25
0	3.60	4.11	4.77	5.35	3.60	4.11	4.77	5.35
10	3.71	4.22	4.85	5.45	4.48	4.94	5.45	6.03
20	3.91	4.38	5.00	5.62	5.19	5.60	6.06	6.57
30	4.18	4.61	5.17	5.77	5.76	6.16	6.60	7.07
40	4.45	4.84	5.39	5.87	6.24	6.64	7.09	7.51
60	4.91	5.28	5.82	6.26	7.02	7.45	7.85	8.25
80	5.33	5.70	6.21	6.63	7.66	8.10	8.48	8.87
100	5.69	6.05	6.57	7.00	8.22	8.66	9.02	9.39
120	6.02	6.37	6.92	7.32	8.69	9.13	9.52	9.83
140	6.32	6.68	7.22	7.63	9.09	9.57	9.93	10.24
160	6.60	6.96	7.50	7.92	9.50	9.96	10.31	10.61
180	6.86	7.23	7.76	8.18	9.85	10.31	10.67	10.92
200	7.10	7.46	8.02	8.44	10.18	10.64	10.97	11.23

walls were equally heated. The eigenvalues and eigenconstants for  $a^* = 0.1, 0.2, 0.5, 1, 2, 5$  and  $10$  are reported in [227].

### 3.3.2 Simultaneously Developing Flow

Montgomery and Wibulswas [92] also numerically obtained a combined hydrodynamic and thermal entry length solution for the rectangular ducts of  $a^* = 1, 0.5, 1/3, 0.25$  and  $1/6$ . In the analysis, they assumed the transverse velocity components  $v$  and  $w$  as zero as well as neglected the axial momentum and thermal diffusion. The  $Nu_{m,T}$  are presented in Table 20 and  $Nu_{x,Hl}$  and  $Nu_{m,Hl}$  are presented in Table 21 for  $Pr = 0.72$  [116]. They investigated the effect of Prandtl number on heat transfer for the duct with  $a^* = 0.5$ . The thermal entry  $Nu_{m,Hl}$  as a function of Prandtl number [116] are presented in Table 22 and Fig. 24.

Table 20. Rectangular ducts  $Nu_{m,T}$  as functions of  $x^*$   
and  $\alpha^*$  for simultaneously developing profiles,  
 $Pr = 0.72$ , from Wibulswas [116]

$\frac{1}{x^*}$	$Nu_{m,T}$				
	Aspect Ratio, $\alpha^*$				
	1.0	0.5	1/3	0.25	1/6
10	3.75	4.20	4.67	5.11	5.72
20	4.39	4.79	5.17	5.56	6.13
30	4.88	5.23	5.60	5.93	6.47
40	5.27	5.61	5.96	6.27	6.78
50	5.63	5.95	6.28	6.61	7.07
60	5.95	6.27	6.60	6.90	7.35
80	6.57	6.88	7.17	7.47	7.90
100	7.10	7.42	7.70	7.98	8.38
120	7.61	7.91	8.18	8.48	8.85
140	8.06	8.37	8.66	8.93	9.28
160	8.50	8.80	9.10	9.36	9.72
180	8.91	9.20	9.50	9.77	10.12
200	9.30	9.60	9.91	10.18	10.51
220	9.70	10.00	10.30	10.58	10.90

Table 21. Rectangular ducts  $Nu_{x,H1}$  and  $Nu_{m,H1}$  as  
functions of  $x^*$  and  $\alpha^*$  for simultaneously  
developing profiles,  $Pr = 0.72$ , from Wibulswas  
[116]

$\frac{1}{x^*}$	$Nu_{x, H1}$				$Nu_{m, H1}$			
	Aspect Ratio, $\alpha^*$				Aspect Ratio, $\alpha^*$			
	1.0	0.5	1/3	0.25	1.0	0.5	1/3	0.25
5					4.60	5.00	5.57	6.06
10	4.18	4.60	5.18	5.66	5.43	5.77	6.27	6.65
20	4.66	5.01	5.50	5.92	6.60	6.94	7.31	7.58
30	5.07	5.40	5.82	6.17	7.52	7.83	8.13	8.37
40	5.47	5.75	6.13	6.43	8.25	8.54	8.85	9.07
50	5.83	6.09	6.44	6.70	8.90	9.17	9.48	9.70
60	6.14	6.42	6.74	7.00	9.49	9.77	10.07	10.32
80	6.80	7.02	7.32	7.55	10.53	10.83	11.13	11.35
100	7.38	7.59	7.86	8.08	11.43	11.70	12.0	12.23
120	7.90	8.11	8.37	8.58	12.19	12.48	12.78	13.03
140	8.38	8.61	8.84	9.05	12.87	13.15	13.47	13.73
160	8.84	9.05	9.38	9.59	13.50	13.79	14.10	14.48
180	9.28	9.47	9.70	9.87	14.05	14.35	14.70	14.95
200	9.69	9.88	10.06	10.24	14.55	14.88	15.21	15.49
220					15.03	15.36	15.83	16.02

Table 22. Rectangular ducts ( $a^* = 0.5$ )  $Nu_{m,HI}$  as functions  
of  $x^*$  and Pr for simultaneously developing  
profiles, from Wibulswas [116]

$\frac{1}{x^*}$	$Nu_{m,HI}$				
	Prandtl Number, Pr				
	$\infty$	10	0.72	0.1	0
20	5.60	5.15	6.94	7.90	8.65
40	6.64	7.50	8.54	9.75	10.40
60	7.45	8.40	9.77	11.10	11.65
80	8.10	9.20	10.83	12.15	12.65
100	8.66	9.90	11.70	13.05	13.50
140	9.57	11.05	13.15	14.50	14.95
180	10.31	11.95	14.35	15.65	16.15
220	10.95	12.75	15.35	16.70	17.20
260	11.50	13.45	16.25	17.60	18.10
300	12.00	14.05	17.00	18.30	18.90
350	12.55	14.75	17.75	19.10	19.80
400	13.00	15.40	18.50	19.90	20.65

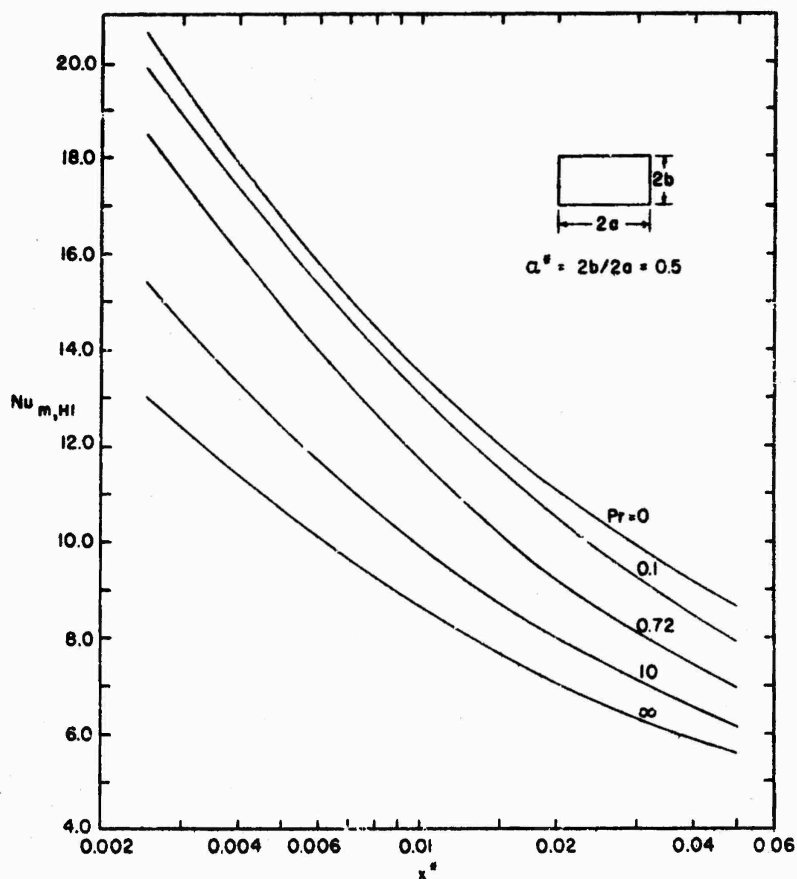


Fig. 24 Rectangular ducts ( $a^* = 0.5$ )  $Nu_{m,HI}$  as functions  
of  $x^*$  and Pr for simultaneously developing pro-  
files, from Wibulswas [116].

#### 4. ISOSCELES TRIANGULAR DUCTS

For the isosceles triangular ducts, the fully developed  $fRe$ ,  $Nu_{Hl}$ , and  $Nu_T$  have been determined by approximate methods as described below. The hydrodynamic entry length solution is available for  $2\phi = 30^\circ$  and  $60^\circ$ . The thermal entry length solution is available for  $2\phi = 60^\circ$  and  $90^\circ$  for the case of transverse velocity components  $v$  and  $w$  as zero for the simultaneously developing flow.

##### 4.1 Fully Developed Flow

The fully developed solutions will be described in detail for the equilateral triangular duct and other isosceles triangular ducts separately. The right angled isosceles triangular duct ( $2\phi = 90^\circ$ ) will be considered in Section 6.

###### 4.1.1 Equilateral Triangular Duct

The fully developed velocity profile for the equilateral triangular duct has been determined by [2,31,33]. For the duct of Fig. 25

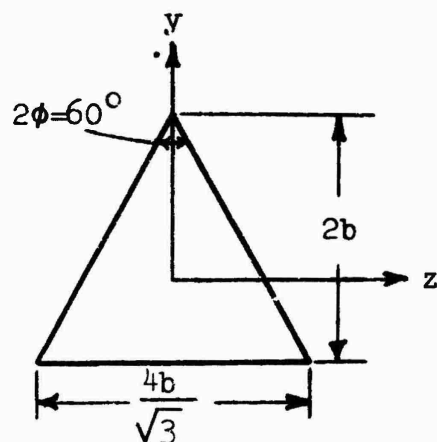


Fig. 25 An equilateral triangular duct

$$u = \frac{c_1}{8b} \left[ -y^3 + 3yz^2 + 2b(y^2 + z^2) - \frac{32}{27} b^3 \right] \quad (152)$$

$$u_m = -\frac{c_1}{15} b^2 \quad (153)$$

$$D_h = \frac{4b}{3} \quad (154)$$

$$fRe = 40/3 = 13.333 \quad (155)$$

References [4,5] report  $Nu_T$  for the equilateral triangular duct as 2.35. Kutateladze [228] report  $Nu_T$  as 2.70. From Schmidt and Newell's graphical results [45],  $Nu_T = 2.47$ . Extrapolating  $Nu_{x,T}$  of [116] to  $1/x^*$  equals to zero, the average  $Nu_T$  is found as 2.47. Until a refined magnitude is available, the  $Nu_T$ , for the equilateral triangular duct, may be taken as 2.47, a result 5.1 percent higher than given in [4,5].

Clark and Kays [44] first evaluated  $Nu_{H1}$  numerically for an equilateral triangular duct by the finite difference method. Marco and Han [31] provided exact solutions for the velocity and temperature distribution for the  $(H1)$  boundary condition. By complex variable techniques, Tao [36] arrived at  $Nu_{H1}$  including thermal energy generation within the fluid. Tyagi [23] extended Tao's analysis by including the viscous dissipation effects. Tyagi's result for the Nusselt number is

$$Nu_{H1} = \frac{28}{9} \left[ \frac{1 + \frac{20}{3} c_5 + c_6}{1 + \frac{40}{9} c_5 + \frac{5}{11} c_6} \right] \quad (156)$$

$$c_5 = \frac{9c_3}{4c_4 b^2} = \frac{-1}{\frac{20}{3} \left[ 1 + \frac{4q''}{SD_h} \right]} \quad (157)$$

$$c_6 = \frac{\mu}{k} \frac{c_1}{c_2} \quad (158)$$

For no internal thermal sources and viscous dissipation effects,

$$Nu_{H1} = 28/9 = 3.111 \quad (159)$$

a result 3.7 percent higher than first reported by Clark and Kays [44] and used in the texts [4,5].

#### 4.1.2 Other Isosceles Triangular Ducts

##### 4.1.2.1 Flow Friction

An exact solution does not exist for the fully developed laminar flow through isosceles triangular ducts with arbitrary apex angles. Nuttall [229] analyzed the torsion of rods of isosceles triangular cross section utilizing the Rayleigh-Ritz variational method. Based on Nuttall's results, the approximate friction factors for isosceles triangular ducts can be calculated. Sparrow [50] developed highly accurate approximate solutions by the point matching method. Sparrow's results for velocity profile and the friction factors, for the duct of Fig. 26, are given by

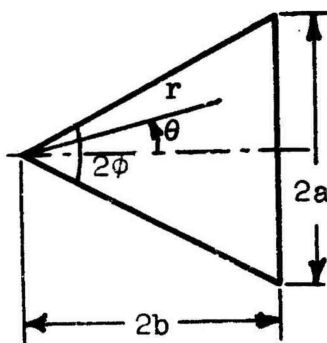


Fig. 26 An isosceles triangular duct.

$$u = -c_1 b^2 \left[ \left(\frac{r}{2b}\right)^2 \left( \frac{\cos 2\theta}{\cos 2\phi} - 1 \right) + \sum_{n=1}^{\infty} c_n \left(\frac{r}{2b}\right)^{N_n} \cos N_n \theta \right] \quad (160)$$

$$u_m = -c_1 b^2 \left[ \frac{1}{3} \left( \frac{1}{\cos 2\phi} - 1 \right) + \frac{2}{\tan \phi} \sum_{n=1}^{\infty} \frac{C_n I_n}{2 + N_n} \right] \quad (161)$$

$$fRe = -\frac{8c_1 b^2}{u_m} \frac{\sin^2 \phi}{(1 + \sin \phi)^2} \quad (162)$$

where  $N_n = \frac{(2n-1)\pi}{2\phi}$  (163)

The constants  $C_n$  and  $I_n$  are tabulated in [50]. Lundgren et al. [19] also determined  $f_D Re$ ,  $K(\infty)$  and other flow parameters for the isosceles triangular ducts. McComas [20] evaluated the hydrodynamic entrance length,  $L_{hy}^+$ . Shah [60] employed the method of least-square-fitting of algebraic-trigonometric polynomials on the boundary and determined the  $fRe$ ,  $K(\infty)$  and  $L_{hy}^+$  for the isosceles triangular ducts. Results of Shah [60] and Sparrow [50] are in excellent agreement. The  $fRe$ ,  $K(\infty)$  and  $L_{hy}^+$  are reported in Table 23 and Fig. 27 [60].

The hydraulic diameter for the isosceles triangular duct of Fig. 26 is

$$D_h = \frac{4b \sin \phi}{1 + \sin \phi} = \frac{2a \cos \phi}{1 + \sin \phi} \quad (164)$$

It would be interesting to consider the two limiting cases of the isosceles triangular ducts: (i)  $2\phi = 180^\circ$  when  $2b$  is kept finite, and (ii)  $2\phi = 0^\circ$ , when  $2a$  is kept finite. In both of these cases, the limiting geometry would appear to be parallel plates with  $2b$  and  $2a$  distance separation respectively. For these parallel plates, the corresponding hydraulic diameters are  $4b$  and  $4a$ . Based on these  $D_h$ ,

$$fRe_{\text{parallel plates}} = 24$$

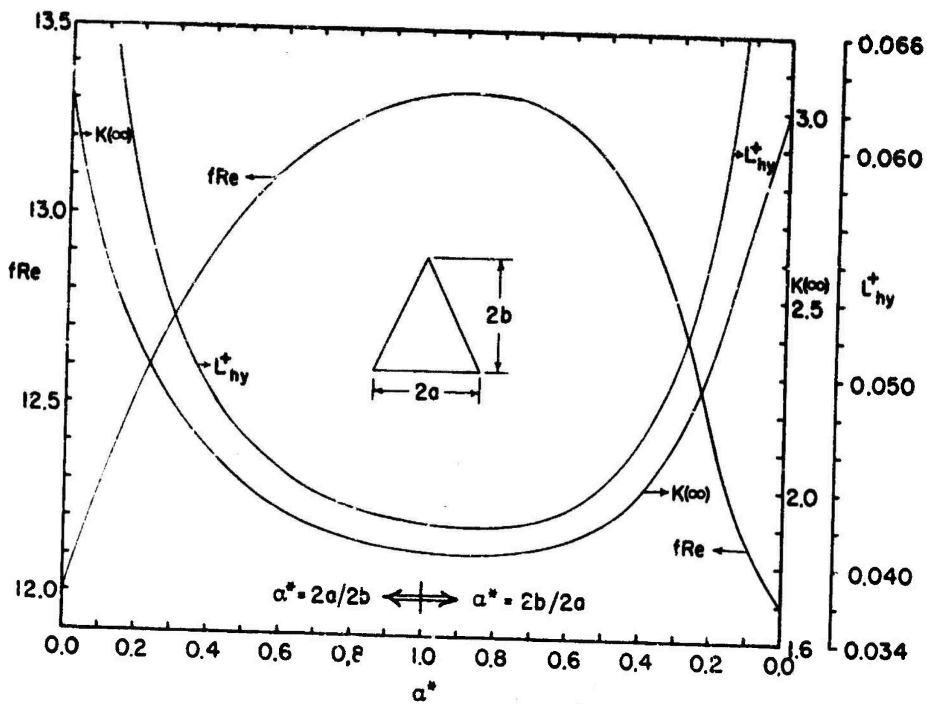


Fig. 27 Isosceles triangular ducts  $f_{Re}$ ,  $K(\infty)$  and  $L_{hy}^+$  for fully developed laminar flow.

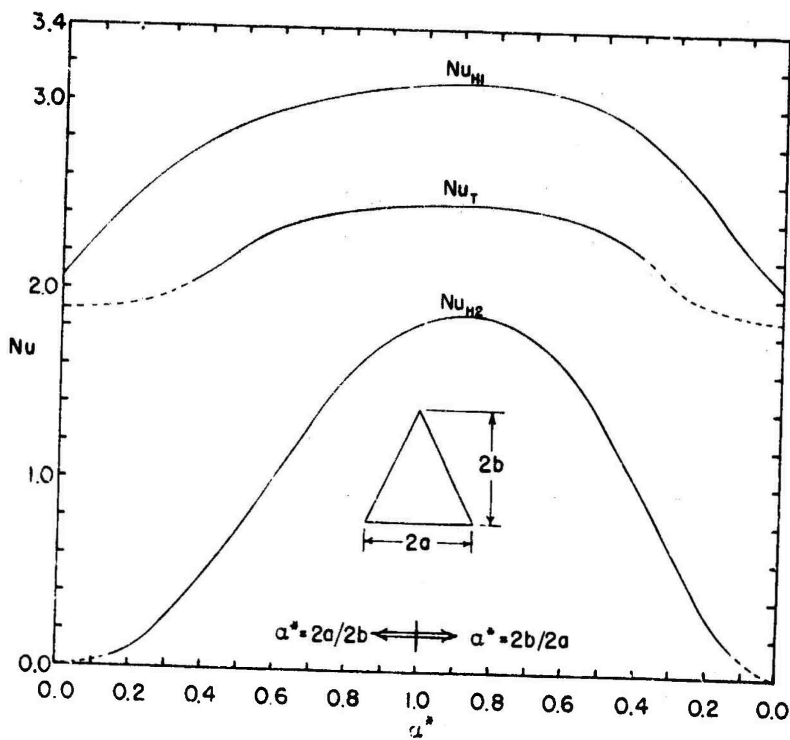


Fig. 28 Isosceles triangular ducts  $Nu_T$ ,  $Nu_{H1}$  and  $Nu_{H2}$  for fully developed laminar flow.

Table 23. Isosceles triangular ducts  $f' Re$ ,  $K(\infty)$ ,  $L_{hy}^+$ ,  $Nu_T$ ,  $Nu_{H1}$  and  $Nu_{H2}$  for fully developed laminar flow

$\frac{2b}{2a}$	$2\phi$ degrees	$\frac{u_{max}}{u_m}$	$K(\infty)$	$L_{hy}^+$	$f' Re$	$Nu_T$ [25]	$Nu_{H1}$	$Nu_{H2}$
$\infty$	0	-	3.000	-	12.000	1.885	2.059	0
8.00	7.153	2.593	2.521	0.0648	12.352	1.90	2.546	0.03927
4.00	14.250	2.442	2.271	0.0533	12.636	1.94	2.575	0.1734
2.00	28.072	2.302	1.991	0.0443	13.026	2.22	2.880	0.7427
1.50	36.870	2.259	1.899	0.0418	13.181	2.38	2.998	1.213
1.00	53.130	2.225	1.824	0.0399	13.321	2.46	3.102	1.847
$\sqrt{3}/2$	60.000	2.222	1.818	0.0398	13.333	2.47	3.111	1.891
0.75	67.380	2.225	1.824	0.0399	13.321	2.45	3.102	1.836
0.50	90.000	2.264	1.909	0.0421	13.153	2.34	2.982	1.345
0.25	126.870	2.416	2.236	0.0515	12.622	1.99	2.603	0.4902
0.125	151.928	2.609	2.583	0.0659	12.212	1.91	2.296	0.1376
0	180.000	-	3.000	-	12.000	1.885	2.059	0

However, for the isosceles triangular duct, the  $D_h$  from Eq. (164) for  $2\phi = 180^\circ$  and  $0^\circ$  is  $2b$  and  $2a$  respectively, one half that of the parallel plate geometry. Consequently, one would expect

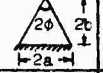
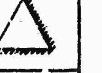
$$f' Re = 12$$

for the isosceles triangular ducts when  $2\phi = 180^\circ$  or  $0^\circ$ . This is the case as mentioned by Sparrow and Haji-Sheikh [230]. Clearly, the limiting triangular geometries do not go to the parallel plates or even each other, but the  $f$  magnitudes are all the same for the same  $(u_m, \rho, \mu)$  conditions.

#### 4.1.2.2 Heat Transfer

Sparrow and Haji-Sheikh [230] solved the momentum and energy equations numerically by the finite difference method and arrived at fully developed  $Nu_{H1}$  for the isosceles triangular ducts of apex angle  $2\phi$  varying from  $0^\circ$  to  $180^\circ$ .

Table 24. Isosceles triangular ducts  $Nu_T$  for fully developed laminar flow when one or more walls are transferring the heat, from Schmidt [138]

$\frac{2b}{2a}$	$\phi$ degrees	$Nu_T$ [138]			
					
$\infty$	0.00	1.885	0.000	1.215	1.215
5.000	5.71	-	0.8222	1.416	1.312
2.500	11.31	2.058	1.20d	1.849	1.573
1.667	16.70	2.227	1.525	2.099	1.724
1.250	21.80	2.312	1.675	2.237	1.802
1.000	26.56	2.344	1.758	2.301	1.831
0.833	30.96	-	-	2.319	1.822
0.714	34.92	2.311	1.812	2.306	1.787
0.625	38.66	-	-	2.274	1.735
0.556	41.99	-	-	2.232	1.673
0.500	45.00	2.162	1.765	2.183	1.606
0.450	48.01	-	-	2.127	1.529
0.400	51.34	-	-	2.055	1.433
0.350	55.01	1.923	1.633	1.968	1.315
0.300	59.04	-	-	1.861	1.173
0.250	63.43	1.51	-	1.733	1.004
0.200	68.20	1.512	1.361	1.581	0.8052
0.150	73.30	1.330	1.229	1.401	0.5779
0.100	78.69	1.126	1.071	1.182	0.3319
0.050	84.29	0.8954	0.8779	0.8930	0.1058
0.000	90.0	(1.215)*	(1.215)*	-	-

\*This  $Nu_T$  magnitude is the expected value for the limiting geometry. For further clarification refer to the text.

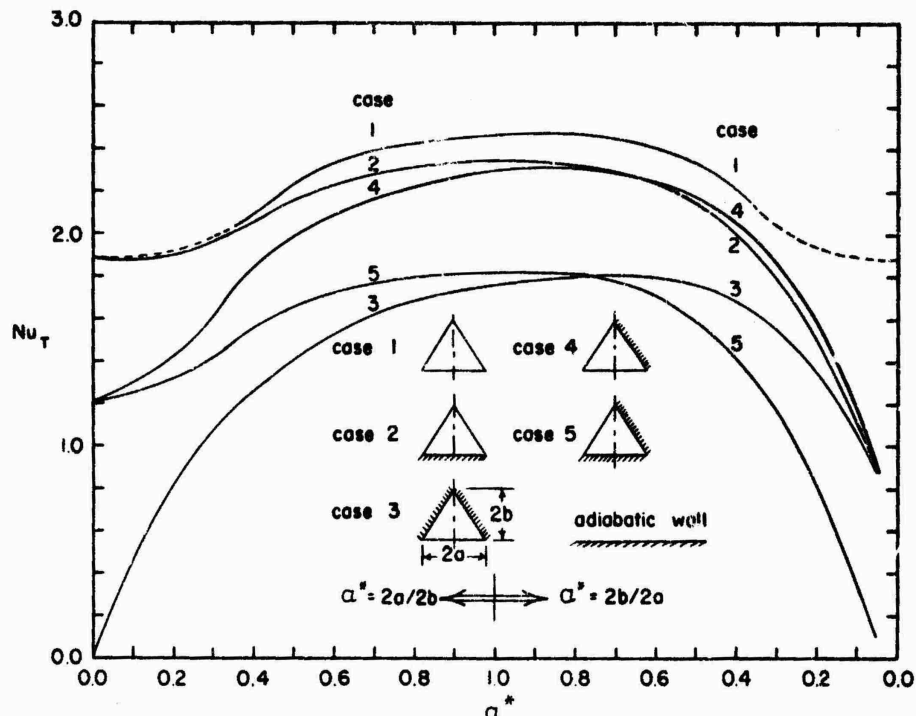


Fig. 29 Isosceles triangular ducts  $Nu_T$  for fully developed laminar flow, when one or more walls are transferring the heat, from Schmidt [138].

They reported the results graphically. After changing the dependent variables, Shah [60] reduced the momentum and energy equation to the Laplace equation. The infinite series solution was then obtained in terms of algebraic-trigonometric polynomials; the unknown coefficients of each term of series were determined by a least-square-fit of known boundary values. Totally first 81 unknown coefficients of the series were evaluated from 90 points on the boundary. The  $Nu_{H1}$  and  $Nu_{H2}$  determined by this method are presented in Table 23 and Fig. 28.

Here, again it would be interesting to investigate the two limiting cases for the isosceles triangular ducts. Based on the energy balance on the duct length of  $5x$ , from Eq. (51),

$$Nu = D_h^2 \frac{u_m}{4\alpha(t_{w,m} - t_m)} \frac{dt_m}{dx}$$

As the  $D_h$  for the limiting case for the isosceles triangular duct is one half that of the parallel plate,  $Nu$  would be one fourth that of the parallel plate, and this is confirmed by Sparrow and Haji-Sheikh [230].

Schmidt and Newell [45] considered the more general case for fully developed  $Nu_{H1}$  and  $Nu_T$  when one or more walls are transferring heat, the rest being adiabatic. They evaluated the results by the finite difference method and presented the  $Nu_{H1}$  and  $Nu_T$  graphically as a function of half apex angle  $\phi$ . The triangular duct was divided into 28 subdivisions in  $z$  direction and 14 in  $y$  direction when the symmetry was present, and was divided into 20 by 10 subdivisions when the complete duct was considered. Schmidt and Newell's  $Nu_T$  when all three walls are transferring heat, based on their graphical results, are presented in Table 23 and Fig. 28. The  $Nu_T$  and  $Nu_{H1}$  [138], when one or two walls are transferring heat are provided in Tables

Table 25. Isosceles triangular ducts  $Nu_{H1}$  for fully developed laminar flow, when one or more walls are transferring the heat, from Schmidt [138]

$\frac{2b}{2a}$	degrees	$Nu_{H1}$ [138]			
*	0.00	2.059	0.000	1.346	1.346
5.000	5.71	2.465	1.003	1.824	1.739
2.500	11.31	2.683	1.515	2.274	1.946
1.667	16.70	2.796	1.807	2.541	2.074
1.250	21.80	2.845	1.978	2.695	2.141
1.000	26.56	2.849	2.076	2.773	2.161
0.833	30.96	-	-	2.801	2.146
0.714	34.99	2.778	2.146	2.792	2.107
0.625	38.66	-	-	2.774	2.053
0.556	41.99	-	-	2.738	1.989
0.500	45.00	2.594	2.111	2.696	1.921
0.450	48.01	-	-	2.646	1.843
0.400	51.34	-	-	2.583	1.746
0.350	55.01	2.332	1.991	2.505	1.628
0.300	59.04	-	-	2.412	1.486
0.250	63.43	2.073	1.843	2.301	1.316
0.200	68.20	1.917	1.746	2.174	1.114
0.150	73.30	1.748	1.635	2.032	0.8741
0.100	78.69	1.576	1.515	1.881	0.5866
0.050	84.29	1.418	1.398	1.737	0.2442
0.000	90.00	1.346	1.346	-	-

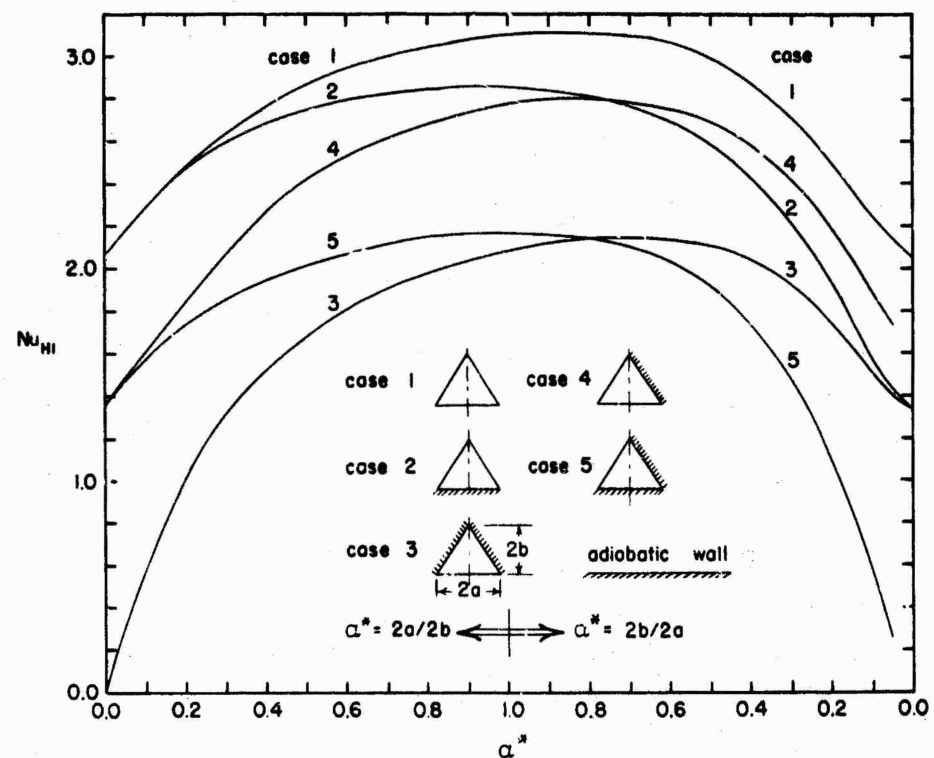


Fig. 30 Isosceles triangular ducts  $Nu_{H1}$  for fully developed laminar flow, when one or more walls are transferring the heat, from Schmidt [138].

24, 25 and Figs. 29 and 30. These  $Nu_T$  and  $Nu_{H1}$  are re-defined with the hydraulic diameter based on the wetted perimeter rather than the heated perimeter as was done in [45].

#### 4.2 Hydrodynamically Developing Flow

The hydrodynamic entry length problem for the equilateral triangular duct was solved by Han and Cooper [78] using Langhaar's linearization and von Kármán's integral procedure with some modifications. The results were presented in tabular and graphical form. Wibulswas [116], in his solution for the combined hydrodynamic and thermal entry length problem for the equilateral triangular duct, solved the hydrodynamic entry length problem by the finite difference method; however, he did not report any hydrodynamic entrance region results. Fleming and Sparrow [86] devised a general method to solve the hydrodynamic entry length problem by introducing a stretched coordinate in the flow direction to linearize the inertia term. They presented the results graphically for the isosceles triangular duct with the apex angle  $2\phi = 30^\circ$  and  $60^\circ$ .

#### 4.3 Thermally Developing Flow

Kutateladze [228] presented graphically the thermal entrance  $Nu_{m,T}$  for hydrodynamically full developed and thermally developing laminar flow through an equilateral triangular duct.

Wibulswas [116] obtained laminar flow  $Nu_{x,T}$ ,  $Nu_{m,T}$ ,  $Nu_{x,H1}$  and  $Nu_{m,H1}$  for an equilateral triangular duct for the slug flow ( $Pr = 0$ ), fully developed flow ( $Pr = \infty$ ) and the simultaneously developing flow for the fluid with  $Pr = 0.72$ . He used the finite difference method and neglected the effect of velocity components  $v$  and  $w$ , as well as the axial viscous and thermal diffusion,  $\mu(\partial^2 u/\partial x^2)$  and  $k(\partial^2 t/\partial x^2)$  respectively. His thermal entrance Nusselt numbers are pre-

Table 26. Equilateral triangular duct  $Nu_{x,T}$ ,  $Nu_{m,T}$ ,  
 $Nu_{x,Hl}$  and  $Nu_{m,Hl}$  as functions of  $x^*$  and  
 $Pr$ , from Wibulswas [116]

$Pr$	$Nu_{x,T}$			$Nu_{m,T}$			$Nu_{x,Hl}$		$Nu_{m,Hl}$			
	*	0.72	0	*	0.72	0	0.72	0	*	0.72	0	
	$x^*$											
1.0	1.17	2.42	1.17	1.15	2.41	1.15	3.37	3.58	4.38	4.02	4.76	6.37
2.0	1.14	2.33	1.14	1.13	2.32	1.13	3.35	3.55	4.35	4.76	5.87	8.04
3.0	1.12	2.26	1.12	1.11	2.24	1.11	3.34	3.54	4.34	5.32	6.80	9.08
4.0	1.10	2.19	1.10	1.09	2.17	1.09	3.32	3.50	4.32	5.82	7.57	9.06
5.0	1.08	2.13	1.08	1.07	2.09	1.07	3.30	3.48	4.30	6.25	6.24	10.65
6.0	1.06	2.07	1.06	1.05	2.02	1.05	3.28	3.46	4.28	6.02	6.76	6.37
8.0	1.04	2.01	1.04	1.03	1.96	1.03	3.26	3.44	4.26	5.27	9.73	12.35
10.0	1.03	1.96	1.03	1.02	1.89	1.02	3.24	3.42	4.24	10.80	13.15	
12.0	1.02	1.91	1.02	1.01	1.83	1.01	3.22	3.40	4.22	11.39	13.82	
14.0	1.01	1.86	1.01	1.00	1.76	1.00	3.20	3.38	4.20	12.05	14.46	
16.0	1.00	1.81	1.00	0.99	1.67	0.99	3.18	3.36	4.18	12.68	15.02	
18.0	0.99	1.76	0.99	0.98	1.62	0.98	3.16	3.34	4.16	13.77	15.90	
20.0	0.98	1.70	0.98	0.97	1.57	0.97	3.14	3.32	4.14	13.80	16.00	

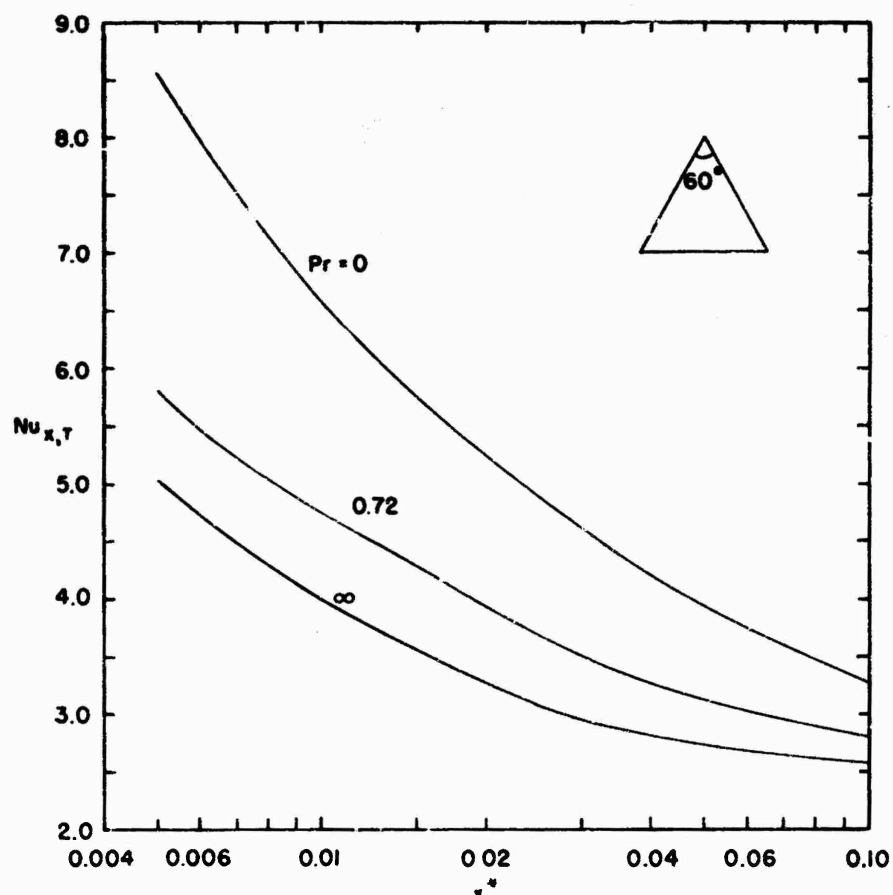


Fig. 31 Equilateral triangular duct  $Nu_{x,T}$ ; the influence of  $Pr$  on  $Nu_{x,T}$  from Wibulswas [116]. Similar influence can be expected for  $Nu_{m,T}$ ,  $Nu_{x,Hl}$  and  $Nu_{m,Hl}$  of Table 26.

sented in Table 26 and Fig. 31. Wibulswas'  $Nu_{m,T}$  are consistently higher by 12-20 percent when compared with  $Nu_{m,T}$  of Kutateladze [228].

Krishnamurty [231], employing Lévêque type approximation, derived expressions for  $\bar{N}$  local and mean Nusselt numbers for an equilateral triangular duct.

Table 27. Equilateral triangular duct with no, one, two and three rounded corners geometrical, flow and heat transfer characteristics, from Shah [60]

	no rounded corners	one rounded corner	two rounded corners	three rounded corners
Perimeter, $P/2a$	3.0000000	2.7717156	2.5434312	2.3151467
Flow area, $A_c/(2a)^2$	0.4330127	0.4139890	0.3949653	0.3759416
Hyd. dia, $D_h/2a$	0.5773503	0.5974480	0.6211535	0.6495339
Centroid from the base, $\bar{y}/2a$	0.2886751	0.2677773	0.3095730	0.2886751
$K(\infty)$	1.818	1.697	1.567	1.441
$u_{max}/u_m$	2.222	2.172	2.114	2.064
$L_{hy}^+$	0.0398	0.0359	0.0319	0.0284
$fRe$	13.333	14.056	14.899	15.993
$Nu_{H1}$	3.111	3.402	3.756	4.205
$Nu_{H2}$	1.892	2.419	2.718	3.780

## 5. EQUILATERAL TRIANGULAR DUCT WITH ROUNDED CORNERS

Only the fully developed laminar flow through the equilateral triangular duct with rounded corners has been analyzed.

### 5.1 Fully Developed Flow

In a triangular passage heat exchanger matrix, due to manufacturing processes, instead of sharp corners, some of the passages have one, two or three rounded corners. The heat transfer and flow friction characteristics of the rounded corner equilateral triangular passage being different from that for the sharp corner equilateral triangular passage, the overall performance characteristics of the matrix may change significantly. Shah [60] has determined the theoretical heat transfer and flow friction characteristics of the idealized passages of Fig. 32. Each rounded corner has a radius of  $a/3$  where  $2a$  is the base of the equilateral triangle.

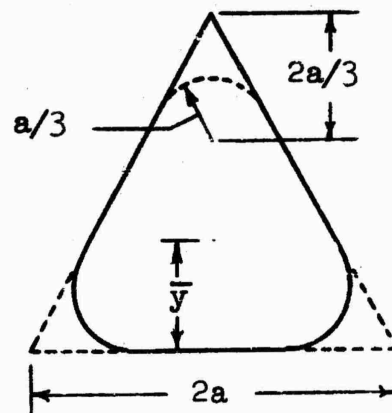


Fig. 32 An equilateral triangular duct with rounded corners.

The flow friction and heat transfer characteristics of these passages was obtained by the least-square-fitting of 72 boundary points to the 71 unknown coefficients of the truncated series solution [60]. These results and the geometrical information is listed in Table 27.

## 6. RIGHT TRIANGULAR DUCTS

For the right triangular ducts, the fully developed  $fRe$  and  $Nu_{Hl}$  have been determined numerically as described below. No hydrodynamic entry length solution has been obtained for this geometry. The thermal entry length solution for simultaneously developing profiles has been obtained for the right-angled isosceles triangular duct ( $\phi = 45^\circ$ ) for the case of transverse velocity components  $v$  and  $w$  as zero.

### 6.1 Fully Developed Flow

#### 6.1.1 Right-Angled Isosceles Triangular Duct

The fully developed velocity profile for the right-angled isosceles triangular duct of Fig. 33 is given by [2,31].

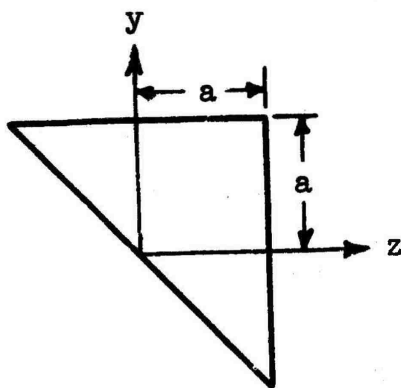


Fig. 33 A right-angled isosceles triangular duct.

$$u = \frac{c_1}{2} \left[ \frac{1}{2}(y + z)^2 - a(y + z) \right. \\ \left. + \frac{2}{a} \sum_{n=0}^{\infty} \frac{(-1)^n \{ \sinh(Nz) \cos(Ny) + \sinh(Ny) \cos(Nz) \}}{N^3 \sinh(Na)} \right] \quad (165)$$

Table 28. Right triangular and Circular sector ducts fRe ,  $K(\infty)$  ,  $Nu_{H1}$  and  $Nu_{H2}$  for fully developed laminar flow

$\phi$ Degrees	$\frac{2b}{2a}$	Right triangular duct			Circular sector duct		
		fRe [230]	$K(\infty)$ [230]	$Nu_{H1}$ [230]	fRe [231]	$K(\infty)$ [231]	$Nu_{H1}$ [231]
0	$\infty$	12.000	2.97	2.059	12.000	2.971	2.059
4	11.430	12.27	2.65	2.27	12.410	2.480	2.384
5	-	-	-	-	-	-	0.051
7.5	5.671	12.49	2.40	2.44	12.729	2.235	2.619
10	-	-	-	-	-	-	0.177
15	3.732	12.68	2.21	2.57	13.310	1.855	3.005
20	2.747	12.83	2.10	2.69	-	-	0.786
22.5	-	-	-	-	13.782	1.657	1.57
30	1.732	13.034	1.95	2.888	14.171	1.580	3.479
40	1.192	13.13	1.88	2.97	14.592	1.530	2.369
45	1.000	13.153	1.88	2.982	-	-	-
50	0.8391	13.13	1.88	2.97	14.928	1.504	3.806
60	0.5774	13.034	1.95	2.888	15.201	1.488	3.906
80	0.1763	12.49	2.40	2.44	15.611	1.468	-
90	0	12.000	2.97	2.059	15.767	1.463	4.088

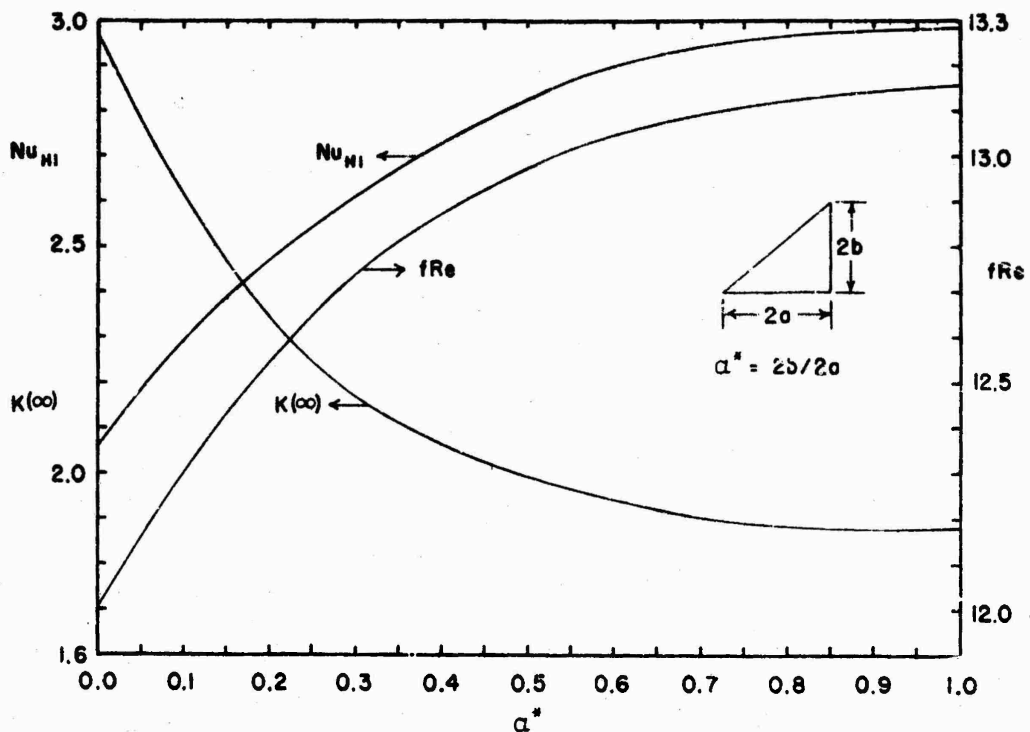


Fig. 34 Right triangular ducts fRe ,  $K(\infty)$  and  $Nu_{H1}$  for fully developed laminar flow, from Sparrow and Haji-Sheikh [230].

$$u_m = - \frac{c_1}{8a^3} \left[ \frac{4}{3} a^5 - \sum_{n=0}^{\infty} \frac{1}{N^5 \tanh(Na)} \right] \quad (166)$$

$$fRe = - \frac{4}{3 + 2\sqrt{2}} \frac{c_1 a^2}{u_m} = 13.153 \quad (167)$$

$$\text{where } N = \frac{(2n+1)\pi}{2a} \quad (168)$$

Marco and Han [31] determined the velocity and temperature distribution for the  $\text{Hl}$  boundary condition for the right-angled isosceles triangular duct. The Nusselt number for this case is [232]

$$Nu_{\text{Hl}} = 2.982 \quad (169)$$

#### 6.1.2 Other Right Triangular Ducts

Sparrow and Haji-Sheikh [230] numerically obtained the fully developed  $fRe$ ,  $K(\infty)$  and  $Nu_{\text{Hl}}$  for right triangular ducts of apex angle varying from  $0$  to  $90^\circ$ . The results were presented graphically. Based on these, Table 28 and Fig. 34 are prepared. Aggarwala and Iqbal [232] obtained the  $fRe$  and  $Nu_{\text{Hl}}$  for two right triangular ducts ( $\phi = 30^\circ$  and  $45^\circ$ ) based on the membrane analogy.

#### 6.2 Hydrodynamically Developing Flow

No hydrodynamic entry length solutions have been found by the authors for the right triangular ducts.

#### 6.3 Thermally Developing Flow

Wibulswas [116] solved the thermal entry length problem for the right-angled isosceles triangular duct ( $\phi = 45^\circ$ ). He obtained the laminar flow  $Nu_{x,T}$ ,  $Nu_{m,T}$ ,  $Nu_{x,Hl}$  and

Table 29. Right-angled isosceles triangular duct  $Nu_{x,T}$ ,  
 $Nu_{m,T}$ ,  $Nu_{x,Hl}$  and  $Nu_{m,Hl}$  for  $Pr = \infty$ , 0.72  
and 0, from Wibulswas [116]

Pr 1/r*	$Nu_{x,T}$			$Nu_{m,T}$			$Nu_{x,Hl}$			$Nu_{m,Hl}$		
	=	0.72	0	=	0.72	0	=	0.72	0	=	0.72	0
10	2.40	2.52	3.75	2.87	3.12	4.81	3.29	4.00	5.31	4.22	5.36	6.86
20	2.53	2.76	4.41	3.33	3.73	5.85	3.58	4.73	6.27	3.98	6.51	7.37
30	2.70	2.98	4.82	3.70	4.20	6.38	3.84	5.23	6.81	5.50	7.32	7.58
40	2.90	3.18	5.17	4.01	4.58	6.97	4.07	5.63	7.23	5.91	7.95	9.20
50	3.05	3.37	5.48	4.28	4.90	7.38	4.28	5.97	7.55	6.25	8.50	9.67
60	3.20	3.54	5.77	4.52	5.17	7.73	4.47	6.30	7.85	6.57	8.99	10.07
80	3.50	3.85	6.30	4.91	5.69	8.31	4.84	6.92	8.37	7.14	9.80	10.75
100	3.77	4.15	6.75	5.23	6.10	8.80	5.17	7.45	8.85	7.60	10.42	11.32
120	4.01	4.43	7.13	5.52	6.50	9.18	5.46	7.95	9.22	8.03	10.90	11.77
140	4.21	4.70	7.51	5.70	6.82	9.47	5.71	8.39	9.58	8.40	11.31	12.14
160	4.40	4.96	7.84	6.00	7.10	9.70	5.95	8.80	9.90	8.73	11.67	12.47
180	4.57	5.22	8.10	6.17	7.33	9.98	6.16	9.14	10.17	9.04	12.00	12.75
200	4.74	5.49	8.38	6.33	7.57	10.13	6.36	9.50	10.43	9.33	12.29	13.04

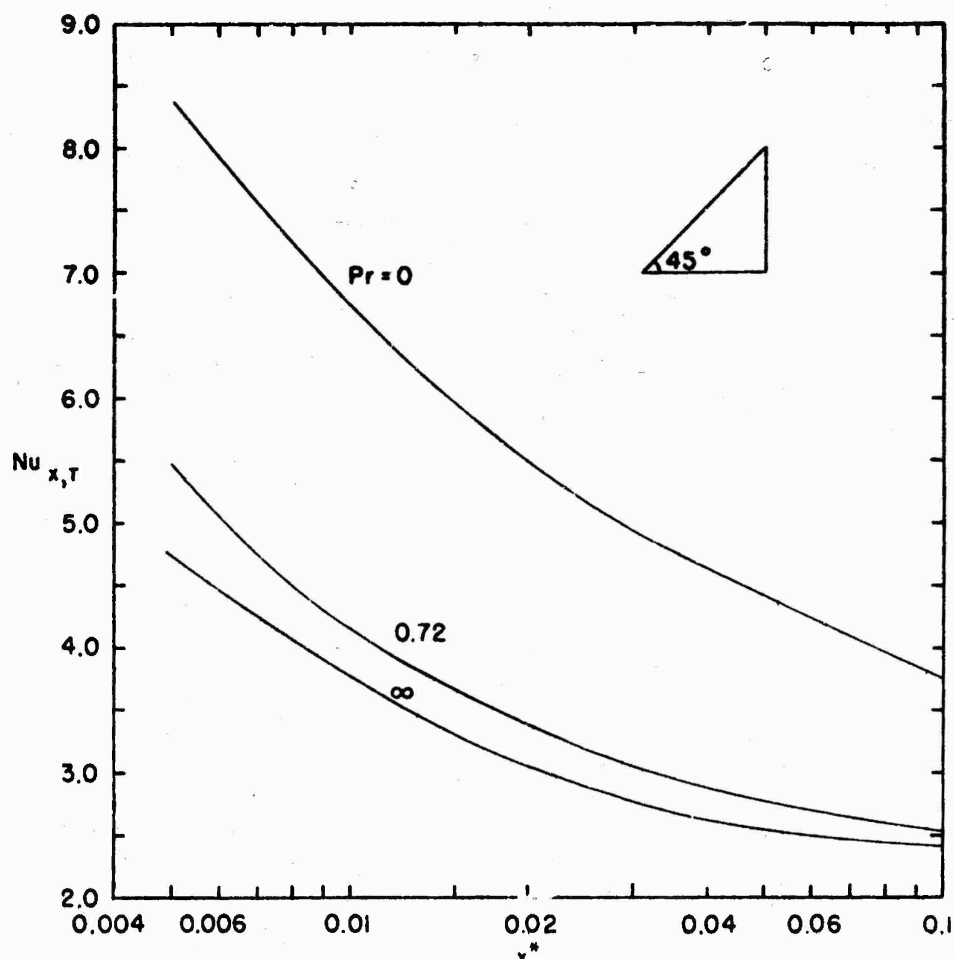


Fig. 35 Right-angled isosceles triangular duct  $Nu_{x,T}$  as functions of  $x^*$  and  $Pr$ , from Wibulswas [116].

$\text{Nu}_{m,H1}$  for the slug flow ( $\text{Pr} = 0$ ), fully developed flow ( $\text{Pr} = \infty$ ), and the simultaneously developing flow for the fluid with  $\text{Pr} = 0.72$ . In his finite difference numerical solution, he used the same idealization as mentioned in the isosceles triangular duct section. His results are presented in Table 29. The effect of  $\text{Pr}$  on  $\text{Nu}_{x,T}$  is shown in Fig. 35. Similar effects of  $\text{Pr}$  on  $\text{Nu}_{m,T}$ ,  $\text{Nu}_{x,H1}$  and  $\text{Nu}_{m,H1}$  may be expected from the data of Table 29.

Table 30. Sine ducts  $u_{\max}/u_m$ ,  $K(\infty)$ ,  $L_{hy}^+$ ,  $fRe$ ,  $\text{Nu}_T$ ,  $\text{Nu}_{H1}$  and  $\text{Nu}_{H2}$  for fully developed laminar flow, from Shah [60]

$\frac{2b}{2a}$	$\frac{u_{\max}}{u_m}$	$K(\infty)$	$L_{hy}^+$	$fRe$	$\text{Nu}_T$ [46]	$\text{Nu}_{H1}$	$\text{Nu}_{H2}$
2.00	2.288	1.884	0.0403	14.564	-	3.310	0.9738
1.50	2.239	1.806	0.0394	14.022	2.60	3.268	1.353
1.00	2.197	1.744	0.0400	13.023	2.45	3.102	1.549
$\sqrt{3}/2$	2.191	1.739	0.0408	12.630	-	3.014	1.474
0.75	2.190	1.744	0.0419	12.234	2.33	2.916	1.337
0.50	2.211	1.810	0.0464	11.207	2.12	2.617	0.8973
0.25	2.291	2.013	0.0553	10.123	1.80	2.213	0.3288
0.125	2.357	2.173	0.0612	9.743	-	2.017	0.09435

## 7. SINE DUCTS

Only the fully developed laminar flow through sine ducts (Fig. 36) has been analyzed. No hydrodynamic and thermal entry length solution has been reported for this geometry.

### 7.1 Fully Developed Flow

The fully developed laminar flow and heat or mass transfer in a sine duct (Fig. 36) has been investigated by Sherony and Solbrig [46]. They obtained the velocity and  $\langle T \rangle$  temperature distribution for the sine duct numerically by the finite difference method, and evaluated  $K(\infty)$  based on Eq. (32),  $L_{hy}^+$  based on Eq. (33),  $fRe$  and  $Nu_T$  for several aspect ratios  $a^* = 2b/2a$ . Their results for  $Nu_T$  are presented in Table 30 and Figs. 37. They also considered the finite wall thermal resistance and determined the fully developed  $Nu_{R1}$  as presented in Table 3.

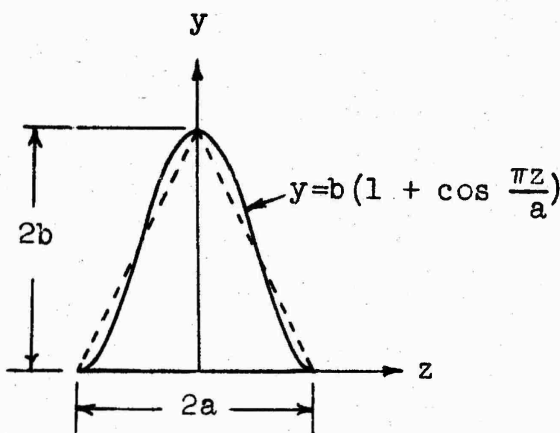


Fig. 36 A sine duct.

Recently, Shah [60] employed the method of least-square-fitting of algebraic-trigonometric polynomials to the known boundary values. He determined the  $fRe$ ,  $K(\infty)$ ,  $L_{hy}^+$ ,  $Nu_{H1}$  and  $Nu_{H2}$  for the sine ducts. The results are presented in Table 30 and Figs. 37 and 38. The results of velocity problems by Refs. [46] and [60] are in good agreement.

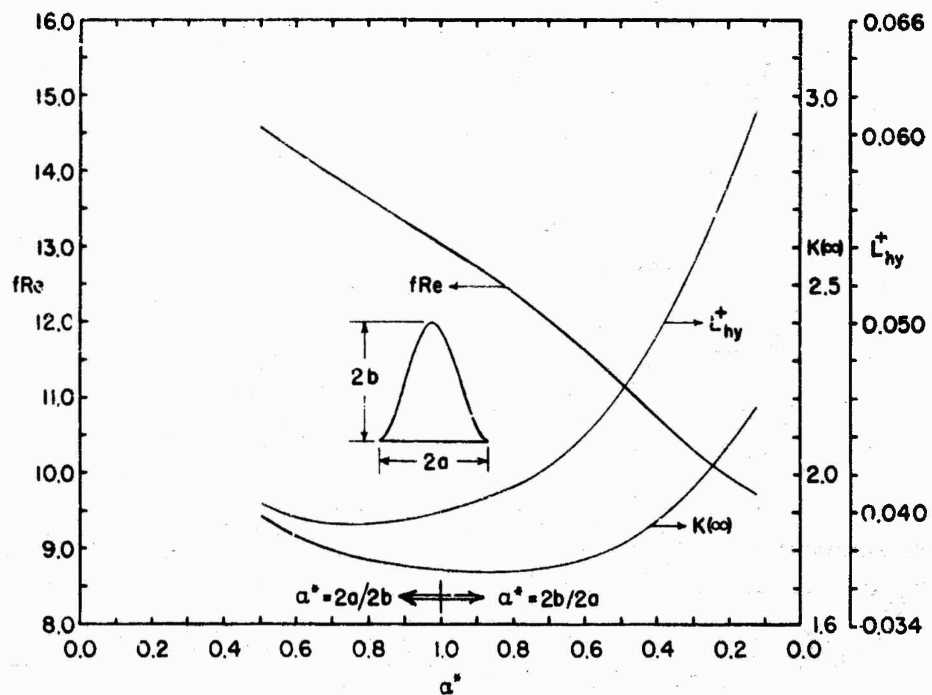


Fig. 37 Sine ducts  $fRe$ ,  $K(\infty)$  and  $L_{hy}^+$  for fully developed laminar flow.

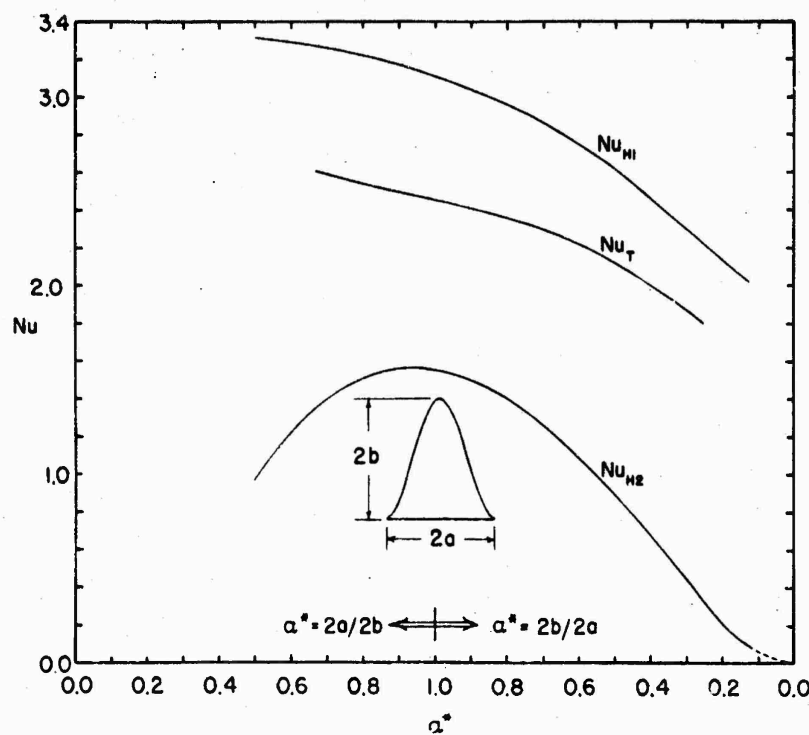


Fig. 38 Sine ducts  $Nu_T$ ,  $Nu_{H1}$  and  $Nu_{H2}$  for fully developed laminar flow.

## 8. CIRCULAR SECTOR DUCTS

Eckert et al. [233,6] presented the fully developed laminar flow velocity profiles for circular sector ducts based on the torsion theory [33]. Eckert et al. [6] derived the laminar  $H_1$  temperature distribution for the circular sector ducts. The results were based on the theory of small deflection of a thin plate [34]. Sparrow and Haji-Sheikh [230] extended the results to cover a wider range of the duct angle. The  $fRe$ ,  $K(\infty)$  and  $Nu_{H1}$  are presented in Table 28 as a function of the circular sector duct angle  $\phi$  [234]. Eckert et al. [6] also derived the laminar  $H_2$  temperature distribution and the Nusselt number. Based on their graphical results,  $Nu_{H2}$  are also presented in Table 28. Figure 39 shows  $fRe$ ,  $K(\infty)$ ,  $Nu_{H1}$  and  $Nu_{H2}$  for fully developed laminar flow through the circular sector ducts.

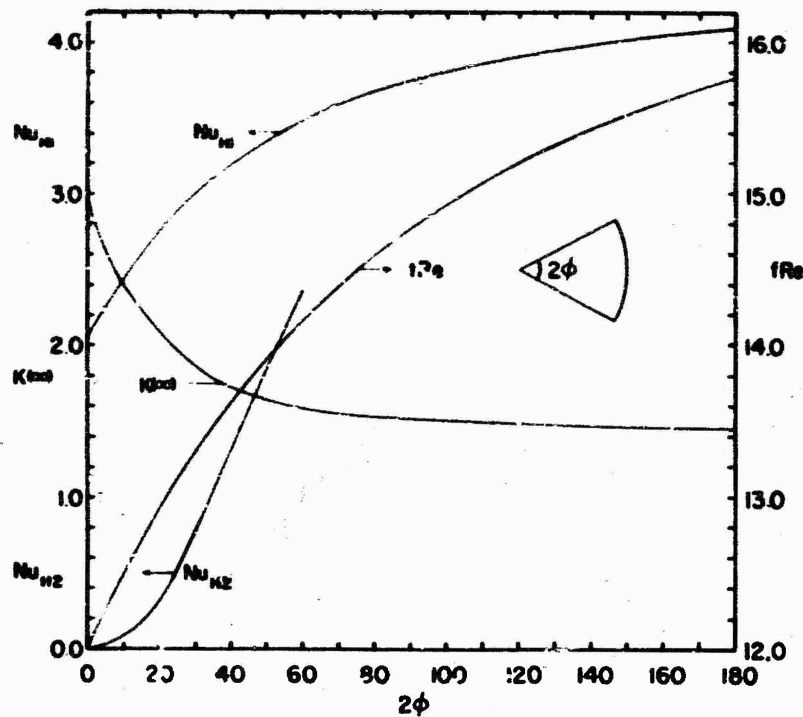


Fig. 39 Circular segment ducts  $fRe$  ,  $K(\infty)$  ,  $Nu_{H1}$  and  $Nu_{H2}$  for fully developed laminar flow.

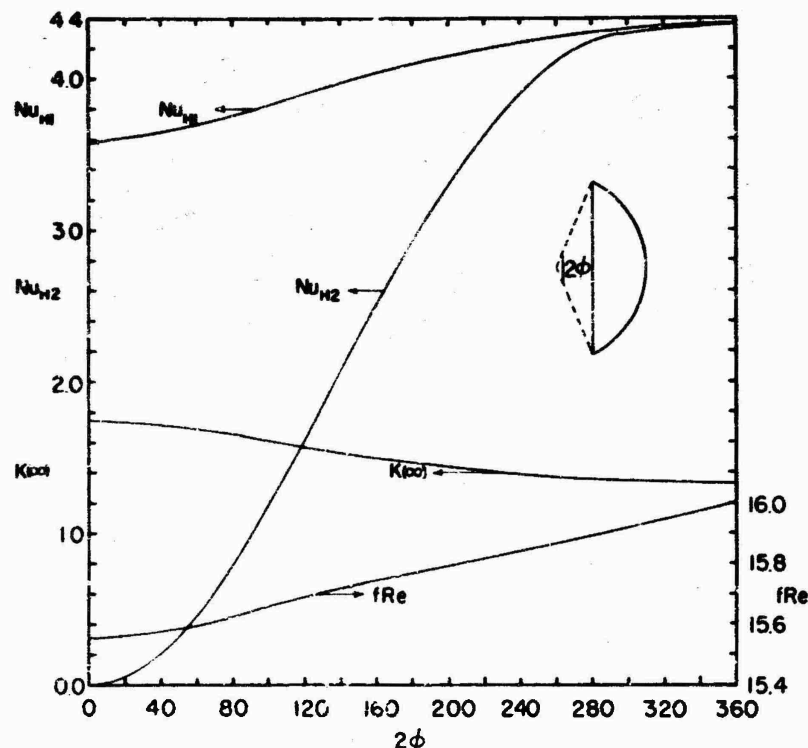


Fig. 40 Circular sector ducts  $fRe$  ,  $K(\infty)$  ,  $Nu_{H1}$  and  $Nu_{H2}$  for fully developed laminar flow, from [57].

## 9. CIRCULAR SEGMENT DUCTS

Sparrow and Haji-Sheikh [57] determined the fully developed laminar flow  $f_{Re}$ ,  $K(\infty)$ ,  $Nu_{H1}$  and  $Nu_{H2}$  for the circular segment duct using the 17-point matching method. Their results are tabulated in Table 31 and Fig. 40.

Table 31. Circular segment ducts, Circular ducts with diametrically opposite flat sides and Moon shaped ducts  $f_{Re}$ ,  $K(\infty)$ ,  $Nu_{H1}$  and  $Nu_{H2}$  for fully developed laminar flow

2φ de- grees	circular segment				flat sided		moon shaped
	$f_{Re}$ [57]	$K(\infty)$ [57]	$Nu_{H1}$ [57]	$Nu_{H2}$ [57]	$f_{Re}$ [239]	$Nu_{H1}$ [239]	$f_{Re}$
0	15.555	1.740	3.580	0.00	24.000	8.235	-
10	15.558	1.739	3.608	0.01316	21.551	-	15.552
20	15.560	1.734	3.616	0.05247	19.822	6.020	15.540
40	15.575	1.715	3.648	0.2017	17.603	4.991	15.492
60	15.598	1.686	3.696	0.4558	16.475	4.483	15.413
80	15.627	1.650	3.756	0.7849	15.986	4.303	15.304
100	-	-	-	-	15.842	4.269	15.169
120	15.690	1.571	3.894	1.608	15.862	4.296	15.027
140	-	-	-	-	15.933	4.335	14.928
160	-	-	-	-	15.980	4.359	15.037
170	-	-	-	-	15.998	4.363	15.321
176	-	-	-	-	-	-	15.657
180	15.766	1.463	4.089	2.923	16.000	4.364	16.000
240	15.840	1.385	4.228	3.882	-	-	-
300	15.915	1.341	4.328	4.296	-	-	-
360	16.000	1.333	4.364	4.364	-	-	-

## 10. CIRCULAR DUCTS WITH DIAMETRICALLY OPPOSITE FLAT SIDES

The fully developed laminar flow  $fRe$  and  $Nu_{Hl}$  for the circular duct with diametrically opposite flat sides are evaluated by Cheng and Jamil [54] by the point matching method. The total number of points matched ranged from 36 for the angle  $\phi = 5^\circ$  to 73 for  $\phi = 85^\circ$ . The results [235] are listed in Table 31 and Fig. 41.

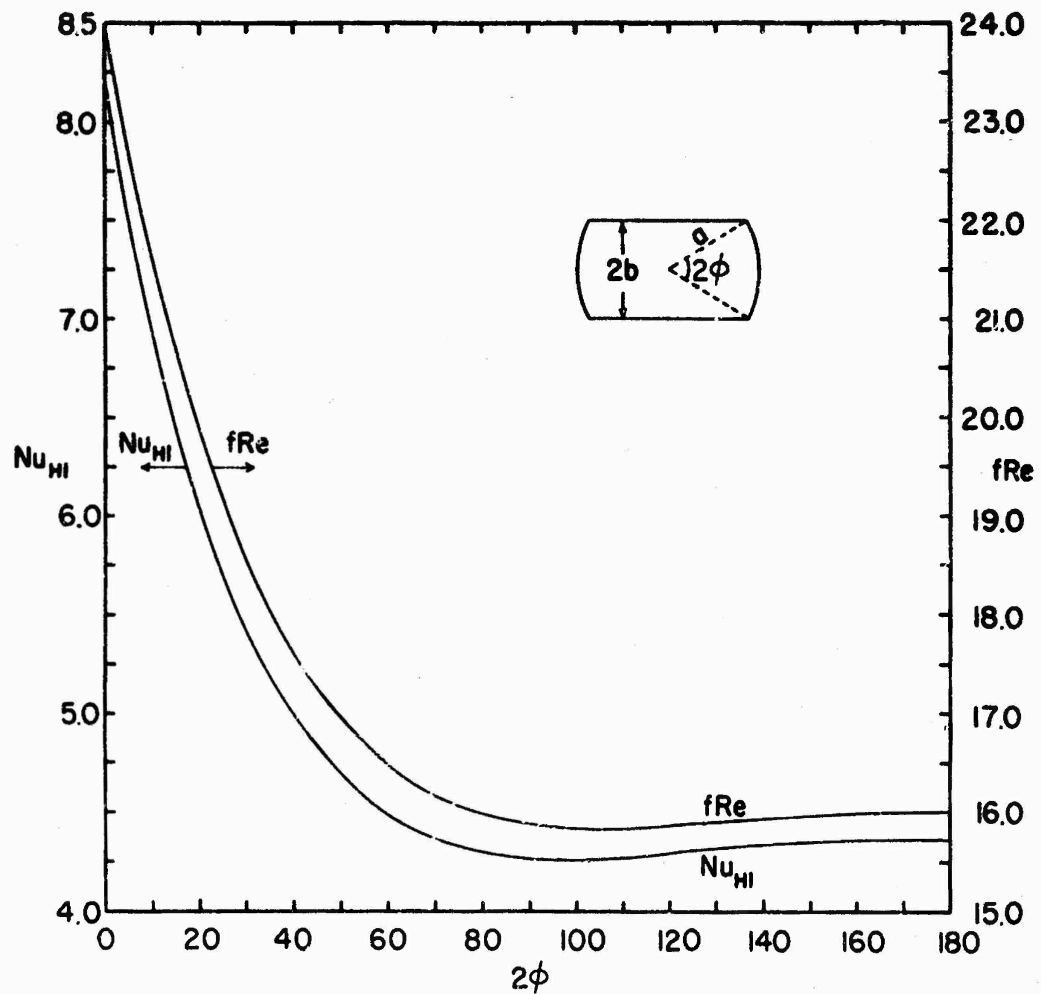


Fig. 41 Circular ducts with diametrically opposite flat sides  $fRe$  and  $Nu_{Hl}$  for fully developed laminar flow.

## 11. REGULAR POLYGONAL DUCTS

For the general n-sided regular polygonal ducts, only the problem of fully developed laminar flow and heat transfer has been attacked so far. For the special cases, namely, the equilateral triangular, square and circular ducts, the reader is referred to the previous sections.

### 11.1 Fully Developed Flow

Tao [38] employed the conformal mapping method for the fully developed laminar flow through a hexagonal duct with linearly varying wall temperature and arbitrary thermal energy generation. He presented the dimensionless heat flux as a function of thermal energy generation within the fluid.

Hsu [236] investigated the fully developed laminar flow heat transfer for the hexagonal duct with and without thermal energy generation within the fluid. He considered two sets of boundary conditions: (i) heat fluxes from three pairs of mutually opposite side walls to be pair-wise the same, but for each pair, the heat flux magnitude can differ, and (ii) heat flux on all six walls uniform and equal. The velocity and temperature fields were determined. The local Nusselt numbers along the wall were presented graphically, and the average  $Nu$  were tabulated for the case of with and without thermal energy generation. The  $Nu_{H2}$  for the hexagonal duct was reported as 3.795 which is about 1.7 percent lower than that listed in Table 32.

Cheng [51] used 9-point matching method to determine fully developed  $fRe$ ,  $Nu_{H1}$ , velocity, shear and temperature distribution etc. for the regular polygonal ducts. Cheng [27] extended his work by including the effect of uniform thermal energy generation and viscous dissipation within the fluid. The dimensionless heat flux and the Nusselt numbers for  $(H1)$  boundary condition were determined by the 10-point matching method and were presented graphically. Shih [53]

independently evaluated  $fRe$  for the regular polygonal ducts using the 12-point matching method. Cheng also employed the 12-point matching method to evaluate fully developed  $Nu_{H2}$  for the regular polygonal ducts [52]. These results are presented in Table 32 and Fig. 42.

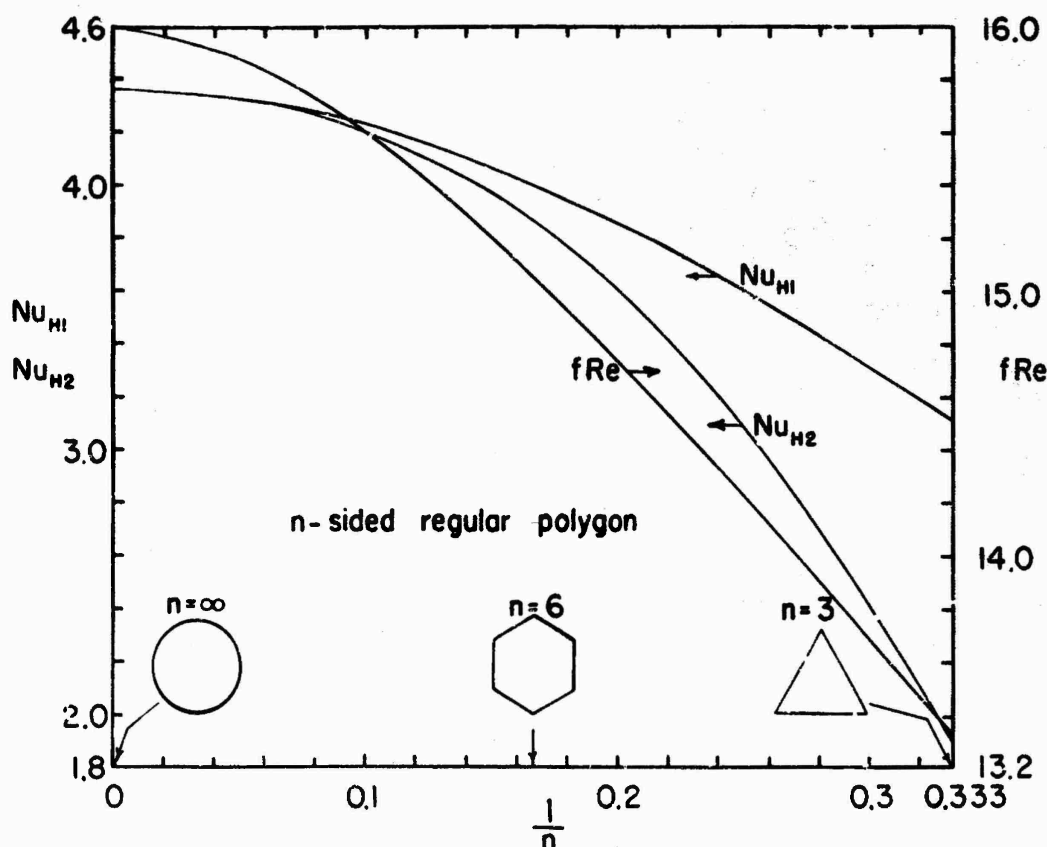


Fig. 42 Regular polygonal ducts  $fRe$ ,  $Nu_{H1}$  and  $Nu_{H2}$  for fully developed laminar flow.

## 12. CUSPED DUCTS

A cusped duct, also referred to as a star-shaped duct, is made of  $n$  concave circular arcs. A bank of circular tubes touching each other forms this cusped duct geometry on the outside of tubes. Shih [53] employed the 12-point matching method and evaluated the fully developed laminar flow friction factor and other related flow parameters for the cusped ducts of sides 3, 4, 5, 6 and 8. The  $f_{Re}$  factors are presented in Table 32.

Table 32. Regular polygonal ducts  $f_{Re}$ ,  $Nu_{H1}$  and  $Nu_{H2}$   
and Cusped ducts  $f_{Re}$  for fully developed laminar flow

n	Regular polygonal ducts			Cusped
	$f_{Re}$	$Nu_{H1}$ [51]	$Nu_{H2}$ [52]	$f_{Re}$ [53]
3	13.333 [53]	3.111	1.892	6.503284
4	14.227 [53]	3.608	3.091	6.605802
5	14.737 [53]	3.859	3.605	6.634380
6	15.054 [53]	4.002	3.862	6.639114
7	15.31 [51]	4.102	4.009	-
8	15.412 [53]	4.153	4.100	6.628657
9	15.52 [51]	4.196	4.159	
10	15.60 [51]	4.227	4.201	
20	15.88 [51]	4.329	4.328	
$\infty$	16.000	4.364	4.364	

### 13. ELLIPTICAL DUCTS

The fully developed laminar flow  $fRe$ ,  $Nu_{H1}$  and  $Nu_T$  have been determined for the elliptical ducts. However, no hydrodynamic entry length solutions have been reported. The thermal entry length solution for the fully developed laminar flow case has been investigated to a limited extent.

#### 13.1 Fully Developed Flow

##### 13.1.1 Velocity Profile and Friction Factors

The velocity profile for the elliptical duct of Fig. 43 with  $2a$  and  $2b$  as major and minor axes is given by [2,33, 36] and the  $fRe$  by [19] as follows.

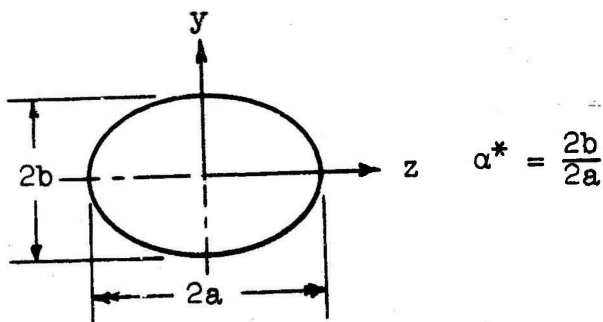


Fig. 43 An elliptical duct.

$$u = \frac{c_1}{2(1 + \alpha^{*2})} \left[ \alpha^{*2} z^2 + y^2 - b^2 \right] \quad (170)$$

$$u_m = - \frac{c_1}{\pi} \frac{b^2}{1 + \alpha^{*2}} \quad (171)$$

$$fRe = 2(1 + \alpha^{*2}) \left[ \frac{\pi}{E(m)} \right]^2 \quad (172)$$

$$D_h = \frac{\pi b}{E(m)} \quad (173)$$

where  $m = (1 - \alpha^2)^{1/2}$  and  $E(m)$  is the complete elliptical integral of the second kind.

Note that one limiting case corresponds to  $\alpha^* = 1$ , a circular duct, for which above formulae indeed reduce to those of the circular duct. But the other limiting case  $\alpha^* = 0$  does not appear to be the parallel plate geometry as discussed below. If the distance  $2b$  is kept constant, and  $2a$  is increased to infinity, the limiting case has  $\alpha^* = 0$  and  $D_h = \pi b$ . The  $D_h$  for the parallel plates separated by the  $2b$  distance is  $4b$ . Similar to the limiting case of the isosceles triangular duct, one might expect that

$$\frac{(fRe)_{\text{elliptical}}}{(fRe)_{\text{parallel plate}}} = \frac{(D_h)_{\text{ell.}}}{(D_h)_{\text{p.p.}}} \quad (174)$$

That is  $fRe$  for the elliptical duct with  $\alpha^* = 0$  would be  $(\frac{\pi b}{4b})(24) = 6\pi$ ; however, from Eq. (172),  $(fRe)_{\alpha^*=0} = 2\pi^2$ , about 5 percent higher. Thus the elliptical duct does not resemble the parallel plate geometry in the limit.

The  $fRe$  were calculated from Eq. (172) on the Stanford IBM 360/67 computer using double precision, and are presented in Table 33 and Fig. 44.

Lundgren et al. [19] determined the dimensionless pressure drop increment  $K(\infty)$  resulting from the flow development in the entrance region. McComas [20] extended Ref. [15] results, and presented the hydrodynamic entrance length  $L_{hy}^+$ . The  $K(\infty)$  and  $L_{hy}^+$  are presented in Table 33 and Fig. 44.

### 13.1.2 Fully Developed $Nu_T$

Dunwoody [237] determined laminar flow fully developed  $Nu_T$  as an asymptote to his thermal entry length solution for the elliptical ducts. Later Schenk and Han [238] confirmed his results for two aspect ratios. James [67] presented the

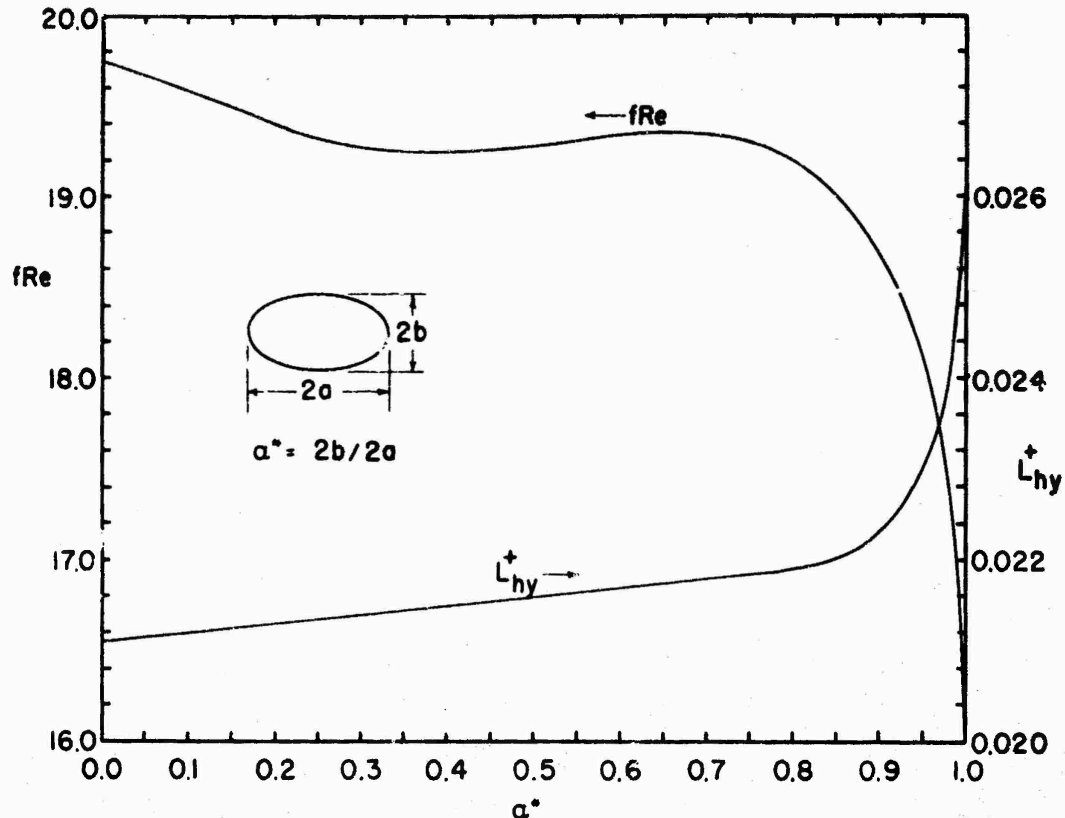


Fig. 44 Elliptical ducts  $fRe$  and  $L_{hy}^+$  for fully developed laminar flow.

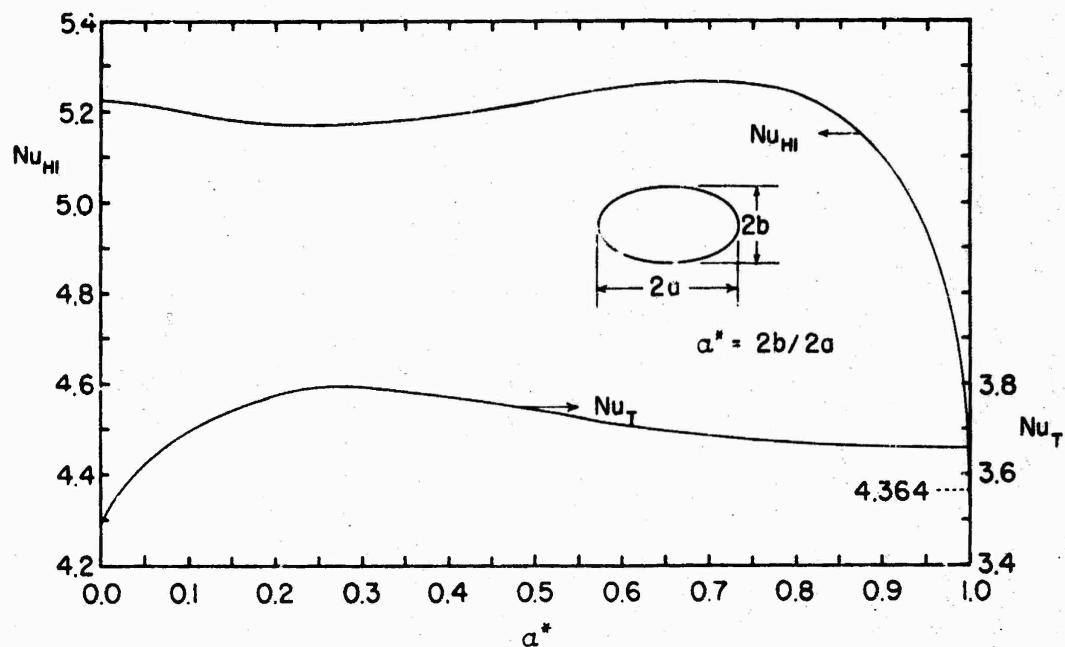


Fig. 45 Elliptical ducts  $Nu_T$  and  $Nu_{Hl}$  for fully developed laminar flow.

Table 33. Elliptical ducts  $fRe$ ,  $K(\infty)$ ,  $L_{hy}^+$ ,  $Nu_{H1}$  and  $Nu_T$  for fully developed laminar flow

$\alpha^*$	$fRe$	$K(\infty)$	$L_{hy}^+$	$Nu_T$	$Nu_{H1}$
1.00	16.000	1.333	0.0260	3.658	4.364
0.99	17.055		0.0244		4.651
0.98	17.443		0.0239		4.757
0.95	18.114		0.0230		4.940
0.90	18.700		0.0223		5.099
0.85	19.020				5.185
0.80	19.202		0.0219	3.669	5.233
0.75	19.299				5.257
0.70	19.340				5.265
2/3	19.347				5.264
0.65	19.346				5.262
0.60	19.329		0.0217		5.252
0.55	19.302				5.238
0.50	19.273			3.742	5.222
0.45	19.250				5.206
0.40	19.239		0.0215		5.191
0.35	19.245				5.180
1/3	19.252				5.177
0.30	19.272				5.172
0.25	19.322			3.792	5.170
0.20	19.394		0.0213		5.173
1/6	19.453				5.178
1/7	19.500				5.184
1/8	19.536			3.725	5.189
1/9	19.565				5.193
0.10	19.588		0.0212		5.196
1/16	19.662			3.647	5.209
0.050	19.684				5.214
0.000	19.739	1.333	0.0211	3.488	5.225

$Nu_T$  for  $\alpha^* = 0$ . All these results are presented in Table 33 and Fig. 45.

### 13.1.3 Fully Developed $Nu_{H1}$

The fully developed laminar heat transfer problem with internal thermal energy sources was first investigated by Tao [36]. He analyzed the problem by the method of complex variables. Tyagi [23] extended Tao's work by including the viscous dissipation. The closed form formulae were presented for the velocity and temperature distributions, bulk mean velocity and temperature, and  $Nu_{H1}$ . In absence of viscous dissipation and thermal energy sources, the  $Nu_{H1}$

are given by Tyagi as

$$Nu_{H1} = \left[ \frac{3\pi}{E(m)} \right]^2 \frac{(1 + a^*^2)[(1 + a^*^4) + 6a^*^2]}{17(1 + a^*^4) + 98a^*^2} \quad (175)$$

The  $Nu_{H1}$  were evaluated from this equation on the Stanford IBM 360/67 computer using double precision and are presented in Table 30 and Fig. 45.

### 13.1.4 Fully Developed $Nu_{R1}$

Based on the Schenk and Han's [238] results for the thermal entry length solution for the  $R1$  boundary condition, the fully developed  $Nu_o$  and  $Nu_{R1}$  are calculated and presented in Table 3 for the elliptical duct with  $a^* = 0.8$ .

### 13.2 Hydrodynamically Developing Flow

To the authors' knowledge, no hydrodynamic entry length solution has been obtained for the elliptical ducts.

### 13.3 Thermally Developing Flow

Dunwoody [237] investigated the  $T$  thermal entry length problem for the fully developed laminar flow through elliptical ducts. Based on his previous work with the free vibrations of membranes with elliptical boundaries, he arrived at the  $Nu_{x,T}$  in a double infinite series form. He evaluated numerically and tabulated the necessary coefficients and eigenvalues for  $a^* = 0.8, 0.5, 0.25, 0.125$  and  $0.0625$ . Schenk and Han [238] extended the work of Dunwoody for the  $a^* = 0.8$  and  $0.25$  to check the accuracy of the results and to obtain more insight into the physical aspects. The results of Refs. [237] and [238] are in excellent agreement. They then considered the finite wall thermal resistance ( $R_w = 10, 1, 0.2$  and  $0$ ) for the elliptical duct with  $a^* = 0.8$ , and tabulated the eigenvalues and eigencorstants for

the thermal entry length problem. Tao [103] applied a variational approach to the same problem for elliptical ducts and presented an expression for the mixed mean fluid temperature in the thermal entrance.

Rao et al. [239] solved the thermal entry length problem for short elliptical ducts with  $\textcircled{T}$  and  $\textcircled{H1}$  boundary conditions. They used the Lévêque approximation near the entrance region to arrive at the solution. Hence, the solution is not applicable to long ducts. The results do not approach asymptotically to the fully developed values. Their results are in fair agreement near the entrance with the results of Schenk and Han [238]. In the Rao et al. empirical formulae for the local and average Nusselt numbers, a correction factor for the temperature dependent viscosity was also included. James [67] also presented the  $\textcircled{T}$  thermal entrance solution, based on Lévêque theory, for short elliptical ducts with  $\alpha^*$  from 1 to 0. His tabulated values for the local  $Nu_{x,T}$  are in excellent agreement with the tabulated values of Rao et al. [239] when the effect of the temperature dependent viscosity in the  $Nu_{x,T}$  expression is eliminated.

## 14. MOON SHAPED DUCTS

Only the fully developed laminar flow through the duct formed by two circular arcs (as shown in Fig. 46) has been analyzed.

### 14.1 Fully Developed Laminar Flow

For the duct formed by two circular arcs, whose cross section is shown in Fig. 46, the geometrical properties are found as follows.

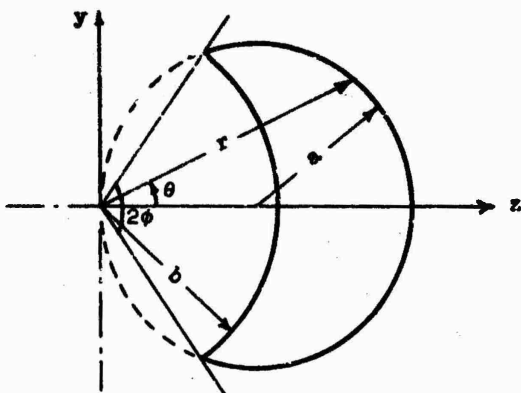


Fig. 46 A moon shaped duct.

$$P = 2(2a + b)\phi \quad (176)$$

$$A_c = (2a^2 - b^2)\phi + a^2 \sin 2\phi \quad (177)$$

$$D_h = 2a \frac{(2 - \alpha^2)\phi + \sin 2\phi}{(2 + \alpha^2)\phi} \quad (178)$$

$$\cos \phi = \frac{b}{2a} \quad \text{and} \quad \alpha^* = \frac{b}{a} \quad (179)$$

Based on the analogy with torsion theory [33], the fully developed laminar velocity profile, solution of Eqs. (3b) and (4), for this duct is given by

$$u = \frac{c_1}{4} \left( r^2 - b^2 \right) \left( 1 - \frac{2a \cos \theta}{r} \right) \quad (180)$$

The mean velocity is calculated as

$$u_m = \frac{c_1 a^2}{-\frac{1}{4}} \frac{\left(\frac{1}{2}a^4 + 2a^2 - 1\right)\phi - \frac{8a^3}{3}\sin\phi + \left(a^2 - \frac{2}{3}\right)\sin 2\phi - \frac{1}{12}\sin 4\phi}{(2-a^2)\phi + \sin 2\phi} \quad (181)$$

The friction factor is then determined from Eq. (29)

$$fRe = -\frac{c_1 D_h^2}{2u_m}$$

where  $D_h$  and  $u_m$  are substituted from Eqs. (178) and (181). The fully developed laminar  $fRe$  factors for this duct were determined from the above formula on the Stanford IBM 360/67 computer using a double precision. The results are presented in Table 31 and Fig. 47.

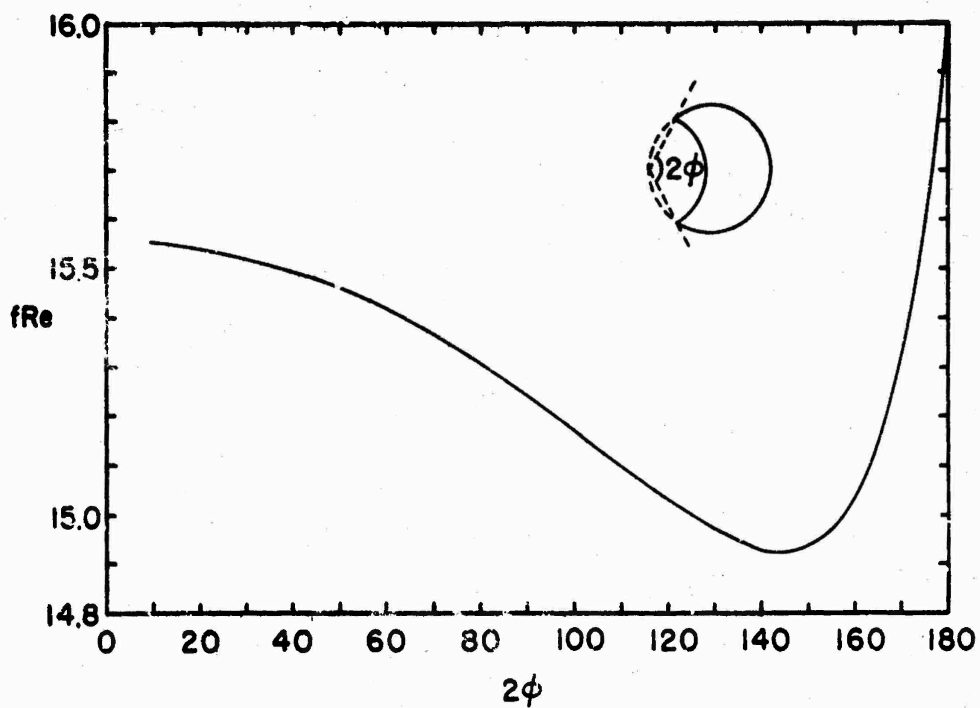


Fig. 47 Moon shaped ducts  $fRe$  for fully developed laminar flow.

## 15. CARDIOID DUCTS

Only the fully developed laminar flow through the cardioid duct (Fig. 48) has been analyzed.

### 15.1 Fully Developed $f_{Re}$ , $Nu_{H1}$ , $Nu_{H2}$

Tao [38] considered laminar flow friction and heat transfer through a cardioid duct for  $H1$  boundary condition by the method of conformal mapping. He included the effect of thermal energy sources within the fluid. Later he considered the flow and heat transfer through a Pascal's limacon [39]. The circular tube and the cardioid duct are limiting cases of the Pascal's limacon. He presented closed form formulae for the fluid velocity and temperature distribution, mean velocity, average and bulk mean temperature, the wall heat flux and  $Nu_{H1}$ . Tyagi [25] extended Tao's work by including the effect of viscous dissipation, gas compression work and the uniform thermal energy sources within the fluid for  $H1$  boundary condition. For the special case of cardioid duct of Fig. 48 with no viscous dissipation, the gas compression work thermal energy sources within the fluid, the  $f_{Re}$  and  $Nu_{H1}$  are given by

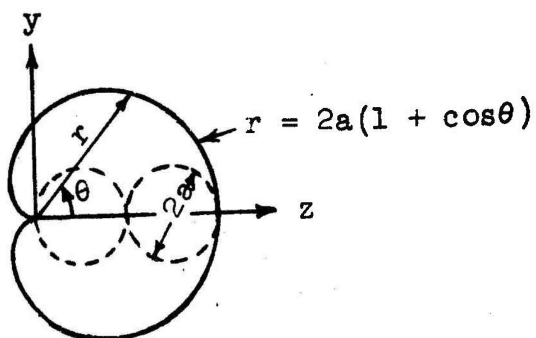


Fig. 48 A cardioid duct.

$$fRe = \frac{27\pi^2}{17} = 15.675 \quad (182)$$

$$Nu_{H1} = \frac{1}{3C} \cdot \frac{75}{2} \pi^2 = 4.208 \quad (183)$$

Note that the  $fRe$  and  $Nu_{H1}$  are 2.0 and 5.4 percent respectively lower than the corresponding circular tube result.

Tao [40] also considered the  $H2$  boundary condition for the cardioid duct using the conformal mapping method, where he included the effect of uniform thermal energy sources within the fluid. Tyagi [24,26] extended the work of Tao [40] by including the effect of viscous dissipation within the fluid. The formulae were presented for the velocity and temperature distribution as well as the flow cross section average and bulk mean fluid temperature. In absence of internal thermal energy sources and the viscous dissipation, the  $Nu_{H2}$  is expressed as

$$Nu_{H2} = \frac{3\pi}{8} \left[ \frac{1}{\pi} \left( \frac{4739}{765} - 8 \ln 2 \right) \right]^{-1} = 5.698 \quad (184)$$

Note that this result is 31 percent higher than that for the circular tube. Even though, Tyagi [24,26] made corrections to the  $Nu_{H2}$  expression of Tao [40] there still seems to be an error, as one would expect  $Nu_{H2}$  to be closer to and lower than the value for the circular tube in view of the agreement shown for  $Nu_{H1}$ .

## 16. CONCENTRIC ANNULAR DUCTS

The simplest form of a two fluid heat exchanger is a double pipe heat exchanger made up of two concentric tubes. One fluid flows through the inside tube, while the other fluid flows through the annular passage formed in between two concentric tubes. Consequently, the heat transfer and fluid friction behavior for the developing and developed profiles has been analyzed for a variety of boundary conditions for both circular tube and concentric annular duct.

The two limiting cases of annular ducts, the circular duct and parallel plates were considered in detail previously; hence only the case of  $0 < r^* < 1$  will be considered here. A literature survey on the pertinent subject up to 1962 is made by Reynolds et al. [240].

### 16.1 Fully Developed Flow

#### 16.1.1 Fully Developed Hydrodynamic Problem

The hydrodynamic problem for the fully developed laminar flow was first solved by Lamb [241]. The velocity distribution and the corresponding friction factors are given by [242,243] as follows.

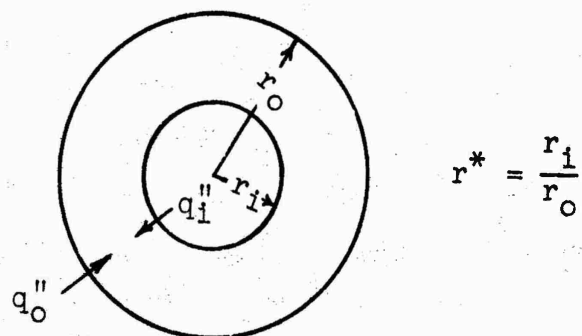


Fig. 49 A concentric annular duct.

$$u = - \frac{c_1}{4} r_o^2 \left[ 1 - \left( \frac{r}{r_o} \right)^2 - (1 - r^{*2}) \frac{\ln(r/r_o)}{\ln r^*} \right] \quad (185)$$

$$u_m = - \frac{c_1 r_o^2}{8} \left[ 1 + r^{*2} + \frac{1 - r^{*2}}{\ln r^*} \right] \quad (186)$$

$$fRe = \frac{16(1 - r^*)^2}{1 + r^{*2} + [(1 - r^{*2})/\ln r^*]} \quad (187)$$

The friction factor is defined on the basis of the average wall shear stress around the perimeter of annulus, i.e.,

$$f = \frac{\tau_i r_i + \tau_c r_o}{r_i + r_o} \frac{2g_c}{\rho u_m^2} \quad (188)$$

The values of  $fRe$  based on Eq. (187) are presented in Table 34 and Fig. 50.

Lundgren et al. [19] determined the fully developed laminar flow pressure drop increment  $K(\infty)$ , based on Eq. (32), for the annular ducts. McComas [20] evaluated the hydrodynamic entrance length  $L_{hy}^+$  for the annular ducts. These  $K(\infty)$  and  $L_{hy}^+$  for the annular ducts are also presented in Table 34 and Fig. 50.

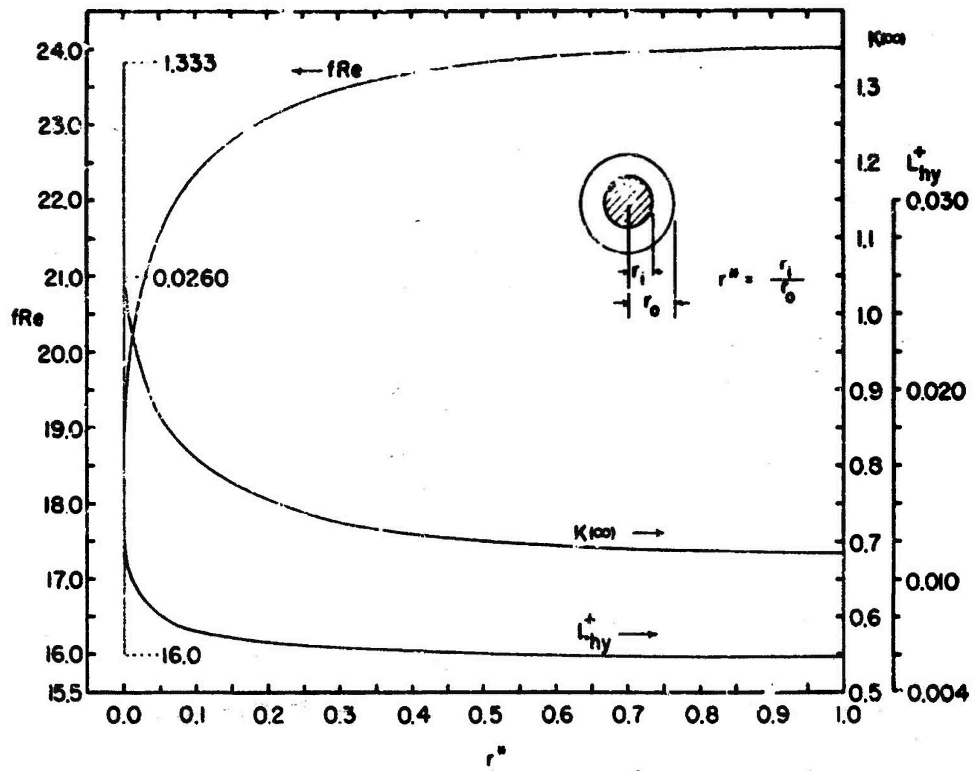


Fig. 50 Concentric annular ducts  $fRe$ ,  $K(\infty)$  and  $L_{hy}^+$  for fully developed laminar flow.

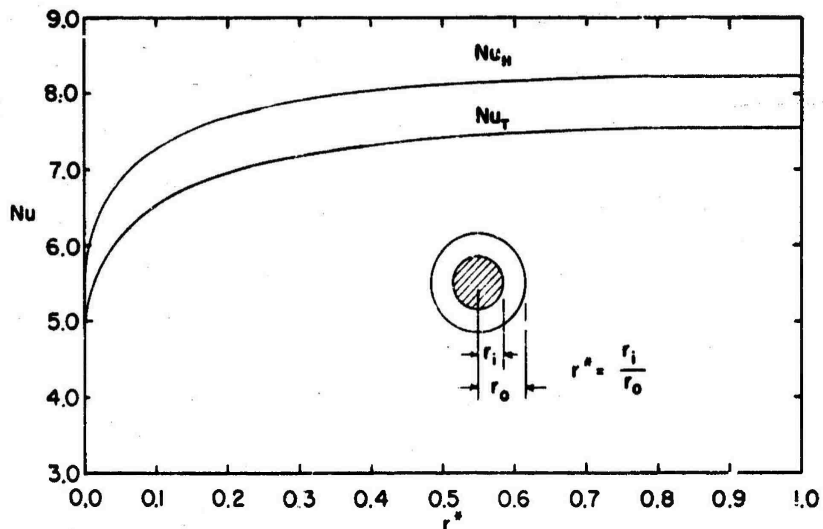


Fig. 51 Concentric annular ducts  $Nu_T$  and  $Nu_H$  for fully developed laminar flow.

Table 34. Concentric annular ducts  $fRe$ ,  $K(\infty)$ ,  $L_{hy}^+$ ,  $Nu_T$  and  $Nu_H$  for fully developed laminar flow

$r^*$	$fRe$	$K(\infty)$	$L_{hy}^+$	$Nu_T$	$Nu_H$
		[20]	[20]		
0	16.000	1.3333	0.0260	3.657	4.364
0.0001	17.945	1.1312	0.01380	-	5.185
0.001	18.671	1.0727	0.01208	-	5.497
0.01	20.028	0.9733	0.00982	-	6.101
0.02	20.629	-	-	5.636	6.383
0.04	21.325	-	-	-	6.725
0.05	21.567	0.8644	0.00800	6.099	6.847
0.06	21.769	-	-	-	6.951
0.08	22.092	-	-	-	7.122
0.10	22.343	0.8087	0.00725	6.517	7.257
0.15	22.790	0.7762	0.00685	-	7.506
0.20	23.088	0.7542	0.00660	-	7.678
0.25	23.302	-	-	7.084	7.804
0.30	23.461	0.7264	0.00630	-	7.900
0.40	23.678	0.7100	0.00613	-	8.033
0.50	23.813	-	-	7.414	8.117
0.60	23.897	0.6935	0.00596	-	8.170
0.70	23.949	-	-	-	8.203
0.80	23.980	0.6872	0.00589	-	8.222
0.90	23.996	0.6860	0.00588	-	8.232
1.00	24.000	0.6857	0.00588	7.541	8.235

### 16.1.2 Fully Developed Heat Transfer Problem

#### 16.1.2.1 Prescribed Constant Temperature or Heat Flux at Walls

Depending upon the temperature or heat flux specified at inner or outer surface of the annulus there are four fundamental problems possible as described in PARALLEL PLATES Section, Fig. 15. For each fundamental problem, there are two solutions, one for each of the two surfaces, thus totaling eight heat transfer solutions. These solutions are identified for the ready reference in the following tabulation.

Table 35. Fundamental solutions for concentric annular ducts

Solutions	Fundamental problems (Fig. 15)
(1) $t_o = t_e = \text{constant}$ , $t_i = \text{constant}$ (2) $t_i = t_e = \text{constant}$ , $t_o = \text{constant}$	first kind
(3) $q_o'' = 0$ , $q_i'' = \text{constant}$ (4) $q_i'' = 0$ , $q_o'' = \text{constant}$	second kind
(5) $q_o'' = 0$ , $t_i = \text{constant}$ (6) $q_i'' = 0$ , $t_o = \text{constant}$	third kind
(7) $t_o = t_e = \text{constant}$ , $q_i'' = \text{constant}$ (8) $t_i = t_e = \text{constant}$ , $q_o'' = \text{constant}$	fourth kind

Jacob and Rees [244] analytically obtained the temperature distribution for the fundamental solution of the second kind for hydrodynamically and thermally fully developed flow. For the boundary condition corresponding to the second kind (inner wall heater or cooled, outer wall insulated), several early investigators [245, 246] correlated heat transfer data empirically considering variable properties of the fluid. Murakawa [247, 248] presented an integral equation formulation for the solution of the first kind and a series solution approach to the same problem including arbitrary peripheral variations. Murakawa did not carry his solutions to the point of numerical computation.

Lundberg et al. [242, 243] systematically approached all four fundamental problems and their various combinations.

Table 36a. Annular ducts fundamental solutions of first kind

$r^*$	$\phi_{11}^{(1)} - \phi_{10}^{(1)}$	$\phi_{00}^{(1)} - \phi_{01}^{(1)}$	$\phi_{mi}^{(1)}$	$\phi_{mo}^{(1)}$	$M_{11}^{(1)} - M_{10}^{(1)}$	$M_{00}^{(1)} - M_{01}^{(1)}$
0	=	0	0	1	=	2.666667
0.0001	217.255262	0.2171295	0.0781242	0.9213758	2359.257938	2.779235
0.001	299.260125	0.2892601	0.1026478	0.8959522	322.254360	2.823294
0.01	42.995154	0.4299515	0.1478340	0.8521660	50.453962	2.908341
0.02	29.050977	0.5010195	0.1699319	0.8300681	30.179421	2.948395
0.04	14.912038	0.5964815	0.1988750	0.8011250	18.613872	2.999279
0.05	12.684712	0.6342356	0.2100902	0.7899098	16.058631	3.018872
0.06	11.137134	0.6682281	0.2200722	0.7799278	14.279700	3.036404
0.08	9.106284	0.728026	0.2374902	0.7625098	11.942512	3.067506
0.10	7.817301	0.7817301	0.2525559	0.7474465	10.498764	3.095280
0.15	5.973968	0.8960951	0.2838370	0.714630	8.361631	3.157077
0.20	4.970679	0.9941359	0.3093762	0.6906258	7.197355	3.213377
0.25	4.328005	1.0820213	0.3311972	0.6688026	6.671392	3.267000
0.30	3.876057	1.1628170	0.3503397	0.6496603	5.966282	3.319113
0.40	3.274070	1.3096280	0.3828461	0.6171539	5.305111	3.420769
0.50	2.885390	1.4426950	0.4098156	0.5901844	4.888963	3.520352
0.60	2.610154	1.5660922	0.4328008	0.5671992	4.601828	3.618506
0.70	2.403149	1.6822040	0.4527569	0.54672431	4.391373	3.715469
0.80	2.240710	1.7925680	0.4703248	0.5296752	4.230347	3.811341
0.90	2.109160	1.8982443	0.4859601	0.5140399	4.103106	3.906173
1.00	2.000000	2.0000000	0.5000000	0.5000000	4.000000	4.000000

Table 36b. Annular ducts fundamental solutions of second kind

$r^*$	$(\theta_{11}^{(2)} - \theta_{10}^{(2)})$	$(\theta_{01}^{(2)} - \theta_{00}^{(2)})$	$(\theta_{mi}^{(2)} - \theta_{mo}^{(2)})$	$(\theta_{10}^{(2)} - \theta_{mo}^{(2)})$	$M_{11}^{(2)}$	$M_{00}^{(2)}$
0	0	0	0.229167	-0.145933	=	4.363636
0.0001	0.0004107	-0.00001389	0.2203366	-0.1388747	2436.900019	4.526185
0.001	0.0029670	-0.00013617	0.2180279	-0.1361083	337.044136	4.586569
0.01	0.0183128	-0.00130725	0.2131133	-0.1307253	50.016694	4.692340
0.02	0.0305763	-0.00255890	0.2112270	-0.1279452	32.705116	4.734244
0.04	0.0687585	-0.004964688	0.2092915	-0.1261220	20.509247	4.778025
0.05	0.0561442	-0.00612338	0.2086820	-0.1228575	17.811277	4.791979
0.06	0.0627609	-0.00726861	0.2081935	-0.1211435	15.933494	4.803225
0.08	0.0762498	-0.00948471	0.2074388	-0.1185589	13.468057	4.820699
0.10	0.0939928	-0.01162135	0.2068290	-0.1162135	11.905784	4.834212
0.15	0.1032909	-0.01464977	0.2057502	-0.1109985	9.687025	4.860262
0.20	0.1176420	-0.02127792	0.2046095	-0.1063896	8.498921	4.882587
0.25	0.1287945	-0.02555181	0.2038840	-0.1022072	7.753473	4.904751
0.30	0.1380995	-0.02950903	0.2029219	-0.0983634	7.241194	4.928005
0.40	0.1518994	-0.03659804	0.2008369	-0.0914951	6.583303	4.979165
0.50	0.1617057	-0.04275661	0.1985493	-0.0855142	6.181015	5.034533
0.60	0.1491558	-0.04614912	0.1941086	-0.0802685	5.911709	5.099125
0.70	0.1768162	-0.05290502	0.1935665	-0.0759786	5.720359	5.166194
0.80	0.1792600	-0.05712724	0.1909658	-0.0714091	5.578491	5.238560
0.90	0.1328193	-0.06089851	0.1883400	-0.0676850	5.4469883	5.309566
1.00	0.185714	-0.0662857	0.185714	-0.0642857	5.384615	5.384615

Table 36c. Annular ducts fundamental solutions of third kind

$r^*$	$\theta_{01}^{(3)}, \theta_{10}^{(3)}, \theta_{mi}^{(3)}, \theta_{mo}^{(3)}$	$\theta_{11}^{(3)}, \theta_{00}^{(3)}$	$M_{11}^{(3)}$	$M_{00}^{(3)}$
0	1	0	=	3.6568
0.02	1	0	32.537	3.9934
0.05	1	0	17.666	4.0565
0.10	1	0	11.560	4.1135
0.25	1	0	7.3708	4.2321
0.50	1	0	5.7382	4.4293
1.00	1	0	4.8668	4.8668

Table 36d. Concentric annular ducts fundamental solutions of the fourth kind

$r^*$	$\theta_{ii}^{(4)}$	$\theta_{oi}^{(4)}$	$\theta_{oo}^{(4)}$	$\phi_{ic}^{(4)}$	$\phi_m^{(4)}$	$\theta_{m0}^{(4)}$	$Nu_{ii}^{(4)} - Nu_{io}^{(4)}$	$Nu_{oo}^{(4)} - Nu_{oi}^{(4)}$
0	0	0	=	=	0	=	=	2.666667
0.2001	0.3906604	-0.0001	0.0356307	-13000.000000	0.0003563	0.2450195	2395.257938	2.779235
0.001	0.3036673	-0.301	3.6573390	-10'0.000000	0.0002942	0.1031988	322.254280	2.823294
0.01	0.0232584	-0.01	2.3258435	-100.000000	0.0034384	0.9820049	50.453967	2.908341
0.02	0.0399184	-0.02	1.9999301	-50.000000	0.0067834	0.9507540	30.179423	2.946355
0.04	0.0670599	-0.04	1.6764976	-25.000000	0.0133365	1.3430843	18.613072	2.999279
0.05	0.0788391	-0.05	1.5767012	-20.000000	0.0165625	1.2654517	16.056431	3.010072
0.06	0.0897697	-0.06	1.4904951	-16.666667	0.0197602	1.1571581	14.279700	3.036404
0.08	0.1090143	-0.08	1.3726786	-12.500000	0.0260794	1.0466609	11.962512	3.067506
0.10	0.1279214	-0.10	1.2792139	-10.000000	0.0323073	0.9561614	10.498704	3.095280
0.15	0.1673929	-0.15	1.1159529	-6.666667	0.0475123	0.7992043	8.341631	3.157077
0.20	0.2011797	-0.20	1.0059987	-5.000300	0.0622398	0.6946499	7.197395	3.213377
0.25	0.2310691	-0.25	0.9241962	-4.000102	0.0785228	0.6181051	6.471392	3.267000
0.30	0.2579942	-0.30	0.8599806	-3.333333	0.0903858	0.5586652	5.946282	3.319113
0.40	0.3054302	-0.40	0.7635756	-2.900000	0.1169328	0.4712036	5.305111	3.420769
0.50	0.3465736	-0.50	0.6931472	-2.000300	0.1420312	0.4090847	4.888963	3.520352
0.60	0.3831192	-0.60	0.6385320	-1.666667	0.1658143	0.36211749	4.601829	3.610566
0.70	0.4162008	-0.70	0.5944582	-1.428571	0.1884015	0.3293132	4.391373	3.715469
0.80	0.4462071	-0.80	0.5576589	-1.250000	0.2098999	0.2956840	4.230347	3.811341
0.70	0.4761223	-0.70	0.5240006	-1.111111	0.2304045	0.2707975	4.103106	3.906173
1.00	0.5000000	-1.00	0.5000000	-1.000000	0.2500000	0.2500000	4.000000	4.000000

Their results for the dimensionless temperatures, heat fluxes and Nusselt numbers for the laminar flow fully developed velocity and temperature profiles are presented in Table 36. The dimensionless temperature  $\theta$  and heat flux  $\Phi$  are defined by Eqs. (133) and (134). In the double subscripted parameters, the first subscript  $i$ ,  $o$ , or  $m$  represents inner wall, outer wall, and bulk mean values respectively; the second subscript  $i$  or  $o$  refers to inner wall and outer wall heated (or cooled) respectively. The superscript refers to the kind of fundamental problem. For example,  $\Phi_{io}^{(1)}$  means dimensionless wall heat flux at the inner wall when the outer wall is heated (or cooled) as specified by the fundamental problem of the first kind. The results of Table 36, based on the equations presented in Ref. [242], were recalculated on the Stanford IBM computer using double precision.<sup>23</sup>

<sup>23</sup>Eqs. (II.D.23) and (II.D.24) of Ref. [242] were in error and were corrected to get the results of Table 36.

When the viscous dissipation and internal thermal energy sources are neglected in Eq. (5), the resulting equation is linear and homogeneous. Consequently, a solution can be established for boundary conditions synthesized from the four fundamental problems by the superposition of the eight solutions of Table 35. The following three problems with axisymmetric boundary conditions, synthesized from the fundamental problems of first, second and fourth kinds, are of engineering interest: (a) constant but different temperatures specified on both walls, (b) constant but different heat fluxes specified on both walls, and (c) constant temperature specified on one wall and constant heat flux specified on the other wall. The temperature, wall heat flux and the Nusselt number relationships for these three problems are presented below. For the case of arbitrarily prescribed axisymmetric heat flux or temperature on whole or part of either wall, the solutions can be determined by the method of superposition. For the details, refer to [242,243]. The Nusselt number for outer and inner wall are defined as

$$Nu_o = \frac{h_o D_h}{k} \quad \text{where} \quad h_o = \frac{q_o''}{t_o - t_m} \quad (189)$$

$$Nu_i = \frac{h_i D_h}{k} \quad \text{where} \quad h_i = \frac{q_i''}{t_i - t_m} \quad (190)$$

In the following formulae,  $\theta$  and  $\Phi$  are found from Table 36. (a) Constant but different temperatures specified on both walls: For  $x \geq x_e$ ,

$$t = t_i \quad \text{on the inner wall}$$

$$t = t_o \quad \text{on the outer wall, and}$$

$t = t_e$  for all  $r$  at  $x < x_e$ . In this case,

**Table 37. Concentric annular ducts Nusselt numbers for specified constant temperatures and axial heat fluxes at inner and outer walls for fully developed laminar flow**

$r^* = \frac{r_1}{r_0}$	Case (a) <sup>25</sup> and (c) <sup>26</sup>		Case (d) constant and equal wall temperatures		Case (b) constant and equal wall heat fluxes		Case (b2) <sup>27</sup>		
	$Nu_i$	$Nu_o$	$Nu_i$	$Nu_o$	$Nu_i$	$Nu_o$	$Nu_i$	$Nu_o$	$\dot{q}_i/\dot{q}_o$
0.00	-	1.667	-	3.657	0	4.364	-	4.364	-
0.01	2.024	2.024	2.024	2.024	-1.622	4.669	-0.912	4.751	0.912
0.02	2.024	2.024	2.024	2.024	-1.327	4.669	-0.700	4.751	0.700
0.04	2.024	2.024	2.024	2.024	-0.912	4.669	-0.497	4.751	0.497
0.06	2.024	2.024	2.024	2.024	-0.620	4.669	-0.300	4.751	0.300
0.08	2.024	2.024	2.024	2.024	-0.427	4.669	-0.166	4.751	0.166
0.10	2.024	2.024	2.024	2.024	-0.320	4.669	-0.083	4.751	0.083
0.15	2.024	2.024	2.024	2.024	-13.249	4.669	-0.772	4.669	0.772
0.20	2.024	2.024	2.024	2.024	-19.655	4.669	-2.200	4.669	2.200
0.25	2.024	2.024	2.024	2.024	-17.142	4.669	-3.971	4.669	3.971
0.30	2.024	2.024	2.024	2.024	-22.199	4.669	-5.022	4.669	5.022
0.40	2.024	2.024	2.024	2.024	-34.976	4.669	-8.162	4.669	8.162
0.50	2.024	2.024	2.024	2.024	-126.768	4.669	-16.314	4.669	16.314
0.60	2.024	2.024	2.024	2.024	-467.712	4.669	-34.253	4.669	34.253
0.70	2.024	2.024	2.024	2.024	-136.359	4.669	-54.524	4.669	54.524
0.80	2.024	2.024	2.024	2.024	-25.166	4.669	-11.993	4.669	11.993
0.90	2.024	2.024	2.024	2.024	-16.355	4.669	-6.766	4.669	6.766
0.95	2.024	2.024	2.024	2.024	-12.111	4.669	-4.970	4.669	4.970
0.98	2.024	2.024	2.024	2.024	-11.466	4.669	-4.759	4.669	4.759
0.99	2.024	2.024	2.024	2.024	-11.077	4.669	-4.620	4.669	4.620
0.995	2.024	2.024	2.024	2.024	-10.715	4.669	-4.500	4.669	4.500
0.999	2.024	2.024	2.024	2.024	-10.411	4.669	-4.400	4.669	4.400
1.00	2.024	2.024	2.024	2.024	-10.163	4.669	-4.300	4.669	4.300

<sup>25</sup>Case (a1): constant but different wall temperatures specified on both walls.

<sup>26</sup>Case (c): constant temperature specified on one wall and constant heat flux specified on other wall.

<sup>27</sup>Case (b2): equal and constant wall temperatures at any axial location, but different and constant axial heat fluxes on both walls.

Note that constant means constant both in time and space.

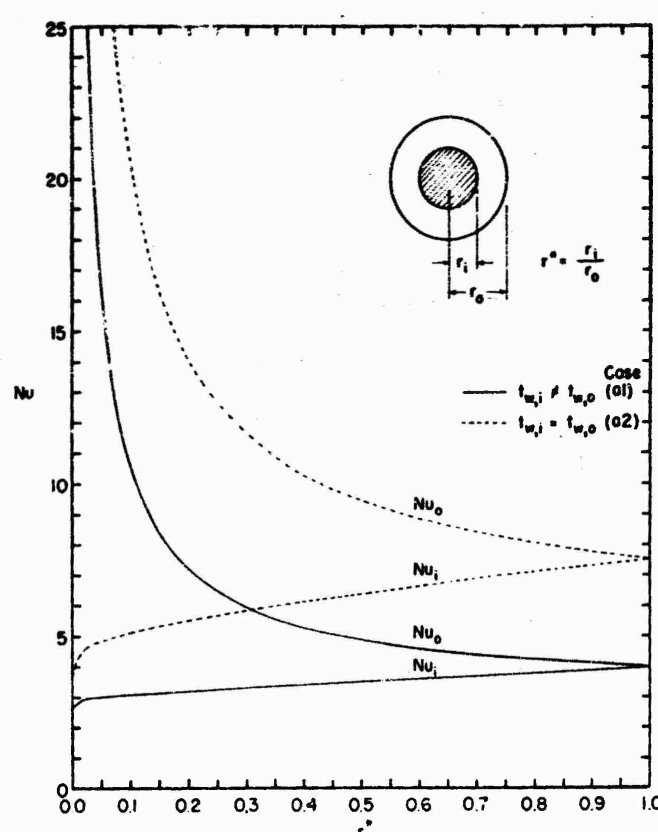


**Fig. 52 Concentric annular ducts  $Nu_i$  and  $Nu_o$  for constant temperatures on both walls for fully developed laminar flow.**

$$t_m = t_i \theta_{mi}^{(1)} + t_o \theta_{mo}^{(1)} + t_e \quad (191)$$

$$q_i'' = \frac{k}{D_h} [(t_i - t_e) \Phi_{ii}^{(1)} + (t_o - t_e) \Phi_{io}^{(1)}] \quad (192)$$

$$q_o'' = \frac{k}{D_h} [(t_i - t_e) \Phi_{oi}^{(1)} + (t_o - t_e) \Phi_{oo}^{(1)}] \quad (193)$$

$$Nu_i = \frac{\Phi_{ii}^{(1)}}{\theta_{mo}^{(1)}} \quad (194)$$

$$Nu_o = \frac{\Phi_{oo}^{(1)}}{\theta_{mi}^{(1)}} \quad (195)$$

The Nusselt numbers for this case, based on Eqs. (194) and (195) are presented as Case (a1) in Table 37 and Fig. 52. The above formulae Eqs. (191) through (195) are valid for the case  $t_i \neq t_o$ . If both the wall temperatures are the same, the nature of the heat transfer problem is changed as discussed in PARALLEL PLATE Section. For this case, Nusselt numbers are obtained as the limiting values of the thermal entrance solution, and are presented as Case (a2) in Table 37 and Fig. 52.

To determine the total heat transfer through or from annular duct (both inner and outer walls) when both walls are at the same temperature  $t_w$  at a given cross section, the heat transfer coefficient  $h$  is defined as follows.

$$q_i' + q_o' = (h_i P_i + h_o P_o)(t_w - t_m) = h(P_i + P_o)(t_w - t_m) \quad (196)$$

Thus the Nusselt number for the total heat transfer is related to  $Nu_o$  and  $Nu_i$  as

$$Nu_T = \frac{Nu_o + Nu_i r^*}{1 + r^*} \quad (197)$$

With the values of  $Nu_i$  and  $Nu_o$  of Case (a2) in Table 37, the Nusselt numbers calculated from Eq. (197) are presented in Table 34 and Fig. 51.

(b) Constant but different heat fluxes specified on both walls: For  $x \geq x_e$ ,

$$q'' = q''_i \text{ on the inner wall}$$

$q'' = q''_o$  on the outer wall, and  
 $t = t_e$  for all  $r$  at  $x < x_e$ . In this case

$$t_i = \frac{D_h}{k} \left[ q''_i \theta_{ii}^{(2)} + q''_o \theta_{io}^{(2)} \right] + t_e \quad (198)$$

$$t_o = \frac{D_h}{k} \left[ q''_i \theta_{oi}^{(2)} + q''_o \theta_{oo}^{(2)} \right] + t_e \quad (199)$$

$$t_m = \frac{D_h}{k} \left[ q''_i \theta_{mi}^{(2)} + q''_o \theta_{mo}^{(2)} \right] + t_e \quad (200)$$

$$Nu_i = \frac{\frac{1}{q''}}{\theta_{ii}^{(2)} - \theta_{mi}^{(2)} - \frac{q''_o}{q''_i} (\theta_{mo}^{(2)} - \theta_{io}^{(2)})} \quad (201)$$

$$Nu_o = \frac{\frac{1}{q''}}{\theta_{oo}^{(2)} - \theta_{mo}^{(2)} - \frac{q''_i}{q''_o} (\theta_{mi}^{(2)} - \theta_{oi}^{(2)})} \quad (202)$$

Note that Kays [5] expresses the above Eqs. (201) and (202) in terms of  $\text{Nu}_{ii}^{(2)}$ ,  $\text{Nu}_{oo}^{(2)}$  and the influence coefficients  $\theta_i^*$  and  $\theta_o^*$  where

$$\text{Nu}_{ii}^{(2)} = \frac{1}{\theta_{ii}^{(2)} - \theta_{mi}^{(2)}}, \quad \text{Nu}_{oo}^{(2)} = \frac{1}{\theta_{oo}^{(2)} - \theta_{mo}^{(2)}} \quad (203)$$

$$\theta_i^* = \frac{\theta_{mo}^{(2)} - \theta_{io}^{(2)}}{\theta_{ii}^{(2)} - \theta_{mi}^{(2)}}, \quad \theta_o^* = \frac{\theta_{mi}^{(2)} - \theta_{oi}^{(2)}}{\theta_{oo}^{(2)} - \theta_{mo}^{(2)}} \quad (204)$$

Two special cases of the specified wall heat fluxes are:

(b1) Constant and equal axial wall heat fluxes specified on both walls so that at any axial location the peripheral wall temperatures are uniform but different at inner and outer wall. (b2) Constant but different wall heat fluxes specified on both walls such that at any axial location, the peripheral wall temperatures at inner and outer walls are uniform and the same. The Nusselt numbers at inner and outer wall are presented in Table 37 and Fig. 53 for both of these particular cases. Note that the heat flux is specified as positive, if the heat transfer is from wall to the fluid. The negative Nusselt number means the heat transfer takes place from the fluid to the wall. Infinite Nusselt number at inner wall means  $t_i = t_m$  and does not mean the infinite heat flux. In the above Case (b2), the ratio  $q_i''/q_o''$  is unique for a given  $r^*$  and is also listed in Table 37.

For Case (b2), the heat transfer coefficient can also be defined, similar to Case (a2), as based on the total wall heat flux and the  $(t_w - t_m)$  temperature difference. The corresponding  $\text{Nu}_H$  were calculated from an equation similar to Eq. (197) with  $\text{Nu}_i$  and  $\text{Nu}_o$  from Case (b2) of Table 37, and are presented in Table 34 and Fig. 51. Note that

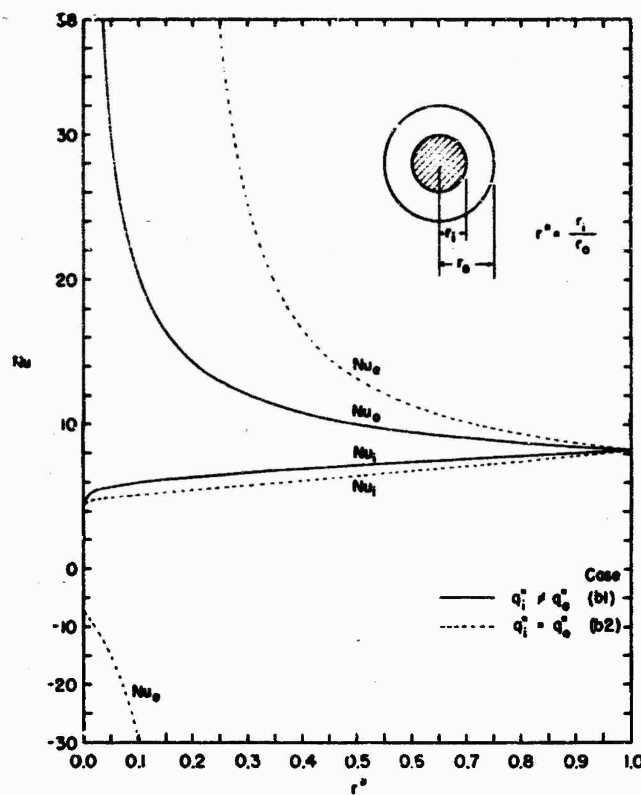


Fig. 53 Concentric annular ducts  $Nu_i$  and  $Nu_o$  for constant axial heat fluxes on both walls for fully developed laminar flow.

fortunately the (H1), (H2) and (H3) boundary conditions are the same for the annular duct, as is the case for circular tube and parallel plates, and hence it is designated as (H) boundary condition.

(c) Constant temperature specified on one wall, and constant heat flux specified on the other wall: For  $x \geq x_e^{24}$

$$t = t_1 \text{ on wall 1}$$

$$q'' = q_2'' \text{ on wall 2, and}$$

<sup>24</sup> Note for this situation, no distinction is needed between inner and outer walls so the subscripts 1 and 2 replace i and o.

$t = t_e$  for all  $r$  at  $x < x_e$ . In this case,

$$t_2 = t_1 + \frac{D_h}{k} q_2'' \theta_{22}^{(4)} \quad (205)$$

$$t_m = t_1 + \frac{D_h}{k} q_2'' \theta_{m2}^{(4)} \quad (206)$$

$$q_1'' = q_2'' \Phi_{12}^{(4)} \quad (207)$$

$$Nu_1 = - \frac{\Phi_{12}^{(4)}}{\theta_{m2}^{(4)}} \quad (208)$$

$$Nu_2 = \frac{1}{\theta_{22}^{(4)} - \theta_{m2}^{(4)}} \quad (209)$$

The  $Nu_i$  and  $Nu_o$  when the wall 1 is i and wall 2 is o are the same as  $Nu_i$  and  $Nu_o$  when wall 1 is o and wall 2 is i. They are also the same as those for Case (a1) of constant but different prescribed wall temperatures and, consequently, are already listed in Table 37.

Dwyer [249] also presented fully developed Nusselt numbers for the boundary condition of the second kind for the laminar, slug and turbulent flow. For laminar flow, his results agree well with the results of Table 36. Dwyer [250] extended his work by considering the bilateral heat transfer in annuli for the Cases (b1) and (b2) above. His tabulated values for Nusselt number for the Cases (b1), (b2) and  $\textcircled{H}$  boundary condition agree well with the results of Table 37 and  $Nu_H$  of Table 34 respectively.

Urbanovich [251,252] included the effect of viscous dissipation and obtained a closed form solution to the following two problems of fully developed laminar flow through

the annulus: (a) inside wall adiabatic, axial heat flux at outer wall constant. He presented formulae for the temperature distribution, heat flux and heat transfer coefficient at the outer wall [251]. (b) axial heat flux at inside wall constant, while at outside wall variable as follows.

$$q''_o = 0 \quad 0 < \phi < 2\pi - \delta \quad (210a)$$

$$q''_o = q''_c(1 + m \cos \phi) \quad -\delta \leq \phi \leq \delta \quad (210b)$$

where  $q''_c$ ,  $m$  and  $\delta$  are constants. The closed form expressions were presented for the fluid temperature distribution and the Nusselt number at the outer wall [252].

#### 16.1.2.2 Exponential Wall Heat Flux, $(H^4)$

Graber [128] analyzed the heat transfer problem for the annular ducts with axial exponential heat flux distribution,  $(H^4)$ , on inner or outer wall only. He introduced a parameter  $F_o$ , defined in Section V.1.1.3 and related to the exponent  $\lambda$  by Eq. (120). The ratio  $Nu_{H^4}/Nu_H$  was presented graphically as functions of  $F_o$  (range from -2 to 8) and  $r^*$  (range from 0 to 1) in [128].

#### 16.2 Hydrodynamically Developing Flow

Murakawa [204] analyzed the laminar flow hydrodynamic entry length problem for the annulus. His final result was

$$\frac{u}{u_m} = \left(1 - \frac{x}{L_{hy}}\right) + \left[\frac{x}{L_{hy}} + \left(\frac{x}{L_{hy}}\right)^2\right] \frac{u_{fd}}{u_m} \quad (211)$$

This result thus requires a knowledge of hydrodynamic entry length  $L_{hy}$ . Sugino [79] and Heaton et al. [80] independently linearized the momentum equation by the Langhaar approach [75] and solved the hydrodynamic entry length problem. Sugino tabulated the dimensionless pressure drop  $\Delta p^*$  as a

function of  $x/D_h Re$  for  $r^* = 0.2, 0.5$  and  $0.833$ . Heaton et al. [80] tabulated  $\Delta p^*$  as a function of  $x/D_h Re$  for  $r^* = 0, 0.02, 0.05, 0.10, 0.25$  and  $1$ . They also tabulated  $u_{\max}/u_m$  and  $fRe$  as a function of  $x/D_h Re$  and  $L_{hy}^+$  for  $r^* = 0, 0.001, 0.02, 0.05, 0.1, 0.25, 0.5$  and  $1$ . The  $L_{hy}^+$  reported by Heaton et al. [80] are approximately double the values reported by McComas [20].

Cheng and Atabek [82] used the linearized momentum equation due to Targ [81] and obtained closed form formulae for the axial velocity and the pressure gradient in the entrance region. Also they have determined and plotted the entrance length as a function of  $r^*$ . Sparrow and Lin [84] linearized the momentum equation introducing a stretched coordinate in the flow direction. They presented first thirty eigenvalues for  $r^* = 0.001, 0.01, 0.05, 0.1, 0.2, 0.4$ , and  $0.8$ . They also presented graphically  $u/u_m$  and  $K(x)$  as a function of  $4x/D_h Re$  for the above values of  $r^*$ .

Manohar [91] solved the momentum equation (14a) numerically for  $r^* = 0.1, 0.3, 0.5$  and  $0.7$ . Near the entrance, the mesh size was taken as  $1/3200$  and was gradually increased up to  $1/400$ . The velocity profiles, pressure distributions and the inlet length were presented in graphical form. The entrance length was also tabulated with two significant digits and agreed with the results of Heaton et al. [82].

### 16.3 Thermally Developing Flow

#### 16.3.1 Hydrodynamically Fully Developed Flow

Murakawa [248,253] presented an integral formulation for the solution of the first kind (Table 35), and a series approach to the same problem including peripheral variations of temperature, but does not present numerical results. Rao et al. [254] derived, based on Léveque approach, a formula for the average Nusselt number for the boundary condition of

the third kind. The effect of natural convection and temperature dependent viscosity was included in the formula by introducing empirical factors.

Viskanta [255,256] obtained complete thermal entry length solutions of first and third kinds. Hatton and Quarmby [257] considered the thermal entry solutions of the second and third kinds only for the case of inner wall heated. Lundberg et al. [242,243] independently solved the thermal entry problem rigorously [Eq. (19a) after neglecting  $v(\partial t/\partial r)$  and  $\alpha(\partial^2 t/\partial x^2)$  terms] and obtained all four kinds of fundamental solutions. These extensive results are presented in tabular and graphical form. Their solution for large  $x^*$  was based on the method of separation of variables and eigenfunction expansion [15]. For small values of  $x^*$ , the above solution converges very slowly, hence Lévêque method [1,99] was employed near the point where the step change occurred.

The simplified assumptions in Lévêque method are as follows. (i) In the downstream region very close to the point of step change in boundary condition, the temperature changes are confined to a boundary layer which is thin compared to the momentum boundary layer. In this region, it is assumed that the velocity distribution is linear having the same slope at the wall. Hence, the axial velocity  $u$  in Eq. (19a) is replaced by a linear velocity distribution in radial direction having the same slope of actual laminar flow velocity distribution at the wall. (ii) For the region close to the wall, the effect of curvature is small hence the term  $\frac{1}{r} \frac{\partial t}{\partial r}$  is neglected from Eq. (19a). The resulting energy equation is

$$\alpha \frac{\partial^2 t}{\partial r^2} = \left[ \left( \frac{\partial u}{\partial r} \right)_w (r - r_w) \right] \frac{\partial t}{\partial x} \quad (212)$$

The solution to this equation is found by the method of similarity transformation where it is further assumed that

(iii) the range of the similarity variable goes to infinity and (iv) far away from the wall, the fluid temperature approaches the inlet temperature of the fluid. The last assumption also implies that the temperature gradient approaches zero far away from the wall. Consequently, Lévêque type solution does not allow a distinction between different kinds of boundary conditions at the opposite wall of multiply connected duct.

Lévêque approximation is valid only in a very restricted thermal entrance region where the depth of heat penetration is of the same order of magnitude as the hydrodynamic boundary layer over which the velocity distribution may be considered linear.

The gap between the limit for Lévêque solution and the point where the eigenvalue solution becomes manageable was bridged by Worsøe-Schmidt [258] by considering a perturbation of Lévêque solution. He successfully relaxed the first two assumptions of Lévêque method, as he considered the fully developed velocity profile and the effect of curvature in the energy equation and obtained a series solution. His tabulated results are complementary to the results by Lundberg et al. [243] for small  $x^*$ .

Nunge et al. [259] investigated the limitations of assumptions common to Lévêque type solution. Lundberg et al. [243] considered the linear velocity profile and neglected the effect of curvature in the energy equation for the region close to the step change in boundary condition; Worsøe-Schmidt considered the curvature and the developed velocity profile; while Nunge et al. [259] assumed curvature and linear velocity profile. They concluded that the improvement brought about by including the effect of curvature over the Lévêque solution is important.

The local Nusselt numbers in the thermal entry region for annuli depend on both the radius ratio  $r^*$  and the axial

distance  $x^*$ . However, Nunge et al. found that when the Nusselt number is defined in terms of  $D_j$ , where  $D_j$  is the diameter of heated surface  $j$ , the radius ratio  $r^*$  is effectively eliminated as a parameter. This newly defined Nusselt number is

$$Nu_{x,j}^* = \frac{h_x D_j}{k} = \frac{h_x D_h}{k} \frac{r_j^*}{1-r^*} = Nu_x \frac{r_j^*}{1-r^*} \quad (213)$$

It is only a function of the dimensionless axial distance for all values of  $r^*$  in the thermal entrance region. It deviates from a single curve correlation as the asymptotic value of the Nusselt number is approached.

As discussed earlier, once the eight solutions to the four fundamental problems (Table 35) are available, the solution for any axially arbitrary, but peripherally uniform boundary condition, can be obtained by the Duhamel's superposition technique. Lundberg et al. [243] solved the following two problems by the superposition technique: (i) heat flux specified on one wall, temperature on the other, and (ii) heat flux specified on both walls. Hatton and Quarmby [257] analyzed the following three problems by the superposition technique: (i) axially linear increase in temperature on inner wall, (ii) axially linear increase in heat flux on inner wall and (iii) half-sine wave heat input variation superimposed on a uniform heat input on inner wall. In all three cases, the outer wall was insulated.

Hsu [260] included the effect of fluid axial heat conduction [Eq. (19a) with  $v = 0$ ] and obtained the fundamental solution of the second kind. In his analysis, he assumed the inlet fluid temperature was uniform at  $x = -\infty$ . Thus he solved the eigenvalue problem for each of the two semi-infinite regions and matched the temperature and axial temperature gradient at  $x = 0$  properly. He presented local

Nusselt number  $Nu_{x,1}$  and  $Nu_{x,2}$  graphically for  $r^* = 0.1$ ,  $0.3$ ,  $0.5$ ,  $0.7$  and  $0.9$  and  $Pe = 1, 5, 10, 20, 30, 50$  and  $\infty$  as a function of  $x^*$  ( $10^{-4} \leq x^* \leq 1$ ). The temperature solutions corresponding to the limiting case of  $Pe = \infty$  are in excellent agreement with the results of Lundberg et al. [243].

Hsu and Hwang [261] considered the finite thermal resistance ( $R_l$  boundary condition) at the inner and outer wall and obtained the thermal entry length solution for fully developed laminar flow through the annulus. The first ten eigenvalues and constants were presented for  $r^* = 0.5$  and  $U_i r_i/k = 1, 5, 10$  and  $U_o r_i/k = 0.5, 1, 2, 2.5, 5, 10$  and  $20$ . Further, they included uniform internal thermal energy generation with  $R_l$  boundary condition, and obtained a solution for the temperature distribution, wall heat fluxes and the Nusselt numbers.

#### 16.3.2 Simultaneously Developing Flow

Murakawa [253] presented an analysis for the combined hydrodynamic and thermal entry length problem when the inner surface of annular duct is heated. The analysis is rather complicated and the numerical results are quoted for one radius ratio only.

Heaton et al. [80] obtained the fundamental solution of second kind for the combined hydrodynamic and thermal entry length problem. The problem was solved by an integral method using the hydrodynamic solution previously described (Langhaar type), and a temperature profile found by an extension of the method used to find the velocity profile. The Nusselt numbers, wall temperatures and bulk mean fluid temperatures are tabulated as a function of  $x^*$  for  $r^* = 0, 0.02, 0.05, 0.10, 0.25, 0.50$  and  $1.00$  and  $Pr = 0.01, 0.70, 10.0$  and  $\infty$ .

For the same reasons as mentioned in PARALLEL PLATES Section V.2.3.2, the three fundamental solutions (exception is the second kind) for the simultaneously developing flow have not been investigated.

## 17. ECCENTRIC ANNULAR DUCTS

Only the case of hydrodynamically and thermally fully developed flow through eccentric annular duct has been analyzed.

### 17.1 Fully Developed Flow

#### 17.1.1 Flow Characteristics

Several investigators [2,262,263] partially investigated laminar flow through eccentric annulus. Heyda [264] determined the Green's function in bipolar coordinates for the potential equation and obtained the velocity distribution in the form of an infinite series. Caldwell [262] carried out the further integration necessary to give the pressure gradient as a function of the flow rate and duct geometry. However, no numerical results were presented. Redberger and Charles [265] solved the momentum equation by the finite difference method after transforming it into bipolar coordinates. They obtained and presented graphically the ratio of mass flow rate of eccentric to concentric cylinders of the same diameter ratio. Snyder and Goldstein [266] independently arrived at the closed form solution for the velocity distribution in bipolar coordinates, and determined the local wall shear stress, and inner wall, outer wall and average friction factors. Jonsson and Sparrow [267] independently analyzed the same problem and numerical results were evaluated for a wider range of governing parameters. For  $r^* = 5/6$  and  $1/2$  at larger eccentricities, the later results of Jonsson and Sparrow are claimed to be slightly more accurate than those of Ref. [266], because slow series convergence and small integration step-size are characteristic at large eccentricities. The wall shear stresses and the average friction factors were presented graphically as a function of eccentricity with  $r^*$  as a parameter in Refs. [266,267]. As tabulated results were not available, Fig.

Table 38. Eccentric annular ducts  $fRe$  for fully developed laminar flow, from graphical results of Jonsson [268]

$e^*$	fRe					
	$r^*=0.05$	$r^*=0.10$	$r^*=0.25$	$r^*=0.50$	$r^*=0.75$	$r^*=0.95$
0.0	21.567	22.343	23.302	23.813	23.967	24.000
0.1	21.37	22.13	23.07	23.48	23.53	23.67
0.2	20.90	21.57	22.30	22.61	22.67	22.75
0.3	20.23	20.77	21.13	21.18	21.27	21.28
0.4	19.43	19.80	19.67	19.50	19.44	19.47
0.5	18.56	18.63	18.20	17.65	17.44	17.47
0.6	17.53	17.30	16.63	15.91	15.60	15.63
0.7	16.60	16.17	15.17	14.26	13.81	13.83
0.8	15.77	15.13	13.80	12.70	12.24	12.23
0.9	15.07	14.27	12.67	11.34	10.90	10.80
1.0	14.63	13.60	11.77	10.26	9.84	9.07

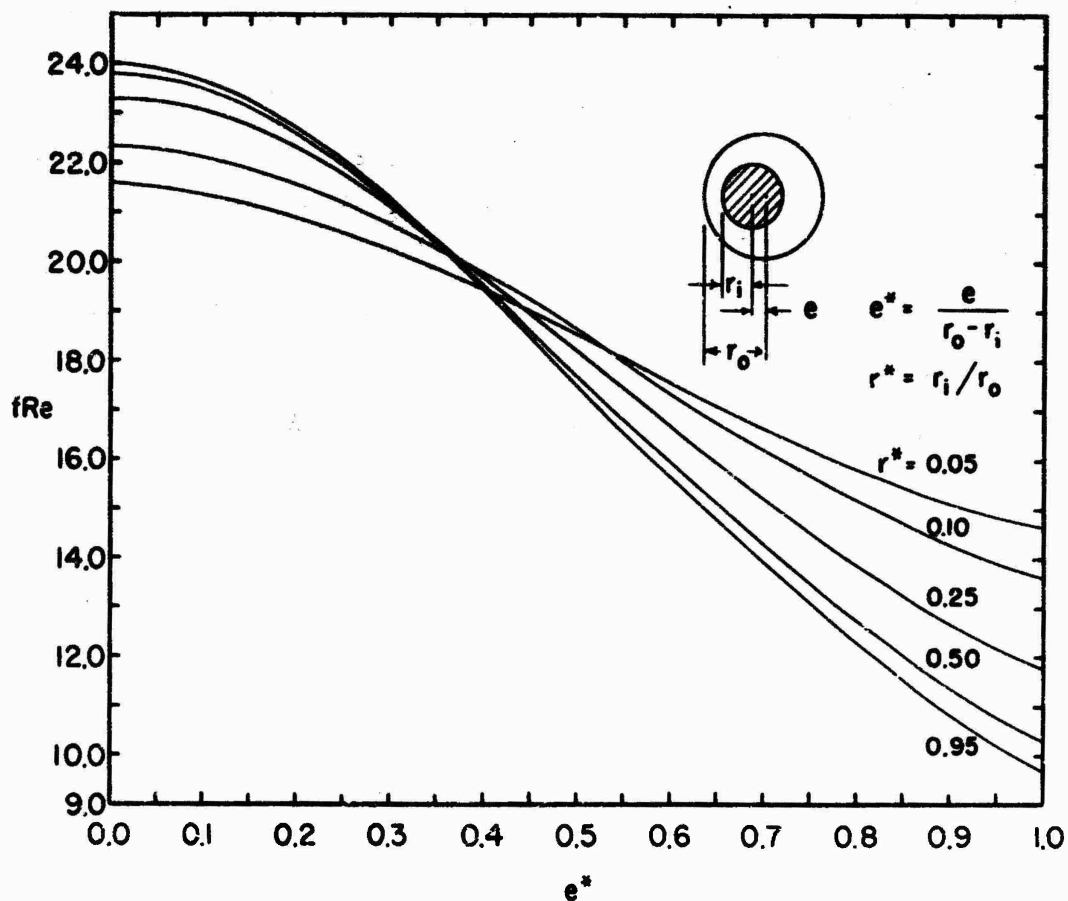


Fig. 54 Eccentric annular ducts  $fRe$  for fully developed laminar flow.

54 and Table 38 were prepared based on the graphical  $fRe$  versus  $e^*$  of Jonsson [268].

At unit eccentricity (inner and outer cylinders just touching), the theoretical results of Caldwell show a minimum at  $r^* \approx 0.75$  in the plot of  $fRe$  versus  $r^*$  with  $fRe = 16, 9.5$  and  $24$  at  $r^* = 0, 0.75$  and  $1$  respectively. Bourne et al. [269] experimentally verified the general shape of this curve. However, their minimum ( $fRe \approx 12.0$  at  $r^* \approx 0.75$ ) is not as small as predicted. It should be noted that Jonsson and Sparrow's [267,268] results do not show a minimum for the unit eccentricity for the range of  $r^*$  0.05 to 0.95. However, the limiting geometry of the eccentric annular duct with unit eccentricity and  $r^*$  approaching one may have a minimum  $fRe \approx 9.62$ , as evidenced by a cross-plot of the  $e^* = 1$  results of Fig. 54. This limiting geometry consists of two circles of the same radius touching each other, leaving essentially no gap for the laminar flow. Just short of  $r^* = 1$  with a flow through gap, one would expect a flow approaching the parallel plate situation and hence a  $fRe$  magnitude of 24. This behavior may justify the existence of a minimum at an  $r^*$  close to unity.

#### 17.1.2 Heat Transfer Characteristics

The only boundary condition analyzed for the eccentric annuli is that of uniform and different axial heat fluxes on both walls such that uniform and equal peripheral wall temperatures result at any axial location. This boundary condition corresponds to Case (b2) of the concentric annular ducts (p. 180). Cheng and Hwang [55] used the 20-point matching method and determined the fully developed  $Nu_H$  with a heat transfer coefficient  $h$  defined by Eq. (196). The effect of internal thermal energy generation was also included in the analysis. Their results for various flow characteristics are in excellent agreement with [266,267].

The Nusselt numbers, with zero thermal energy sources, are presented in Table 39 and Fig. 55.

Table 39. Eccentric annular ducts  $Nu_H$  for fully developed laminar flow, from Cheng and Hwang [55]

$e^*$	$Nu_H$			
	$r^*=0.25$	$r^*=0.50$	$r^*=0.75$	$r^*=0.90$
0.00	7.804	8.117	8.214	8.232
0.01	7.800	8.111	8.208	8.226
0.10	7.419	7.608	7.659	7.667
0.20	6.524	6.473	6.432	6.422
0.40	4.761	4.393	4.227	4.192
0.60	3.735	3.247	3.024	2.975
0.80	3.203	2.644	2.384	2.324
0.90	3.038	2.446	2.171	2.106
0.99	2.925	2.305	2.016	1.947

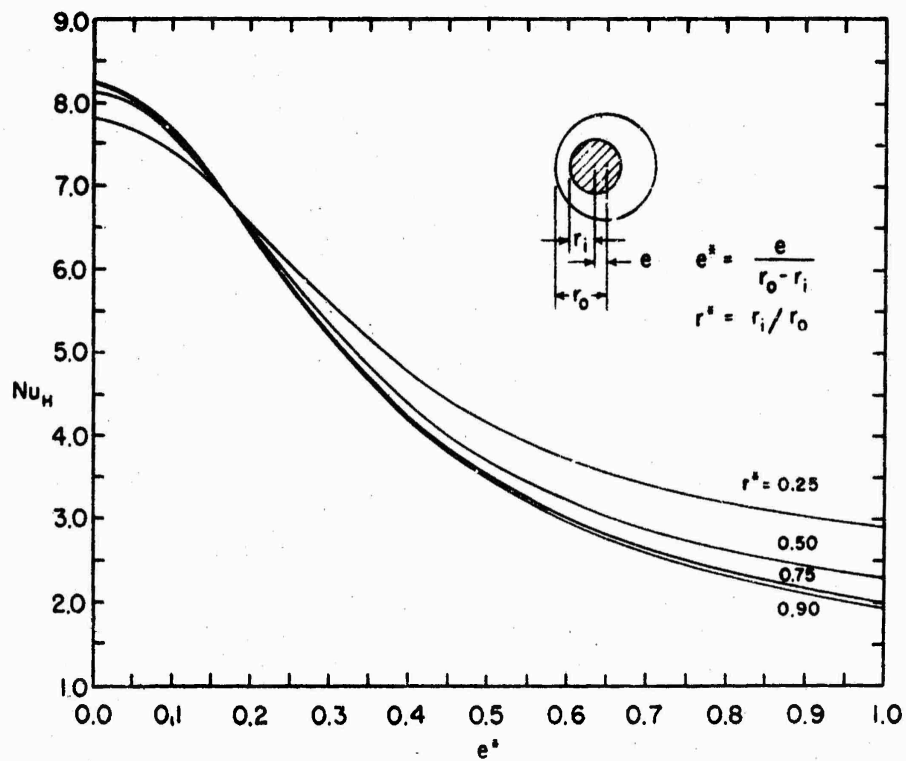


Fig. 55 Eccentric annular ducts  $Nu_H$  for fully developed laminar flow.

## 18. ANNULAR SECTOR DUCTS

### 18.1 Fully Developed Flow Characteristics

The fully developed laminar flow characteristics of annular sector duct geometry has been studied by Sparrow et al. [270]. The problem was solved by the method of separation of variables and the use of linear superposition. The expressions for velocity distributions, flow rate and the fRe were presented in an infinite series form. The fRe magnitudes are tabulated in [270] for the sector angle  $\phi$  from  $5^\circ$  to  $60^\circ$  and  $r^*$  from 0.05 to 0.95. Also, fRe is shown graphically in [270] for  $2\phi$  from  $5^\circ$  to  $360^\circ$  and  $r^*$  from 0.05 to 0.95.

Based on the equations presented in [270], the fRe factors were determined on the Stanford computer using double precision. Up to the first 1200 terms in the infinite series were used. The fRe factors are presented in Table 40 and Fig. 56 for a wide range of  $r^*$  and  $\phi$ . Incidentally, Eq. (7) of [270] takes a different form for  $\phi = 90^\circ$  and  $270^\circ$  for  $n = 1$  and 3 respectively and the appropriate formula was derived for this case to arrive at the results of Table 40.

Table 40. Annular sector ducts fRe for fully developed laminar flow

$r^*$	$5^\circ$	$10^\circ$	$15^\circ$	$20^\circ$	$30^\circ$	$40^\circ$	$50^\circ$	$60^\circ$	$90^\circ$	$120^\circ$	$150^\circ$	$180^\circ$	$210^\circ$	$240^\circ$	$270^\circ$	$300^\circ$	$330^\circ$	$350^\circ$
0.11	12.47	12.77	12.93	13.124	13.466	13.765	14.027	14.259	14.810	15.190	15.479	15.706	15.888	16.047	16.191	16.326	16.451	16.532
0.15	13.676	13.937	13.670	13.796	14.020	14.212	14.376	14.518	14.649	15.105	15.339	15.575	15.815	16.063	16.306	16.561	16.765	16.903
0.20	14.469	14.473	14.550	14.597	14.576	14.616	14.650	14.682	14.693	15.007	15.208	15.616	15.960	16.301	16.627	16.932	17.215	17.391
0.25	15.654	15.315	15.207	15.114	14.949	14.859	14.761	14.704	14.629	14.998	15.374	15.808	16.237	16.645	17.021	17.364	17.675	17.986
0.30	16.335	16.123	15.775	15.557	15.205	14.932	14.748	14.661	14.687	15.964	15.572	16.095	15.591	17.043	17.469	17.811	18.133	18.329
0.35	17.111	16.678	16.192	15.846	15.281	14.895	14.658	14.566	14.714	15.247	15.659	16.455	16.994	17.472	17.881	18.259	18.583	18.779
0.40	17.679	17.452	16.462	15.971	15.236	15.778	14.560	14.467	14.621	15.505	16.215	16.833	17.429	17.917	18.330	18.704	19.023	19.216
0.45	18.318	17.142	16.579	15.960	15.095	14.623	14.434	14.430	15.020	15.845	16.620	17.307	17.883	18.371	18.786	19.143	19.452	19.635
0.50	18.754	17.502	16.525	15.726	14.994	14.471	14.378	14.405	15.328	16.251	17.082	17.777	18.350	18.820	19.231	19.574	19.865	20.045
0.55	19.117	17.502	16.526	15.726	14.994	14.471	14.378	14.405	15.328	16.251	17.082	17.777	18.350	18.820	19.231	19.574	19.865	20.045
0.60	19.333	17.358	16.420	15.696	14.994	14.471	14.378	14.405	15.328	16.251	17.082	17.777	18.350	18.820	19.231	19.574	19.865	20.045
0.65	19.477	17.277	15.774	15.555	14.925	14.376	14.378	14.405	15.328	16.251	17.082	17.777	18.350	18.820	19.231	19.574	19.865	20.045
0.70	19.535	17.162	15.450	14.630	14.293	14.536	15.131	15.711	17.247	14.367	14.181	19.793	20.266	20.663	20.946	21.203	21.417	21.542
0.75	19.532	16.142	14.994	14.372	14.123	14.492	15.649	16.312	17.904	18.388	18.752	20.415	20.746	21.085	21.360	21.587	21.776	21.987
0.80	19.469	16.142	14.994	14.372	14.123	14.492	15.649	16.312	17.904	18.388	18.752	20.415	20.746	21.085	21.360	21.587	21.776	21.987
0.85	19.346	16.928	14.257	14.164	15.286	16.277	17.156	17.879	19.389	20.312	20.829	21.369	21.699	21.955	22.159	22.326	22.465	22.595
0.90	19.111	16.612	14.319	14.420	15.141	17.271	18.151	18.867	20.213	21.533	21.903	22.172	22.382	22.549	22.684	22.797	22.962	23.100
0.95	19.376	16.492	15.808	17.394	18.514	19.330	19.940	21.090	21.736	22.149	22.436	22.648	22.810	22.939	23.043	23.190	23.340	23.440
0.95	19.055	17.619	19.179	20.153	21.298	21.912	22.351	22.664	23.152	23.269	23.363	23.440	23.500	23.561	23.621	23.681	23.740	23.800

The fRe =  $2^{\phi}$  for all  $f$  at  $r^* = 1$ .

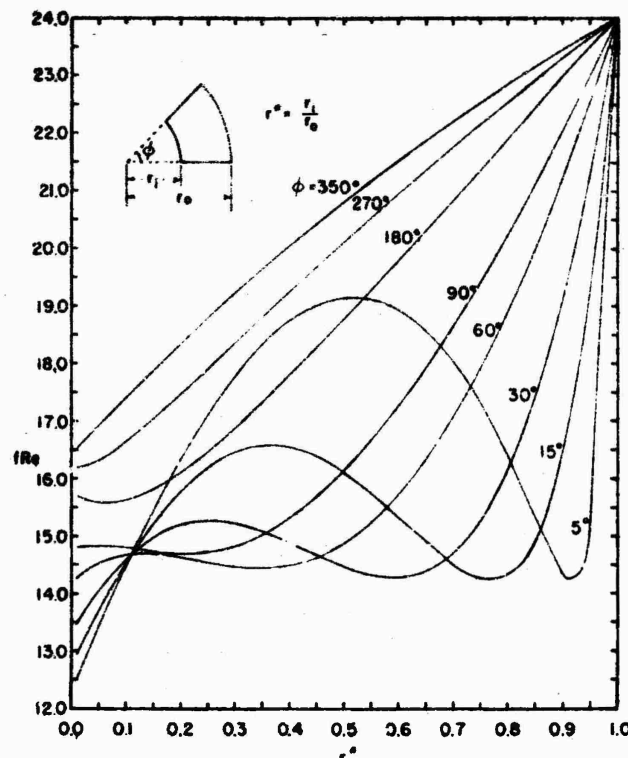


Fig. 56 Annular sector ducts  $f_{Re}$  for fully developed laminar flow.

Table 42. Regular polygonal ducts with central circular cores  $Nu_{H1}$  for fully developed laminar flow, from Cheng and Jamil [54]<sup>28</sup>

$a/\epsilon_1$	$Nu_{H1}$								
	n=3	n=4	n=5	n=6	n=7	n=8	n=9	n=10	n=20
0.00	3.111	3.608	3.859	4.002	4.102	4.153	4.196	4.227	4.329
0.05	4.938	5.723	6.094	6.303	6.431	6.525	6.588	6.635	6.778
0.1	5.296	6.104	6.467	6.670	6.794	6.885	6.946	6.992	7.142
1/9	5.354	6.163	6.523	6.722	6.845	6.935	6.995	7.040	7.189
0.125	5.417	6.228	6.582	6.778	6.898	6.986	7.045	7.090	7.236
1/7	5.486	6.297	6.644	6.834	6.951	7.037	7.094	7.138	7.280
1/6	5.560	6.370	6.705	6.887	6.998	7.080	7.136	7.177	7.314
0.2	5.626	6.438	6.755	6.924	7.027	7.102	7.154	7.192	7.321
0.25	5.655	6.474	6.760	6.906	6.995	7.060	7.104	7.138	7.251
1/3	5.511	6.351	6.593	6.697	6.757	6.801	6.831	6.854	6.933
0.5	4.466	5.317	5.488	5.498	5.480	5.465	5.453	5.444	5.419

<sup>28</sup>The  $Nu_{H1}$  for  $n = \infty$  corresponds to  $Nu_H$  of concentric annular ducts, Table 34.

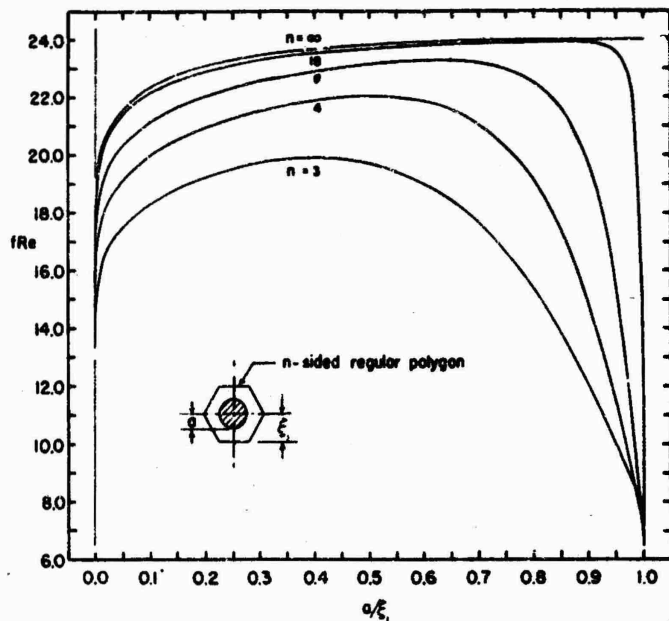


Fig. 57 Regular polygonal ducts with central circular cores  
 $f_{Re}$  for fully developed laminar flow, from  
Ratkowsky [271].

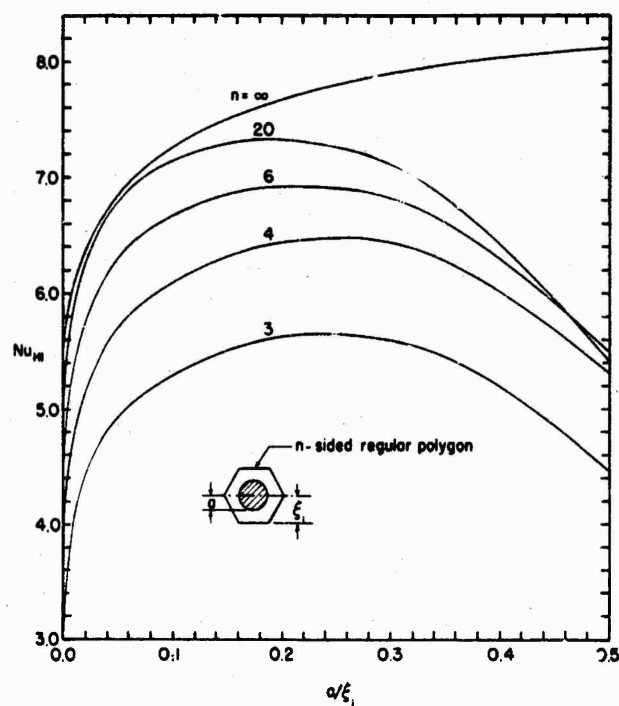


Fig. 58 Regular polygonal ducts with central circular cores  
 $Nu_{H1}$  for fully developed laminar flow, from Cheng  
and Jamil [54].

## 19. REGULAR POLYGONAL DUCTS WITH CENTRAL CIRCULAR CORES

Only the case of hydrodynamically and thermally fully developed flow has been analyzed.

Cheng and Jamil [54] studied the fully developed laminar flow in regular polygonal ducts with central circular cores. They employed a 10-point matching method to evaluate Nusselt numbers. For the heat transfer problem, they considered the boundary condition corresponding to Case (b2) of concentric annular duct, i.e., constant but unequal axial heat fluxes specified at inner and outer walls such that it results into uniform and equal wall temperatures peripherally. They also presented the results graphically in [56]. For this duct,  $f_{Re}$  are presented in Table 41a and  $Nu_{Hl}$  in Table 42 and Fig. 58.

Independently, Ratkowsky and Epstein [58] studied the flow characteristics of the same problem by the least-square fitting of harmonic functions to known boundary values. Their friction factors are in excellent agreement with Cheng and Jamil results. These  $f_{Re}$  results are presented in Table 41b [271] and Fig. 57. Tables 41a and 41b provide the comparison of two different numerical methods.

Two limiting cases of this geometry (see Fig. 57),  $a/\xi_1$  equals 0 and 1 are of interest. For  $a/\xi_1$  equals zero, the corresponding geometry is the n-sided regular polygonal duct, which has been discussed in Section V.11. Ratkowsky and Epstein [58] have analyzed the other limiting case ( $a/\xi_1 = 1$ ) in detail. Theoretically, they have shown that when  $n \rightarrow \infty$ ,  $f_{Re} \rightarrow 56/9 = 6.222$ .

**Table 4la.** Regular polygonal ducts with central circular cores fRe for fully developed laminar flow, from Cheng and Jamil [54]

$a/t_1$	fRe									
	n=3	n=4	n=5	n=6	n=7	n=8	n=9	n=10	n=20	(exact)
1/1.1	10.797	14.304	16.980	19.135	20.681	21.730	22.428	22.391	23.906	
0.50	19.728	22.026	22.793	23.115	23.289	23.394	23.466	23.519	23.716	23.813
1/3	19.821	21.669	22.329	22.658	22.858	22.992	23.085	23.160	23.427	23.546
0.25	19.512	21.255	21.934	22.295	22.521	22.675	22.788	22.869	23.172	23.308
0.20	19.215	20.922	21.624	22.009	22.252	22.418	22.537	22.627	22.952	23.088
1/6	18.965	20.654	21.374	21.775	22.028	22.203	22.329	22.423	22.761	22.901
1/7	18.755	20.433	21.165	21.577	21.839	22.020	22.149	22.246	22.594	22.737
0.125	18.578	20.247	20.987	21.407	21.675	21.860	21.993	22.092	22.446	22.591
1/9	18.425	20.086	20.833	21.259	21.532	21.719	21.854	21.955	22.314	22.461
0.10	18.293	19.945	20.696	21.126	21.404	21.593	21.730	21.832	22.195	22.343
0.05	17.514	19.104	19.866	20.310	20.596	20.793	20.935	21.041	21.417	21.567

**Table 4lb.** Regular polygonal ducts with central circular cores fRe for fully developed laminar flow, from Ratkowsky [271]

$a/t_1$	fRe				
	n=3	n=4	n=6	n=8	n=18
1.000	7.803	7.000	6.618	6.478	6.477
0.991	-	-	-	-	17.822
0.987	-	-	-	11.041	-
0.981	-	-	-	-	21.594
0.979	-	-	10.889	-	-
0.96875	9.179	9.858	-	-	-
0.966	-	-	-	-	23.071
0.950	-	-	15.346	18.789	23.533
0.9375	10.508	12.316	-	-	-
0.900	-	-	19.550	22.035	23.890
0.875	12.934	16.208	-	-	-
0.850	-	-	21.563	23.011	23.927
0.800	15.316	19.083	22.478	23.408	23.915
0.750	16.579	20.254	22.921	23.542	-
0.711	-	-	-	-	23.872
0.700	-	-	23.140	23.591	-
0.684	-	21.190	-	-	-
0.675	18.013	-	-	-	-
0.650	-	-	23.222	23.573	-
0.600	18.977	21.819	23.234	23.537	-
0.550	-	-	23.190	23.468	-
0.5454..	19.436	21.982	-	-	-
0.511	19.689	22.022	23.115	23.391	23.695
0.500	19.838	21.394	-	-	-
0.4545..	-	-	-	-	-
0.45	-	-	23.007	23.291	-
0.40	19.900	21.888	22.876	23.178	-
0.35	19.856	-	22.715	23.039	-
0.318	-	-	-	-	23.358
0.30	19.727	-	22.525	22.876	-
0.250	19.514	21.252	22.293	22.672	-
0.200	19.217	20.920	22.007	22.416	-
0.150	-	-	21.637	22.075	-
0.125	18.579	20.244	-	-	-
0.100	-	-	21.127	21.592	22.162
0.0625	17.746	19.358	-	-	-
0.05	-	-	20.308	20.791	-
0.03125	17.072	18.611	-	-	-
0.025	18.886	18.400	19.583	20.071	-
0.020	16.713	18.202	-	-	-
0.0125	-	17.823	-	-	-
0.0000	13.332	14.225	15.052	15.410	15.860

## 20. CIRCULAR DUCT WITH CENTRAL REGULAR POLYGONAL CORES

Only the case of hydrodynamically and thermally fully developed flow has been analyzed.

Cheng and Jamil [54,56] studied fully developed laminar flow through an annulus with a circle as the outside boundary and a concentric regular polygon as the inside boundary. As the number of sides of regular polygonal core decreased from 20 towards 3, the shear stress distributions and normal temperature gradients along the inner regular polygonal boundary exhibited a wavy character, with a very small region having negative shear stress distribution. In spite of the difficulty with local values, Cheng and Jamil stated that the integrated overall quantities, such as  $f_{Re}$  and  $Nu_{H1}$  were sufficiently accurate for practical purposes [56]. The  $(H1)$  boundary condition is the same as the boundary condition, Case (b2) of CONCENTRIC ANNULAR DUCTS.  $Nu_{H1}$  were based on the heat transfer coefficient defined in Eq. (196). Their  $f_{Re}$  and  $Nu_{H1}$  were based on 6-point matching method (on one side of regular polygon). The  $f_{Re}$  are presented in Table 43a and  $Nu_{H1}$  in Table 44 and Fig. 60.

Hagen and Ratkowsky [59] studied the same problem by using the method of least-square fitting of harmonic functions. They did not encounter the negative shear stress distribution and its wavy character, however the fitting procedure became more difficult as the number of sides of the polygon became smaller. A total of 6 to 16 harmonic functions were utilized in the solution of momentum equation. Their  $f_{Re}$  values [271] are reported in Table 43b and Fig. 59.

Table 43a. Circular duct with central regular polygonal cores f<sub>Re</sub> for fully developed laminar flow, from Jamil [235]

t <sub>1/a</sub>	f <sub>Re</sub>									
	n=3	n=4	n=5	n=6	n=7	n=8	n=9	n=10	n=20	n-> (exact)
0.50	21.629	21.268	21.776	21.776	21.745	21.733	21.730	21.732	21.775	21.813
1/3	21.072	21.612	21.595	21.488	21.417	21.427	21.439	21.452	21.546	-
0.25	21.857	21.298	21.173	21.166	21.177	21.193	21.207	21.220	21.217	21.308
0.20	21.676	21.051	21.367	22.366	22.369	22.395	23.008	23.019	22.973	23.008
1/6	23.413	22.557	22.734	22.737	22.816	22.823	22.835	22.837	22.804	22.901
1/7	23.191	22.693	22.646	22.649	22.660	22.671	22.691	22.662	22.652	22.737
0.125	23.000	22.563	22.416	22.517	22.526	22.536	22.518	22.527	22.516	22.591
1/9	22.840	22.344	22.400	22.399	22.506	22.514	22.597	22.504	22.392	22.561

Table 43b. Circular duct with central regular polygonal cores f<sub>Re</sub> for fully developed laminar flow, from Katkowsky [271]

t <sub>2/a</sub>	f <sub>Re</sub>				
	n=3	n=4	n=6	n=8	n=18
1.000	15.750	15.674	15.595	15.574	15.518
0.375	-	16.839	-	-	22.928
0.350	17.148	17.958	19.743	21.210	23.661
0.325	-	18.300	-	-	-
0.300	18.422	19.713	21.713	23.668	23.927
0.285	19.498	20.936	22.708	-	-
0.260	20.352	21.796	23.206	23.677	23.944
0.235	21.048	22.343	23.435	23.764	-
0.210	21.530	22.722	23.535	21.778	23.696
0.185	21.321	22.933	23.575	23.741	-
0.160	22.198	23.051	23.573	23.707	23.837
0.135	22.337	23.094	23.516	23.700	-
0.110	22.563	23.079	23.490	23.661	23.753
0.085	22.376	23.039	23.411	23.544	-
0.060	22.349	22.981	23.341	23.564	23.622
0.35	22.308	22.914	23.250	23.372	-
0.30	22.235	22.826	23.122	23.258	23.412
0.25	22.111	22.682	22.975	23.114	-
0.20	21.979	22.589	22.800	22.917	23.050
0.15	21.903	22.599	22.591	22.649	-
0.100	21.641	21.353	22.171	22.242	22.322
0.075	-	21.744	-	-	-
0.050	21.080	-	21.542	21.542	21.560
0.000	16.000	16.000	16.000	16.000	16.000

Table 44. Circular duct with central regular polygonal cores  $\frac{Nu_{H1}}{Nu_H}$  for fully developed laminar flow, from Jamil [235]<sup>29</sup>

t <sub>1/a</sub>	$\frac{Nu_{H1}}{Nu_H}$					
	n=4	n=5	n=6	n=7	n=8	n=9
0.0	4.364	4.364	4.364	4.364	4.364	4.364
1/3	7.157	7.321	7.115	7.320	-	7.325
0.125	7.138	7.186	7.195	7.388	7.390	7.395
1/7	7.467	7.467	7.459	7.464	7.467	7.057
1/6	7.518	7.517	7.514	7.550	7.555	7.558
0.20	7.616	7.616	7.615	7.618	7.614	7.660
0.175	7.643	7.713	7.744	7.751	7.763	7.776
1/4	7.773	7.914	7.858	7.884	7.838	7.909
0.150	-	7.718	7.910	7.989	8.027	8.049

<sup>29</sup>The  $\frac{Nu_{H1}}{Nu_H}$  for n = corresponds to  $Nu_H$  of concentric annular ducts, Table 4.

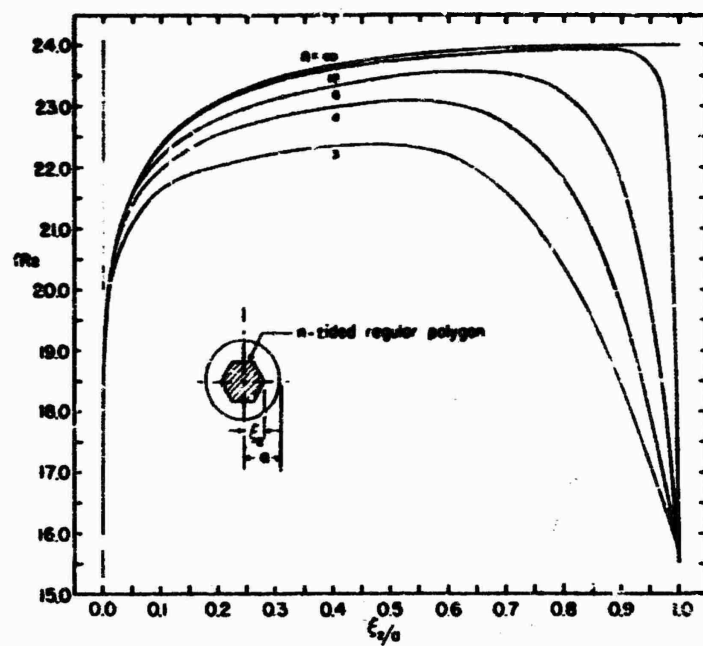


Fig. 59 Circular duct with central regular polygonal cores  $f_{Re}$  for fully developed laminar flow, from Ratkowsky [271].

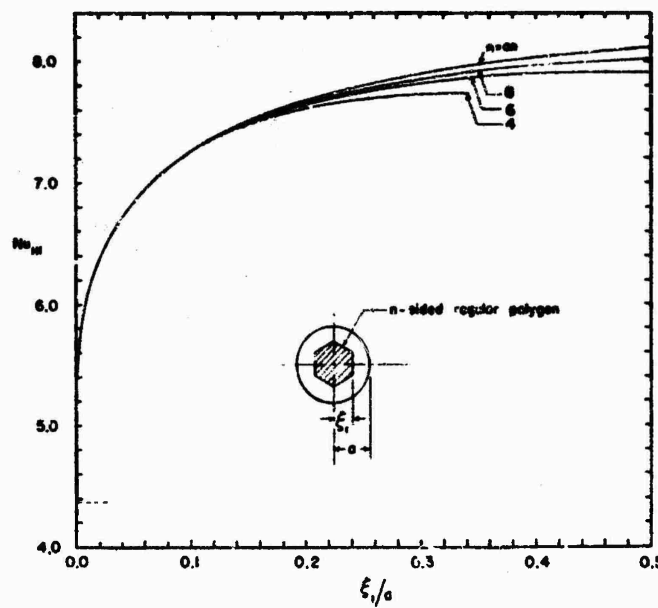


Fig. 60 Circular duct with central regular polygonal cores  $Nu_{Hl}$  for fully developed laminar flow, from Jamil [235].

## 21. LONGITUDINAL FLOW BETWEEN CYLINDERS

The laminar flow over straight circular cylinders arranged in triangular or square array has been analyzed only for fully developed flow as described below.

### 21.1 Flow Friction

Sparrow and Loeffler [48] obtained an analytical solution by the 6-point matching method for the longitudinal flow between cylinders arranged in equilateral triangular and square array as shown in Fig. 61.

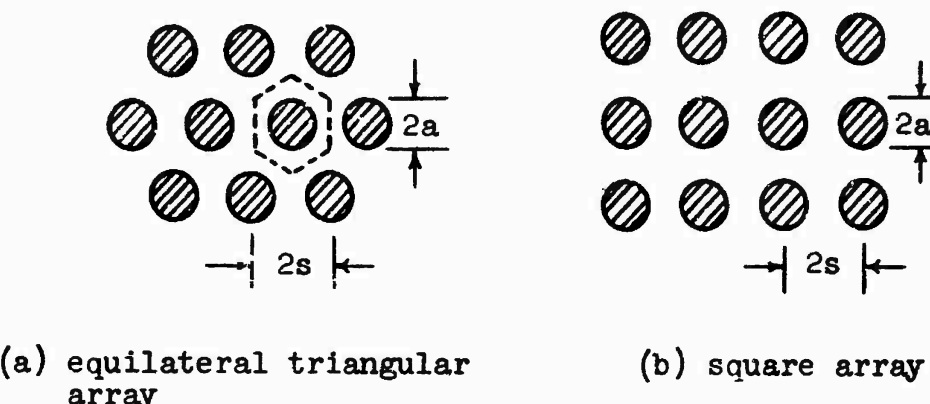


Fig. 61 Triangular and square array arrangements for longitudinal flow between cylinders.

They presented a pressure-drop-flow parameter  $(-\frac{dp}{dx})(\frac{a^4}{\mu})/Q$  and also  $(fRe)(2a/D_h)$  graphically as a function of porosity  $\sigma$  (range 0.1 ~ 1.0). The porosity,  $\sigma$ , is defined as the ratio of free flow area to frontal area (= free flow area plus the cross sectional area of rods). The porosity  $\sigma$  and pitch-to-diameter ratio ( $2s/2a$ ) are related as

$$\sigma = 1 - \frac{\sqrt{3} \pi}{6(s/a)^2} \quad \text{for triangular array} \quad (214a)$$

$$\sigma = 1 - \frac{\pi}{4(s/a)^2} \quad \text{for square array} \quad (214b)$$

They developed, for the limited range of  $\sigma > 0.8$  ( $s/a > 2.1$ ) for triangular array and  $\sigma > 0.9$  ( $s/a > 2.8$ ) for a square array, the following approximate expression for the friction factor

$$(fRe) \left( \frac{2a}{D_h} \right) = \frac{8\sigma^2}{2(1-\sigma) - \ln(1-\sigma) - (1-\sigma)^2/2 - 1.5} \quad (215)$$

where

$$\frac{D_h}{2a} = \frac{2\sqrt{3}}{\pi} \left( \frac{s}{a} \right)^2 - 1 \quad \text{for triangular array} \quad (216a)$$

$$\frac{D_h}{2a} = \frac{4}{\pi} \left( \frac{s}{a} \right)^2 - 1 \quad \text{for square array} \quad (216b)$$

Axford [272] refined the Sparrow and Loeffler analysis for the triangular array by matching 15 boundary points instead of six. He tabulated extensively various parameters of interest. The following equation for the friction factors for the triangular array can be derived from his results.

$$fRe = \frac{\pi}{6M(s/a)^4} \left[ \frac{2\sqrt{3}}{\pi} \left( \frac{s}{a} \right)^2 - 1 \right]^3 \quad (217)$$

The values of parameter  $M$ , a function of  $(s/a)$ , are tabulated by Axford correct to five significant figures. Using Eq. (217), the  $fRe$  values for the triangular array are presented in Table 45 and Fig. 62. For  $(s/a) > 2.1$ ,  $fRe$  can also be evaluated accurately from Eq. (215). Sholokhov et al. [273] obtained an electric analog solution and a finite difference solution of the same problem.

Table 45. Longitudinal flow between cylinders (triangular array)  $fRe$ ,  $Nu_{H1}$ ,  $Nu_{H2}$  for fully developed laminar flow

$s/a$	$fRe$	$Nu_{H1}$ [47]	$Nu_{H2}$ [47]
1.000	6.50	1.36	0.149
1.001	7.17	-	-
1.004	8.64	1.52	0.26
1.01	10.639	1.82	0.404
1.02	12.441	2.14	0.580
1.03	13.075	2.48	0.795
1.04	14.478	2.82	1.06
1.05	-	3.18	1.36
1.06	-	3.54	1.70
1.07	-	-	-
1.10	30.177	4.62	2.94
1.15	33.141	-	-
1.16	24.950	7.48	6.90
1.18	26.301	-	-
1.25	27.417	9.19	10.03
1.40	-	10.38	10.28
1.50	31.035	11.26	11.22
1.60	-	12.08	12.05
1.75	-	13.28	13.26
1.80	-	13.62	13.66
1.90	-	14.47	14.46
2.00	39.384	15.27	15.26
2.01	58.46	-	-
2.00	79.80	-	-

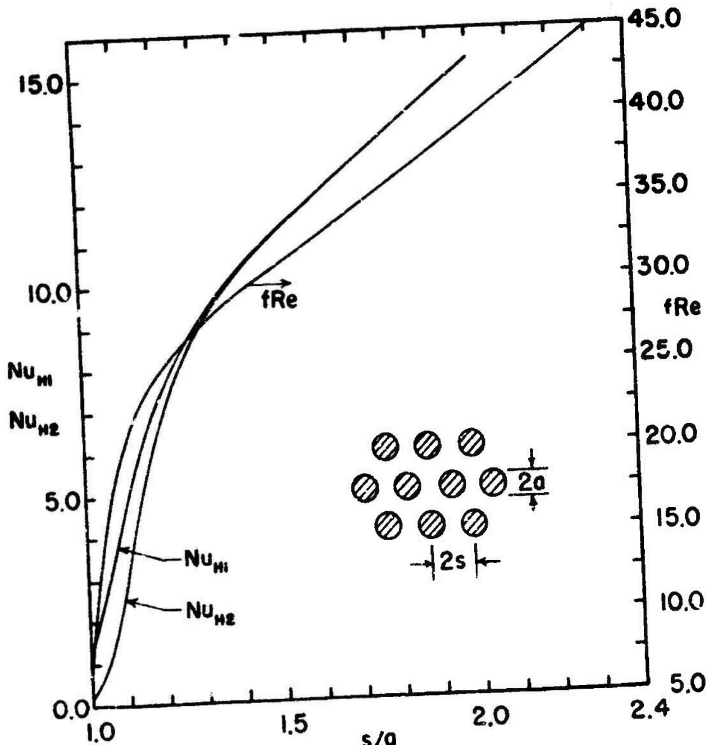


Fig. 62 Longitudinal flow between cylinders  $fRe$ ,  $Nu_{H1}$  and  $Nu_{H2}$  for fully developed laminar flow.

Sholokhov presented graphically the pressure-drop-flow parameter and velocity distribution for a wide range of pitch-to-diameter ratios. The results compare favorably with those of Sparrow and Loeffler [48].

### 21.2 Heat Transfer

Sparrow et al. [49] further solved the  $(H_1)$  heat transfer problem for the laminar flow between cylinders arranged in an equilateral triangular array. They have presented graphically the  $Nu_{H_1}$  for the pitch-to-diameter ratio ( $2s/2a$ ) of 1.1 to 4.0. For  $(s/a) > 2$ , they showed that  $Nu_{H_1}$  can be accurately calculated from an equivalent-annulus model described in the following paragraph.

The equivalent-annulus model is defined as follows. The hexagonal flow area associated with each rod in Fig. 60(a), is approximated by a circle of equal area, and the fluid dynamical and heat transfer behaviors of the system are assumed to be the same as those in the area between the inner radius and the radius of maximum velocity of an annulus. This model implicitly assumes that the transverse flow of heat is entirely in the radial direction, which means that there is no circumferential variation of either the surface temperature of the rod or its surface heat flux.

In tube bundles, neither the inside nor the outside tube wall surface temperature is, in fact, uniform peripherally. The same is also true of the heat fluxes on the inside and outside tube wall [272]. To predict quantitatively the magnitude of the circumferential variations of the inside and outside tube wall temperatures and heat fluxes, Axford [272] set up the energy and momentum balances for the velocity and temperature fields in all regions of tube bundle. He then solved these equations simultaneously. In this approach, the assumption of either a peripherally uniform heat flux or temperature on the outside tube wall is removed and replaced by temperature and heat flux continuity at the fluid-

tube wall interfaces. Axford found that the peripheral variations of the outside tube wall temperature and heat fluxes become quite sensitive to changes in the pitch-to-diameter ratio of the tube bundles as this ratio approached unity. Hence, he concluded that the single region analysis (e.g. as done by Sparrow et al. [49]) with  $H_1$  or  $H_2$  boundary conditions contained an inherent source of error for decreasing (s/a) ratios.

Dwyer and Berry [47] investigated, by the finite difference method, the  $H_2$  boundary condition for the longitudinal laminar flow over cylinders arranged in an equilateral triangular array. They calculated both the  $Nu_{H1}$  and  $Nu_{H2}$  as a function of pitch-to-diameter ( $2s/2a$ ) ratio range of 1.001 to 2. These results are presented in Table 45 and Fig. 62. For s/a ratio greater than 2, the  $Nu_{H1}$  and  $Nu_{H2}$  are almost identical, and can be evaluated from the equivalent-annulus model analysis by Sparrow et al. [49].

## 22. MISCELLANEOUS GEOMETRIES

For the flow geometries considered in this section, only the fully developed laminar flow case has been analyzed; no hydrodynamic and thermal entrance solution are available.

Gunn and Darling [274] determined the fully developed laminar  $fRe$  (by the finite difference numerical method) for the ducts shown in Fig. 63.

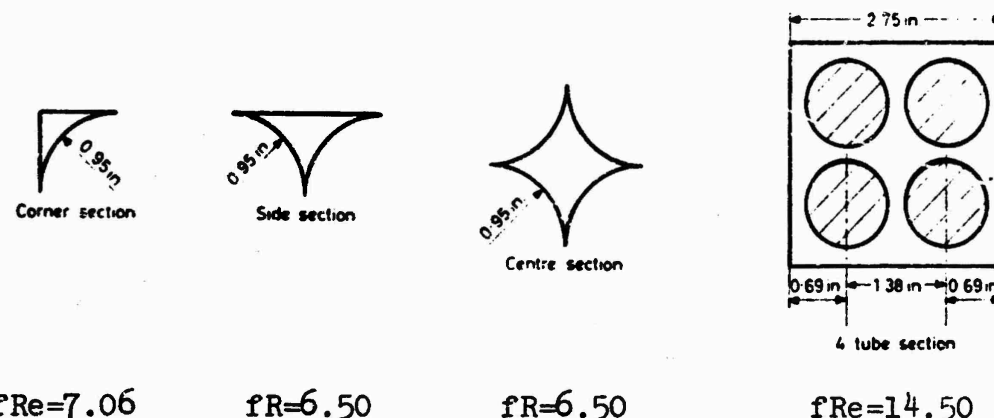


Fig. 63 Geometries and results considered by Gunn and Darling [274].

They presented analytical velocity profiles for each of the above four ducts. They also experimentally determined  $fRe$  in agreement with the theoretical values within 5 percent.

In a series of papers [37, 41, 42, 275, 276, 277], Sastry employed exact and approximate methods of conformal mapping to solve the laminar flow velocity and forced convection  $\textcircled{H1}$  heat transfer problem. In Ref. [37], he analyzed a cross-section bounded confocal ellipses, with internal thermal energy generation included. An example was worked out for the elliptical ducts. In Ref. [41] he investigated the  $\textcircled{H1}$  laminar forced convection problem for curvilinear polygonal ducts. In Ref. [42], he solved the  $\textcircled{H1}$  heat transfer problem for an arbitrary duct which can be conformally trans-

formed onto a unit circle by the mapping function

$$z = w(\zeta) = \sum_{n=0}^{\infty} a_n \zeta^n \quad (218)$$

The formulae were presented for  $u$ ,  $u_m$ ,  $t$ ,  $t_m$ ,  $q''$  and  $Nu_{H1}$  in terms of the constants  $a_n$ . The method was illustrated by applications to cardioid and ovaloid cross sections.

Sastry further employed the Schwarz-Neumann alternating method (an approximate method of conformal mapping) and solved the forced convection  $(H1)$  heat transfer problem for the ducts: (i) outer boundary was a circle and inner boundary was an ellipse [275], and (ii) outer boundary was a circle and inner boundary was a square with rounded corners [276]. The results of sections bounded by concentric circles, confocal ellipses and eccentric circles can be deduced by mapping cross sections onto a region bounded by concentric circles. This approach was used to evaluate the heat transfer of laminar forced convection in a duct bounded by concentric circle in [276].

Additionally, Sastry [277] analyzed the laminar flow velocity problem for doubly connected regions using the transformation

$$z = \sum_{-\infty}^{\infty} a_n \zeta^n \quad (219)$$

which mapped the section conformally onto an concentric annular ring. Examples were worked out for concentric, eccentric and confocal elliptical ducts. Using Schwarz-Neumann alternating method, the laminar flow through an elliptical duct with a central circular core was analyzed.

Kun [278] analyzed the fully developed laminar flow through an internally finned tube (as shown in Fig. 64) by

means of Green's function. He presented graphically the fully developed  $Nu_{Hl}$  as a function of fin length  $\xi$  with the angle  $\phi$  as a parameter.

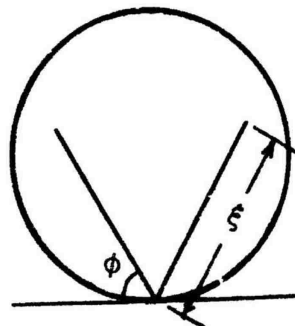


Fig. 64 An internally finned tube.

## Part 2. Curved Ducts

The pressure drop and heat transfer characteristics for flow through a curved duct is needed for a variety of technical applications. The first theoretical analysis was done by Dean [279] in 1927 for fully developed laminar flow of an incompressible fluid in curved pipe of circular cross section. Since then a considerable effort has been made to determine analytically and experimentally the flow friction and heat transfer behavior of curved ducts. A thorough literature survey up to 1968 on the curved duct characteristics is presented by Cheng and Akiyama [280,281].

Due to curvature effects, an additional parameter, called Dean number  $K = Re \sqrt{a/R}$ , appears as a nondimensional parameter for the curved ducts flow friction and heat transfer characteristics. The nondimensional parameters will have suffix c for curved ducts, and suffix s for corresponding straight duct.

In the following sections, the theoretical analysis is reviewed for curved ducts of circular, rectangular, elliptical and annular cross sections. Unless specifically mentioned, it is assumed that flow is steady state, laminar and hydrodynamically as well as thermally fully developed. The fluid is assumed as Newtonian, incompressible fluid with constant properties. Only the centrifugal body force is present due to the effect of curvature. The thermal energy sources, viscous dissipation and axial heat conduction as well as free convection, mass diffusion, chemical reaction, electromagnetic effects etc. are neglected.

## 23. CURVED CIRCULAR DUCTS

For the curved circular duct only the fully developed laminar flow and heat transfer have been analyzed.

### 23.1 Flow Friction

Dean [279,282] employed perturbation method and first analyzed the fully developed laminar flow of an incompressible fluid in a curved circular pipe. His analysis is valid for small Dean numbers only ( $0 \leq K \leq 25$ ). Topakoğlu [283] refined Dean's analysis with a different approach. Topakoğlu obtained an approximate solution based on the power series expansion of the stream function and the normal component of velocity in terms of the curvature of pipe. The solution is valid for small Dean numbers (Topakoğlu does not specify the range, however). The friction factors are expressed as

$$\frac{f_c}{f_s} = \left[ 1 - \frac{1}{48} \left( \frac{a}{R} \right)^2 \left\{ \frac{1.541}{2419.2} Re^4 + \frac{1.1}{3.6} Re^2 - 1 \right\} \right]^{-2} \quad (220)$$

For high Dean numbers, White [284] in 1929 correlated his experimental data and the existing experimental data in the literature on helical coils and arrived at

$$\frac{f_c}{f_s} = \left[ 1 - \left\{ 1 - \left( \frac{11.6}{K} \right)^{0.45} \right\}^{\frac{1}{0.45}} \right]^{-1} \quad (221)$$

for  $11.6 < K < 2000$  and  $f_s = 16/Re$ . This correlation has been experimentally confirmed by many investigators.

Adler [285] introduced the important concept of boundary layer for secondary flow along the wall in his analysis for laminar flow with high Reynolds number. Barua [286] employed the boundary layer approximation in his analysis for the secondary flow. The boundary layer approximations are

Table 46. Curved circular ducts  $f_c/f_s$  and  $\frac{Nu_{Hl,c}}{Nu_{H,s}}$  for fully developed laminar flow

K	$f_c/f_s$	$Q = \sqrt{K^2 Pr}$	$\frac{Nu_{Hl,c}}{Nu_{H,s}}$
20.0	1.127	3.5	1.023
40.0	1.184	4	1.017
50.0	1.241	5.0	1.143
60.0	1.296	6.0	1.312
80.0	1.399	8.0	1.660
100.0	1.494	10.0	2.000
200.0	1.883	20.0	3.074
300.0	2.192	30.0	5.453
400.0	2.455	40.0	7.226
500.0	2.689	50.0	9.012
600.0	2.900	60.0	10.805
800.0	3.278	80.0	14.403
1000.0	3.611	100.0	18.009

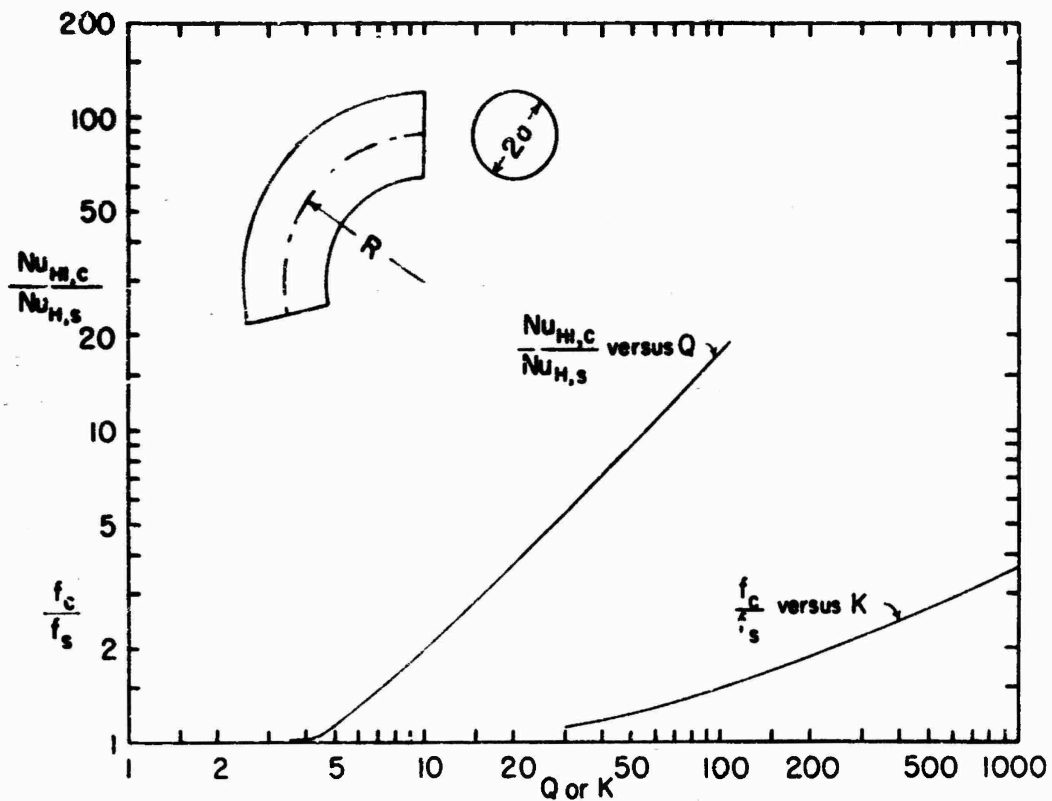


Fig. 65 Curved circular duct  $f_c/f_s$  and  $\frac{Nu_{Hl,c}}{Nu_{H,s}}$  for fully developed laminar flow.

valid for high Dean number region. Itō [287] assumed that the flow consisted of a frictionless central core surrounded by a boundary layer. He employed the Pohlhausen's approximate method to analyze the flow and arrived at the following formula for the friction factor.

$$\frac{f_c}{f_s} = 0.1008 K^{\frac{1}{2}} \left[ \left( 1 + \frac{1.729}{K} \right)^{\frac{1}{2}} - \frac{1.315}{K^{1/2}} \right]^{-3} \quad (222)$$

The above formula agrees well with White's [284] and Itō's own test data for  $K > 30$ . This  $f_c/f_s$  ratio for the curved circular duct is presented in Table 46 and Fig. 65.

Recently, Akiyama and Cheng [288] obtained a finite difference solution for the curved pipes using a combination of, what is described as, line iterative method and boundary vorticity method. Their fully developed laminar flow friction factors agrees with the data of White [284] and Itō [287] as well as with the empirical equation of Itō [Eq. (222)]. Eq. (222) does not fit the experimental data below Dean numbers of about 30. Akiyama and Cheng's numerical results fit the experimental data very well even in this range. Unfortunately, these numerical results were not available at the time of write-up of this report.

Itō [289] also experimentally investigated the friction factors for laminar and turbulent flow in curved pipes. The lower critical Reynolds number where the transition from laminar to turbulent flow starts was correlated as

$$Re_{crit} = 2 \times 10^4 \left( \frac{a}{R} \right)^{0.32} \quad (223)$$

This equation gives good agreement with experimental results in the range  $15 < R/a < 860$ . For  $R/a > 860$ , the critical Reynolds number for a curved pipe practically coincides with that for a straight pipe.

### 23.2 Heat Transfer

Several investigators have studied experimentally the heat transfer through curved circular ducts, such as tube coils by Seban and McLaughlin [290] and helical and spiral coiled tubes by Kubair and Kuloor [291].

Mori and Nakayama [292,293] first analyzed the laminar heat transfer in a curved pipe for  $\textcircled{H1}$  and  $\textcircled{T}$  boundary conditions based on boundary layer approximations along the pipe wall. The  $\textcircled{H1}$  and  $\textcircled{T}$  Nusselt numbers for the curved pipe were surprisingly found to be the same based on theoretical analysis, and are given by

$$\text{Nu}_c = \frac{0.864}{\zeta} K^{\frac{1}{2}} (1 + 2.35 K^{-\frac{1}{2}}) \quad (224)$$

$$\zeta = \frac{2}{11} \left[ 1 + \sqrt{\left( 1 + \frac{77}{4} \frac{1}{Pr^2} \right)} \right] \quad \text{for } Pr \geq 1 \quad (225a)$$

$$\zeta = \frac{1}{5} \left[ 2 + \sqrt{\left( \frac{10}{Pr^2} - 1 \right)} \right] \quad \text{for } Pr \leq 1 \quad (225b)$$

for Dean number  $K > 30$  for  $Pr \gg 1$  and  $K > 60$  for  $Pr \approx 1$ .

For small Dean numbers, where the above results are not applicable, Özışik and Topakoğlu [294] obtained fully developed  $\text{Nu}_{H1}$  for a curved circular pipe by a method of series expansion. They also considered the effect of internal thermal energy generation. For no internal thermal energy generation the Nusselt number was expressed as

$$\text{Nu}_{H1,c} = \frac{48}{11} \left( \frac{f_s}{f_c} \right) \left/ \left( 1 - \frac{a^2}{R^2} J_n \right) \right. \quad (226)$$

where

$$J_n = \frac{1}{264} \left[ -71.6 + \frac{Re^2}{403.2} \left\{ 165.47 + 7Pr + \right. \right. \\ \left. \left. + \frac{Re^2}{100.8} \left( 9.96576 + \frac{6.95513}{1.1} Pr^2 \right) \right\} \right] \quad (227)$$

Recently, Akiyama and Cheng [288] analyzed the fully developed laminar flow heat transfer through curved pipes under the  $\text{Hl}$  boundary condition. The finite difference solution was obtained using a combination of line iterative method and boundary vorticity method. Akiyama and Cheng [288] have clarified the effect of Prandtl number on heat transfer by showing that all the heat transfer results for  $Pr \geq 1$  can be approximated as follows.

$$\frac{Nu_{Hl,c}}{Nu_{H,s}} = 0.181Q \left[ 1 - \frac{0.839}{Q} + \frac{35.4}{Q^2} - \frac{207}{Q^3} + \frac{419}{Q^4} \right] \quad (228)$$

where  $Q = (K^2 Pr)^{1/4} \geq 3.5$  for  $Pr \geq 1$ . For  $Q \leq 3.5$ , the secondary flow effect due to curvature is estimated to be less than 1.5 percent in terms of the ratio  $Nu_{Hl,c}/Nu_{H,s}$ . The ratio  $Nu_{Hl,c}/Nu_{H,s}$ , from Eq. (228), is presented in Table 46 and Fig. 65.

Table 47. Curved rectangular ducts  $f_{Re}$  and  $Nu_{Hl}$  for fully developed laminar flow,  $Pr = 0.73$ , from Akiyama [281]

2b/2a = 0.2			2b/2a = 0.5			2b/2a = 1			2b/2a = 2			2b/2a = 5		
K	f <sub>Re</sub>	Nu <sub>Hl</sub>	K	f <sub>Re</sub>	Nu <sub>Hl</sub>	K	f <sub>Re</sub>	Nu <sub>Hl</sub>	K	f <sub>Re</sub>	Nu <sub>Hl</sub>	K	f <sub>Re</sub>	Nu <sub>Hl</sub>
0	19.486	5.7414	0	15.517	4.1264	0	14.204	3.6099	0	15.577	4.1264	0	19.046	5.7314
3.3160	19.046	5.7415	12.832	15.540	4.1366	12.510	14.264	3.6116	4.0637	15.517	4.1266	3.7148	19.046	5.7315
33.095	13.075	5.7508	18.075	15.602	4.1645	13.296	14.296	3.6476	12.834	15.537	4.1359	15.441	19.107	5.7732
46.627	19.146	5.7946	22.018	15.669	4.2024	19.142	14.312	3.7245	18.086	15.593	4.1627	16.279	19.259	5.8076
56.643	19.236	5.8403	25.258	15.769	4.2501	26.564	15.020	3.9238	25.259	15.706	4.2531	25.870	19.361	5.9719
65.328	19.326	5.8864	28.056	15.892	4.2979	31.505	15.470	4.1037	30.440	16.044	4.3660	63.347	19.879	6.0992
72.708	19.413	5.9303	30.537	15.995	4.3456	35.625	15.839	4.2578	34.559	16.315	4.4088	69.736	20.209	6.2230
79.298	19.498	5.9735	32.779	16.094	4.3924	39.090	16.154	4.3524	38.007	16.502	4.5950	75.152	20.514	6.3228
85.276	19.581	6.0156	34.800	16.164	4.4432	51.067	17.150	4.4503	50.287	17.703	5.0071	79.932	20.846	6.4761
			36.544	16.360	4.5182	60.974	18.286	5.1501	56.818	16.518	4.4004	84.184	21.146	6.5996
			52.307	17.047	4.8115	81.394	18.972	5.6630	67.681	19.190	5.6133	88.082	21.431	6.7046
			70.422	17.899	5.2136	91.499	19.481	6.0934	76.655	20.063	6.1106	93.673	21.703	6.8015
			83.575	18.462	5.4645	100.01	19.922	6.0634	85.571	20.735	6.1583	106.76	22.059	7.1226
			96.232	18.893	5.6736	117.64	20.722	6.4389	93.220	21.266	6.5951	118.31	23.009	7.3883
			103.36	19.247	5.8246				121.46	23.052	7.3739	128.11	24.632	7.9353
									156.63	25.440	8.3662	136.57	25.375	8.2809
									179.74	27.553	9.1501			

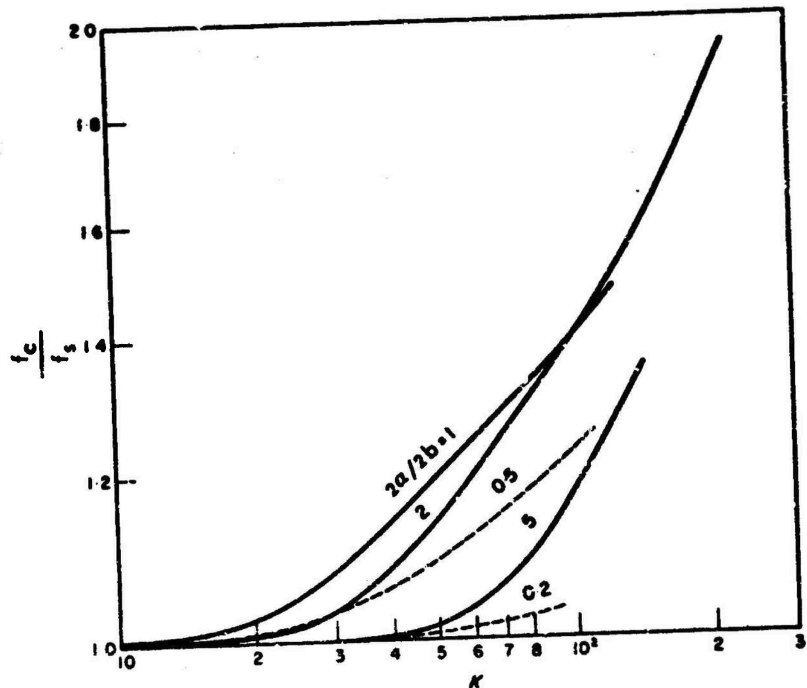


Fig. 66 Curved rectangular ducts  $f_c/f_s$  for fully developed laminar flow, from Cheng and Akiyama [280].

## 24. CURVED RECTANGULAR DUCTS

### 24.1 Flow Friction

Itō [295] first reported the theory on laminar flow through curved rectangular ducts using series expansion in Dean number and obtained formulae for the velocity components as functions of  $\alpha^*$  and  $K$ . The results are applicable for  $K \leq 600$ . Cumming [296] also investigated the same problem by using a perturbation method. Dean and Hirst [297] analyzed the curved square channel by assuming uniform stream for secondary flow.

Mori and Uchida [298] employed the boundary layer approximation to analyze the laminar flow and heat transfer through a square channel.

The perturbation method is applicable for low Dean number region, the boundary-layer technique is valid for high Dean number region. Cheng and Akiyama [280] presented the friction factors which are valid from low to a reasonably high Dean number. They employed the point successive over-relaxation numerical method to arrive at the results of Table 47 for the aspect ratio  $2b/2a = 0.2, 0.5, 1, 2$  and 5 [281]. The  $f_c/f_s$  for rectangular ducts are shown in Fig. 66.

Eichenberger [299] presented a theoretical analysis for the entrance region problem in a curved rectangular channel with secondary flow for an inviscid fluid.

### 24.2 Heat Transfer

Ustimenko et al. [300] presented flow and heat transfer results for fully developed laminar flow in curved flat channels with different heat fluxes at the inner and outer walls with no secondary flow effects.

Using boundary layer approximations, Mori and Uchida analyzed the fully developed laminar flow through a curved square channel with axially uniform wall temperature gradient [298] and rectangular channels with axially uniform wall heat

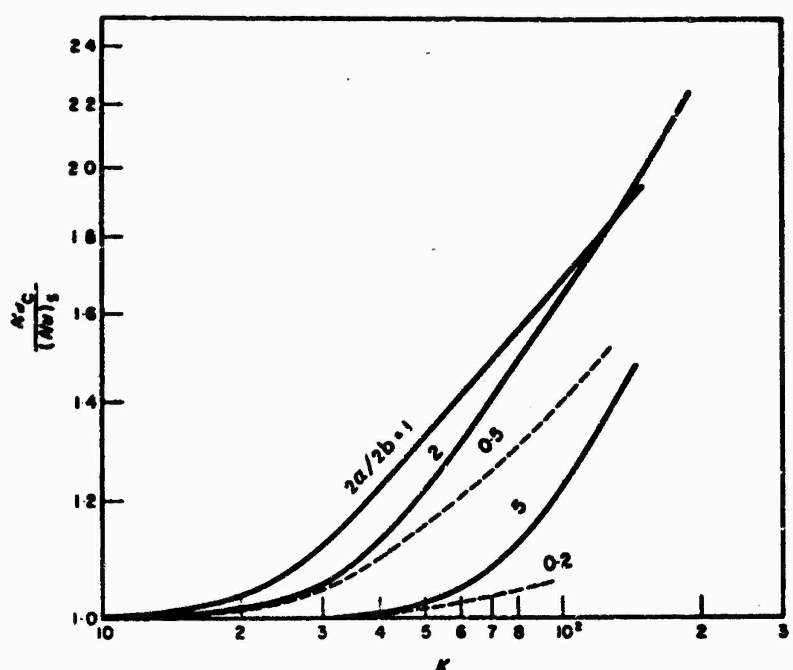


Fig. 67 Curved rectangular ducts  $\frac{Nu_{Hl,c}}{Nu_{Hl,s}}$  for fully developed laminar flow, from Cheng and Akiyama [280].

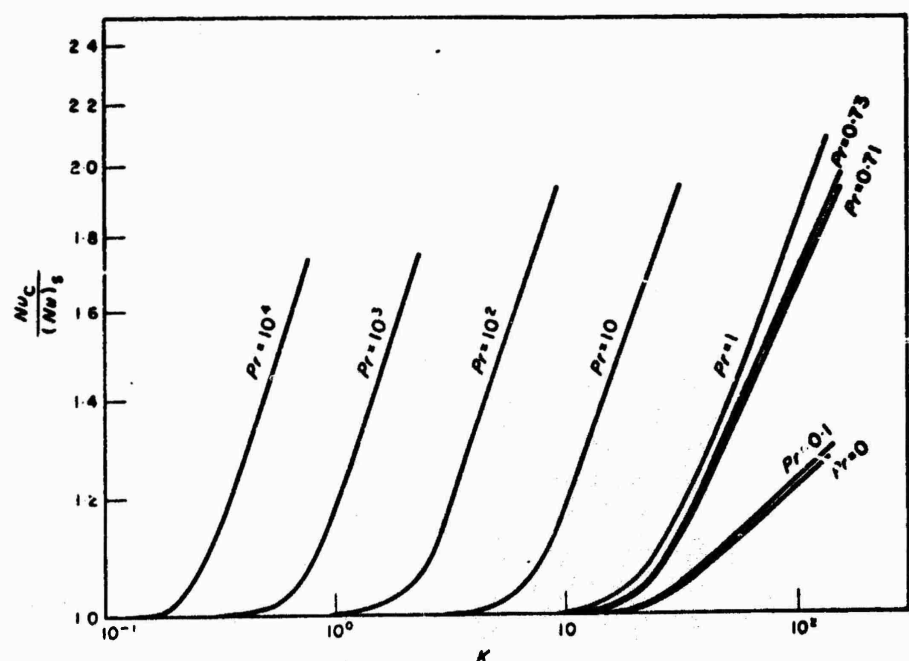


Fig. 68 Curved square duct  $\frac{Nu_{Hl,c}}{Nu_{Hl,s}}$  as functions of  $K$  and  $Pr$  for fully developed laminar flow, from Cheng and Akiyama [280].

flux conditions [301]. Their results are applicable in high Dean number region.

Cheng and Akiyama [280] investigated laminar  $(H_1)$  heat transfer in rectangular ducts by employing a point successive over-relaxation method. The  $Nu_{H_1,c}/Nu_{H_1,s}$  from Akiyama [281] are presented in Table 48 and Fig. 67 for  $2b/2a = 0.2, 0.5, 1, 2$  and  $5$  for  $Pr = 0.73$ . Also, the effect of Prandtl number was investigated for the curved square duct, and is presented in Table 49 and Fig. 68 [281].

Table 48. Curved square duct  $fRe$  and  $Nu_{H_1}$  for fully developed laminar flow; the influence of  $Pr$  on  $fRe$  and  $Nu_{H_1}$ , from Akiyama [281]

$Pr = 0.1$	$Pr = 0.71$	$Pr = 1$	$Pr = 10$	$Pr = 100$	$Pr = 1000$									
K	$fRe$	$Nu_{H_1}$	K	$fRe$	$Nu_{H_1}$	K	$fRe$	$Nu_{H_1}$	K	$fRe$	$Nu_{H_1}$	K	$fRe$	$Nu_{H_1}$
0	14.204	3.6099	0	14.204	3.6099	0	14.204	3.6099	0	14.204	3.6099	0	14.204	3.6099
19.442	14.204	3.6099	19.453	14.204	3.6099	19.453	14.204	3.6099	19.453	14.204	3.6099	19.453	14.204	3.6099
31.574	14.172	3.7067	31.574	14.172	3.7067	31.574	14.172	3.7067	31.574	14.172	3.7067	31.574	14.172	3.7067
61.276	17.835	4.1453	61.276	17.835	4.1453	61.276	17.835	4.1453	61.276	17.835	4.1453	61.276	17.835	4.1453
86.670	19.243	4.3497	86.670	19.243	4.3497	86.670	19.243	4.3497	86.670	19.243	4.3497	86.670	19.243	4.3497
123.65	20.980	4.5637	123.65	20.980	4.5637	123.65	20.980	4.5637	123.65	20.980	4.5637	123.65	20.980	4.5637
			26.464	15.020	3.8165	33.253	14.310	3.6766	7.6983	14.213	3.9112	1.4105	14.204	3.6490
			31.573	15.470	1.0640	21.401	14.766	3.9221	8.8873	14.220	4.0845	1.8124	14.204	3.7105
			35.626	15.839	4.2339	29.240	15.295	4.1897	10.853	14.239	4.4392	2.3456	14.204	3.8406
			39.050	18.154	4.3715	61.276	17.835	5.5575	12.510	14.265	4.7293	2.6107	14.204	4.0812
			51.867	17.190	4.8213	86.667	19.243	6.2918	13.956	14.296	4.9770	3.5114	14.204	4.4758
			68.974	18.266	5.1134	100.12	19.901	6.6402	15.850	14.352	5.2669	4.2133	14.206	4.8679
0.34405	14.205	4.6104	81.369	18.975	5.6227	117.64	20.722	7.737	17.504	14.417	5.4066	4.9053	14.206	5.2107
0.44416	14.205	4.6871	91.501	19.481	5.8488	127.39	21.983	7.029	19.442	14.512	5.7697	5.6171	14.207	5.5022
0.62813	14.205	5.7260	100.12	19.901	6.0318	26.584	14.766	6.0875	23.401	15.020	5.2795	14.206	5.7259	
0.72930	14.205	6.0964	117.64	20.722	6.3842				15.020	14.3457	6.8569	14.271	6.8595	

## 25. CURVED ELLIPTICAL DUCTS

Itō [295] investigated the laminar flow characteristics through the curved elliptical ducts using the series expansion for the velocity in terms of Dean number. He obtained the formulae for velocity components as a function of  $a^*$  and  $K$ . The results are applicable for  $K \leq 40$ .

Cumming [296] also analyzed the laminar flow through curved elliptical ducts using the perturbation method.

## 26. CURVED CONCENTRIC ANNULAR DUCTS

Only the laminar flow through curved concentric annulus without any heat transfer has been analyzed.

Kapur et al. [302] studied laminar flow through curved annuli for the large radius of curvature of the annulus in comparison to the outer radius of annulus. Analysis was based on simplified momentum and continuity equations. Expressions were derived for the flow parameters.

Topakoğlu [283] extended his curved circular pipe to the curved annular pipe and obtained the secondary flow streamlines for the flow between two concentric curved pipes.

Dean [279], in his analysis, could not get the effect of curvature on the relation between rate of flow and pressure gradient. Topakc̄lu and Kapur et al. extended Dean's problem to the curved annulus, so they did not bring this curvature effect in their analysis. In order to show the effect of curvature, Srivastava [303] considered higher approximations following Dean [282] and obtained the reduction in flow for the curved annulus with  $r^* = 1/2$ .

## VI. DISCUSSION AND COMPARISONS

A brief discussion is provided in this chapter of the following topics:

1. The dependency of Nusselt number on various parameters
- 2.1 A comparison of different wall flux boundary conditions  $(H_1)$ ,  $(H_2)$  and  $(H_3)$
- 2.2 A comparison of the  $(H_1)$  and  $(T)$  boundary conditions
3. A comparison of  $Nu$  for various geometries
4. A comparison of limiting geometries
5. A suggested correlation for fully developed heat transfer results
6. Application of fully developed heat transfer results to gas turbine regenerator design

### VI.1 The Dependency of Nusselt Number on Various Parameters

Theoretical laminar forced convection heat transfer results ( $Nu$ ) presented in Chapter V are dependent on (i) duct geometry, (ii) inlet velocity and temperature profiles and (iii) thermal boundary conditions.

(i) In turbulent flow, the heat transfer results are reasonably well correlated by using  $D_h$  as a characteristic dimension; hence, clearly, the turbulent flow results are not a strong function of the duct geometry. In contrast, it is well established that for laminar flow, the dependence of heat transfer results on the duct geometry is not removed by using  $D_h$  as a characteristic dimension. In light of present compilation of analytical results, it is suggested that a search be made for another characteristic dimension for a given geometry. This new dimension will allow a Nusselt number definition that result in magnitudes less dependent on the duct geometry.

(ii) Laminar forced convection heat transfer theory results are dependent on the idealized velocity and/or temperature profile at the inlet. Usually, these profiles are specified as either uniform or fully developed at the entrance. As these idealized profiles are used to approximate the real life situation in technical applications, the designer should be explicitly aware of both the actually expected and idealized profiles associated with the theory results.

(iii) There are a variety of thermal boundary conditions of technical interest, as outlined in Sections II.1.3 (Table 1) and II.3.1. The theoretical laminar forced convection heat transfer rates are quite sensitive to these thermal boundary conditions. It has been the practice to assume that the  $\textcircled{H1}$  and  $\textcircled{T}$  boundary conditions are the two usual extremes in the heat exchanger designs. However, reviewing the material of Chapter V or Table 50 on p. 228 reveals that this may not be the case; e.g.  $Nu_{H2}$  are lower than  $Nu_T$  for the rectangular ducts ( $\alpha^* < 0.75$ ) and isosceles triangular ducts. Consequently, the question of what boundary conditions can be assumed is of major significance to a designer of laminar flow heat transfer systems. As the  $\textcircled{H1}$ ,  $\textcircled{H2}$ ,  $\textcircled{H3}$  and  $\textcircled{T}$  boundary conditions are all of considerable technical importance, the implicit idealizations used in the boundary condition specification and the reasons for different Nusselt numbers are discussed in the following subsections.

#### VI.2.1 A Comparison of Different Wall Flux Boundary Conditions $\textcircled{H1}$ , $\textcircled{H2}$ and $\textcircled{H3}$

The thermal boundary condition of approximately constant axial heat rate per unit of tube length ( $q' \approx \text{constant}$ ) is realized in many cases; for example, electric resistance heating, nuclear heating, counterflow heat exchanger with equal thermal capacity rates ( $W_c_p$ ) etc. For this case, there

are three idealized boundary conditions,  $(H_1)$ ,  $(H_2)$  and  $(H_3)$ , that have been analyzed to varying degrees. These three boundary conditions are essentially the same for straight ducts having constant peripheral curvature and no "corners effects"; e.g. circular duct, parallel plates, annular ducts. These same boundary conditions for the ducts having corners and/or different curvature around the periphery (e.g. rectangular, triangular, sine, elliptical ducts) are essentially different and yield different  $Nu$  magnitudes. Before further discussion, the implicit idealizations used for the thermal conductivity of the material for these boundary conditions are summarized in Table 49.

Table 49. Idealizations of wall thermal conductivity for thermal boundary conditions

boundary condition	$k_w$ in axial direction	$k_w$ in peripheral direction
$(H_1)$	zero	infinite
$(H_2)$	zero	zero
$(H_3)$	zero	finite
$(T)$	infinite	infinite

Since, only the wall temperature at the wall-fluid interface is needed as a boundary condition, the radial thermal conductivity of the material is not involved in the analysis. From Table 49, it can be seen that the  $(H_1)$  and  $(H_2)$  boundary conditions are the special cases of the  $(H_3)$  boundary condition. As indicated above, they become identical for ducts such as the straight circular duct because then there is no peripheral variation of wall temperature and the magnitude of  $k_w$  is of no significance.

For a heat exchanger with highly conductive materials (e.g. copper, aluminum), the  $\textcircled{H1}$  boundary condition may prevail when axial  $q'$  is constant. However, for a heat exchanger with low thermal conductivity materials (e.g. glass ceramic, teflon), the  $\textcircled{H2}$  boundary condition may be realized if the wall thickness all around the periphery is uniform. For a more general problem, with constant axial  $q'$ , the  $\textcircled{H3}$  boundary condition would be most appropriate.

The Nusselt number for the  $\textcircled{H1}$  boundary condition is higher than that for the  $\textcircled{H2}$  boundary condition. The  $Nu_{H3}$  falls in between  $Nu_{H1}$  and  $Nu_{H2}$ . The heat transfer coefficient for the  $\textcircled{H1}$  boundary condition based on the definition of Eq. (43), is found as

$$h_{H1} = \frac{1}{t_w - t_m} \frac{q'}{P}, \quad \left\{ \begin{array}{l} q' = \text{constant with } x \\ t_w = \text{constant with } s \end{array} \right. \quad (229)$$

Similarly the heat transfer coefficient for the  $\textcircled{H2}$  boundary condition is found as

$$h_{H2} = \frac{1}{\frac{1}{P} \int t_w ds - t_m} \frac{q'}{P} \quad \left\{ \begin{array}{l} q' = \text{constant with } x \\ q'' = q'/P, \text{constant with } s \end{array} \right. \quad (230)$$

For the  $\textcircled{H2}$  boundary condition,  $q'' = -k(\partial t / \partial n) = \text{constant}$  around the periphery. This thermal energy is transferred to the fluid in the central section of the duct where the bulk of the fluid flows. The fluid mean effective conduction path length  $s_f$  for the thermal energy transfer is higher from the corners to the bulk of fluid when compared to the wall regions away from the corners. Consequently, as indicated in the following expression, the corner temperature difference is higher. This increases the peripheral average

age  $t_w$  in Eq. (230) with a reduction of  $h_{H2}$  relative to its counterpart  $h_{H1}$ .

$$q'' = k \frac{\Delta t}{\Delta n} = k \frac{(t_w - t_m)}{\delta_f} = \text{constant} \quad (231)$$

The  $Nu_{H2}$  can be significantly lower than the  $Nu_{H1}$  for an acute cornered duct geometry. Consequently judgment must be exercised before applying the theoretical data to a design. This also suggests that more theoretical information is needed for the noncircular duct (H2) and (H3) heat transfer problem. Additionally, more experimental measurements of actual peripheral wall temperatures would be useful to approximate the thermal boundary condition.

#### VI.2.2 A Comparison of (H1) and (T) Boundary Conditions

In the previous section, the examples were mentioned where the (H1) boundary condition may be realized in a practical situation.

The (T) boundary condition may be approximated for the heat transfer in the condenser, evaporators etc. In this case, the temperature of fluid on one side is uniform and constant, and the thermal resistance of wall and constant fluid temperature side is relatively small and is treated as zero. For this situation, it is implicitly assumed that  $k_w$  in axial direction is arbitrary, but that  $k_w$  in radial direction is infinite. The other possible idealized situation for the (T) boundary condition is described in Table 49. For that situation, the thermal conductivity of the material is assumed to be infinite both in axial and peripheral direction. The radial thermal conductivity or the radial wall temperature profile for this case is not involved in the analysis.

The  $Nu_{H1}$  is higher than the  $Nu_T$  for all the duct

Table 50. Solutions for heat transfer and friction for fully developed flow

GEOMETRY ( $L/D_h > 100$ )	$Nu_{H1}$	$Nu_{H2}$	$Nu_T$	$fRe$	$\frac{Nu_{H1} Pr^{-1/3}\dagger}{fRe}$	$\frac{Nu_{H1}}{Nu_T}$
 $\frac{b}{a} = \frac{\sqrt{3}}{2}$	1.014	1.474	2.39*	12.630	0.269	1.26
 $\frac{b}{a} = \frac{\sqrt{3}}{2}$	1.111	1.891	2.47	13.333	0.263	1.26
 $\frac{b}{a} = 1$	3.603	3.091	2.976	14.227	0.286	1.21
	4.002	3.862	3.33*	15.054	0.299	1.20
 $\frac{b}{a} = \frac{1}{2}$	4.123	3.017	3.391	15.548	0.299	1.22
	4.164	4.364	3.657	16.000	0.307	1.19
 $\frac{b}{a} = 1.5$	5.099	-	3.66	18.700	0.307	1.39
 $\frac{b}{a} = \frac{1}{4}$	5.311	2.930	4.439	18.233	0.329	1.20
 $\frac{b}{a} = \frac{1}{5}$	5.450	2.904	5.597	20.585	0.355	1.16
 $\frac{b}{a} = \infty$	8.245	6.425	7.541	24.000	0.386	1.09
 insulated	5.385	-	4.861	24.000	0.253	1.11

\* Interpolated values

$\dagger_{Pr = 0.72}$

geometries. The physical reasoning for this behavior can be given from the review of dimensionless fluid temperature profiles. These dimensionless temperature profiles  $(t_w - t)/(t_w - t_m)$  are shown in Fig. 69 for the circular tube with heat transfer from the wall to the fluid. It can be seen that there is an inflection point in the fluid tempera-

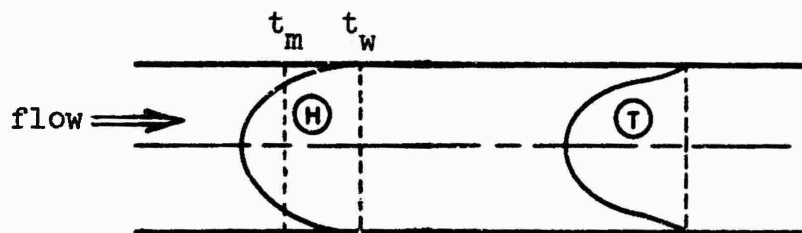


Fig. 69 Fluid temperature profiles for  $\textcircled{H}$  and  $\textcircled{T}$  boundary conditions.

ture profile for  $\textcircled{T}$  boundary condition because  $t_w$  is constant. For the  $q' = \text{constant}$  boundary condition,  $t_w$  is continuously "running away" from  $t_m$  so that an inflection in the profile does not develop. The heat transfer coefficient, from Eq. (46), is found as

$$k \left( \frac{\partial t}{\partial r} \right)_{r=a} = h(t_w - t_m) \quad (232)$$

for the circular tube. From Fig. 69, for the same  $(t_w - t_m)$ , the fluid temperature gradient at the wall is smaller for the  $\textcircled{T}$  boundary condition because of the inflection. Thus, from Eq. (232) the  $h$  and consequently  $\text{Nu}$  is lower for  $\textcircled{T}$  boundary condition when compared to  $\textcircled{H}$  boundary condition. This result may be generalized to apply to the noncircular ducts.

### VI.3 A Comparison of $\text{Nu}$ for Various Geometries

The flow friction modulus  $fRe$  and Nusselt numbers  $\text{Nu}$  for several duct geometries of technical interest are summarized in Table 50. From the discussion of previous

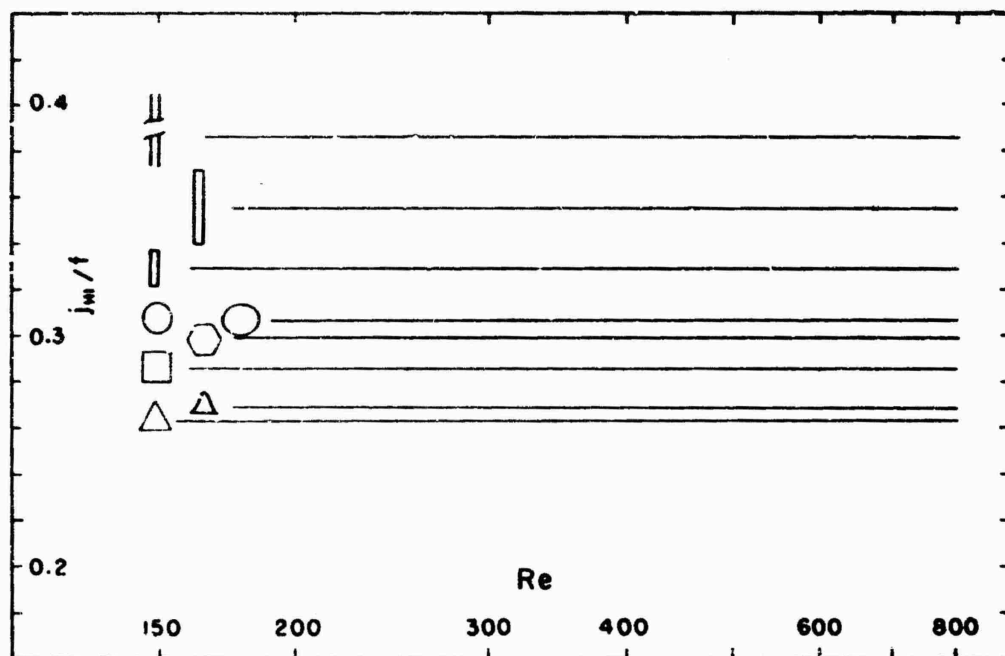


Fig. 70 Flow area "goodness" factors for some duct geometries of Table 50.

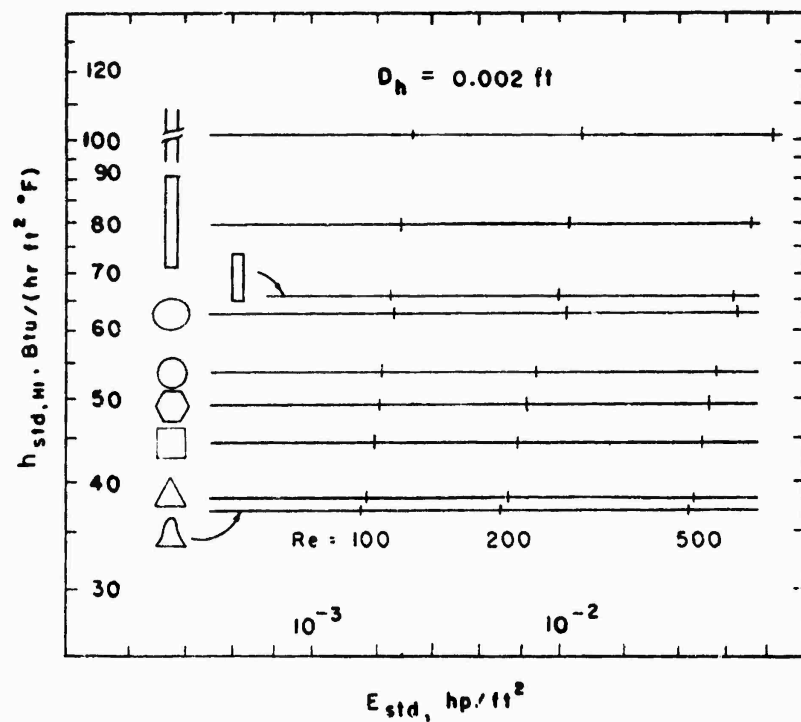


Fig. 71 Volume "goodness" factors for some duct geometries of Table 50.

section, as expected, both  $Nu_{H2}$  and  $Nu_T$  are lower than  $Nu_{H1}$ . For the duct geometries having strong corner effects,  $Nu_{H2}$  is even lower than the  $Nu_T$ , but otherwise  $Nu_{H2}$  is higher than  $Nu_T$ . The ratio of maximum to minimum  $Nu_{H1}$ ,  $Nu_{H2}$ ,  $Nu_T$  and  $fRe$  is found as 2.7, 5.6, 3.2 and 1.9 respectively for the geometries considered in Table 50. The ratio  $Nu_{H1}/Nu_T$  varies from 1.09 to 1.39 for the geometries of Table 50.

From the design point of view, the performance of heat exchanger cores made up of these different geometries may be compared in the following two complimentary different ways: (i) comparing the flow area "goodness" factors  $NuPr^{-1/3}/f = j/f$  and (ii) comparing the core volume "goodness" factors  $h_{std}$  versus  $E_{std}$ .

(i) It can be shown that the flow area "goodness" factor  $j_{H1}/f$  is

$$\frac{j_{H1}}{f} = \frac{1}{A_c^2} \left[ \frac{Pr^{2/3}}{2g_c \rho} \frac{N_{tu} W^2}{\Delta p} \right] \quad (233)$$

With the bracketed quantities constant, this area "goodness" factor is inversely proportional to  $A_c^2$ , where  $A_c$  is the core free flow area. The  $j_{H1}/f$  is presented in Fig. 70 for most of the duct geometries of Table 50. This factor ranges from 0.263 (equilateral triangular duct) to 0.386 (parallel plates). Thus parallel plates relative to the triangular duct present an improvement of 47% ( $= 0.386/0.263 - 1$ ) for  $j/f$  and consequently a 21% ( $= \sqrt{1.47} - 1$ ) smaller free flow requirement. The exchanger porosity must be considered in order to translate this free flow area advantage into a frontal area improvement. Note that in the flow area "goodness" factor comparison, no estimate of total heat transfer area or the volume can be inferred. This is the function of the volume "goodness" factor to follow.

(ii) The core volume "goodness" factor is a plot of  $h_{std}$  versus  $E_{std}$ , where

$$h_{std} = \frac{c_p \mu}{Pr^{2/3}} \frac{1}{D_h} j Re = \frac{k}{D_h} Nu \quad (234)$$

$$E_{std} = \frac{\mu^3}{2g_c \rho^2} \frac{1}{D_h^3} f Re^3 \approx u_m r_h \frac{\Delta p}{L} \quad (235)^*$$

The higher the  $h_{std}$  for a given  $E_{std}$ , the lower is the heat transfer area requirement; and it can be shown that when the  $D_h$  is fixed, the lower is the heat exchanger volume requirement for a given core porosity.

A common hydraulic diameter  $D_h = 0.002$  ft is used to eliminate the influence of the scale of surface geometries. Using the physical properties of air at one atmosphere pressure and 500°F, the  $h_{std,H1}$  and  $E_{std}$  were calculated from Eqs. (234) and (235) at  $Re = 100, 200$  and  $500$  for most of the geometries of Table 50. The results are plotted in Fig. 71. From this figure, for a given friction power expenditure, the heat transfer power per unit area and temperature difference, or convection coefficient  $h_{std}$ , can vary from 37 to 101 Btu/(hr ft<sup>2</sup> °F) (a factor of 2.7) from sine duct to the parallel plate geometry. Based on Fig. 71, the parallel plate heat exchanger would require 63% ( $1 - 1/2.7$ ) less heat transfer area compared to the sine duct heat exchanger. Moreover, the parallel plate heat exchanger would

---

\*The  $\Delta p$  formulation applies rigorously to constant density flow and approximately for gas flows.

have a significantly smaller frontal area. This simple argument is possible only because both "goodness" factor lines are horizontal.

Parallel plate heat exchanger may not prove to be practical for several reasons. But it is clear from Figs. 70 and 71 that there are other configurations that possess significant advantages relative to the triangular and sine duct geometries.

#### VI.4 A Comparison of Limiting Geometries

Comparisons of limiting cases of several geometries of Chapter V are of interest. These differences for fully developed  $fRe$  and  $Nu_{H1}$  are qualitatively rationalized here as they are revealed by the available tabular information of Chapter V.

The limiting cases of elliptical, triangular and sine duct geometries are obtained when the aspect ratio  $2b/2a$  approaches either 0 or  $\infty$ , with one dimension remaining finite. The geometries under consideration are shown in Fig. 72(a) and 72(b). Only the corners of geometries are depicted. The corner shape has a strong influence on the fully developed  $fRe$  and  $Nu_{H1}$ . The more acute the passage is at the corner, the greater is the "corner effect". Because, the flow is more stagnant resulting in lower temperature and velocity gradients and lower  $fRe$  and  $Nu_{H1}$  as a consequence.

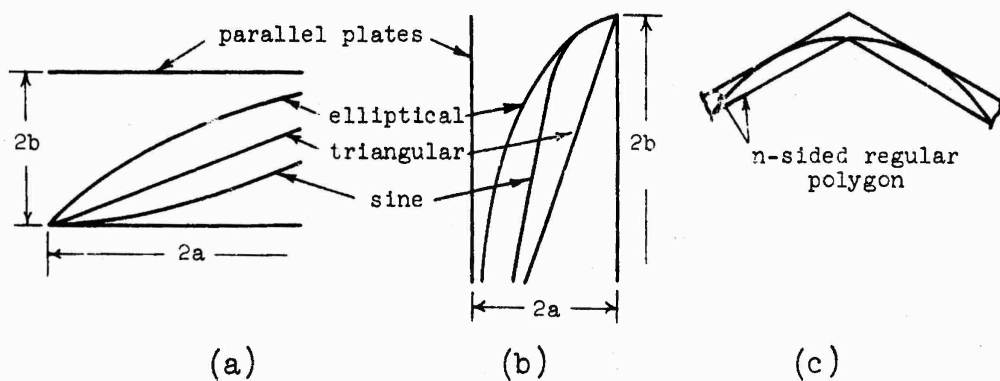


Fig. 72 Corner effects for limiting geometries.

In Fig. 72(a) ( $2b/2a \rightarrow 0$ ), the height of the channel  $2b$  is kept finite while the width  $2a$  is approaching infinity. Using the "corner effects" argument, the geometries in decreasing order of  $fRe$  and  $Nu_{Hl}$  are: parallel plates (no corners), elliptical duct, triangular duct and then the sine duct with the most acute corner.

In Fig. 72(b) ( $2b/2a \rightarrow \infty$ ), the width of the channel  $2a$  is kept finite while the height  $2b$  is approaching infinity. Based on the "corner effects" argument, the geometries in decreasing order of  $fRe$  and  $Nu_{Hl}$  are: parallel plates, elliptical duct, sine duct and triangular duct. Note that the order of performance is reversed for the sine and triangular ducts in Fig. 72(a) and (b). The trends shown in Figs. 73 and 74 support this conclusion.

In Fig. 72(c), the number of sides  $n$  of the inscribed and circumscribed regular polygon is approaching infinity. Based on the "corner effects", the geometries in decreasing order of  $fRe$  and  $Nu_{Hl}$  are: circular duct with inscribed  $n$ -sided regular polygon, and  $n$ -sided regular polygon duct with a circular core touching tangentially.

#### VI.5 A Suggested Correlation for Fully Developed Heat Transfer Results

If the cylindrical flow passage of a heat exchanger is very long compared to the thermal entry length for a given boundary condition, the effect of thermal entrance region may be very small. In that case, the fully developed heat transfer results may be accurate for design purposes. Otherwise, the effect of the thermal entrance regime may be significant, and the design using fully developed heat transfer results may be too conservative.

In case of the velocity problem, the pressure drop in a duct longer than the hydrodynamic entry length was determined by defining a pressure drop increment  $K(\infty)$ . With the knowledge of fully developed  $fRe$  and  $K(\infty)$ , the friction

pressure drop can be determined conveniently from

$$\frac{\Delta p}{\rho u_m^2/2g_c} = f_{fd} \frac{L}{r_h} + K(\infty) . \quad (31)$$

An approximate theory was devised by Lundgren et al. [19] to evaluate  $K(\infty)$  for any arbitrary duct with the knowledge of fully developed velocity profile [see Eq. (32)]. Thus the designer can readily assess the hydrodynamic entry length effects.

It is proposed that a similar scheme may also be used for the laminar heat transfer in a long duct. An incremental thermal entry length heat transfer number,  $N(\infty)$ , may be defined as

$$Nu_m \frac{L}{r_h} = Nu_{fd} \frac{L}{r_h} + N(\infty) . \quad (236)$$

As no theory exists in heat transfer literature to evaluate  $N(\infty)$ , and as sufficient information is not available for any one duct geometry (except circular tube), it is recommended that efforts be directed to obtain this information for other geometries. For circular tubes, on the other hand, the information provided in Table 8 allows  $N(\infty)$  to be determined.

With such information for  $N(\infty)$ , the designer can readily assess the thermal as well as the hydrodynamic entry length effects.

#### VI.6 Application of Fully Developed Laminar Flow Results to Gas Turbine Regenerator Design

A gas turbine regenerator is usually either a recuperative type counterflow, a multipass cross-counterflow or a rotary type (periodic flow) heat exchanger. In either case, on one "side" cold compressed air flows and on the other "side" hot turbine exhaust gases pass through to the atmo-

sphere. The thermal capacity rate ( $C = W_{cp}$ ) of both the air and gas are approximately equal,  $C_{min} \approx C_{max}$ . A significant portion of thermal energy from the hot gas is transferred to the air prior to further heating in the combustion chamber. In this way a substantial fuel savings result. The designer aims for a compact, low weight, durable and high effectiveness heat exchanger. The wall heat flux from the hot gas to the air side may be approximated as constant over most of the regenerator flow length. The influence of thermal boundary conditions and idealized geometries on the gas turbine regenerator design is discussed below.

#### VI.6.1 Influence of Thermal Boundary Conditions

The discussion of Section VI.2.1 for constant axial wall heat flux case may be summarized as: (i) for a heat exchanger with highly conductive materials, the  $(H_1)$  boundary condition may prevail, (ii) with low thermal conductivity materials (e.g. glass ceramic), the  $(H_2)$  boundary condition may be realized, if the wall thickness all around the periphery is constant, and (iii) for a more general problem, the  $(H_3)$  boundary condition would be most appropriate. Further, in Chapter II, it was mentioned that in addition  $\Delta t$  and  $(H_4)$  thermal boundary conditions, conceptually, may also be applicable to the gas turbine regenerator. As Nusselt numbers for each of the above boundary conditions are different, and substantially so if a strong "corner effect" passage geometry is employed, the specification of the most appropriate idealized thermal boundary condition becomes important. Before examining the question of an appropriate boundary condition for the regenerator, the pertinent literature is reviewed below specially for  $(H_3)$ ,  $\Delta t$  and  $(H_4)$  boundary conditions; other boundary conditions are covered in Chapter V and Tables 50 and 51.

The  $(H_3)$  boundary condition is analyzed only for a square duct by Lyczkowski et al. [11] for fully developed flow. The

$(H_3)$  and  $(H_1)$  boundary conditions on each pair of opposite sides of a rectangular duct have been considered by Han [216] again for fully developed flow. The  $(\Delta t)$  boundary condition has been investigated only for the circula. tube by Kays [12] for thermally developing flow. The  $(H_4)$  boundary condition is analyzed for the circular tube by Hall et al. [127] and Hasegawa et al. [10], and for the annular duct family by Graber [128] for fully developed flow. This survey indicates that insufficient work has been done for the laminar heat transfer with  $(H_3)$ ,  $(\Delta t)$  and  $(H_4)$  boundary conditions.

Experimental results for triangular passage glass ceramic matrices [304] generally fall in between the theoretical prediction for the  $(H_1)$  and  $(T)$  boundary conditions. Even though the glass ceramic has low thermal conductivity (0.42 Btu/hr ft  $^{\circ}$ F), the  $(H_2)$  boundary condition which falls below  $(T)$  for the isosceles triangle (Fig. 28) is not realized. This may be due to the fact that the wall is thicker at somewhat rounded corners. Thus peripheral conduction may reduce the peak temperatures and consequently th "corner effects" below the prediction for the  $(H_2)$  boundary condition.

Current design data for the gas turbine regenerator matrix are based on the experimental data rather than the theory predictions. The many reasons for this choice will not be discussed here. However, the theory results provide a valuable base line for comparison with experiments. The experimental data is usually obtained by a transient, single-blow, technique [4]. An open question remains as to the appropriate boundary conditions for the test core in the experimental facility. Do they approximate the boundary conditions for the prototype application, the regenerator in service? Consequently, characterization of the transient boundary conditions in the test facility in terms of the

equivalent idealized steady state conduction is an important area of investigation.<sup>t</sup>

### VI.6. Influence of Idealized Geometry

A variety of duct geometries are considered in Chapter 7 and those most important for the regenerator application are summarized in Table 50. A comparison of the heat transfer and flow friction behavior of these idealized geometries for the gas turbine regenerator design is of interest. As discussed in Section VI.3, these comparisons may be made on the basis of: (i) flow area "goodness" factor and (ii) volume "goodness" factors, as is done in Figs. 70 and 71. The higher flow area "goodness" factors make for the lower frontal area requirements (for the same through flow porosity). Also, the higher volume "goodness" factors (the line of  $h_{std}$  versus  $E_{std}$ ) results in the lower exchanger volumes as well as the pressure drop for the same passage  $D_h$ . From these viewpoints, the rectangular duct family with  $\alpha^* \leq 0.25$  appears to be the most promising from Figs. 70 and 71. A more detailed comparison of circular, elliptical, isosceles triangular, sine, rounded corner triangular and cusped ducts may be made as follows, as these geometries can be more readily fabricated relative to the  $\alpha^* \leq 0.25$  rectangular duct surface.

#### (a) Circular duct and elliptical duct with $\alpha^*$ close to 1.

The current interest of glass ceramic surfaces for the regenerator of a vehicular gas turbine engine has increased efforts to produce compact, low weight and high effectiveness circular tube matrix. If a significant number of passages are squashed and become elliptical during core

<sup>t</sup>For the single blow transient testing technique, refer to [4, 305, 306]. For the periodic testing technique, refer to [307, 308].

fabrication, the performance of a mix of elliptical and circular passage geometries may differ substantially from the idealized circular passage geometry.

A slight flattening of circular tubes to an elliptical shape can have a significant effect on the theoretical  $f_{Re}$  and  $\text{Nu}_{Hl}$ . Inspection of the following table prepared from the results of Table 33 illustrates this point.

$\alpha^*$	$\frac{f_{Re}}{f_{C}} \cdot \frac{\text{Nu}_{Hl}}{58/11}$
1.00	1.000
0.99	1.066
0.98	1.090
0.95	1.132
0.90	1.169

Note that both the ratio  $f_{Re}/f_{C}$  and  $\text{Nu}_{Hl}/(58/11)$  are the same in the above table.

Comparison of the circular tube and an elliptical duct with  $\alpha^* = 0.9$  is made in Fig. 70 and 71 in terms of area "goodness" and volume "goodness" factors. For these two geometries, area goodness factors are the same, resulting the same frontal area requirement for equal through flow porosities. However, it is surprising to notice that  $n_{std}$  for the elliptical duct is 17% higher. Theoretically, this would result in a 15% ( $1-1/1.17$ ) lower heat transfer area requirement and 15% lower pressure drop requirement for the elliptical duct core.

The future trend for glass ceramic regenerator surfaces is to employ hexagonal and/or circular passages in contrast to the present use of triangular passages. Based on the theoretical results, it appears that the elliptical passage matrix offer an improvement in performance over both the circular tube and hexagonal passage matrix. Before applying

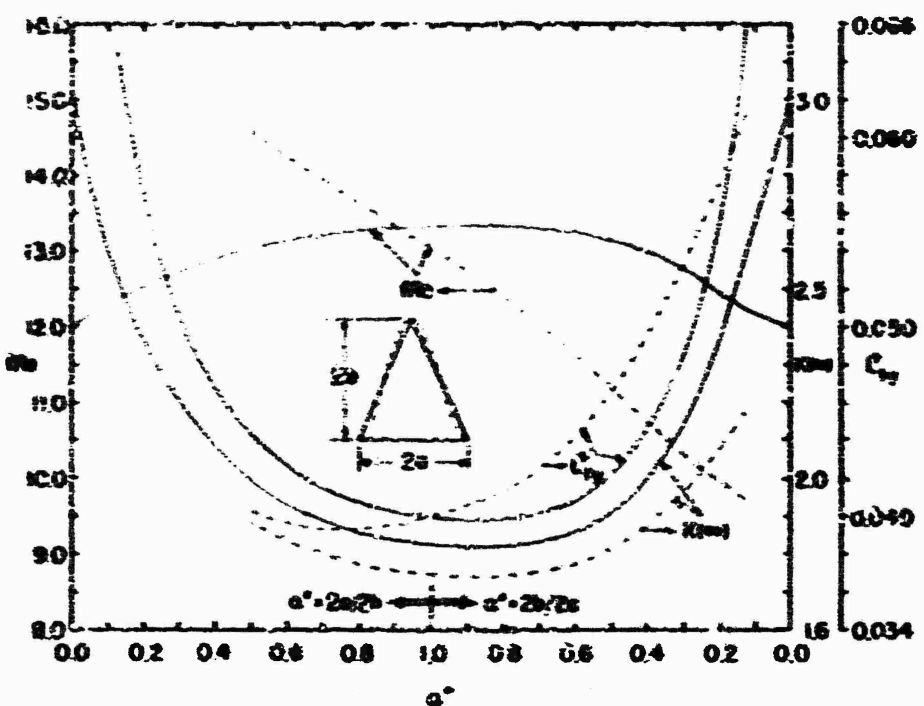


Fig. 73 Comparison of flow friction behavior -- isosceles triangular and sine ducts.

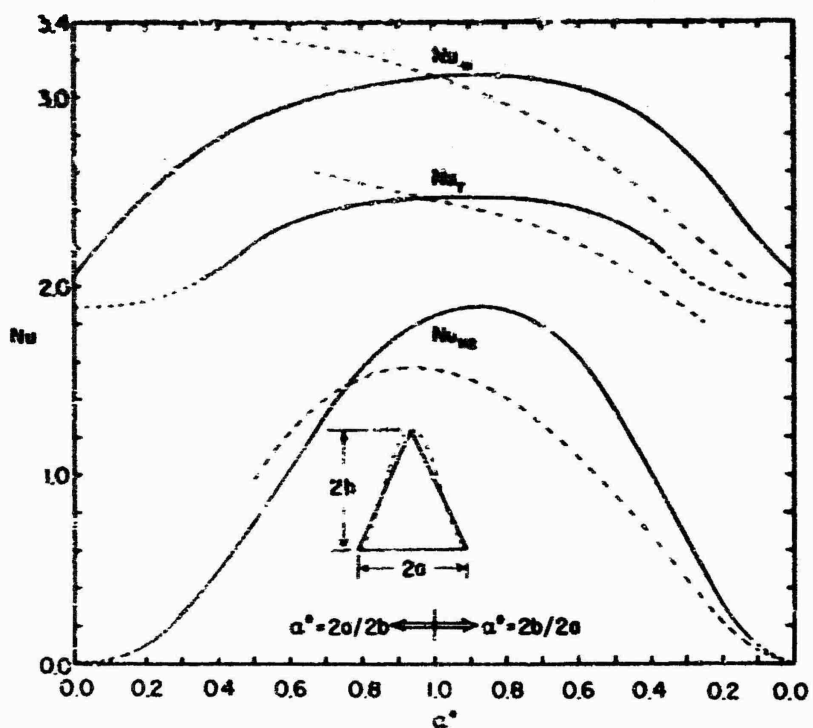


Fig. 74 Comparison of heat transfer behavior -- isosceles triangular and sine ducts.

this result in a prototype design, however, it is recommended that experimental work be carried out on appropriate matrices to verify the suggested advantages.

(b) Isosceles triangular and sine ducts. In manufacturing process of a triangular passage matrix, frequently the passages of a fabricated matrix approximate a sine duct. For such a matrix, the flow friction and heat transfer behavior would differ from the triangular passage behavior. These comparisons are made in Figs. 73 and 74. The following observations are made from these figures: (i) for  $0 \leq 2b/2a \leq 1$ , the  $fRe$ ,  $K(\infty)$ ,  $Nu_T$ ,  $Nu_{H1}$  and  $Nu_{H2}$  are lower for the sine duct, and (ii) for  $0 \leq 2a/2b < 1$ , the  $fRe$ ,  $Nu_T$ ,  $Nu_{H1}$  and  $Nu_{H2}$  (for  $2a/2b < 0.75$ ) are higher for the sine duct.

To translate this performance in terms of area and volume "goodness" factors, the equilateral triangular duct and sine duct of the same aspect ratio are compared in Figs. 70 and 71. From these figures, the surfaces differ only about 5 percent. Consequently, for the same required performance, the heat exchangers, made from either equilateral triangular or sine duct geometry of the same aspect ratio, will have approximately the same frontal area and volume.

(c) Equilateral triangular duct with rounded corners.

The rounded corners geometries of Section V.5 are compared in the following table in terms of area and volume goodness factors.

Based on the area and volume "goodness" factors, the three rounded corners geometry appears to be superior to the all sharp corner geometries. Note that the flow area of the three rounded corners geometry is 13% lower (Table 27); and this factor must also be accounted for in the evaluation of advantages of this geometry.

Equilateral triangular duct with specified rounded corners	$\epsilon/\epsilon_0$	$Re_{KL}$	$f_{HL}/f^1$	$h_{ste}^2$
no rounded corner	13.333	3.111	0.263	38.2
one rounded corner	14.050	3.402	0.273	41.8
two rounded corners	14.899	3.756	0.284	46.2
three rounded corners	15.993	4.205	0.295	51.7

<sup>1</sup>For  $Pr = 0.700$

<sup>2</sup>For air properties at one atmosphere and  $500^{\circ}\text{F}$

(d) A combined geometry of cusped and circular ducts.

In a circular tube core, the n-sided cusped geometry is formed between the tubes. The heat transfer area associated with the cusped geometry is of the same order of magnitude as that associated with circular tubes. If there is a significant amount of fluid flowing through these cusps (for  $n \geq 4$ ) the associated heat transfer area becomes effective. The overall performance for a matrix with these combined geometries may be substantially higher than for a circular tubes matrix. The combined geometry question needs to be explored further when heat transfer characteristics of the n-sided cusped geometry are derived.

(e) Performance of a combined geometry. In the preceding sections, several combined geometries were considered, e.g., circular and elliptical passages, circular and cusped passages, triangular passages with rounded corners. As the theoretical heat transfer and flow friction characteristics of these individual passages are available (or become available in the case of cusped ducts), the combined performance of mixed passages can be determined as outlined in [309]. It is recommended that the combined performance of the above geometries be investigated as these geometries are of current interest for the vehicular gas turbine regenerator application.

## VII. SUMMARY AND CONCLUSIONS

1. This report provides an up-to-date compilation, using a common format, of available analytical solutions for laminar flow through straight and curved ducts. These analytical solutions for flow friction and forced convection heat transfer are summarized from over 300 references for 25 duct geometries. The results are presented in tabular and graphical nondimensionalized form in Chapter V. As a summary, Table 51 is prepared so that the reader may readily locate specific solutions.
2. The tabular and graphical information available in the heat transfer literature has been augmented in this presentation by (i) calculating, when readily feasible, more detailed and accurate results for some geometries using the Stanford computer (e.g. rectangular, elliptical, moon shaped, concentric annular and annular sector ducts), (ii) providing more current and complete information obtained by corresponding with authors, and (iii) applying knowledge of the limiting cases of boundary conditions and of geometries.
3. The following new results are presented for fully developed laminar flow [60]:  $Nu_{H2}$  for rectangular ducts;  $fRe$ ,  $u/u_{max}$ ,  $K(\infty)$ ,  $L_{hy}^+$ ,  $Nu_{H1}$  and  $Nu_{H2}$  for isosceles triangular ducts, sine ducts and equilateral triangular ducts with rounded corners.
4. All the thermal boundary conditions analyzed for the fully developed laminar flow through straight simply connected ducts are systematically summarized in Table 1.
5. The H1 boundary condition is relatively the most simple one for the mathematical analysis. Consequently, it is the boundary condition applied to the greatest number of duct geometries. However, this boundary condition, which

Table 51. Summary index of available laminar flow solutions  
for straight and curved ducts

Geom. v	Re	$\mu_{KL}$	$\mu_T$	Hydrodynamic entry length	$\frac{\tau}{\delta}$ / $\frac{H}{\delta}$ Thermal entry length	$\frac{\tau}{\delta}$ / $\frac{H}{\delta}$ Hydro. and thermal entry length
	Straight circular duct	16	48/11	3.657	Tables 5,6 Figs. 9,10	[141,142, 157,22,161] Table 6 Figs. 12,13 14
	Parallel plates	24	140/17	7.541	Tables 10, 11a,11b	[141,176, 161] [115,80]
	Rectangular ducts $b/a \sim 0 - 1$	Table 15 Fig. 19	Table 13 Fig. 20	Table 13 [86,220] Fig. 20	Tables 17, 18,19 Fig. 23	Tables 20,21 Fig. 24
	Isosceles tri- angular ducts $\beta = 0 - 180^\circ$	Table 23 Fig. 27	Table 23 Fig. 28	Table 23 [78,86] Fig. 28	Partially [78,86]	$2\phi=60^\circ$ only Table 26 Fig. 31 $2\phi=60^\circ$ only Table 26 Fig. 31
	Right triangular duct $\beta = 0 - 180^\circ$	Table 28 Fig. 34	Table 28 Fig. 34	$\phi = 45^\circ$ only	none	$\phi=45^\circ$ only Table 29 Fig. 35 $\phi=45^\circ$ only Table 29 Fig. 35
	n-sided regular polygonal ducts $n = 3 - \infty$	Table 32 Fig. 42	Table 32 Fig. 42	$n=3,4,\infty$ only see above	$n=3,4,\infty$ only see above	$n=3,4,\infty$ only see above
	Elliptical ducts $b/a \sim 0 - 1$	Table 33 Fig. 44	Table 33 Fig. 45	Table 33 Fig. 45	none	[237,238] none
	Concentric annular ducts $r_i/r_o \sim 0 - 1$	Table 34 Fig. 50	Table 34 Fig. 51	Table 34 [75,76 80,87] Fig. 51	[242,243 256,257, 260]	[76]

**Table 51 (cont'd). Summary index of available laminar flow solutions for straight and curved ducts**

Geometry	$fRe$	$Nu_{Hl}$	Geometry	Velocity problem	Temperature problem
	Table 27	Table 27		[48]	none
	Table 30 Fig. 37	Table 30 Fig. 38		[39]	none
	Table 28 Fig. 40	Table 28 Fig. 40		[41]	[41]
	Table 31 Fig. 39	Table 31 Fig. 39		[42]	[42]
	Table 31 Fig. 41	Table 31 Fig. 41		[37,277]	[37]
	Table 32	none		[276]	[276]
	Table 31 Fig. 47	none		[275]	[275]
	15.675	4.208		[277]	none
	Table 38 Fig. 54	Table 39 Fig. 55		[278]	[278]
	Table 40 Fig. 56	none		Table 46 Fig. 65	Table 46 Fig. 65
	Table 41 Fig. 57	Table 42 Fig. 58		Table 47 Fig. 66	Tables 48, 49 Fig. 67
	Table 43 Fig. 59	Table 44 Fig. 60		[295,296]	none
	Table 45 Fig. 62	Table 45 Fig. 62		[302,283, 303]	none

yields the largest convection coefficient, may in fact not be the most appropriate one for the technical applications at hand.

6. The present results do not allow the prediction of Reynolds number range over which laminar flow applies. The designer is interested in knowing the specific range of Reynolds number for the laminar, transition and turbulent flow regimes for a specified duct geometry. Much work remains to be done for the transition region. The results of this report are only applicable for a "true" laminar flow.
7. The hydrodynamic and thermal entrance lengths are defined in different manners as follows in the heat transfer literature. The hydrodynamic entrance length  $L_{hy}$  is defined as the duct length required to achieve the duct centerline velocity (the maximum) as 99% of the corresponding fully developed magnitude when the entering flow is uniform. The thermal entrance length  $L_{th}$  is defined as the duct length required to achieve the value of local Nusselt number  $Nu_x$  as  $1.05 \cdot Nu_{fd}^+$ . The  $L_{hy}^+$  is presented for a majority of geometries. Hence, at a given Reynolds number, the required  $L/D_h$  to achieve hydraulically fully developed flow may be determined. The  $L_{th}$  is not determined for most of the duct geometries. For the geometries for which the thermal entrance solutions are available,  $L_{th}^*$  can be established, but this has not yet been achieved on a systematic basis.
8. The comparison of a circular tube and an elliptical duct ( $\alpha^* = 0.9$ ) revealed that both the ducts have the same area "goodness" factor. However, the elliptical duct is superior to the circular duct on the basis of the volume "goodness" factor. Thus, an elliptical passages glass ceramic matrix may be superior to a circular tube

matrix for the vehicular gas turbine regenerator of the periodic-flow type.

9. Other comparisons and areas of investigations for the gas turbine regenerator design are suggested in Section VI.6.

## VIII. RECOMMENDATIONS

Recommendations are divided into three categories:

1. extension of the present work; 2. new compilations; and
3. general comments on the presentation of future work.

### 1. Extension of the Present Work

From Chapter V summarizing the analytical solutions available for different geometries and Table 51, it appears that a large number of solutions are not available for many of the geometries of current technical interest. These are as follows.

- (i) For fully developed flow, no general method exists for the  $\textcircled{T}$  and  $\textcircled{H3}$  heat transfer through an arbitrary duct. A general method is needed.
- (ii) The thermal entry length  $L_{th}^*$  for the circular tube can be determined from the results of Table 8. The  $L_{th}^*$  for any other duct geometry has not been determined for any boundary condition. Similar to hydrodynamic entry length  $L_{hy}^+$  [Eq. (33)], approximate or exact theories are needed to evaluate  $L_{th}^*$  for an arbitrary duct with arbitrary thermal boundary conditions.
- (iii) For fully developed heat transfer, a theory is needed to determine the incremental thermal entry heat transfer number  $N(\infty)$  [see Eq. (236)] for an arbitrary duct with arbitrary thermal boundary conditions.
- (iv) Very few thermal entry length solutions (exceptions are the circular tube and parallel plates) are available for noncircular ducts. Much work is needed for the thermal entry length problem for at least  $\textcircled{T}$ ,  $\textcircled{H1}$ ,  $\textcircled{H2}$  and  $\textcircled{\Delta t}$  boundary conditions.
- (v) For the vehicular gas turbine regenerator of the periodic flow type, the matrix with rectangular, isosceles triangular, sine or hexagonal passages

has been considered for the heat transfer from hot gas to cold air. The typical material used for such a matrix is glass ceramic having low thermal conductivity. The thermal boundary condition realized for this application may approximate the  $H_3$ . Hence, as a minimum, fully developed  $H_3$  heat transfer results are urgently needed for the above geometries.

- (vi) The cusped duct geometry is technically important, as it is formed as a combined geometry in a circular tube matrix. Only the flow friction results are available for the n-sided cusped duct geometry. Heat transfer results are urgently needed for the possible use in glass ceramic matrices [see above (v)].
- (vii) Other areas of investigations for the regenerator design are suggested in Section VI.6.

## 2. New Compilations

- (i) Summary of analytical work for laminar duct flow forced convection heat transfer with variable fluid properties.
- (ii) Summary of analytical work for combined forced and free convection laminar flow heat transfer.
- (iii) Summary of experimental work related to laminar duct flow heat transfer.
- (iv) A critical comparison of the experimental results with the compilations of the above items (i), (ii), (iii) and of the present report.
- (v) Summary of transition flow regime Reynolds number range for various duct geometries, as well as, duct flow friction and heat transfer characteristics.

## 3. General Comments on Future Presentation

It is evident that research work in laminar duct flow is carried out throughout the world by many different branches of applied sciences and engineering. The results obtained

directly from all these different sources are in differing formats. The designer of laminar flow systems frequently cannot interpret the results. With the needs of the designer in mind, the following brief comments are appropriate.

- (i) A variety of new methods have been devised for fully developed and developing flow heat transfer problem. But the examples are generally worked out only for known solutions. It is recommended that after qualifying a new method with known results, that new solutions be obtained.
- (ii) There is a considerable amount of duplication of solutions for the circular tube and parallel plate ducts. Once the exact (or more accurate) solutions are available, it is recommended that further solutions to the same problem should not be carried out using the obsolete approximate methods. For example, for a circular tube, even after the thermal entry length problem has been solved employing the accurate velocity profiles (from numerical solutions), papers have continued to appear for the same problem employing the approximate velocity profiles in the entrance region.
- (iii) In many cases, a refinement is made to an already approximately solved problem; however, the final results are compared only by small scale graphs. It is recommended for the future that comparisons be presented in tabular form or alternatively, the tabular results should be forwarded to an agency from which the information can be readily available. One such agency in the USA is: ASIS National Auxiliary Publications Service, c/o CCM Information Sciences, Inc., 909 Third Avenue, New York, N.Y. 10022.

(iv) There exists a tendency to present the theoretical results in terms of a particular set of dimensionless parameters deduced from normalizing the differential equations and boundary conditions in a special way. Many different sets of dimensionless parameters can be formulated for a particular duct. Such results may not be useful to a designer, because he cannot readily interpret them in terms of the familiar conventional set. It is therefore recommended that the conventional parameters, as used in this report, should be employed in reporting new work. These are:  $\text{Nu}$ ,  $\text{Re}$ ,  $\text{Pr}$ ,  $\text{St}$ ,  $x^*$ ,  $D_h$ ,  $L_{hy}$ ,  $K_p$ .

(v) Throughout the thermal entrance heat transfer literature, the dimensionless axial distance is defined variously as  $x^*$ ,  $1/x^*$ ,  $cx^*$  (where  $c$  is a constant) etc. and these dimensionless distances are all designated as Graetz number! McAdams [29] defines the Graetz number  $Gz$  as  $Gz = \frac{Wc_p}{kL} = \frac{PeP}{4L}$  and this definition is consistently used in chemical engineering literature. To avoid the confusion of various definitions used for dimensionless axial distance, it is suggested that (i) McAdams' definition of Graetz number be accepted, (ii) the dimensionless axial distance  $x^* = x/D_h Pe$  be used for the thermal entry length problem and (iii)  $x^*$  should not be designated as the Graetz number. According to the foregoing recommendations,

$$x^* = \frac{x}{D_h Pe} = \frac{x}{4L} \frac{P}{D_h} \frac{1}{Gz} \quad (237)$$

(vi) The dimensionless total wall heat flux  $\Phi$  (Eq. 72) is inappropriately designated as a mean Nusselt number  $\text{Nu}_{m,T}$ . The "mean heat transfer coefficient" in  $\Phi$  does not represent a thermal conductance in

a thermal circuit for a heat exchanger nor does it approach the fully developed value at large  $x^*$  ( $x^* \rightarrow \infty$ ). Consequently, the dimensionless parameter should not be designated as  $Nu_{n,T}$ .

- (vii) Reviewing Fig. 4 and Eq. (11a) on p. 12, the wall conductance  $U_w$  consists of two components: wall conductance and the other side of wall fluid conductance. Hence,  $1/R_w$  [Eq. (54)] is not a Nusselt number or a Biot number and should not be identified as such. To avoid confusion, it is recommended that the terminology  $R_w$ , the wall thermal resistance, be used for the  $\textcircled{R1}$  boundary condition. The  $R_w$  has a simple physical significance of its own as described before, Eq. (54) on p. 33.

## REFERENCES

The titles of the journals are abbreviated as in the World List of Scientific Periodicals, Butterworths, London, Fourth Edition (1964).

1. T. B. Drew, Mathematical attacks on forced-convection problems: a review, Trans. Am. Inst. chem. Engrs 26, 26-80 (1931).
2. H. L Dryden, F. D. Muraghan and H. Bateman, Hydrodynamics, Committee on Hydrodynamics, Division of Physical Sciences, Bulletin 84, National Research Council, Washington, D.C., pp. 197-201 (1932), also as Dover Publication, New York (1956).
3. W. M. Rohsenow and H. Choi, Heat, Mass and Momentum Transfer, Prentice-Hall Inc., Englewood Cliffs, N. J. (1961).
4. W. M. Kays and A. L. London, Compact Heat Exchangers, 2nd Edn., McGraw-Hill, New York (1964).
5. W. M. Kays, Convective Heat and Mass Transfer, McGraw-Hill, New York (1966).
6. E.R.G. Eckert, T. F. Irvine, Jr. and J. T. Yen, Local laminar heat transfer in wedge-shaped passages, Trans. Am. Soc. mech. Engrs 80, 1433-1438 (1958).
7. W. C. Reynolds, Effect of wall heat conduction on convection in a circular tube with arbitrary circumferential heat input, Int. J. Heat Mass Transfer 6, 925 (1963).
8. R. Siegel and J. M. Savino, An analytical solution of the effect of peripheral wall conduction on laminar forced convection in rectangular channels, J. Heat Transfer 87C, 59-66 (1965).
9. T. F. Irvine, Jr., Non-circular duct convective heat transfer, Modern Developments in Heat Transfer, edited by Warren Ibele, pp. 1-17, Academic Press, New York (1963).
10. S. Hasegawa and Y. Fujita, Nusselt numbers for fully developed flow in a circular tube with exponentially varying heat flux, Mem. Fac. Engng Kyushu Univ. 27 (1), 77-80 (1967).

11. R. W. Lyczkowski, C. W. Solbrig and D. Gidaspow, Forced convective heat transfer in rectangular ducts - general case of wall resistances and peripheral conduction, Institute of Gas Technology, Tech. Info. Center, File 3229, 3424 S. State Street, Chicago, Ill. 60616 (1969).
12. W. M. Kays, Numerical solutions for laminar-flow heat transfer in circular tubes, Trans. Am. Soc. mech. Engrs 77, 1265-1274 (1955).
13. J. R. Sellers, M. Tribus and J. S. Klein, Heat transfer to laminar flow in a round tube or flat conduit - the Graetz problem extended, Trans. Am. Soc. mech. Engrs 78, 441-448 (1956).
14. J. W. Mitchell, An expression for internal flow heat transfer for polynomial wall temperature distribution, J. Heat Transfer 91C, 175-177 (1969).
15. R. Siegel, E. M. Sparrow and T. M. Hallman, Steady laminar heat transfer in a circular tube with prescribed wall heat flux, Appl. scient. Res. 7A, 386-392 (1958).
16. R. N. Noyes, A fully integrated solution of the problem of laminar or turbulent flow in a tube with arbitrary wall heat flux, J. Heat Transfer 83C, 96-98 (1961).
17. Z. Rotem, The effect of thermal conduction of the wall upon convection from a surface in a laminar boundary layer, Int. J. Heat Mass Transfer 10, 461-466 (1967).
18. E. J. Davis and W. N. Gill, The effects of axial conduction in the wall on heat transfer with laminar flow, Int. J. Heat Mass Transfer 13, 459-470 (1970).
19. T. S. Lundgren, E. M. Sparrow and J. B. Starr, Pressure drop due to the entrance region in ducts of arbitrary cross section, J. bas. Engng 86D, 620-626 (1964).
20. S. T. McComas, Hydrodynamic entrance lengths for ducts of arbitrary cross section, J. bas. Engng 89D, 847-850 (1967).
21. L. Schiller, Die entwicklung der laminaren geshwindigkeitsverteilung und ihre bedeutung für zähigkeitsmessungen, Z. angew. Math. Mech. 2, 96-106 (1922).
22. D. K. Hennecke, Heat transfer by Hagen-Poiseuille flow in the thermal development region with axial conduction, Wärme-und stoffübertragung 1, 177-184 (1968).

23. V. P. Tyagi, Laminar forced convection of a dissipative fluid in a channel, J. Heat Transfer 88C, 161-169 (1966).
24. V. P. Tyagi, Forced convection of a dissipative liquid in a channel with Neumann conditions, J. appl. Mech. 33, 18-24 (1966).
25. V. P. Tyagi, A general non-circular duct convective heat transfer problem for liquids and gases, Int. J. Heat Mass Transfer 9, 1321-1340 (1966).
26. V. P. Tyagi, General study of a heat transmission problem of a channel-gas flow with Neumann type thermal boundary conditions, Proc. Camb. phil. Soc. 62, 555-573 (1966).
27. K. C. Cheng, Dirichlet problems for laminar forced convection with heat sources and viscous dissipation in regular polygonal ducts, A.I.Ch.E. Jl 13, 1175-1180 (1967).
28. H. D. Baehr and E. Hicken, Neue kennzahlen und gleichungen für den wärmeübergang in laminar durchströmten kanälen, Kältetechnik - Klimatisierung 21, 34-38 (1969).
29. W. H. McAdams, Heat Transmission, 3rd Edn., p. 135. McGraw-Hill, New York (1954).
30. F. W. Schmidt and B. Zeldin, Laminar heat transfer in the entrance region of ducts, Appl. scient. Res. 23, 73-94 (1970).
- 30a. R. P. Stein, Liquid metal heat transfer, in Advances in Heat Transfer, Vol. 3, p. 146. Academic Press, New York (1966).
31. S. M. Marco and L. S. Han, Note on limiting laminar Nusselt numbers in ducts with constant temperature gradient by analogy to thin-plate theory, Trans. Am. Soc. mech. Engrs 77, 625-630 (1955).
32. K. C. Cheng, Analogy solution of laminar heat transfer in non-circular ducts by Moiré method and point-matching, J. Heat Transfer 88C, 175-182 (1966).
33. S. P. Timoshenko and J. N. Goodier, Theory of Elasticity, 3rd Edn., McGraw-Hill, New York (1970).
34. S. Timoshenko and S. Woinowsky-Krieger, Theory of Plates and Shells, 2nd Edn., McGraw-Hill, New York (1959).

35. K. C. Cheng, Laminar heat transfer in noncircular ducts by Moiré method, J. Heat Transfer 87C, 308-309 (1965).
36. L. N. Tao, On some laminar forced-convection problem, J. Heat Transfer, 83C, 466-472 (1961).
37. U. A. Sastry, Heat transfer by laminar forced convection in multiply connected cross section, Indian J. Pure appl. Phys. 3, 113-116 (1965).
38. L. N. Tao, Method of conformal mapping in forced convection problems, in International Development in Heat Transfer, part III, pp. 598-606, Am. Soc. mech. Engrs, New York (1961).
39. L. N. Tao, Heat transfer of laminar forced convection in indented pipes, in Developments in Mechanics, edited by J. E. Lay and L. E. Malvern, Vol 1, pp. 511-525, Plenum Press, New York (1961).
40. L. N. Tao, The second fundamental problem in heat transfer of laminar forced convection, J. appl. Mech. 29, 415-420 (1962).
41. U. A. Sastry, J. Sci. Engng Res. 7 (Pt. 2), 281 (1963).
42. U. A. Sastry, Solution of the heat transfer of laminar forced convection in non-circular pipes, Appl. scient. Res. 13A, 269-280 (1964).
43. M. J. Casarella, P. A. Laura, and M. Chi, On the approximate solution of flow and heat transfer through non-circular conduits with uniform wall temperature, Br. J. appl. Phys. 18, 1327-1335 (1967).
44. S. H. Clark and W. M. Kays, Laminar-flow forced convection in rectangular tubes, Trans. Am. Soc. mech. Engrs 75, 859-866 (1953).
45. F. W. Schmidt and M. E. Newell, Heat transfer in fully developed laminar flow through rectangular and isosceles triangular ducts, Int. J. Heat Mass Transfer 10, 1121-1123 (1967).
46. D. F. Sherony and C. W. Solbrig, Analytical investigation of heat or mass transfer and friction factors in a corrugated duct heat or mass exchanger, Int. J. Heat Mass Transfer 13, 145-159 (1970).
47. O. E. Dwyer and H. C. Berry, Laminar-flow heat transfer for in-line flow through unbaffled rod bundles, Nucl. Sci. Engng 42, 81-88 (1970).

48. E. M. Sparrow and A. L. Loeffler, Jr., Longitudinal laminar flow between cylinders arranged in regular array, A.I.Ch.E. Jl 5, 325-330 (1959).
49. E. M. Sparrow, A. L. Loeffler, Jr. and H. A. Hubbard, Heat transfer to longitudinal laminar flow between cylinders, J. Heat Transfer 83C, 415-422 (1961).
50. E. M. Sparrow, Laminar flow in isosceles triangular ducts, A.I.Ch.E. Jl 8, 599-604 (1962).
51. K. C. Cheng, Laminar flow and heat transfer characteristics in regular polygonal ducts, Proc. Third Int. Heat Transfer Conf., Vol. I, pp. 64-76, A.I.Ch.E., New York (1966).
52. K. C. Cheng, Laminar forced convection in regular polygonal ducts with uniform peripheral heat flux, J. Heat Transfer 91C, 156-157 (1969).
53. F. S. Shih, Laminar flow in axisymmetric conduits by a rational approach, Can. J. chem. Engng 45, 285-294 (1967).
54. K. C. Cheng and M. Jamil, Laminar flow and heat transfer in ducts of multiply connected cross sections, Am. Soc. mech. Engrs Paper No. 67-HT-6 (1967).
55. K. C. Cheng and G. J. Hwang, Laminar forced convection in eccentric annuli, A.I.Ch.E. Jl 14, 510-512 (1968).
56. K. C. Cheng and M. Jamil, Laminar flow and heat transfer in circular ducts with diametrically opposite flat sides and ducts of multiply connected cross sections, Can. J. chem. Engng 48, 333-334 (1970).
57. E. M. Sparrow and A. Haji-Sheikh, Flow and heat transfer in ducts of arbitrary shape with arbitrary thermal boundary conditions, J. Heat Transfer 88C, 351-358 (1966).
58. D. A. Ratkowsky and N. Epstein, Laminar flow in regular polygonal ducts with circular centered cores, Can. J. chem. Engng 46, 22-26 (1968).
59. S. L. Hagen and D. A. Ratkowsky, Laminar flow in cylindrical ducts having regular polygonal shaped cores, Can. J. chem. Engng 46, 387-388 (1968).
60. R. K. Shah, Laminar flow forced convection heat transfer and flow friction in straight and curved ducts -- a summary of analytical solutions, Ph.D. Thesis, Stanford Univ., Stanford, Calif., to be published.

61. E. M. Sparrow and R. Siegel, A variational method for fully developed laminar heat transfer in ducts, J. Heat Transfer 81C, 157-167 (1959).
62. S. C. Gupta, A variational principle for fully developed laminar heat transfer in uniform channels, Appl. scient. Res. 10A, 85-101 (1961).
63. W. E. Stewart, Application of reciprocal variational principles to laminar flow in uniform ducts, A.I.Ch.E. Jl 8, 425-428 (1962).
64. D. Pnueli, A computational scheme for the asymptotic Nusselt number in ducts of arbitrary cross-section, Int. J. Heat Mass Transfer 10, 1743-1748 (1967).
65. B. A. Finlayson and L. E. Scriven, On the search for variational principles, Int. J. Heat Mass Transfer 10, 799-821 (1967).
66. I. L. MacLaine-Cross, An approximate method for calculating heat transfer and pressure drop in ducts with laminar flow, J. Heat Transfer 91C, 171-173 (1969).
67. P. A. James, Forced convection heat transfer in narrow passages, Can. J. chem. Engng 48, 330-332 (1970).
68. A. H. Shapiro, R. Siegel and S. J. Kline, Friction factor in the laminar entry region of a smooth tube, Proc. 2nd U.S. National Congress of Appl. Mech. pp. 733-741, Am. Soc. mech. Engrs, New York (1954).
69. W. D. Campbell and J. C. Slattery, Flow in the entrance of a tube, J. bas. Engng 85D, 41-46 (1963).
70. V. E. Gubin and V. S. Levin, Fluid flow at the starting length of circular tube, Inzh.-fiz. Zh. 15, 98-102 (1968).
71. H. Schlichting, Laminare kanaleinlaufstromung, Z. angew. Math. Mech. 14, 368-373 (1934).
72. H. Schlichting, Boundary Layer Theory, 6th Edn., pp. 176-178, McGraw-Hill, New York (1968).
73. Atkinson and S. Goldstein, Modern Developments in Fluid Dynamics, edited by S. Goldstein, Vol 1, pp. 304-308, Oxford University Press, London (1938).

74. M. Collins and W. R. Schowalter, Laminar flow in the inlet region of a straight channel, Physics Fluids 5, 1122-1124 (1962).
75. H. L. Langhaar, Steady flow in the transition length of a straight tube, J. appl. Mech. 9, A55-A58 (1942).
76. L. S. Han, Hydrodynamic entrance lengths for incompressible flow in rectangular ducts, J. appl. Mech. 27, 403-409 (1960).
77. L. S. Han, Simultaneous development of temperature and velocity profiles in flat ducts, in International Development in Heat Transfer, part III, pp. 591-597, Am. Soc. mech. Engrs, New York (1961).
78. L. S. Han and A. L. Cooper, Approximate solutions of two internal flow problems - solution by an integral method, Proc. 4th U.S. National Congress of Appl. Mech. 2, 1269-1278 (1962).
79. E. Sugino, Velocity distribution and pressure drop in the laminar inlet of a pipe with annular space, Bull. Japan Soc. mech. Engrs 5, 651-655 (1962).
80. H. S. Heaton, W. C. Reynolds and W. M. Kays, Heat transfer in annular passages. Simultaneous development of velocity and temperature fields in laminar flow, Int. J. Heat Mass Transfer 7, 763-782 (1964). Also as Report No. AHT-5, Dept. of Mech. Engng, Stanford University, Stanford, California (1962).
81. N. A. Slezkin, Dynamics of Viscous Incompressible Fluids, (in Russian) Gostekhizdat, Moscow (1955).
82. C. C. Chang and H. Atabeck, Flow between two co-axial tubes near the entry, Z. angew. Math. Mech. 42, 425-430 (1962).
83. E. M. Sparrow, S. H. Lin and T. S. Lundgren, Flow development in the hydrodynamic entrance region of tubes and ducts, Physics Fluids 7. 338-347 (1964).
84. E. M. Sparrow and S. H. Lin, The developing laminar flow and pressure drop in the entrance region of annular ducts, J. bas. Engng 86D, 827-834 (1964).
85. C. L. Wiginton and R. L. Wendt, Flow in the entrance region of Ducts, Physics Fluids 12, 465-466 (1969).

86. D. P. Fleming and E. M. Sparrow, Flow in the hydrodynamic entrance region of ducts of arbitrary cross section, *J. Heat Transfer* 91C, 345-354 (1969).
87. J. R. Bodcia and J. F. Osterle, Finite difference analysis of plane Poiseuille and Couette flow development, *Appl. scient. Res.* 10A, 265-276 (1961).
88. R. W. Hornbeck, Laminar flow in the entrance region of a pipe, *Appl. scient. Res.* 13A, 224-232 (1964).
89. E. B. Christiansen and H. E. Lemmon, Entrance region flow, *A.I.Ch.E. Jl* 11, 995-999 (1965).
90. R. Manohar, Analysis of laminar-flow heat transfer in the entrance region of circular tubes, *Int. J. Heat Mass Transfer* 12, 15-22 (1969).
91. R. Manohar, An exact analysis of laminar flow in the entrance region of an annular pipe, *Z. angew. Math. Mech.* 45, 171-176 (1965).
92. S. R. Montgomery and P. Wibulswas, Laminar flow heat transfer for simultaneously developing velocity and temperature profiles in ducts of rectangular cross-section, *Appl. scient. Res.* 18, 247-259 (1967).
93. J. A. Miller, Laminar incompressible flow in the entrance region of ducts of arbitrary cross section, *J. Engng Pwr* 92A, 113-118 (1971).
94. J. S. Vrentas, J. L. Duda and K. G. Bargeron, Effect of axial diffusion of vorticity on flow development in circular conduits: part I numerical solutions, *A.I.Ch.E. Jl* 12, 837-844 (1966).
95. M. Friedmann, J. Gillis and N. Liron, Laminar flow in a pipe at low and moderate Reynolds numbers, *Appl. scient. Res.* 19, 426-438 (1968).
96. F. W. Schmidt and B. Zeldin, Laminar flows in inlet sections of tubes and ducts, *A.I.Ch.E. Jl* 15, 612-614 (1969).
97. Y. L. Wang and P. A. Longwell, Laminar flow in the inlet section of parallel plates, *A.I.Ch.E. Jl* 10, 325-328 (1964).
98. J. Gillis and A. Brandt, Air Force European Office of Aerospace Research Scientific Report 63-73, Rehovoth, Israel (1964).

99. M. A. Lévêque, Les lois de la transmission de chaleur par convection, Annls Mines 13, 201-299, 305-362, 381-415 (1928).
100. J. Newman, Extension of the Lévêque solution, J. Heat Transfer 91C, 177-178 (1969).
101. A. Burghardt and A. Dubis, A simplified method of determining the heat transfer coefficient in laminar flow (in Polish), Chemia stosow. Ser. B, Vol. 7 (3), 281-303 (1970).
102. E. M. Sparrow and R. Siegel, Application of variational methods to the thermal entrance region of ducts, Int. J. Heat Mass Transfer 1, 161-172 (1960).
103. L. N. Tao, Variational analyses of forced convection in a duct of arbitrary cross section, Proc. Third Int. Heat Transfer Conf., Vol. I, pp. 56-63, A.I.Ch.E., New York (1966).
104. I. N. Sadikov, Laminar heat transfer over the initial section of a rectangular channel, J. Engng Phys. 8, 287-291 (1965).
105. I. N. Sadikov, Heat transfer in the entrance regions of plane and rectangular passage (in Russian), Inzh.-fiz. Zh. 7 (9), 44-51 (1964).
106. I. N. Sadikov, Laminar heat transfer in a two-dimensional channel with a nonuniform temperature field at the entrance, J. Engng Phys. 8, 192-196 (1965).
107. U. Grigull and H. Tratz, Thermischer einlauf in ausgebildetu laminarer rohrströmung, Int. J. Heat Mass Transfer 8, 669-678 (1965).
108. S. R. Montgomery and P. Wibulswas, Laminar flow heat transfer in ducts of rectangular cross-section, Proc. Third Int. Heat Transfer Conf. Vol I, pp. 85-98 (1966).
109. R. D. Chandler, J. N. Panaia, R. B. Stevens and G. E. Zinsmeister, The solution of steady state convection problems by the fixed random walk method, J. Heat Transfer 90C, 361-363 (1968).
110. R. K. McMordie and A. F. Emery, A numerical solution for laminar-flow heat transfer in circular tubes with axial conduction and developing thermal and velocity fields, J. Heat Transfer 89C, 11-16 (1967).

- 111. D. Butterworth and T. D. Hazell, Forced convective laminar flow heat transfer in the entrance region of a tube, Proc. Fourth Int. Heat Transfer Conf., Vol II, FC 3.1, pp. 1-11, Paris-Versailles (1970).
- 112. S. Kakaç and M. R. Özgü, Analysis of laminar flow forced convection heat transfer in the entrance region of a circular pipe, Wärme-und Stoffübertragung 2, 240-245 (1969).
- 113. R. W. Hornbeck, An all-numerical method for heat transfer in the inlet of a tube, Am. Soc. mech. Engrs Paper No. 65-WA-HT-36 (1965).
- 114. E. Bender, Wärmeübergang bei ausgebildeter und nicht ausgebildeter rohrströmung mit temperaturabhängigen stoffwerten, Wärme-und Stoffübertragung 1, 159-168 (1968).
- 115. C. L. Hwang and L. T. Fan, Finite difference analysis of forced convection heat transfer in entrance region of a flat rectangular duct, Appl. scient. Res. 13A, 401-422 (1964).
- 116. P. Wibulswas, Laminar-flow heat transfer in non-circular ducts, Ph.D. Thesis, London University (1966).
- 117. L. Graetz, On the heat capacity of fluids, (in German), Annln Phys. 18, 79-94 (1883).
- 118. L. Graetz, On the heat capacity of fluids, (in German), Annln Phys. 25, 337-357 (1885).
- 119. Wilhelm Nusselt, The dependence of the heat-transfer coefficient on tube length, (in German), Z. Ver. dt. Ing. 54, 1154-1158 (1910).
- 120. V. S. Pahor and J. Strand, Die Nusseltsche zahl für laminare strömung im zylinderischen rohr mit konstanter wandtemperatur, Z. angew. Math. Phys. 7, 536-538 (1956).
- 121. D. A. Labuntsov, Heat emission in pipes during laminar flow of a liquid with axial heat conduction taken account, Soviet Phys. Dokl. 3, 33-35 (1958).
- 122. R. L. Ash and J. H. Heinbockel, Note on heat transfer in laminar, fully developed pipe flow with axial conduction, Z. angew. Math. Phys. 21, 266-269 (1970).
- 123. R. L. Ash, Private communication, Old Dominion University, Norfolk, Virginia (July 1971).

124. H. Glaser, Heat transfer and pressure drop in heat exchangers with laminar flow, MAP Voelkenrode, Reference: MAP-VG-96-818T (March 1947).
125. J. M. Madejski, Temperature distribution in channel flow with friction, Int. J. Heat Mass Transfer 6, 49-51 (1963).
126. W. C. Reynolds, Heat transfer to fully developed laminar flow in a circular tube with arbitrary circumferential heat flux, J. Heat Transfer 82C, 103-112 (1960).
127. W. B. Hall, J. D. Jackson, and P. H. Price, Note on forced convection in a pipe having heat flux which varies exponentially along its length, J. mech. Engng Sci. 5, 48-52 (1963).
128. H. Graber, Heat transfer in smooth tubes, between parallel plates, in annuli and tube bundles with exponential heat flux distribution in forced laminar or turbulent flow, (in German), Int. J. Heat Mass Transfer 13, 1645-1703 (1970).
129. W. B. Hall and P. H. Price, The effect of a longitudinally varying wall heat flux on the heat transfer coefficient for turbulent flow in a pipe, Proc. Int. Dev. Heat Transfer, Boulder, Colorado, 607-613 (1961).
130. Trevor Dury, The development of a smooth circular tube test section with variable heat flux distribution for experiments on the forced convection cooling of supercritical pressure carbon dioxide, M.S. Thesis, Victoria University of Manchester, (May 1970).
131. S. Sideman, D. Luss and R. E. Peck, Heat transfer in laminar flow in circular and flat conduits with (constant) surface resistance, Appl. scient. Res. 14A, 157-171 (1964).
132. C. J. Hsu, Exact solution to entry region laminar heat transfer with axial conduction and the boundary condition of the third kind, Chem. Engng Sci. 23, 457-468 (1968).
133. H. L. Toor, The energy equation for viscous flow, Ind. Engng Chem. 48, 922-926 (1956).
134. J. C. Chen, Laminar heat transfer in tube with nonlinear radiant heat flux boundary condition, Int. J. Heat Mass Transfer 9, 433-440 (1966).

135. Ya. S. Kadaner, Yu. P. Rassadkin and E. L. Spector, Heat transfer for laminar liquid flow in tube with radiational heat removal, Inzh.-iz. Zh. 20, 31-37 (1971).
136. J. Boussinesq, Hydrodynamique, Comptes Rendus 110, 1160-1238 (1890); 113, 9-15, 49-51 (1891).
137. R. Manohar, Private communication, Dept. of Math., Univ. of Saskatchewan, Saskatoon, Saskatchewan, Canada (1970).
138. F. W. Schmidt, Private communication, Mech. Engng Dept., Pennsylvania State Univ., University Park, Pa. (1971).
139. M. Abramowitz, On solution of differential equation occurring in problem of heat convection laminar flow in tube, J. Math. Phys. 32, 184-187 (1953).
140. R. P. Lipkis, Heat transfer to an incompressible fluid in laminar motion, M.Sc. Thesis, Univ. of California, Los Angeles (1954).
141. G. M. Brown, Heat or mass transfer in a fluid in laminar flow in a circular or flat conduit, A.I.Ch.E. Jl 6, 179-183 (1960).
142. B. K. Larkin, Higher-order eigenfunctions of the Graetz problem, A.I.Ch.E. Jl 7, 530 (1961).
143. O. Kuga, Laminar and turbulent heat transfer of liquid metal in a circular tube with non-isothermal surface (in English), Proc. 1967 semi-International Symposium, Heat Transfer Vol II, 155-159, Japan Soc. mech. Engrs (1968).
144. E. Hicken, Der einfluss einer über dem querschnitt unterschiedlichen anfangstemperatur auf den wärmeübergang in laminar durchströmten röhren, Wärme-und Stoffübertragung 1, 220-224 (1968).
145. B. C. Lyche and R. B. Bird, The Graetz-Nusselt problem for a power-law non-Newtonian fluid, Chem. Engng Sci. 6, 35-41 (1956).
146. I. R. Whiteman and W. B. Drake, Heat transfer to flow in a round tube with arbitrary velocity distribution, Trans. Am. Soc. mech. Engrs 80, 728-732 (1958).
147. H. Barrow and J. F. Humphreys, The effect of velocity distribution on forced convection laminar flow heat transfer in a pipe at constant wall temperature, Wärme- und Stoffübertragung 3, 227-231 (1970).

148. L. Topper, Forced heat convection in cylindrical channels: Some problems involving potential and parabolic velocity distribution, Chem. Engng Sci. 5, 13-19 (1956).
149. H. L. Toor, Heat transfer in forced convection with internal heat generation, A.I.Ch.E. Jl 4, 319-323 (1958).
150. S. N. Singh, Heat transfer by laminar flow in a cylindrical tube, Appl. scient. Res. 7A, 325-340 (1958).
151. B. S. Petukhov and F. F. Tsvetkov, Calculation of heat transfer during laminar flow of a fluid in pipes within a range of small Péclet numbers (in Russian), Inzh.-fiz. Zh. 4, 10-17 (1961); also translation No. FTD TT-61-321 (January 29, 1962).
152. V. V. Shapovalov, Heat transfer during the flow of an incompressible fluid in a circular tube, allowing for axial heat flow, with boundary conditions of the first and second kind at the tube surface, J. Engng Phys. 11, 153-155 (1966).
153. T. Bes, Convection and heat conduction in a laminar fluid flow in a duct (in English), Bull. Acad. pol. Sci. Sér. Sci. tech. 16 (1), 41-51 (1968).
154. A. S. Jones, Extensions to the solution of the Graetz problem, Int. J. Heat Mass Transfer 14, 619-623 (1971).
155. O. Kuga, Laminar flow heat transfer in circular tubes with non-isothermal surfaces (in Japanese), Tran. Japan Soc. mech. Engrs 31 (222), 295-298 (1965).
156. V. V. Shapovalov, Heat transfer in laminar flow of incompressible liquid in a tube, Inzh.-fiz. Zh. 12, 672-674 (1967).
157. C. J. Hsu, Heat transfer in a round tube with sinusoidal wall heat flux distribution, A.I.Ch.E. Jl 11, 690-695 (1965).
158. E. M. Sparrow and R. Siegel, Laminar tube flow with arbitrary internal heat sources and wall heat transfer, Nucl. Sci. Engng 4, 239-254 (1958).
159. R. M. Inman, Experimental study of temperature distribution in laminar tube flow of a fluid with internal heat generation, Int. J. Heat Mass Transfer 5, 1053-1058 (1962).

160. C. J. Hsu, An exact mathematical solution for entrance region laminar heat transfer with axial conduction, *Appl. scient. Res.* 17, 359-376 (1967).
161. C. J. Hsu, An exact analysis of low Péclét number thermal entry region heat transfer in transversely nonuniform velocity fields, *A.I.Ch.E. J.* 17, 732-740 (1971).
162. V. V. Shapovalov, Heat transfer in laminar flow of incompressible liquid in a tube (in Russian), *Inzh.-fiz. Zh.* 12, 672-674 (1967).
163. O. Kuga, Heat transfer in a pipe with non-uniform heat flux (in Japanese), *Trans. Japan Soc. mech. Engrs* 32 (233), 83-87 (1966).
164. T. K. Bhattacharyya and D. N. Roy, Laminar heat transfer in a round tube with variable circumferential or arbitrary wall heat flux, *Int. J. Heat Mass Transfer* 13, 1057-1060 (1970).
165. J. Schenk and J. M. DuMoré, Heat transfer in laminar flow through cylindrical tubes, *Appl. scient. Res.* 4A, 39-51 (1954).
166. E. M. Rosen and E. J. Scott, The Lévêque solution with a finite wall resistance, *J. Heat Transfer* 83C, 98-100 (1961).
167. A. A. McKillop, J. C. Harper and H. J. Bader, Heat transfer in entrance-region flow with external resistance, *Int. J. Heat Mass Transfer* 14, 863-866 (1971).
168. I. Benicio, V. Dussan and T. F. Irvine, Jr., Laminar heat transfer in a round tube with radiating heat flux at the outer wall, *Proc. Third Int. Heat Transfer Conf.* Vol. V, pp. 184-189 (1966).
169. S. Sikka and M. Iqbal, Laminar heat transfer in a circular tube under solar radiation in space, *Int. J. Heat Mass Transfer* 13, 975-983 (1970).
170. P. Goldberg, M.S. Thesis, Mech. Engng Dept., M.I.T., Cambridge, Mass. (Jan. 1958).
171. C. Tien and R. A. Pawelek, Laminar flow heat transfer in the entrance region of circular tubes, *Appl. scient. Res.* 13A, 317-331 (1964).

172. B. S. Petukhov and Chzhan Chzhen-Yun, Heat transfer in the hydrodynamic inlet region of a round tube with laminar flow, Proc. Second All Soviet Union Conf. on Heat and Mass Transfer, Vol. 1 (May 1964).
173. D. N. Roy, Laminar heat transfer in the inlet of a uniformly heated tube, J. Heat Transfer 87C, 425-426 (1965).
174. D. L. Ulrichson and R. A. Schmitz, Laminar flow heat transfer in the entrance region of circular tubes, Int. J. Heat Mass Transfer 8, 253-258 (1965).
175. B. Zeldin and F. W. Schmidt, Developing flow with combined forced-free convection in an isothermal vertical tube, Am. Soc. mech. Engrs Paper No. 71-HT-6.
176. P. A. McCuen, W. M. Kays and W. C. Reynolds, Heat transfer with laminar and turbulent flow between parallel planes with constant and variable wall temperature and heat flux, Report No. AHT-3, Dept. of Mech. Engng, Stanford University, Stanford, Calif. (1962).
177. W. Nusselt, Der wärmeaustausch am berieselungskühler, Z. Ver. dt. Ing. 67, 206-210 (1923).
178. R. H. Norris and D. D. Streid, Laminar-flow heat transfer coefficients for ducts, Trans. Am. Soc. mech. Engrs 62, 525-533 (1940).
179. H. Hahnemann and L. Ghert, Wärme-und Kältetech 44, 167 (1942).
180. S. Pahor and J. Strand, A note on heat transfer in laminar flow through a gap, Appl. scient. Res. 10A, 81-84 (1961).
181. J. R. Bodoia, The finite difference analysis of confined viscous flows, Ph.D. Thesis, Carnegie Inst. Technol. (1959).
182. H.F.P. Purday, Streamline Flow, Constable and Co. Ltd, London, p. 146 (1949).
183. J. A. Prins, J. Mulder and J. Schenk, Heat transfer in laminar flow between parallel planes, Appl. scient. Res. 2A, 431-438 (1951).

184. C. S. Yih and J. E. Cermak, Laminar heat convection in pipes and ducts, Civil Engng Dept., Colorado Agricultural and Mechanical College, Fort Collins, Colorado, Report No. 5 ONR Contract No. N90nr-82401, NR 063-071/1-19-49 (Sept. 1951).
185. V.V.G. Krishnamurty and C. Venkata Rao, Heat transfer in non-circular conduits: Part II - Laminar forced convection in slits, Indian J. Technol. 5, 166-167 (1967).
186. M. V. Bodnarescu, Beitrag zur theorie des wärmeübergangs in laminarer strömung, ForschHft. Ver. dt. Ing. 450, Vol. 21, pp. 19-27 (1955).
187. H. C. Agrawal, Heat transfer in laminar flow between parallel plates at small Péclét numbers, Appl. scient. Res. 9A, 177-189 (1960).
188. E. M. Sparrow, J. L. Novotny and S. H. Lin, Laminar flow of a heat-generating fluid in a parallel-plate channel, A.I.Ch.E. Jl 9, 797-804 (1963).
189. J. Klein and M. Tribus, Forced convection from non-isothermal surfaces, Am. Soc. mech. Engrs Paper No. 53-SA-46 (1953).
190. J. Schenk and H. L. Beckers, Heat transfer in laminar flow between parallel plates, Appl. scient. Res. 4A, 405-413 (1954).
191. R. D. Cess and E. C. Shaffer, Summary of laminar heat transfer between parallel plates with unsymmetrical wall temperatures, J. Aerosp/Space Sci. 26, 538 (1959).
192. A. P. Hatton and J. S. Turton, Heat transfer in the thermal entry length with laminar flow between parallel walls at unequal temperatures, Int. J. Heat Mass Transfer 5, 673-680 (1962).
193. R. D. Cess and E. C. Shaffer, Heat transfer to laminar flow between parallel plates with a prescribed wall heat flux, Appl. scient. Res. 8A, 329-344 (1958).
194. R. D. Cess and E. C. Shaffer, Laminar heat transfer between parallel plates with an unsymmetrically prescribed heat flux at the walls, Appl. scient. Res. 9A, 64-70 (1960).
195. J.A.W. van der Does de Bye and J. Schenk, Heat transfer in laminar flow between parallel plates, Appl. scient. Res. 3A, 308-316 (1952).

196. V. J. Berry, Non-uniform heat transfer to fluids flowing in conduits, *Appl. scient. Res.* 4A, 61-75 (1953).
197. J. Schenk, Heat loss of fluids flowing through conduits, *Appl. scient. Res.* 4A, 222-224 (1953).
198. J. Schenk and H. L. Beckers, Heat transfer in laminar flow between parallel plates, *Appl. scient. Res.* 4A, 405-413 (1954).
199. R. M. Butler and A. C. Plewes, Evaporation of solids into laminar air streams, *Chem. Engng Prog. Symp. Ser.* 10, Vol. 50, 121-127 (1954).
200. J. Schenk, A problem of heat transfer in laminar flow between parallel plates, *Appl. scient. Res.* 5A, 241-244 (1955).
201. S.C.R. Dennis and G. Poots, An approximate treatment of forced convection in laminar flow between parallel plates, *Appl. scient. Res.* 5A, 453-457 (1956).
202. E. M. Sparrow, Analysis of laminar forced-convection heat transfer in entrance region of flat rectangular ducts, NACA TN 3331 (Jan. 1955).
203. N. A. Slezkin, Flow of a viscous heat-conducting gas in a pipe, *J. Appl. Math. Mech.* 23, 473-489 (1959).
204. K. Murakawa, Theoretical solutions of heat transfer in the hydrodynamic entrance length of double pipes, *Bull. J.S.M.E.* 3 (11), 340-345 (1960).
205. K. Stephan, Wärmeübergang und druckabfall bei nicht ausgebildeter laminarströmung in rohren und in ebenen spalten, *Chemie-Ingr-Tech.* 31, 773-778 (1959).
206. W. E. Mercer, W. M. Pearce and J. E. Hitchcock, Laminar forced convection in the entrance region between parallel flat plates, *J. Heat Transfer* 89C, 251-257 (1967).
207. J. A. Miller and D. D. Lundberg, Laminar convective heat transfer in the entrance region bounded by parallel flat plates at constant temperature, *Am. Soc. mech. Engrs Paper No. 67-HT-48* (1967).
208. R. Siegel and E. M. Sparrow, Simultaneous development of velocity and temperature distributions in a flat duct with uniform wall heating, *A.I.Ch.E. Jl* 5, 73-75 (1959).

209. J. A. Miller, Discussion of Ref. [77], Int. Dev. in Heat Transfer, Part VI, (1961).
210. D. B. Holmes and J. R. Vermeulen, Velocity profiles in ducts with rectangular cross sections, Chem. Engng Sci. 23, 717-722 (1968).
211. J. B. Miles and J. Shih, Reconsideration of Nusselt number for laminar fully developed flow in rectangular ducts, an unpublished paper, Mech. Engng Dept., Univ. of Missouri, Columbia, Missouri (1967).
212. N. P. Ikryannikov, Temperature distribution in laminar flow of an incompressible fluid in a rectangular channel allowing for energy dissipation, J. Engng Phys. 10, 180-182 (1965).
213. J. M. Savino and R. Siegel, Laminar forced convection in rectangular channels with unequal heat addition on adjacent sides, Int. J. Heat Mass Transfer 7, 733-741 (1964).
214. H. M. Cheng, Analytical investigation of fully developed laminar-flow forced convection heat transfer in rectangular ducts with uniform heat flux, M.S. Thesis, Mech. Engng Dept., M.I.T. (September 1957).
215. N. P. Ikryannikov, Temperature distribution in a laminar incompressible fluid flow in a rectangular channel at boundary conditions of the second kind (in Russian), Inzn.-fiz. Zh. 16, 30-37 (1969).
216. L. S. Han, Laminar heat transfer in rectangular channels, J. Heat Transfer 81C, 121-128 (1959).
217. J. M. Savino and R. Siegel, Extension of an analysis of peripheral wall conduction effects for laminar forced convection in thin-walled rectangular channels, NASA TN D-2860 (1965).
218. E. M. Sparrow, C. W. Hixon and G. Shavit, Experiments on laminar flow development in rectangular ducts, J. bas. Engng 89D, 116-124 (1967).
219. R. J. Goldstein and D. K. Kreid, Measurement of laminar flow development in a square duct using a Laser-Doppler flowmeter, J. appl. Mech. 34, 813-818 (1967).
220. C. L. Wiginton and C. Dalton, Incompressible laminar flow in the entrance region of a rectangular duct, J. appl. Mech. 37, 854-856 (1970).

221. G. S. Beavers, E. M. Sparrow and R. A. Magnuson, Experiments on hydrodynamically developing flow in rectangular ducts of arbitrary aspect ratio, Int. J. Heat Mass Transfer 13, 689-702 (1970).
222. S.C.R. Dennis, A. McD. Mercer and G. Poots, Forced heat convection in laminar flow through rectangular ducts, Q. appl. Math. 17, 285-297 (1959).
223. R. W. Lyczkowski, Discussion of Ref. [108], Proc. Third Int. Heat Transfer Conf. Vol VI, pp. 73-74 (1967).
224. V.V.G. Krishnamurty and N. V. Sambasiva Rao, Heat transfer in non-circular conduits: Part IV - Laminar forced convection in rectangular channels, Indian J. Technol. 5, 331-333 (1967).
225. J. R. DeWitt and W. T. Snyder, Thermal entrance region heat transfer for rectangular ducts of various aspect ratios and Péclét numbers, AD693564, Clearinghouse for Federal Scientific and Technical Information, Springfield, Virginia 22151 (Sept. 1969).
226. E. Hicken, Das temperaturfeld in laminar durchströmten kanälen mit rechteck-querschnitt bei unterschiedlicher beheizung der kanalwände, Wärme-und Stoffübertragung 1, 98-10<sup>4</sup> (1968).
227. E. Hicken, Wärmeübergang bei ausgebildeter laminarer kanalströmung für am umfang veränderliche rand beidringungen, Diss. Techn. Hochsch. Braunschweig (1966).
228. S. S. Kutateladze, Fundamentals of Heat Transfer, Academic Press, New York (1963).
229. H. C. Nuttall, Torsion of uniform rods with particular reference to rods of triangular cross section, J. appl. Mech. 19, 554-557 (1952).
230. E. M. Sparrow and A. Haji-Sheikh, Laminar heat transfer and pressure drop in isosceles triangular, right-triangular and circular sector ducts, J. Heat Transfer 87C, 426-427 (1965).
231. V.V.G. Krishnamurty, Heat transfer in non-circular conduits: Part III - Laminar forced convection in equilateral triangular ducts, Indian J. Technol. 5, 167-168 (1967).
232. B. D. Aggrawala and M. Iqbal, On limiting Nusselt numbers from membrane analogy for combined free and forced convection through vertical ducts, Int. J. Heat Mass Transfer 12, 737-748 (1969).

- 13. E.R.G. Eckert and T. F. Irvine, Jr., Flow in corners of passages with noncircular cross sections, Trans. Am. Soc. mech. Engrs 78, 709-716 (1956).
- 134. A. Haji-Sheikh, Private communication, Dept. Mech. Engng, Univ. of Texas at Arlington, Arlington, Texas, U.S.A. (1970).
- 135. M. Jamil, Laminar forced convection in noncircular ducts, M.Sc. Thesis, Mech. Engng Dept., Univ. of Alberta, Edmonton, Alberta, Canada (1967).
- 136. C. J. Hsu, Laminar heat transfer in a hexagonal channel with internal heat generation and unequally heated sides, Juel. Sci. Engng 16, 305-318 (1966).
- 137. N. T. Dunwoody, Thermal results for forced heat convection through elliptical ducts, J. appl. Mech. 29, 165-170 (1962).
- 138. J. Schenk and B. S. Han, Heat transfer from laminar flow in ducts with elliptical cross-sections, Appl. scient. Res. 17, 96-114 (1967).
- 139. S. Someswara Rao, N. Ch. Pattabhi Ramacharyulu and V.V.G. Krishnamurty, Laminar forced convection in elliptical ducts, Appl. scient. Res. 21, 185-193 (1969).
- 140. W. C. Reynolds, R. E. Lundberg and P. A. McCuen, Heat transfer in annular passages. General formulation of the problem for arbitrarily prescribed wall temperatures or heat fluxes, Int. J. Heat Mass Transfer 6, 483-493 (1963).
- 141. H. Lamb, Hydrodynamics, 6th Edn., Dover Publications New York (1952).
- 142. R. E. Lundberg, W. C. Reynolds and W. M. Kays, Heat transfer with laminar flow in concentric annuli with constant and variable wall temperature and heat flux, NASA TN D-1972, Washington, D.C.; also as Report No. AHT-2, Dept. Mech. Engng, Stanford Univ., Stanford, Calif. (1961).
- 143. R. E. Lundberg, P. A. McCuen and W. C. Reynolds, Heat transfer in annular passages. Hydrodynamically developed laminar flow with arbitrarily prescribed wall temperatures or heat fluxes, Int. J. Heat Mass Transfer 6, 495-529 (1963).
- 144. M. Jacob and K. A. Rees, Heat transfer to a fluid in laminar flow through an annular space, Trans. Am. Inst. chem. Engrs 37, 619-648 (1941).

245. E. S. Davis, Heat transfer and pressure drop in annuli, Trans. Am. Soc. mech. Engrs 65, 755-760 (1943).
246. C. Y. Chen, G. A. Hawkins and H. L. Solberg, Heat transfer in annuli, Trans. Am. Soc. mech. Engrs 68, 99-106 (1946).
247. K. Murakawa, Analysis of temperature distribution of nonisothermal laminar flow of pipes with annular space, Trans. Japan Soc. mech. Engrs 18 (67), p. 43 (1952).
248. K. Murakawa, Heat transmission in laminar flow through pipes with annular space, Trans. Japan Soc. mech. Engrs 88 (19), p. 15 (1953).
249. O. E. Dwyer, On the transfer of heat to fluids flowing through pipes, annuli and parallel plates, Nucl. Sci. Engng 17, 336-344 (1963).
250. O. E. Dwyer, Bilateral heat transfer in annuli for slug and laminar flows, Nucl. Sci. Engng 19, 48-57 (1964).
251. L. I. Urbanovich, Temperature distribution and heat transfer in a laminar incompressible flow in an annular channel with the account for energy dissipation (in Russian), Inzh.-fiz. Zh. 14, 740-742 (1968).
252. L. I. Urbanovich, Heat transfer in laminar incompressible liquid flow in an annulus with asymmetric boundary conditions of the second kind relatively to the axis (in Russian), Inzh.-fiz. Zh. 15, 326-328 (1968).
253. K. Murakawa, Heat transfer in entry length of double pipes, Int. J. Heat Mass Transfer 2, 240-251 (1961).
254. C. Venkata Rao, C. Syamala Rao and V.V.G. Krishnamirty, Heat transfer in non-circular conduits: Part I - Laminar forced convection in annuli, Indian J. Technol. 5, 164-166 (1967).
255. R. Viskanta, Heat transfer with laminar flow in concentric annuli with constant and arbitrary variable axial wall temperature, Argonne National Lab., Report 6441 (1961).
256. R. Viskanta, Heat transfer with laminar flow in a concentric annulus with prescribed wall temperatures, Appl. Scient. Res. 12A, 463-476 (1964).
257. A. P. Hatton and A. Quarmby, Heat transfer in the thermal entry length with laminar flow in an annulus, Int. J. Heat Mass Transfer 5, 973-980 (1962).

268. P. M. Worsøe-Schmidt, Heat transfer in the thermal entrance region of circular tubes and annular passages with fully developed laminar flow, Int. J. Heat Mass Transfer 10, 541-551 (1967).
269. R. J. Nunge, E. W. Porta and R. Bentley, A correlation of local Nusselt numbers for laminar flow heat transfer in annuli, Int. J. Heat Mass Transfer 13, 927-933 (1970).
270. C. J. Hsu, Theoretical solutions for low Péclét number thermal entry region heat transfer in laminar flow through concentric annuli, Int. J. Heat Mass Transfer 13, 1907-1924 (1970).
271. C. J. Hsu and C. J. Hwang, Heat or mass transfer in laminar flow through a concentric annulus with convective flux at walls, Chem. Engng Sci. 21, 209-221 (1966).
272. A. Caldwell, J. Royal Tech. College (Glasgow) 2, p. 203 (1931).
273. N.A.V. Piercy, M. S. Hooper and H. F. Winny, Viscous flow through pipes with cores, Phil. Mag. Ser. 7, Vol. 15, 647-676 (1933).
274. J. F. Heyda, A Green's function solution for the case of laminar incompressible flow between non-concentric circular cylinders, J. Franklin Inst. 267, 25-34 (1959).
275. P. J. Redberger and M. E. Charles, Axial laminar flow in a circular pipe containing a fixed eccentric core, Can. J. chem. Engng 40, 148-151 (1962).
276. W. T. Snyder and G. A. Goldstein, An analysis of fully developed laminar flow in an eccentric annulus, A.I.Ch.E. Jl 11, 462-467 (1965).
277. V. K. Jonsson and E. M. Sparrow, Results of laminar flow analysis and turbulent flow experiments for eccentric annular ducts, A.I.Ch.E. Jl 11, 1143-1145 (1965).
278. V. K. Jonsson, Experimental studies of turbulent flow phenomena in eccentric annuli, Ph.D. Thesis, Univ. Minnesota, Minneapolis (1965).
279. D. E. Bourne, O. Figueiredo and M. E. Charles, Laminar and turbulent flow in annuli of unit eccentricity, Can. J. chem. Engng 46, 289-293 (1968).

270. E. M. Sparrow, T. S. Chen and V. K. Jonsson, Laminar flow and pressure drop in internally finned annular ducts, Int. J. Heat Mass Transfer 7, 583-585 (1964).
271. D. A. Ratkowsky, Private communication, Senior Research Scientist, Tasmanian Regional Laboratory, CSIRO, Stowell Avenue, Hobart, Tasmania, Australia 7000 (1970).
272. R. A. Axford, Two-dimensional, multiregion analysis of temperature fields in reactor tube bundles, Nucl. Engng & Des. 6, 25-42 (1967).
273. A. A. Sholokhov, N. I. Buleev, Yu. I. Cribanov and V. E. Minashin, Longitudinal laminar fluid flow in a bundle of rods (in Russian), Inzh.-fiz. Zh. 14, 389-394 (1968).
274. D. J. Gunn and C.W.W. Darling, Fluid flow and energy losses in non-circular conduits, Trans. Instn chem. Engrs 41, 163-173 (1963).
275. U. A. Sastry, Heat transfer of laminar forced convection in doubly connected region, Indian J. Pure app. Phys. 2 (7), 213-215 (1964).
276. U. A. Sastry, Heat transfer by laminar forced convection in multiply connected regions, Acta Technica (Budapest) 51, 181-192 (1965).
277. U. A. Sastry, Viscous flow through tubes of doubly connected regions, Indian J. Pure appl. Phys. 3 (7), 230-232 (1965).
278. L. C. Kun, Friction factor and limiting Nusselt numbers for laminar flow in internally finned tubes by means of Green's function, Ph.D. Thesis, State Univ. of New York at Buffalo, New York (Sept. 1970).
279. W. R. Dean, Note on the motion of fluid in a curved pipe, Phil. Mag. Ser. 7, Vol. 4, pp. 208-223 (1927).
280. K. C. Cheng and M. Akiyama, Laminar forced convection heat transfer in curved rectangular channels, Int. J. Heat Mass Transfer 13, 471-490 (1970).
281. M. Akiyama, Laminar forced convection heat transfer in curved rectangular channels, M.Sc. Thesis, Mech. Engng Dept., Univ. of Alberta, Edmonton, Alberta, Canada (1969).

282. W. R. Dean, The stream-line motion of fluid in a curved pipe, Phil. Mag. Ser. 7, Vol. 4, pp. 673-695 (1928).
283. H. C. Topakoğlu, Steady laminar flows of an incompressible viscous fluid in curved pipes, J. Math. Mech. 16, 1321-1338 (1967).
284. C. M. White, Streamline flow through curved pipes, Proc. R. Soc. Ser. A, Vol. 123, pp. 645-663 (1929).
285. M. Adler, Strömung in gekrümmten röhren, Z. angew. Math. Mech. 14, 257-275 (1934).
286. S. N. Barua, On secondary flow in stationary curved pipes, Q. J. Mech. appl. Math. 16, 16-77 (1963).
287. H. Itō, Laminar flow in curved pipes, Z. angew. Math. Mech. 49 (11), 653-663 (1969), also in The Reports of the Institute of High Speed Mechanics, Tohoku University, Sendai, Japan, Vol. 22, 161-180 (1970).
288. M. Akiyama and K. C. Cheng, Boundary vorticity method for laminar forced convection heat transfer in curved pipes, Int. J. Heat Mass Transfer 14, 1659-1675, (1971).
289. H. Itō, Friction factors for turbulent flow in curved pipes, J. bas. Engng. 81D, 123-134 (1959).
290. R. A. Seban and E. F. McLaughlin, Heat transfer in tube coils with laminar and turbulent flow, Int. J. Heat Mass Transfer 6, 387-395 (1963).
291. V. Kubair and N. R. Kuloor, Heat transfer to Newtonian fluids in coiled pipes in laminar flow, Int. J. Heat Mass Transfer 9, 63-75 (1966).
292. Y. Mori and W. Nakayama, Study on forced convective heat transfer in curved pipes (1st report, Laminar region), Int. J. Heat Mass Transfer 8, 67-82 (1965).
293. Y. Mori and W. Nakayama, Study on forced convective heat transfer in curved pipes (third report, Theoretical analysis under the condition of uniform wall temperature and practical formulae), Int. J. Heat Mass Transfer 10, 681-695 (1967).
294. M. N. Özişik and H. C. Topakoğlu, Heat transfer for laminar flow in a curved pipe, J. Heat Transf. 90C, 313-318 (1968).

295. H. Ito, Theory on laminar flows through curved pipes of elliptic and rectangular cross sections, The Reports of the Institute of High Speed Mechanics, Tohoku University, Sendai, Japan, Vol. 1, 1-16 (1951).
296. H. G. Cuming, The secondary flow in curved pipes, Aeronautical Research Council, Reports and Memoranda, No. 2880 (1952).
297. W. R. Dean and J. M. Hurst, Note on the motion of fluid in a curved pipe, Mathematika 6, 77-85 (1959).
298. Y. Mori and Y. Uchida, Study on forced convective heat transfer in curved square channel (1st report, Theory of laminar region), Trans. Japan Soc. mech. Engrs 33, 1836-1846 (1967).
299. H. P. Eichenberger, Secondary flow within a bend, J. Math. Phys. 32, 34-42 (1953).
300. B. P. Ustimenko, K. A. Zhurgembauer and D. A. Nusupbekova, Calculation of convective heat transfer for an incompressible liquid in complex-configuration channels, Proc. Second All-Soviet Union Conf. Heat Mass Transfer 1, 124-143 (1966).
301. Y. Mori and Y. Uchida, Forced convective heat transfer in curved channels, Proc. 1967 Semi-Int. Symp., Heat Transfer Vol. I, pp. 181-190, Japan Soc. mech. Engrs, (1968).
302. J. N. Kapur, V. P. Tyagi and R. C. Srivastava, Streamline flow through a curved annulus, Appl. scient. Res. 14A, 253-267 (1964).
303. R. S. Srivastava, On the motion of fluid in a curved annulus, Z. angew. Math. Phys. 21, 490-493 (1970).
304. A. L. London, M.B.O. Young and J. H. Stang, Glass ceramic surfaces, straight triangular passages--heat transfer and flow friction characteristics, J. Engng Pwr 92A, 381-389 (1970).
305. P. F. Pucci, C. P. Howard and C. H. Fiersall, Jr., The single-blow transient testing technique for compact heat exchanger surfaces, J. Engng Pwr 89A, 29-40 (1967).
306. A. J. Wheeler, Single-blow transient testing of matrix-type heat exchanger surfaces at low values of  $Ntu$ , TR No. 68, Dept. Mech. Engng, Stanford Univ., Stanford Calif. (1968).

307. J. H. Stang and J. E. Bush, The periodic technique  
for testing compact heat exchanger surfaces, TR No.  
67, Dept. Mech. Engng, Stanford Univ., Stanford, Calif.  
(1968).
308. J. H. Stang, Some contributions to the techniques for  
testing compact heat exchanger surfaces, TR No. 74,  
Dept. Mech. Engng, Stanford Univ., Stanford, Calif.  
(1970).
309. A. L. London, Laminar flow gas turbine regenerators --  
the influence of manufacturing tolerances, J. Engng  
Pwr 92A, 46-56 (1970).

## APPENDIX A

Following is a partial listing of technical journals in which laminar flow heat transfer literature has been located.

1. American Institute of Chemical Engineers Journal (USA)
2. Annalen der Physik (Germany)
3. Annales des mines (France)
4. Applied Scientific Research (Netherlands)
5. British Journal of Applied Physics (UK)
6. Bulletin de l'Academie polonaise des sciences, série des sciences techniques (Poland)
7. Bulletin. Japan Society of Mechanical Engineers (Japan)
8. Chemia Stosowana (Poland)
9. Canadian Journal of Chemical Engineering (Canada)
10. Chemical Engineering Progress Symposium Series (USA)
11. Chemical Engineering Science (UK)
12. Chemie-Ingenieur-Technik (Germany)
13. Forschungshefte. Verein Deutscher Ingenieure (Germany)
14. Indian Journal of Pure and Applied Physics (India)
15. Indian Journal of Technology (India)
16. Industrial and Engineering Chemistry. Industrial (from 1959 International Edition) (USA)
17. International Journal of Heat and Mass Transfer (UK)
18. Inzhenerno-fizicheskii zhurnal (USSR)
19. Journal of the Aero/Space Sciences (USA)
20. Journal of Applied Mathematics and Mechanics (English translation of a Russian magazine)
21. Journal of Applied Mechanics. (USA)
22. Journal of Basic Engineering (USA)
23. Journal of Engineering Physics (English translation of a Russian magazine)
24. Journal of Engineering for Power (USA)
25. Journal of the Franklin Institute (USA)
26. Journal of Heat Transfer (USA)

27. Journal of Mathematics and Mechanics (USA)
28. Journal of Mathematics and Physics (USA)
29. Journal of Mechanical Engineering Science (UK)
30. Journal of Science and Engineering Research (India)
31. Kältetechnik-Klimatisierung (Germany)
32. Mathematika (UK)
33. Memoirs of the Faculty of Engineering, Kyushu University (Japan)
34. Nuclear Science and Design (Netherland)
35. Nuclear Science and Engineering (USA)
36. Philosophical Magazine (UK)
37. Physics of Fluids (USA)
38. Proceedings of the Cambridge Philosophical Society. Mathematical and Physical Sciences (UK)
39. Proceedings of the Royal Society (UK)
40. Quarterly of Applied Mathematics (USA)
41. Quarterly Journal of Mechanics and Applied Mathematics (UK)
42. Soviet Physics: Doklady (English translation of a Russian magazine)
43. Transactions of the American Institute of Chemical Engineers (USA)
44. Transactions of the American Society of Mechanical Engineers (USA)
45. Transactions of the Institution of Chemical Engineers (UK)
46. Transactions of the Japan Society of Mechanical Engineers (Japan)
47. Wärme- und Stoffübertragung (Germany)
48. Zeitschrift für angewandte Mathematik und Mechanik (Germany)
49. Zeitschrift für angewandte Mathematik und Physik (Germany)
50. Zeitschrift des Vereins deutscher Ingenieure (Germany)

It is interesting to note the wide spread of published sources for this one class of problem which attests to both its technical and mathematical interest.